POLITECHNIKA KOSZALIŃSKA
WYDZIAŁ INŻYNIERII LĄDOWEJ, ŚRODOWISKA I GEODEZJI

ROZPRAWA DOKTORSKA nt.

# Hybrydowe metody eliminowania mikrozanieczyszczeń organicznych z wody i ścieków

**mgr inż. Lucyna Lewandowska**

Promotor: **Dr hab. Paweł K. Zarzycki**

**Koszalin 2022**

KOSZALIN UNIVERSITY OF TECHNOLOGY

FACULITY OF CIVIL ENGINEERING, ENVIRONMENTAL AND GEODETIC SCIENCE

PhD THESIS

# Hybrid methods enabling elimination of organic micropollutants in water and sewage

MSc **Lucyna Lewandowska**

PhD Supervisor: **Paweł K. Zarzycki**, PhD, DSc

**Koszalin 2022**

**PhD THESIS CONTENTS**

# 1. INTRODUCTION

## *1.1. Key problems overview*

The rapid development of industrial zones, the extensive production of pharmaceuticals, cosmetics, chemicals, fuels and fertilizers, as well as food and other related products has resulted in massive releases of toxic micro-pollutants into the air, water and soil. Access to safe drinking water and wastewater treatment is now considered to be a global problem. Based on recent research the main issue is the presence of micropollutants in water and water related media.

There are many micropollutants that can be present, generated in and carried by aquatic ecosystems. The key problem is that they form a highly heterogeneous mixture and exist in various concentrations, usually ranging from pg to ng per liter. They may be chemically resistant, but even under certain conditions (*e.g.* UV radiation and/or high temperatures) bioactive decomposition products may be formed. Additionally, the problem is that the micropollutants can present a wide range of polarities. This can significantly reduce the adsorption capacity of the materials, which are commonly applied for removal of these chemicals during wastewater treatment processes **[Atta-ur-Rahman 2016]**, **[Grumezescu 2017]**, **[Grumezescu 2018]**, **[Zarzycki 2020]**.

It has been well documented that micropollutants have a strong negative impact on animal and human populations. This is the main reason why authorities from many countries around the world are trying to deal with this problem. In the European Union, a number of regulations concerning this problem have been introduced. Notably, on October 23, 2000, Directive 2000/60 EC was implemented and then updated by Directive 2014/101 / EU on October 30, 2014, establishing a framework for Community action in the field of water policy. This was issued in order to create a program for the protection of inland surface waters, transitional, coastal and underground waters, including procedures for dealing with water pollution disclosed in Art. 16 of Directive 2000/60 / EC WFD. Moreover, this regulation sets forth a list of priority substances, which was finally adopted by Decision 2455/2001 /EC. Finally, this list included 33 priority substances or groups of substances (PS). Among the PS substances, priority hazardous substances were also identified, mainly those which are toxic, persistent and bioaccumulative (Directive 2000/60 / EC 2000, Joint Implementation Strategy WFD 2000/60 / EC 2009) (**Table 1**),

**[EU 2013]**. It should be highlighted that commonly used wastewater treatment methods involving coagulation, flocculation, precipitation, adsorption, ion exchange, electrodialysis membrane separation, and aerobic, anaerobic oxidation methods are not really effective for micropollutant elimination **[Świderska 2018]**. This is caused by the fact that such chemicals are not primary targets of these processes. Moreover, elimination processes of the main elements like carbon, nitrogen or phosphorus often results in undesirable synthesis of micropollutants and their uncontrolled release to the environment **[Ślączka 2013]**, **[Kaleniecka 2018]**, **[Jain 2021]**. Therefore, quantification of such chemicals, optimalization of wastewater treatment, as well as research into new active materials or nanomaterials enabling effective elimination of micropollutants are the priority of modern environmental engineering. The evidence that this problem is critical is presented in **Figure 1**, where a rapid increase in the number of publications focusing on sewage micropollutants during last 10 years has been recorded.

## *1.2. Short outline of micropollutant occurrence during wastewater treatment processes*

Micropollutants can be present in the environment in two forms: **(i)** free and **(ii)** physically adsorbed or chemically conjugated. It is considered that the active molecules should be free. For example, estrogens are biologically active as endocrine disrupting compounds, while conjugated estrogens (sulfates, glucuronides or hemisuccinates) are reported as non-active **[Lamparczyk 1992]**. For that reason, micropollutants which are present in sewage can be transformed during wastewater treatment, via simple deconjugation reactions, into free active molecules. It should be noted that this process can be performed without complicated synthesis of the given micropollutants. In general, wastewater treatment involves both simple and complex processes. Frequently applied physicochemical methods often involve active chemicals including chlorine compounds, ammonia, permanganate, alum, sodium hydroxide, hydrochloric acid, ozone and iron salts, coagulation and filtration aids, ion exchange resins and regenerators. They may be effective at removing the main pollutants but are energy and operation intensive. These methods are usually combined with mechanical waste processing and require advanced engineering knowledge and infrastructure. Unfortunately, in terms of micropollutants, conventional techniques are not efficient enough to completely remove low (but still

dangerous) levels of organic toxins and heavy metals from raw contaminated wastewater. However, they may reduce the levels of various pollutants to some extent **[Yamamura 2011]**, **[Rajasulochana 2016]**, **[Zinicovskaia 2016]**, **[Kumar 2021]**. This is a difficult issue because micropollutants belong to different chemical classes and form highly non-homogeneous groups of low molecular mass compounds including persistent metalorganic chemicals (**Table 1**). The conventional approach for the removal of micropollutants from wastewater involve a number of diverse processes including: photocatalytic degradation, biological oxidation, ion exchange, flocculation/coagulation, precipitation, adsorption and/or membrane filtration.

However, to increase the selectivity and efficiency of micropollutant removal, researchers still seek new nanomaterials, particularly, based on waste organic materials. As active, inexpensive and environmentally friendly adsorbents the compounds extracted from orange expeller, fungi or green algae are frequently studied. Most recently, there has been an increasing interest in the application of newly discovered carbon nanomaterials, including graphene and derivatives like graphene oxide or carbon nanotubes for micropollutant removal from wastewater **[Chatzimitakos 2017]**, **[Kumawat 2017]**, **[Vanni 2017**], **[Piaskowski 2018]**.

Over the last decade, there has been a growing interest in the development of inexpensive hybrid technologies that combine nanoparticles, generated from processed waste materials. They have been utilised by many research teams to act as selective media for removing micropollutants from wastewater **[Ren 2018]**, **[Amri 2020]**, **[Manoj 2020]**. This is a complex task and many different approaches have been proposed and explored as is visible in the graphs presented (**Figure 2**). Recently, the determination of various micropollutants in complex matrices have been significantly improved. This is mainly because of the development and miniaturization of mass spectrometry detection technology and the discovery of a number of effective and selective pre-purification or separation nanomaterials. These tools can be used in miniaturized and automatic quantification systems. As a consequence of effective micropollutant quantification, researchers may seek smart elimination processes of such chemicals during wastewater treatment. From principles, these processes must be effective but in addition selective, inexpensive and consume low amounts of energy. Nowadays, nanotechnology is being researched as a promising technology and has shown remarkable achievements in various fields, including wastewater treatment **[Ślączka 2017]**, **[Świderska 2018]**,

**[Zarzycki 2022]**. Nanostructures offer new opportunities to create more effective catalysts and redox active media for wastewater treatment due to their small size, large surface area and ease of functionalization, as well as exceptional control over microstructure shape. Nano objects can be created by simple chemical reactions involving various physicochemical interactions and/or be derived from larger natural objects such as cell structures (cellulose, cyclodextrins), bacteria (microbial cellulose), fungi (chitosan) as well as tissues (pyrolytic carbon, graphene oxide, carbon nanotubes, sporopollenin) **[Kiziltas 2015]**, **[Nazerah 2016]**, **[Mitura 2018]**, **[Peña-Gonzalez 2018]**.
It was found that some nanomaterials may effectively interact with given low molecular mass compounds. Recently, there has been increasing research into the application of such systems to remove a number of pollutants from wastewater, such as heavy metals, organic and inorganic solvents, biological dyes and toxins, and pathogen causing diseases such as cholera and typhoid as well as Covid-19 viruses **[Kumar 2014]**, **[Aydin 2021]**, **[El-Said 2021]**, **[Zhang 2021]**. It should be noted that nanomaterials can act as part of sensing devices enabling detection of the above-mentioned molecules and biological structures in wastewater **[Lu 2021]**, **[Srivastava 2021]**, **[Vashisht 2021].**

## *1.3. Colorants as target micropollutants*

Colorants are common chemicals in a number of global industries which produce textiles, food products, cosmetics and pharmaceuticals as well as printer inks, leather and plastics. Currently, the textile industry is considered to be the main consumer of colorants. The amount of dye chemicals used in this industry is difficult to estimate but ranges from between $1 \times 10^5$ and $3 \times 10^5$ tons. It should be noted that the total annual consumption of colorants may be around $7 \times 10^5$ tons, globally **[Kant 2012]**, **[Kuppusamy 2017].** Based on these data it can be expected that synthetic colorants may be parent compounds for a number of bioactive micropollutants, particularly those which consist of aromatic rings. From principles, colorants are relatively easy to detect. Unfortunately, they are difficult to eliminate from wastewater and/or surface water due to the fact that they often contain chemical structures with aromatic rings. The relatively high stability of the selected dyes, together with their toxic, mutagenic and carcinogenic nature raises health and environmental concerns.

Based on their chemical structure, particularly the presence of chromophores and/or auxochromic groups, synthetic dyes can be classified into several categories. The most common are azo, anthraquinone, sulfur, indigo, triphenylmethyl and phthalocyanine derivatives. Auxochrome structures may increase the intensity of the colors. Increasing their solubility in water can be easily performed by the incorporation of acid groups into the colorant structure, *e.g*. a sulfone group (-$SO_3H$) or a carboxyl group (-COOH) can be added. Such modified chemicals are usually used in sodium salt form.

Nowadays, due to the wide range of colors and shades available, the azo dyes are the most commonly used commercial colorants. These colorants are also non-expensive for production and have high water or moisture resistance **[Siti Zuraida 2013].** It should be mentioned that these chemicals may be easily transformed into highly toxic decomposition molecules because the parent structures consist of aromatic rings as well as different reactive ligands including nitrates and sulphates and also heavy metals like lead, cadmium or mercury. They are frequently applied as textile colorants, which then are processed by wastewater treatment plants and may be released to water environments as toxic pollutants or micropollutants **[Raducan 2008].** Dyeing processes may include harmful additives, which also can be released into wastewater. The list of potential toxic chemicals includes microplastics, organic acids, soaps, hydrocarbon softeners and other surfactants. In addition, auxiliary agents based on formaldehyde acting as dye fixers or chlorine-containing stain removers increase the pollution problems associated with the colorants industry. This is because chlorine may react with the organic sewage matrix and generate additional toxic products **[Kant 2012]**, **[Buntić 2017]**, **[Dil 2017]**, **[Vashisht 2021]**.

One of the main problems for the human population is that such pollutants can be back transferred from surface waters to food **[Rybczyńska 2016].** In addition, drinking polluted water may result in long term accumulation of micropollutants in the body. Non-polar chemicals may be permanently adsorbed within fat tissues like central nervous systems and these deposits may lead to severe disease **[Li 2017]**, **[Melo 2017]**. Interestingly, dye pollutants may be fairly stable during wastewater treatment and this may result in low biodegradability of colorants and their degradation products **[Janović 2017]**, **[Manavi 2017]**, **[Rajasimman 2017]**.

Generally, elimination of dyes from wastewater may be carried out using two different approaches **[Kant 2012].** The first method is based on biodegradation where

colorants are transferred to biomass that is acting in a different form *e.g*. in the solid or sediment phase. The second method involves different types of mineralization **[Hamdaoui 2008]**, **[Asfaram 2017]**, **[Kuppusamy 2017]**, **[Rajasimman 2017].** It is clear that efficient elimination of dye micropollutants must be processed by hybrid methods, combining a number of physicochemical processes and interactions like: adsorption, coagulation, flocculation, supramolecular host-guest interactions, ion exchange, electrochemical oxidation, ozonation, ion exchange as well as sonication, photocatalysis, irradiation and membrane processes **[Zarzycki 2009]**, **[Kant 2012]**, **[Asfaram 2017]**, **[Kuppusamy 2017], [Piaskowski 2018]**, **[Rajasimman 2017]**, **[Kaleniecka 2019]**.

The problem is that hybrid systems may involve expensive reagents or generate new hazardous micropollutants **[Kuppusamy 2017]**. Very efficient oxidation technologies can be non-selective and generate reactive hydroxyl radicals. The consequence of this is the production of toxic low-molecular mass compounds containing chlorine. These methods are considered to be expensive because they involve complicated protocols and equipment **[Buntić 2017]**. Non-destructive processes during wastewater treatment such as coagulation, flocculation, membrane colorant removal protocols can further be divided into separation and adsorption processes, while destructive processes include biodegradation and oxidation **[Piaskowski 2018]**.

In this PhD thesis as the target micropollutants, four synthetic dyes were investigated, namely: Brilliant Blue, Ponceau 4R, Sunset Yellow and Malachite Green (**Table 2**, **Figure 3**). Selection of these chemicals was based on different criteria: **(i)** overall toxicity, **(ii)** food and general industry usage (*e.g.* as textile colorants), **(iii)** water solubility, which is important in terms of the pollution impact on surface waterecosystems, **(iv)** possible molecular interactions with various adsorbents and nanoparticles due to the presence of differently charged ligands and ion behavior in an electric field, **(v)** complex supramolecular formation between host and guest molecules in the presence of macrocycles (*e.g.* cyclodextrins), **(vi)** detection possibility on planar analytical systems using simple RGB data acquisition. The general characteristics of these substances are described below.

**Sunset Yellow FCF (E110)** (**Table 2**, **Figure 3**) is considered to be a common synthetic food dye within the azo compounds group. This substance enhances or gives the final color of soft drinks, candies and snacks. Elimination of wastewater pollution by E110 is problematic because of the high molecular stability of this chemical and its ability to form

toxic intermediates. Due to the high visible light adsorption of Sunset Yellow molecules, even a low amount of this substance may block visible light within the water column from 0 to 15 m, approximately. Therefore, this micropollutant may have significant effect on surface water ecosystems **[Yagub 2014]**. According to EFSA (European Food Safety Authority) data, E110 may be acceptable as a food additive with a limited daily intake that is equal to 1 mg/kg bodyweight **[Ismail 2016]**. A number of researchers highlight several adverse health effects (including allergies, attention deficit, and hyperactivity), which are associated with this most commonly used synthetic colorant **[Amchova 2015]**, **[Ismail 2016]**. These observations justify the necessity of extensive research focusing on developing new methods for the efficient and selective removal of E110 from sewage as well as surface water ecosystems. So far, traditional methods applied for the removal of Sunset Yellow include: adsorption, precipitation, oxidation and ion exchange as well as electrochemical and photocatalytic protocols **[Ghaedi 2012]**, **[Rajamanickam 2014]**, **[Ahmad 2015]**, **[Rajamanickam 2015]**, **[Aliabadi 2018]**, **[Ahmad 2019]**. Within these methods adsorption-based removal protocols are most commonly applied using molecular sieves, activated carbons and various polymeric matrices with active ligands (polypyrrole, polyaniline) **[Roosta 2015]**, **[Xu 2017]**, **[Aliabadi 2018]**. Most recently, new protocols based on magneto and graphene materials formed as nanocomposites have also been proposed **[Yakout 2018]**, **[Mirzajani 2019]**, **[Coros 2020]**.

**Malachite Green (MG)** (di[4-dimethylamino-phenyl]phenyl cation) (**Table 2**, **Figure 3**) is a widely used cationic dye that belongs to triphenylmethane group. It is an important water-soluble dye **[Khan 2013]**, **[Wang 2015]**. Due to its relative high stability and vibrant color this synthetic dye is commonly used for dyeing silk, cotton, jute, and paper, wool and leather products **[Ngah 2010]**. Interestingly, Malachite Green can be applied as an effective fungicide, frequently used in the aquaculture industry **[Roosta 2014]**. MG is extensively used in the fish farming industry to treat various infections caused by parasites, both fungal and bacterial. There are some studies documenting that Malachite Green may be mutagenic and carcinogenic as well as affecting the nervous system and brain in humans since it may enter the food chain **[Shirmardi 2013]**. Therefore, the use of MG as a veterinary drug in aquaculture has been restricted in many countries including the USA, Canada, the UK and the EU. Importantly, in the USA this dye has been banned for food-related applications since 1983. Considering the fact that MG is still used in the textile industry, this compound is reported to be an important pollutant of wastewater.

It is notable that MG may be present in various dissolved dyestuffs and other products, for example, dispersing agents, salts, emulsifiers or leveling agents. MG removal from effluent is an expensive process and is considered to be a major problem for the textile industry. The removal process resulting mainly from MG fading can be catalyzed by small concentrations of cationic surfactants. This reaction has been successfully applied for MG removal from wastewaters **[Raducan 2008]**. MG level can be also decreased by contact with a $Fe_3O_4$/CD/GO ($Fe_3O_4$ /cyclodextrin/graphene oxide) composite containing macrocycles and graphene oxide molecules. These new hybrid nanomaterials have been found to be very promising structures for dye removal from polluted water **[Wang 2015]**. An additional problem is that there are a number of forms and metabolites of MG that may be adsorbed by tissues and cells. For example, animals may metabolize malachite green into a leuco form, which is strongly non-polar (log P = 5.7). The consequence of this is that this metabolite is strongly retained in, for example, catfish muscles where it may be active for a long period of time (HL = 10 days). In comparison, for the parent dye the HL value = 2.8 days. This clearly indicates why MG must be efficiently removed from the waste and water environments **[Veterinary Residues Committee 2012]**.

**Ponceau 4R (P4R)**, Acid red (AR18), is a 1-(4-sulfo-1-napthylazo)-2-napthol-6,8-disulfonic acid, trisodium salt (**Table 2, Figure 3**). This synthetic azo colorant is primary applied for the dyeing of food and textile products **[Koupaie 2012]**. The major environmental problem reported with this chemical is the high loss of the colorant during the industrial dyeing process. It may be expected that 10 – 50% of P4R can remain in the effluent after dyeing processes **[Khandegar 2013]**. Similar, to Malachite Green, Ponceau 4R is highly soluble in polar solvents, particularly in water. The consequence of this is a serious impact on hydrobiontes even at a low concentration. This is possible due to the high visible light absorption of P4R molecules decreasing the photosynthesis rate of plants, as well as generation of several intermediate products that can be either toxic, carcinogenic, or mutagenic to aquatic life **[Khandegar 2013]**, **[Azarian 2014]**, **[Lu 2019]**, **[Wang 2019]**. Therefore, the treatment of effluents containing P4R is important to reduce the toxic impact of this chemical on aquatic life forms **[Amri 2020]**. Ponceau 4R is commonly used in Europe, Asia and Australia, however, it is not accepted for human consumption within the USA. In Europe, the acceptable daily intake of P4R is 0.7 mg/kg, whilst the WHO/FAO (World Health Organization/Food and Agriculture Organization) ADI (Acceptable Daily Intake) recommendation is 4 mg/kg **[Abbey 2013]**. It should be noted

that azo dyes, including P4R still have broad industry application due to the variety of their chemical structures and simple production **[Gupta 2008]**. Generally, P4R, as other azo dyes, is resistant to biodegradation because it consists of complex aromatic structures. Therefore, after improper discharge, they may persist in the water environment for a long time **[Irikura 2016]**, **[Li 2016]**. There have been many attempts to eliminate azo dye chemical pollution, including Ponceau 4R, from wastewater using physiochemical methods namely: reverse osmosis, coagulation and flocculation, ultra-filtration, ion exchange, adsorption and membrane processes and advanced oxidation processes (AOPs) **[Mozia 2005]**. It has been found that common physiochemical methods seem to be ineffective, expensive and may result in the production of a large volume of sludge causing a number of secondary problems like biomass treatment and disposal **[Malakootian 2013]**. For that reason, there are a lot of studies involving complementary wastewater treatment based on alternatives such as electrochemistry **[Movahedian 2006]**, **[Arqiani 2013]**, **[Zhang 2013]**, **[Yousefi 2018]**.

**Brilliant Blue (BB)**, (asethyl - [4 - [[4 - [ethyl -[(3 - sulfophenyl) methyl] amino] phenyl] - (2 - sulfophenyl) methylidene] - 1 - cyclohexa - 2, 5 - dienylidene] - [(3 -sulfophenyl) methyl] azanium) (**Table 2**, **Figure 3**) is a frequently applied water soluble dye used in the food and drug industries. BB has various staining applications, for example, as an additive to inks, paints and textile/leather products **[Sabnis 2010]**. Recently, this chemical has been considered to be a toxic substance due to some concerns related to its effects on carcinogenicity and reproductive and neurological disorders. Therefore, application of this dye was restricted in several countries. Following health studies, the European Union Scientific Committee for Food (SCF) decreased the acceptable daily intake (ADI) of BB from 12.5 mg/kg/day in 1975 to 6 mg/kg/day in 1990 **[Borzelleca 1990]**, **[Aguilar 2010]**. BB additive is a typical example where other ingredients present in the final product (like beverages) may significantly participate in degradation process by *e.g.* adduct formation **[Eskilsson 2002]**, **[Gottlieb 2003]**, **[Gosetti 2006]**. This phenomenon strongly affects the elimination of colorant molecules from waste. In such cases, quantification of trace amounts of Brilliant Blue seems to be essential. There are a number of protocols which have been devised for such purpose based on simple spectrophotometry **[Capitán-Vallvey 1996]**, separation science involving liquid column chromatography **[Minotti 2007]**, **[Alves 2008]**, capillary electrophoresis **[Huang 2005]**, **[Fraige 2009]** and paper chromatography **[Sumiko Tsuji 2001]** as well as different

methods using electrospray mass spectrometry **[Ma 2006]**, **[Tsai 2015]**, cloud point extraction **[Pourreza 2011]**, cathodic stripping voltammetry **[Florian 2002]** and two phase interaction systems **[Shiri 2012]**. Recently, more advanced methods for BB determination have been developed, the results of which can be also used as the starting point for elimination studies of dye pollution from waste and surface water ecosystems. For example, methodology based on nanomagnetic molecularly imprinted polymers (MMIP) can be efficiently used for BB and different kinds of dye extraction from water media **[Parisi 2010]**, **[Okutucu 2010]**, **[Marcinkowska 2013]**, **[Mirzajani 2016]**, **[Lee 2016]**. In such technology, a given template from the polymeric matrix gives specific recognition sites enabling target compound elimination **[Arabzadeh 2016]**. This protocol is frequently combined with solid-phase extraction (SPE) allowing fast pre-purification, concentration and separation of target molecules **[Arabzadeh 2010]**, **[Panjali 2015]**, **[Arabzadeh 2018]**.

## *1.4. Potential active additives for water and sewage purification from micropollutants*

Elimination of micropollutants from sewage is a complex task. As mentioned above, there is a growing interest in finding new nanomaterials that can be applied in environmental engineering specifically for improving elimination of micropollutants from sewage (**Figure 2**). There are different classes and forms of nanomaterials like metal, organic and carbon-based nanoparticles, macrocyclic inclusion compounds, zeolites, self-assembled monolayers on mesoporous supports or hybrid polymers/biopolymers. All of them are characterized by a high surface to volume ratio **[Baruah 2019]**. Usually, the native forms are chemically active, which enable functionalization of such structures with various destination ligands. They can easily be adapted for sorption, chemical transformation matrices and therefore can be used in technological sewage treatment processes **[Nedyalkova 2017]**, **[Baruah 2019]**, **[Jain 2021]**. However, there is also the problem of unknown toxicity of nanomaterials and their disintegration products, especially in the case of uncontrolled emission to the aquatic ecosystems and environment. Below, there is a list and short characteristic of the selected adsorbents and nanomaterials that were of interest in terms of the experimental work presented in this PhD thesis.

### 1.4.1. Carbon-based nanomaterials

Pure carbon and carbon-related nanomaterials may be considered the most versatile particles that are presently studied in physics, chemistry, and bioengineering. Extensive research focusing on classic and new carbon particles is being carried out worldwide, and a number of new commercial products have been successfully implemented in different industries and technology areas, including electronic, medicine/pharmacy, cosmetic, food and agriculture, wastewater treatment or environmental protection and civil engineering **[Grumezescu 2017]**. From principles, carbon nanoparticles are easy to functionalize with various organic ligands and therefore, there are a virtually unlimited number of derivatives available which can be adapted to the given applications **[Sun 2017]**. Particularly, carbon nanoparticles based on fullerenes, nanotubes, graphene, as well as nanodiamonds or carbon dots (CDs) are presently of great interest due to their relatively low toxicity, biocompatibility, easy synthesis, and unique physicochemical properties **[Grumezescu 2018a]**, **[Neethirajan 2018]**, **[Zarzycki 2020b**], **[Kalniecka 2020b]**.

**Activated carbon (AC)**. In particular, this material is a common adsorption base that is very efficient but predominantly non selective. AC are produced in several forms (powder, granules) that are available with various pore sizes **[Gopinathan 2017]**, **[Ferreira 2017]**. In general, AC surface area varies from 500-2000 $m^2$ /g and it can easily be modified by attachment of different functional groups. This may increase selectivity for interaction with micropollutants **[Świderska 2018]**. One of disadvantage of AC is that such material is relatively expensive in terms of overall production cost in comparison with other adsorbents **[Raval 2017]**. Therefore, there is increasing research focusing on non-expensive precursors, mainly waste materials like extravagant pods, coconut stalks, or guava seeds **[Vargas 2011]**, **[Ozdemir 2014]**, **[Pezoti 2016]**. This material is commonly applied in wastewater treatment technologies in different modes and spatial forms or as support for different active molecules (**Figure 4**), **[Biswas 2016]**, **[Chang 2016]**, **[Maddigpu 2018]**, **[Świderska 2018]**, **[Zarzycki 2021]**.

**Graphene oxide (GO)** is one of the most commonly investigated carbon-based nanomaterials derived from graphene, which presents as an ordered honeycomb network structure. GO can be described as a highly oxidative form of a graphene monolayer. The chemical structure of this substance depends greatly on the synthesis

protocol **[Le 2019]**. Generally, GO may consist of a variety of oxygen containing ligands, including hydroxyl, carboxyl, carbonyl, and epoxy groups. These functional groups are attached to both the sides of the basal plane (*e.g*., hydroxyl and epoxy groups) or on the GO particle edges (*e.g*., carboxyl and carbonyl groups) **[Nazerah 2016]**. The consequence of the presence of functional groups in the GO structure is that such particles are relatively polar and can easily be dispersed in water, forming fairly stable suspensions. This property of GO is critical for a number of industrial applications. Graphene oxide is especially attractive to researchers because of its low production costs and unique physicochemical properties, enabling various applications. It should be noted that GO can be simply synthesized using chemical exfoliation of graphite. This approach is attractive because it does not involve complex equipment or metallic catalysts and therefore, no further complex purification steps are needed. There are a number of approaches for the synthesis of GO that have been described in literature, mainly based on the Hummers and Offeman protocol (**Figure 5**), **[Hummers 1958]**, **[Zarzycki 2020b]**, **[Coros 2020]**.

### 1.4.2. Biopolymers and various organic nanostructures

Nowadays, natural polymers like cellulose-based structures play an important role in green analytical chemistry. Cellulose is complex at any scale and contains both crystal and amorphic conglomerates. Many physicochemical properties have been discovered in the structure of these materials made of nanofibers and nanocrystals **[French 2014]**, **[Mu 2015]**, **[Usov 2015]**. Due to such properties and general trends, they find application in planar and column chromatography and in analytical and preparative applications **[Okamoto 1984]**, **[Astec Cellulose DMP Efficient 2010]**. Cellulose-containing materials, such as printing papers or filter papers, are widely researched as active carriers for sensors, flexible electronics and microfluidic devices (paper microfluidic devices; PAD) **[Kurra 2013]**, **[Lisowski 2013]**, **[Lin 2014]**. Polysaccharides such as cyclodextrins, nanomagnetic polymers, covalent organic polymers, extracellular polymeric substances, etc. are commonly used polymeric adsorbents **[Reddy 2013]**, **[Alaba 2018]**. Nanocelluloses, which are derived from cellulose, are non-toxic, ubiquitous, have excellent adsorption properties and their surfaces can be easily modified. All this makes them suitable for waste water remediation **[Abdi 2020]**. The enormous potential of lignin-derived nanomaterials for water and wastewater treatment has recently been discovered. They have been found

to be effective in catalytic degradation of dyes and the removal of nitroarenes and heavy metals **[Chen 2019]**.

**Cellulose**, this biopolymer is based on glucose monomers. Cellulose is complex at any scale: it contains both crystalline and amorphous zones. It is classified as an unbranched biopolymer composed of 3,000 - 14,000 D-glucose molecules, which are linked by β-1,4-glycosidic bonds. Cellulose crystalline regions contain molecular chains that are arranged in a highly ordered structure forming large agglomerates. These structures are stabilized by a complex network of hydrogen bonds **[Habibi 2010]**, **[Gong 2018]**. Changes in the three-dimensional structure of cellulose result in different physicochemical properties of this polymer and therefore this topic is studied extensively. In general, a number of cellulose polymorphs including cellulose I, cellulose II, cellulose III and cellulose IV have been identified **[Morán 2008]**, **[Gong 2010]**, **[Yue 2012]**, **[Jin 2016]**. It should be highlighted that, due to its particular 3D structure this biopolymer may adsorb water molecules as well as non-polar target chemicals from the water phase. Native cellulose and its derivatives are commonly used in separation science mainly due to the fact that this material may work both in normal phase and reversed phase mode **[Zarzycki 2022]**.

**Cyclodextrins (CDs, cyclic oligosaccharides)** belong to group of macrocyclic compounds forming donut-like shaped molecules. Native cyclodextrins (alpha, beta and gamma possessing 6,7 and 8 glucose units) can easily be manufactured using green chemistry biosynthesis. They are virtually non-toxic for the environment, animals and humans. The solubility of CDs is strongly affected by temperature and by the presence of organic co-solvents **[Zarzycki 2016]**, **[Kaleniecka 2020a]**. The main interest in these molecules is due to their inclusion properties, enabling the creation of highly selective host-guest complexes in water solutions. These properties were discovered at the beginning of the 1950s and since then have been extensively investigated worldwide **[Cramer 1954]**, **[Connors 1987]**, **[Lehn 1995]**. The internal cavity of cyclodextrin is chiral, therefore, these molecules can selectively interact with chiral guest molecules and recognize enantiomers. This was extensively applied in separation science for the effective fractionation of racemic mixtures **[Zarzycki 2016]**. Currently, these materials are being extensively used in food, cosmetics and drugs products, mainly to enhance active component stability. There is also an interest in the synthesis of cyclodextrins containing polymers that may work as adsorption matrices for the isolation of

micropollutants from sewage. Most recently cyclodextrins have been used as active chemicals enabling the elimination of bisphenols from water samples **[Ohta 2017]**, **[Grumezescu 2018b]**, **[Kaleniecka 2019]**.

**Pine pollen (PP)**. This biomaterial is produced by plants in the form of durable microcapsules. Pine pollen structure is multicompartmental (**Figure 6B**) and its wall membranes contain highly resistant polymers, particularly sporopollenin, cellulose and other polysaccharides. Pollen can be locally present in the natural environment in large quantities (**Figure 6A**). These biological structures have a number of unique properties primarily enabling them to protect and deliver a wide range of biocomponents to destination plant organs. Pine pollen contains up to 25% by mass of wall membranes forming empty spaces, which allow them to be easily transported by wind, water, insects or birds. Pollen size may range from 5 to 250 μm (*e.g*. *Myosotis L.* and *Cucurbita L*. respectively) **[Punt 1999]**, **[Punt 2007].** Pollen membranes consist of unique biopolymers called sporopollenins. These materials are considered to be one of the most resistant natural biomaterials in nature and its residues can be present in sedimentary rocks from 500 million years ago **[Feagri 1964]**, **[Brooks 1978a]**, **[Mackenzie 2014]**. Currently, properties of this biomaterial are being widely studied. Pollen can be used as natural microcapsulation particles also after the isolation of clean sporopollenin exine capsules **[Mackenzie 2014]**, **[Li 2016a]**, **[Prabhakar 2017]**. In the experimental part of this PhD thesis, PP was used as a reaction mixture additive for testing biodegradation of the given dyes. Under such conditions, multiple mechanisms can be expected in the reaction mixture including physical and chemical adsorption as well as PP biomass effect on activated sludge microorganisms **[Zarzycki 2021]**.

**Dandelion Pappus (DP)**. This biomaterial forms feather-like microstructures enabling dandelion seed transportation over large distances using wind as a dispersal method (**Figure 7A**). This material is characterized by a complex surface structure visible under both an optical microscope and SEM imaging (**Figure 7B**). Pappus filaments are formed from cellulose but also contain a number of different organic substances *e.g.*, waxes. They may change pappus surface polarity and protect it from moistening. Recently, a dandelion plant was used as a useful matrix in determination of trace element pollution in various ecosystems **[Bijelić 2018]**. Dandelion pappus biomass is present in large amounts in the environment, can be detected in sediments, and this material may affect benthic biota **[Laima 2002]**, **[Tauber 2005]**. Most recently, a number of new

applications of such biomaterial were reported, including new supercapacitors or as an extraction matrix for micropollutant analysis **[Virtanem 2017]**, **[Zarzycki 2022]**.

### 1.4.3. Inorganic nanostructures

**Egyptian blue (EB)**. This blue pigment was probably discovered in ancient Egypt in the third millennium BC. The original protocol for the preparation of this chemical is unknown. One potential preparation protocol was described by Vitruvius in De Architectura in the 1st century BC. Interestingly, the chemical composition of this dye has been found to be similar on various archeological artifacts, which have been located in various parts of the Roman Empire **[Ullrich1987]**, **[Riederer 1997]**, **[Delamare 1998 a, b]**. Generally, EB can be obtained by heating a mixture of silica sand, limestone sand, copper minerals or bronze fragments and flux compounds like natron or plantash. In Vitruvius' recipe, calcium carbonate was not mentioned, probably because the sand used in Pozzuoli area had the appropriate limestone content. Recently, it has been discovered that EB synthesis temperature must be within the range 850 - 950°C. Temperatures exceeding 1000°C result in EB decomposition or the production of a green colored substance **[FitzHugh 1997/2012]**, **[Bianchetti 2000]**, **[Baraldi 2001]**, **[Mozzocchini 2004]**, **[Errington 2016]**, **[Panagopoulou 2016]**. More recently, it has been discovered that this ancient mineral pigment can be considered a complex nanomaterial and may spontaneously delaminate in water, resulting in the formation of various nanoparticles. Moreover, it may act as an efficient fluorophore, transferring visible light into near infrared wavelengths which has number of applications in civil engineering and forensic studies **[Binet 2021]**, **[Berdahl 2018]**, **[Errington 2016]**. This material can be relatively easy to produce in different forms in laboratory conditions (**Figure 8**), **[Zarzycki 2021]**.

### 1.4.4. Activated sludge and duckweed

**Activated sludge (AS)** can be considered a strongly non-homogeneous biomass that is dispersed in the water phase. It consists of various microorganisms including aerobic and anaerobic bacteria, fungi, protozoa and algae. Suspended microbes form flocks that may work as small bioreactors that spontaneously perform a number of complex biochemical processes. As a result of such activity, various organic pollutants can be removed from wastewater. Therefore, AS is one of the more important components of biological purification in the technological processes

of wastewater treatment (Figure 9), **[Verlicchi 2012]**, **[Jain 2021]**.

**Duckweed** (*Lemna minor L*.; common duckweed), (Figure 10) belongs to the subfamily Lemnoideae of the *Araceae* family. It is a cosmopolitan freshwater aquatic plant that floats on the water surface. Typically, this tiny organism consists of one to four leaves with one root hanging in the surface water space. This plant may generate a high volume of biomass because duckweed reproduction is mainly vegetative: its leaves may quickly divide and form separate individuals **[Appenroth 2013]**. Duckweed biomass is commonly used as an animal food and also for bioremediation, enabling nutrient removal from wastewater. It has been demonstrated that duckweed biomass may effectively remove a number of heavy metals from the water phase including lead, zinc, copper and arsenic **[Goswami 2014]**, **[Sasmaz 2015]**. However, it has been found that higher heavy metal concentrations may significantly reduce the biomass growth rate **[Rahmani 1999]**. Interestingly, duckweed organisms are fairly temperature tolerant, therefore, they have great potential for economic use in different climate zones, especially in wastewater treatment plants, for both municipal and industrial wastewater treatment **[Rahmani 1999]**. In some cases, duckweed biomass from wastewater plant has been used as a compost material, a soil additive and also a protein source for livestock **[Skilicorn 1993]**. It should be mentioned that such material should be tested for heavy metal content before any agricultural applications **[Hillman 1978]**, **[Skilicorn 1993]**, **[Huang 2004]**, **[Baby 2010]**. There is also an issue with accumulation or removal of organic micropollutants, such as pharmaceuticals, from wastewater by duckweed biomass **[Iatrou 2017]**, **[Gatidou 2017]**. Recent studies indicate that this organism may increase the removal rate of bisphenol micropollutants **[Kaleniecka 2019]**.

## *1.5. Technological processes in sewage water treatment (Jamno Treatment Plant)*

The “Jamno” Municipal Wastewater Treatment Plant (JMWTP) is located in the Koszalin area. This semi-automated industrial facility was launched in 1995. JMWTP can be considered a typical example of a sewage treatment plant based on both mechanical and biological technological processes involving chemical support for

wastewater treatment (**Figure 11**), **[Kozak 2007]**, **[Uchwała Rady Miejskiej w Koszalinie 2020]**. Wastewater is supplied to this system through a sewage collector from the Koszalin city. The treatment plant also collects large sewage volumes from neighboring areas including Świeszyno and Sianów. The facility consists of several complementary parts:

1) mechanical, which includes: mechanical grates, a sand trap with sand outflow and preliminary sedimentation tanks,
2) biological; this part consists of several bioreactors including dephosphating, denitrification and nitrification chambers as well as secondary sedimentation tanks with recirculation pumping stations and a blower station,
3) a treatment facility dedicated to sewage sludge, which includes: thickeners, a fermentation chamber and sludge centrifuges as well as a chemical reactor, mobile pumping station and leachate pumping station.
4) a sludge storage hall and thermal treatment of sewage sludge, including a sludge dryer as well as air deodorization stations after the deep drainage process.

The estimated capacity of JMWTP is around 36 x $10^3$ $m^3$ per day. In the years 2000 - 2002, the second stage of this facility was improved enabling biological sewage treatment. This resulted in a high degree of nutrient reduction in the treated wastewater. Biological reactors are equipped with control and measurement equipment, which allows continuous monitoring and automation of the treatment process. It should be highlighted that JMWTP generates sludge in the form of pellets, which are characterized by high dry matter and carbon content.

## *1.6. Hybrid methods approach for micropollutant removal from water and during wastewater technological processes*

As described above, micropollutant removal from the water phase is complexand cannot be efficiently completed using classic wastewater treatment processes. In the case of the given target components, there are a number of classical and hybrid approaches proposed as listed and described in **Table 3**. Unfortunately, these processes have been found to be ineffective for micropollutants that are characterized

by a wide range of polarities and molecular masses **[Popowicz 2015]**, **[Baptisstella 2018]**, **[Bridle 2022]**. Therefore, alternative hybrid methods have been extensively developed, combining various complementary purification protocols and a number of bio- and nano-materials. This is, in fact, the present priority of research focusing on micropollutant removal conducted in European Union countries. As a possible solution to this problem, a hybrid approach combining microfluidic nano-devices with supramolecular chemistry processes (*e.g*. host-guest interactions) can be proposed.
In this case, the selectivity of a given purification system may be accurately tuned by the application of different host molecules, for example macrocyclic oligosaccharides including cyclodextrins, and its efficiency increased by a high area (volume) of active channels within microfluidic devices. These devices can be arranged in the form of large arrays and therefore, dedicated to work on a large scale.

It is worth noting that in nature, a similar concept was successfully implemented by several filtrating organisms like sponges and ascidians, which are composed of large 3D structures (**Figure 12**). These organisms may effectively filtrate extremely large volumes of water using simple, multiplied and low-rate flow channel systems adsorbing small particles and water-soluble nutrients.

A similar concept based on complex biostructures (blood circulation in lungs) was part of a grant application proposal entitled: Antibiotic and Endocrine Disruptor Removal From Wastewater By Absorption In Microfluidics Systems (ARAMIS). The project was prepared for Horizon 2020 FETOPEN-2018-2020 (Novel ideas for radically new technologies) in cooperation with Eden Microfluidics (France), Lappeenrannan-Lahden Teknillinen Yliopitsto LUT (Finland), Black Hole Lab (France), Sumy State University (Ukraine). The main goal of the ARAMIS project was the removal and recycling of a number of bioactive micropollutants including, antibiotics and steroidal hormones using new hybrid microfluidics, biopolymers and host-guest complexes involving cyclodextrins. The core part of this approach was based on Eden Microfluidics devices (**Figure 13**), **[www 5]** and the implementation of several selective supramolecular chemistry processes for the efficient extraction of target micropollutants from sewage. Eden Microfluidics has developed a new microfluidic design for high - volume applications **[www 6]**, by taking inspiration from natural processes like blood circulation in the lungs. They patented a similar structure based on high-density microchannels placed inside in a 12-cm CD-like microfluidic cartridge. This structure has been demonstrated to deliver

flow rates of 15 L/day driven by low pressure (1 bar only). The large-scale purification platform may be highly modular and consists of a stack of cartridges, bonded together and providing for large volumes of water and sewage processing. The microdevice for the ARAMIS project was designed for the selective adsorption of given micropollutants by the application of hybrid cyclodextrins and chitosan biopolymers received from waste sources.

To the best of my knowledge, the method mentioned above or similar approaches can be a promising solution for the efficient purification of wastewater from different micropollutants. At this stage of my research, screening of new selective nanomaterials should be performed.

# 2. MAIN AIMS OF PhD THESIS

The aims and main protocol steps of this PhD thesis which focus on the investigation of hybrid methods enabling the elimination of given organic dyes acting as organic micropollutants from water phase are as follows:

**[1]** Synthesis and characterization of various nanomaterials including graphene oxide nanoparticles and Egyptian Blue dye for the elimination of target micropollutants from different matrices. This step was necessary to obtain the proper quality of nanomaterials for artificial colorants elimination research.

**[2]** Elaboration of new simple analytical protocols based on direct colorimetry and/or microplanar chromatographic separation for the fast estimation and quantification of target chemicals during elimination studies.

**[3]** Investigation of molecular interactions between inorganic adsorbents and various biopolymers (cellulose in different forms, potato starch, nutrient agar, TLC cellulose, TLC polyamide, TLC silica gel 60 W, HPTLC silica gel RP-18W), nanoparticle additives (graphene oxide) and selected charged organic dyes ions using electroplanar separation protocols. Results of these studies enable the rapid and preliminary selection of further active matrices in ion form for elimination.

**[4]** Study of hybrid systems involving given biopolymers, nanomaterials and living organisms (β-cyclodextrin, pine pollen, dandelion pappus, microcrystalline cellulose, activated carbon, graphene oxide, Egyptian Blue, activated sludge and duckweed) based on different experimental setups (24 hours, 16 days) to study the elimination of selected dyes (Brilliant Blue, Sunset Yellow, Malachite Green, Ponceau 4R) from the water phase. This part of the PhD thesis was designed as a multiparameter experiment requiring the application of multivariate statistical calculations for data mining.

**[5]** Results of the main research enabled additional studies focusing on the application of coated cellulose with graphene oxide as an efficient adsorbent for analytical applications of micropollutants.

# 3. EXPERIMENTAL PART

## *3.1. General chemicals and reagents*

### 3.1.1. Organic solvents

Acetone, Sigma Aldrich 99.9% HPLC, Steinheim, Germany
Methanol: LiChrosolv 99.8% for LC, Merck, Darmstadt, Germany
Acetonitrile (LiChrosolv; 99.9%) Merck, Darmstadt, Germany
*n*-Hexane Fluka Chemika 95%, Buchs, Switzerland
Etanol 99.8%, bezwodny cz.d.a., Eurochem BGD, Tarnów, Poland
Ethanol 95% spożywczy rektyfikowany (Spirytus Kaliski, 95%), Kalisz, Poland
Binary organic/water chromatographic mobile phases were prepared using freshly distilled water.

### 3.1.2. Internal/external standards

Methyl Red, ACS reagent crystalline, Sigma Aldrich, Saint Louis, USA
7,8 Dimethoxyflavone, Sigma Aldrich, Saint Louis, USA
Chlorophyll standard from spinach, Sigma Aldrich, Saint Louis, USA

### 3.1.3. Studied dyes (target chemicals)

Sunset Yellow FCF, P.P.H. „Standard" sp. z o o., Lublin, Poland
Ponceu 4R, P.P.H. „ Standard" sp. z o.o, Lublin, Poland
Brilliant Blue, Roha Europe, Valencia,Spain
Malachite Green oxalate salt, Sigma Aldrich, Saint Louis, USA

### 3.1.4. Inclusion chemicals, biopolymers and nanoparticles

β-Cyclodextrin, 2127, K19365427/450/100g, Merck, Darmstadt, Germany
Cellulose microcrystalline, ~50 μm, Avicel, Sigma-Aldrich, Saint Louis , USA
Activated carbon Norit SA SUPER 94 001-6, Amersfoort, Netherlands
Egyptian Blue 1.1.1. and 1.1.1a. synthesized in TUK (Technical Universisty of Koszalin) laboratory

Graphene oxide, Lyophylized, previously synthesized in TUK laboratory using a modified Hummer's method.

### 3.1.5. Biological materials

**Pine pollen** was collected from pine trees in the Koszalin (Poland) area in May 2017. This material was air dried, sieved and stored in a sealed glass container until the experiment was performed.

**Dandelion pappus** was collected in the Koszalin (Poland) area in May 2020, air dried and stored in a glass container. For the purpose of these experiments the pappus feathers were separated from the dandelion seeds.

**Activated sludge** samples were collected from the Jamno Wastewater Treatment Plant (located within the Koszalin city area, Poland) and biomass samples were acquired from the activated sludge pumping station. In particular, excessively concentrated sludge was collected from the bottom of the secondary settling tank. This material was additionally centrifuged (using an MPW 350, Warszawa, Poland) for 10min. at 700rpm and appropriate volumes of this stock biomass was mixed with the remaining sample components for the 24 hours biodegradation experiment.

**Duckweed biomass** was collected in 2012 by PKZ (surface water ecosystem, Koszalin; N 54$^{o}$ 11.579' E016$^{o}$ 11.021'); This biomaterial was stored in a small aquarium (28 L; 20-26$^{o}$C; 14/24 h photoperiod; light source: 25 W incandescent light bulb). This container was regularly refilled with tap water and contained two to five small fish (*Ancistrus dolichopterus*) fed with common fish food.

### 3.1.6. Remaining chemicals and materials

Silicon dioxide, Brenntag, Essen, Germany
Sodium hydrogen carbonate, pure p.a., Chempur, Piekary Śląskie, Poland
Calcium carbonate, pure p.a., Chempur, Piekary Śląskie, Poland
Copper oxide, pure p.a., Chempur, Piekary Śląskie, Poland
Boric acid, cz.d.a., POCh, Gliwice, Poland
Paraffin wax, Chempur, Piekary Śląskie, Poland
Sulphuric acid (VI) 95% POCh Gliwice, Poland
Orthophosphoric acid 85%, Chempur, Piekary Śląskie, Poland

Potassium permanganate, POCh Gliwice, Poland

Hydrogen peroxide 30%, POCh Gliwice, Poland

Hydrochloric acid, 35 - 38%, POCh Gliwice, Poland

Formic Acid 85%, cz.d.a., Chempur, Piekary Śląskie, Poland

Filtrating paper, Polska Grupa Laboratoryjna Sp. z o.o., PGL, Warszawa, Poland

Office paper POL Jet 80, Sp.z o.o., Kwidzyn, Poland

Whatman chromatography paper, GE Healthcare UK Limited, Little Chalfont, UK, China

Thin Japanese paper for aircraft paper models, Distributed by www.modele.sklep. pl Warszawa, Poland

Thick Japanese paper for aircraft paper models, Distributed by www.modele.sklep. pl Warszawa, Poland

TLC cellulose without fluorescence indicator, glass-based pre-coated plates, Merck, Darmstadt, Germany

Potato starch (potato flour), Kupiec, Sp. z o.o., Krzymów, Poland

Nutrient agar, 451 and 1003 μm, Merck, Darmstadt, Germany

TLC polyamide 11 F254, glass-based pre-coated plates, Merck, Darmstadt, Germany

TLC silica gel 60 W F254 S, glass-based pre-coated plates, Merck, Darmstadt, Germany

TLC silica gel 60 RP-18 F254S, Merck, Darmstadt, Germany

HPTLC silica gel RP-18W, glass-based pre-coated plates, Merck, Darmstadt, Germany

TLC aluminum oxide 60 F254 type E, glass-based plates, Merck, Darmstadt, Germany

### 3.1.7. Equipment and research facility

Electron microscope SEM; JSM-5500LV, JEOL, Tokyo, Japan

Optical microscope Motic BA310 LED; equipped with a Moticam 3, 3.0 MP USB digital camera Group, Ltd., Xiamen, China

Canon EOS 1100D SLR Digital camera

Photo aquisition system consisting of a ring of 12 LED lamps (JDR, SMDHLCW-250; 3.5W; 6400 K; 250 Lumens, Sanico Electronics, Warszawa, Poland); Designed and manufactured by P.K.Z.

Scanner Microtek ScanMaker 4800 / MRS-1200T48U, Microtek International, Inc., USA

Zeta Potential Analyzer, ZetaPALS Brookhaven Instruments Corporation, Holtsville, NY, USA

Oven N 61/H 20 kW, Nabertherm GmbH, Lilienthal/Bremen, Germany

Oven Ecocell, BMT, Brno-Zábrdovice, Czech Republic

Retsch Ball Mill S100, Haan, Germany

Centrifuge MPW-350, MPW Med Instruments, Warszawa, Poland

Centrifuge MPW-53, MPW Med Instruments, Warszawa, Poland.

Ultrasonic washer Sonic - 1, Polsonic Sp. Zo.o., Warszawa, Poland

Magnetic stirrer MR – Hei - End, Heidolph, Schwabach, Germany

Refrigerated Vapor Traps RVT 4104, Thermo Electron Corporation, Asheville, NC, USA

Oil vacuum pump VLP80, Thermo Milford, MA, USA

Thermogravimetric analyzer NETZSCH TG 209F3, Selb, Germany

pH- meter Handylab pH11 Schott, SI Analytics GmbH, Mainz, Germany

High voltage power supply EV232 (0 – 3000 V, 0 – 150 mA, 0 – 150 W; Consort, Belgium

Multimeters for current MT-1210 Pro'sKit, Prokit's IndustriesCo. Ltd., China

Multimeters for data acquisition Appa 207, Appa TechnologyCorp., Taiwan

Radwag WAS 100/X, Radom, Poland

Laboratory shaker Laboshake Gerhardt GmbH 500, Königswinter, Germany

Thermostat Huber CC®-K6, Offenburg, Germany

Thermostat Julabo FP 51, Julabo Labortechnik GmbH, Seelbach, Germany

Temperature controlled micro-TLC chamber according to design provided by PKZ **[Zarzycki 2008]**

Horizontal electrophoresis chamber, Enduro E1010-10 Horizontal Gel Box, Labnet International, Inc. Completion, Warszawa, Poland

Dewar chambers (200 mL, approximately; 10 units), home-made open-air, invented and manufactured by PKZ

## *3.2. Separation protocols*

### 3.2.1. Electroplanar separation

Electroseparation experiments were conducted using a commercially available horizontal electrophoresis chamber (Enduro E1010-10 Horizontal Gel Box). Active layers were positioned inside an electrophoresis chamber using a homemade plastic support (**Figure 14**). The electroplanar separation system consisted of a separation

chamber unit connected to an adjustable power supply and two additional digital multimeters to monitor voltage and current. Dye samples were manually transferred to the separation layer (using a Hamilton syringe; 2.5 µL of methanolic solution containing 1.25 µg dye mass). In the case of 0.5 mm and 1.0 mm agar layers, 2.5 µL of dye sample was mixed with 5 µL or 10 µL, respectively, of running electrolyte. After electrophoretic separation, the wet strips were covered with a thin transparent film (top clear film) and immediately scanned.

This equipment was used in two modes, as a separation unit using commercially available layers or as a testing device for the electromigration of dyes in the presence of thin- layers modified with graphene oxide.

GO barriers were generated from raw (water suspended nanoparticles, directly after synthesis) and lyophilized graphene oxide (dry material reconstituted in distilled water). These nanoparticles were applied horizontally or along the edge of the stationary phase (parallel to the mobile phase development). As stationary phases, cellulose strips and commercially available glass based cellulose TLC plates were used.

### 3.2.2. Micro-thin-layer chromatography (micro-TLC) process

Micro-plate development was performed under temperature-controlled conditions using a removable unit working inside a liquid circulating metal oven designed and constructed by PKZ (**Figure 15**), **[Zarzycki 2008]**. The general protocol scheme for qualitative and quantitative measurements is presented in **Figure 16**. The developed chromatograms were acquired directly after the separation process and the plates were dried at room temperature using the photo acquisition system described in Chapter 3.5. For the determination of analytes, the reaction mixture or a properly prepared extract (2 x 1 µL sample) were directly loaded. The mobile phase development distance was 45 mm. For Brilliant Blue samples, the developing distance was shortened to 40 mm due to the migration of the target component close to the front of the mobile phase. This made it possible to quantify BB using the peak baseline reference. Additionally, external standards were simultaneously chromatographed: Methyl Red (100 ng/point); and 7.8 DMF (1000 ng/point) on a TLC plate. All chromatographic runs included 100% methanol as the mobile phase and HPTLC glass coated plates 60RP18WF254S, as the stationary phase. BB quantification was carried out at a temperature of 20°C **[Suszyński 2015]**, **[Ślączka 2017]**, **[Włodarczyk 2014]**.

## *3.3. Biological tests*

Experimental work using hybrid methods for micropollutant elimination was performed using two separate tests. General protocol sequences of 24 hours (**A**) and 16 days (**B**) tests are summarized in **Figure 17**.

### 3.3.1. Biodegradation test in conical glass (24 h)

This biodegradation test was performed using conical glass flasks (250 mL Erlenmeyer flasks) attached to a laboratory shaker with a shaking speed set at 150 rpm. The reaction mixtures consisted of freshly collected and concentrated activated sludge (concentration 1,5 g/L) as well as given additives including GO, activated carbon, cellulose, beta-cyclodextrin, pine pollen, dandelion pappus and two types of Egyptian Blue. Detailed experimental data are presented in **Figure 18**. After test completion all samples were filtrated through a cellulose filter (diameter 125 mm, hard type) and stored in a fridge at 5°C for further target component quantification.

### 3.3.2 Biological experiment in Dewar chambers (16 days test)

This biodegradation test was performed within thermostatic cylindrical glass containers (internal diameter = 40 mm, h = 230 mm) open to the air which were connected to an external circulating thermostat (**Figure 19** and **Figure 20**). The detailed protocol for this test was described in the scheme presented within **Figure 17B**. The Dewar chambers were illuminated with LED fluorescent lamps (LED Tube-SWS061W, diameter 0.26 mm, length 0.6 m, TempColor 2800 - 3000 K) with the photoperiod set as 10 h/24h. Reactors were filled with 200 mL of Brilliant Blue (BB) solution (deionized water; 5 mg/L), duckweed biomass (0.03g, approximately) and 200 mg/L of each of the following additives respectively: graphene oxide, activated carbon, β-cyclodextrin, cellulose, dandelion pappus, pollen, Egyptian Blue type 1.1.1. and Egyptian Blue type 1.1.1a.

## *3.4. Synthesis protocols*

### 3.4.1. Graphene oxide

This nanomaterial was prepared according to Hummers methodology **[Hummers 1958]** slightly modified according to the equipment available at the Technical University of Koszalin (TUK) laboratory **[Zarzycki 2020]**. The detailed protocol for GO synthesis and analysis are included in Chapter 4.1.

### 3.4.2. Egyptian Blue pigment

Synthesis of Egyptian blue was performed according to the Bologna method **[Mazzocchin 2004]**. The heating process was performed under specific conditions, which were found to be critical for final products Detailed protocol and obtained EB form analysis are included in Chapter 4.2.

## *3.5. Data acquisition, post-processing and computations*

An optical microscope view of the cellulose layers (for electrophoretic separations) was acquired using a Motic BA310 LED optical microscope equipped with a digital camera under side light visualization mode. Digital photos were acquired with Motic Image Plus 2.0 (Motic China Group Co., Ltd., 2007). Additionally, the dye pattern resulting from the electrophoresis experiments was acquired with an office scanner using MicroScan Wizard 5, version 5.812. Quantitative electromigration data, including point shifts and point cross-section profiles that were necessary to calculate the Resolution Ratio (Rs) values, were extracted from raw digital images using ImageJ software (v. 1.48 Wayne Rasband, National Institutes of Health, USA; **[www 7].**

For the electropherogram images presented in this PhD thesis, a global manual balance filter was applied to increase the contrast for the visual evaluation of the spots. It should be highlighted that all retention parameters were measured based on raw, unprocessed pictures.

Quantitative data from micro-TLC plates was extracted from raw digital images (acquired by a Canon EOS 1100D SLR digital camera and home lighting equipped with both UV and visible light sources) using ImageJ software, version 1.48 Wayne Rasband,

National Institutes of Health, USA; **[www 7].** The digital SLR camera was fitted with a Tamron 55 - 200 lens and a HAMA filter (UV 390/52 mm). Pictures were taken from a distance of 94.5 cm with the following setting (F16; 1/4s). The acquisition system included a ring of 12 LED lamps. Two glass plates coated with carbon black and magnesium oxide were used as black and white patterns. The picture acquisition system described above was designed and constructed by PKZ.

The quantitative data of the tested samples were analyzed using the PCA procedure *via* the XLSTAT XLSTAT-Pro/3DPlot statistical-visualization package (version 2008.2.01) provided by Addinsoft (Paris, France) and plotted with Microsoft Excel 2002. The adequacy of multivariate calculations for experimental data was assessed by performing the Bartlett sphericity test.

# 4. RESULTS AND DISCUSSION

The key part of the experimental work presented in this PhD dissertation was the proposal and testing of given nanomaterials as active substances enabling elimination of organic micropollutants from the water phase. Nanomaterials, even if they are available on the market are usually expensive (*e.g.* the cost of 1g of graphene oxide from the supplier, Sigma Aldrich, was about 200 Euro, in 2020). Moreover, due to nanoparticle stability problems, they must be extensively characterized before application as active substances. Therefore, in this work, detailed synthesis protocols and the results of product physicochemical analysis/characterization concerning graphene oxide and Egyptian Blue substances were described.

## *4.1. Graphene oxide synthesis and physicochemical characterization*

Graphene oxide nanoparticles were prepared according to the Hummers protocol **[Hummers 1958]**. This was justified by the high cost of GO material available on the market, as well as the uncertain composition and stability of given GO standards during storage time **[Chowdhury 2013, Yeh 2015, Wang 2020]**. In practice, graphene oxide can be relatively easily and inexpensively prepared by chemical exfoliation of raw graphite. This approach is attractive because it does not involve complex equipment or metal catalysts. For this reason, no further complex purification steps are needed. There are a number of approaches in the literature to describe the synthesis of GO, mainly based on the Hummers and Offeman protocols **[Hummers 1958]**.

Based on the literature search, the synthesis of graphene oxide was started using high-purity graphite powder. The synthesis protocol was combined in accordance with the studies published by: **[Hummers 1958]**, **[Marcano 2010]**, **[Panwar 2015]**, **[Yuan 2017]**, **[Zaaba 2017]**, **[Saleem 2018]**. Moreover, due to GO particle spatial variability, a number of various GO forms are possible. Therefore, the self-synthesis step allows for the production of one large batch of GO nanoparticles under controlled and reproducible conditions for further studies. In addition, the described process enables the acquisition of different forms of dry GO by modification by, for example, the drying process. This step has been found to be critical for GO nanoparticle form.

The synthesis procedure presented in this PhD manuscript was slightly modified according to the equipment available at the TUK laboratory **[Zarzycki 2020]**. All the key steps applied for GO preparation are summarized in **Figure 21**. The pictures included in this figure clearly show that this approach involved the most basic laboratory equipment possible. The reaction mixture changed color as bulk graphite material (**Figure 21 B**, step 1) was transformed into brown graphene oxide particles (**Figure 21 B**, step 8). Then, the water suspension of synthesized GO material (raw graphene oxide) was separated into two parts, which were dried using different methods namely using an air circulating oven (60ºC, 18 hours) and the lyophilisation procedure. In the lyophylisation procedure, the sample was frozen at a temperature of minus 100ºC and then the water was removed at room temperature inside a low-pressure chamber for 18 hours. All the details of the lyophilisation process and the equipment that was used for the dehydration of the raw GO water suspension are included in **Figure 22**. Using the above drying protocols, two different forms of graphene oxide were obtained. These materials are presented in the large scale and the magnified optical microscopy pictures presented in **Figure 23**. As can be seen, the water suspension sample which was dried under air circulating oven conditions, has resulted in a dark/brown solid material, whilst the lyophilized sample of GO was transformed into a light sponge-like substance. This material was very light with an estimated apparent density equal to 14 - 22 mg/mL.
A detailed view of the lyophilized GO under an optical microscope has been documented in **Figure 24**. It has been found that the lyophilized form of GO can easily be re-suspended in tap water. This material is fairly polar and can be spontaneously wetted and partially dispersed in tap or distilled water at room temperature, similar to polar starch particles (**Figure 25**).

Measured values of particle size and zeta potential parameters of lyophilized GO material reconstituted in water, as well as for active carbon particles (Norit SA Super) at a concentration of 0.2 mg/mL, are presented in **Table 5**. Taking into account data reported by **[Krishnamoorthy 2013]**, the observed value of zeta potential at a level of –20,6 mV for my graphene oxide particles (dispersed in a water environment characterized by a pH close to 3), confirms the possibility of the existence of a stable GO suspension. This is probably due to the presence of ionized carboxylic groups on the GO surface, resulting in electrostatic repulsive forces between individual particles which enabled the formation of a stable suspension. On the contrary, activated carbon

particles cannot form a stable suspension in water (the measured zeta potential value for these particles was around -13,3 mV).

Both forms of graphene oxide (after direct air drying and lyophilization) were inspected by scanning electron microscopy (SEM; (**Figure 26A**) and analyzed using energy X-ray dispersive spectroscopy (EDS; **Figure 26 B**, **C**). These measurements were also performed for different carbon particles, which were used as the reference materials, namely graphite (from which the GO was produced) and activated carbon (Norit SA Super). Additionally, Norit SA Super was used as an additive for micropollutant degradation studies. SEM data presented within **Figure 26A** clearly indicate that the surface of both air-dried and lyophilized GO samples have a similar pattern, however, lyophilized graphene oxide is much more porous and contains large scale structures.

EDS measurements have revealed that the graphite sample consists of pure carbon, whilst Norit SA Super contains several metal impurities. These elements were probably included in the vegetable raw material used for Norit SA Super production **[Świderska 2018]**. Both graphene oxide samples consisted of carbon and oxygen elements, however, in slightly different quantities. This may be a reason for the difference in the content of oxygen ligands for both materials. The recorded presence of sulfur atoms can be explained as an impurity that remained after GO synthesis where sulfuric acid was used as the reagent.

It has been observed that graphene oxide samples were unstable during storage time. Particularly, at room temperature and over a few months, both liquid and solid materials changed color from light to dark brown. This problem has been extensively investigated in separate studies and presented in graphical form within Figure 4 ***[S1]*** included in the reference **[Piaskowski 2020]**. Experimental data using the synthesized GO samples above in different forms have revealed that the 2D/G peak intensity ratio was less than 1, which suggest a multi-layered graphene structure of synthesized materials **[Shen 2013], [Khan 2017]**. GO samples may contain carbon atoms with different hybridization and/or partial exfoliation because of ID/G ratio values close to 0.8. Importantly, the observed decrease in ID/G value for samples measured during storage time may suggest reorganization of the GO layers. In addition, similar spectra shapes of 2D peaks of both air dried and lyophilized samples indicate that the number of layers in both materials are similar despite the different macroscopic views of these samples.

## *4.2. Synthesis and analysis of Egyptian Blue particles*

Synthesis of Egyptian blue was performed according to the Bologna method **[Mazzocchin 2004],** (**Figure 27 A**). In particular, this nanomaterial was prepared using sequential heating involving a ceramic oven (**Figure 27 B**). Reagent powder was placed inside the cold oven in normal air environment and the temperature was raised to 860°C. The heating time was 4 h and then the material was cooled inside the oven to room temperature (taking 19 h) (**Figure 27 C**). The overall heating time was 24 h (including 1h for temperature stabilization starting from room temperature to 860°C). Then, the cold sinter was ground in a ball mill (**Figure 27 D**) and the heating process was repeated using an oven temperature of 950ºC. Pigment dye samples (labeled as EB type 1.1.1. and EB type 1.1.1a.) were obtained using different spatial arrangements of the raw pigment produced at 860°C that was then re-heated at 950°C. It should be noted that EB 1.1.1. material was re-heated at 950°C directly on a fireclay brick base (**Figure 8 B**) whilst EB 1.1.1a. material was placed within a porcelain steamer (ID = 9 cm, approximately; **Figure 8 C**). After the heating and re-heating stages, all sintered materials were ground using a ball mill set at 450 rpm, for 2 x 15 min with rotation changes using two types of grinding balls (10 mm, 30 mm).

Results of physicochemical analysis using SEM, EDS, and FTIR presented in **Figure 28** confirm identity of synthesized dye and commercially available Egyptian Blue samples.

## *4.3. Optimization of electroplanar chromatography*

This part of the experimental work was necessary to establish proper electroseparation conditions for further interaction studies involving various dyes and graphene oxide nanoparticles. The proposed research involves a number of protocols concerning the selection of potential stationary phases and electrolytes that may work with the selected power source, voltage range and chamber/electroplanar layer spatial arrangement. For this step, a simple planar electrophoresis/ chromatography system for

the fast screening of different natural polymers applied as stationary phases enabling efficient separation of low molecular mass compounds, particularly dyes, was extensively investigated **[Lewandowska 2017]**. This simple system was found to be very useful for the fast evaluation of separation efficiency and chromatographic/electrophoretic properties of stationary phases, particularly cellulose-based strips and/or classical glass-based thin-layer chromatographic plates. The separation equipment utilized a simple open-air electrophoresis box with a homemade support for the positioning of active separation layers and electrode connection strips.

Electrophoresis involving cellulose layers was extensively developed in the 1950s and 1960s **[Kunkel 1951]**, **[Martin 1954]**, **[Brown 1955]**, **[Wunderly 1961]**. Recently, there has been an increasing interest in the application of cellulose-based materials in analytical chemistry since a number of discoveries concerning cellulose physicochemical properties, their chirality, and also their relationship to nanofibers and nanocrystal structures were reported **[Usov 2015]**, **[French 2014]**, **[Mu 2015]**. Due to such properties and general trends in the application of natural polymers for green analytical chemistry protocols, cellulose-based stationary phases are still manufactured, for planar and column chromatography and for both analytical and preparative applications **[Okamoto 1984]**, **[Astec Cellulose 2010]**. Cellulose-containing materials like printing or filtrating papers have been extensively investigated as the active supports for sensors, flexible electronics, and microfluidic devices (paper-based microfluidic devices; PADs) **[Lisowski 2013], [Lin 2014], [Kurra 2013]**.

The main goal of this research was to test a planar electrochromatographic system, which is as simple as possible and can be used as a fast separation tool for the analysis of colorants and their interactions with GO nanoparticles. The system investigated work under open-air conditions and involved a number of natural polymers (cellulose, starch, agar) and common TLC stationary phases (silica, octadecylsilica, polyamide, aluminum oxide). In particular, the initial data set generated, concerned critical parameters including active layer type, geometry, applied voltage, electrolyte composition, and pH. This may help the further design of hybrid separation devices involving natural polymeric layers.

As the first optimization step, pure cellulose layers (chromatographic and cellulose filtrating papers) and cellulose-based materials (office and various papers) as active stationary phases for electroplanar chromatography were tested. Moreover,

commercially available TLC plates were investigated including cellulose pre-coated plates and other TLC or HPTLC plates, as well as nutrient agar layers on glass support as the reference stationary phases. Detailed data of the active layers that were tested for separation of selected dyes (Methyl Red, Ponceau 4R) are listed in **Table 6**. In addition, two biopolymeric layers based on potato starch and nutrient agar were manufactured according to the protocol visualized in **Figure 29**.

Electroseparation experiments were conducted using a commercially available electrophoresis box, however, the active layers were placed on the top of a homemade plastic support. This was prepared to secure the proper electric current flow through the active layer, particularly for flexible cellulose strips (**Figure 14**). Experiments were performed under two strip arrangement modes: using 20 cm long active material (filtrating paper, office paper, and chromatographic paper (**Figure 14 A**) or 10 cm long active material placed on the glass support and connected to the anode/cathode jars with 6 cm long filtrating paper strips (**Figure 14 A**). In both systems, the effective length of the conducting layer from anode to cathode jar was 18 cm. Dye samples were introduced in the center of the active layer strip, and electroseparation conditions (current and voltage) were monitored using appropriate digital multimeters. Preliminary studies concerning the linearity of current *versus* the applied voltage (potential difference $\Delta V$ ranging from 100 V to 1000 V) were performed using a filtrating paper strip with a cross-section area = 2 $mm^2$ (20 mm × 0.1 mm). This strip was pre-soaked with working electrolyte as a conductive layer. This experiment revealed that, for typical electrolytes and buffers based on boric or formic acids, non-linear Ohm's Law plots were observed, starting from a potential difference of approximately 500 V (**Figure 30**). This can be explained by ohmic heating (Joule heating), as relatively high electric power was generated. For the electrolytes studied, the maximal values of power ($\Delta V$ = 1000 V) were ~0.43 W, 0.71 W, 1.67 W, and 2.24 W for electrolyte numbers I, II, III, and IV, respectively. Therefore, for further separation studies, a 500 V electric potential was applied along the strips, to avoid electrolyte heating and evaporation. Under such conditions, significantly lower power loss values were recorded: ~0.11 W, 0.16 W, 0.35 W, and 0.45 W for electrolyte numbers I, II, III, and IV, respectively.

As can be seen from the data presented within **Figure 31**, under these conditions ($\Delta V$ = 500 V), baseline separation of the dye pair on filtrating paper was observed using an electrolyte composed of 100 mM boric acid. Considering the low current value

observed on the Ohm's Law plot, this liquid was selected as the final running electrolyte for testing dye separation on different layers. Similar power loss values for a potential difference of 180 V had been reported previously for a system consisting of a 2 cm × 17 cm cellulose strip and a sodium bicarbonate water solution at a concentration of 35.7 mM (3 g/L and pH 9.1) applied as the working electrolyte **[Hyde 2015]**.

According to the data presented in **Table 6**, the investigated layers were characterized by different densities, internal structures and their thickness values, varied from 19 μm to 1003 μm, for layer No.4 (thick Japanese paper) and layer No.13 (nutrient agar layer). The stationary phase layers were also characterized by different degrees of electrolyte soaking due to the different cellulose or stationary phase particle size, shape, and overall density. **Figure 32** contains optical microscope pictures of the cellulose layers investigated. As can be seen, these materials are composed of long cellulose fibers (No.1 – 5; different papers) and cellulose microcrystalline powder (No.6; TLC pre - coated plate). Layer No.2 (office paper) combines cellulose fibers and additional components used for improving office paper characteristics for printing, while layers No.4 and No.5 (Japanese papers) present as a very low-density net of pure cellulose fibers. Therefore, the question was how the composition of the strip material may affect the electric current for the electric potential investigated ($\Delta V$ = 500 V). According to the graphs presented in (**Figure 33**), there is generally an increase in current value in relation to the increase in layer thickness. The relatively low value of the determination coefficient and slope coefficient of the calculated linear regression equation may indicate that the electric current can be limited by overall conductivity of the connection strips (filtrating paper; 2 $mm^2$ cross-section area) in comparison to nutrient agar layers No.12 and No.13, characterized by 9 $mm^2$ and 20 $mm^2$ cross-section areas respectively. The observed electric current variation can be also affected by whole stationary phase density and the electrolyte/stationary phase ratio, which was not fully controlled in such experiments. This is because only simple capillary force pre-soaking of active layers was performed.

The data presented in **Figure 34** summarize the results of dye electroseparation on all the active layers studied. It should be noted that, for this part of the experiment, the electroseparation run time was increased to 20 min, in comparison to the data presented in **Figure 31**. This was changed to achieve a sufficient dye migration distance for resolution parameter ($R_S$) calculation. It has been observed that there was

no electrophoretic shift of the tested dyes on polyamide TLC plate (No.8) and RP-18W coated HPTLC plate (No.10). In such case, both dyes were strongly adsorbed within the application point area. Similar behavior is observed for thin Japanese paper (No.4); however, in such case, a small shift of methyl red to the negatively charged electrode (cathode) was registered, probably due to the existing electroosmotic flow. Short migration of the dye to the positively charged electrode (anode), still without significant spot separation, was observed on various layers, especially: office paper (No.2), thick Japanese paper (No.5), and nutrient agar (1mm layer; No.13). Measurable separation was recorded on chromatographic paper (No.3), silica gel TLC (No.9), and aluminum oxide (No.11) TLC plates. In such cases, the methyl red spot remained within the application point area and ponceau 4R shifted to the anode. This resulted in the separation factor values $R_S$ = 0.54,0.61 and 0.78 (No.3, 11, and 9, respectively). Baseline spot separation was obtained on strips consisted of filtrating paper (No.1; $R_S$ = 1.07) and nutrient agar (0.5 mm layer; No.12; $R_S$ = 1.08), where both dyes moved to the anode from the application point. The best separation under the selected analytical conditions was observed for the starch layer on filtrating paper support (No.7; $R_S$ = 2.26) and cellulose pre-coated TLC plate (No.6; $R_S$ = 2.89). In both cases, almost no shift for Methyl Red was observed, while Ponceau 4R dye moved strongly to the positively charged electrode.

The investigations conducted have revealed substantial differences between the electrophoretic migrations of target dyes within cellulose type layers and also in comparison with the remaining stationary phases studied. On all stationary phases investigated, Ponceau 4R dye migrated faster to the positively charged electrode in comparison to Methyl Red for which no shift or slow migration to the anode was observed. This is in agreement with the chemical structure of the dyes investigated: Methyl Red contains less electrically charged functional groups than Ponceau 4R dye (one carboxylic and three sulfonic acid groups, respectively), which may result in multiple charged ions and stronger Ponceau 4R acceleration to the anode direction. Typically, electroseparation in the liquid phase is based on differences in the electrophoretic acceleration depending on the average charge of the analyte and its molecular weight and size. Due to the p$K_a$ values of Methyl Red (p$K_a$ = 5.1) **[The Merck Index 1976]** and Ponceau 4R (p$K_a$ = 11.19) **[Perez-Urquiza 2001]**, these molecules cannot be fully dissociated under the applied electrolyte conditions (pH = 4.3).

Nevertheless, it has been reported that the addition of organic liquids (*e.g.* alcohols) to the working electrolyte may significantly change the p$K_a$ values of dyes **[Srour 2008]**. It should be noted that Methyl Red color may change from red at pH below 4.2, to yellow above pH = 6.2, and orange between these two pH values **[The Merck Index 1976]**. According to the observed color changes of Methyl Red spots on the wet electrophoretic strips, from orange (*e.g.* cellulose plate No.1) to yellow (*e.g.* neutral aluminum oxide TLC type E – neutral or nutrient agar No.12), it can be hypothesized that the stationary phase may also significantly change the local pH of the running electrolyte. This may result in, for example, high electrophoretic mobility of Ponceau 4R on starch (No.7) and the microcrystalline cellulose pre-coated TLC plate (No.6). Therefore, this effect can improve or degrade dye separation on a selected stationary phase. On the other hand, the significant difference in the migration and separation of dyes on 0.5 mm and 1 mm agar layers is probably due to the high resistance of the connection strips (cross-section area 2 $mm^2$) resulting in similar electric current flow for both thin and thick agar layers (with 9 $mm^2$ and 20 $mm^2$ cross-section areas, respectively). In such case, a small dye shift can be observed for thick agar layers.

## *4.4. Interaction studies between graphene oxide nanoparticles and target dyes involving electroplanar chromatography*

### 4.4.1. Electromigration experiments

In this part of the research, the electroseparation equipment described above was used to test the viability of graphene oxide materials as a stationary phase component. This concept was based on the consideration of the physicochemical properties of GO. The high polarity of these nanoparticles and fairly complex surface composition containing oxygen functional groups enable dispersion in water or water-based electrolytes. This structure and physicochemical property suggest normal phase (NP) retention/electromigration mechanism. These ligands should interact with target analytes and therefore, affect their retention/electromigration behavior. The result of this experiment gives the possibility of understanding the basic interaction mechanisms between target analytes and the active matrix as well as the fast selection of separation conditions for micropollutants that may be isolated by graphene oxide matrices. This experiment proposal could result in an initial data set enabling the design of further technological processes of micropollutant purification involving GO nanoparticles **[Zarzycki 2020a]**.

The first approach to this problem was simply to cover the cellulose strips with a raw graphene oxide suspension in water and to dry off the resulting layer at a temperature of 60ºC for 24 hours (**Figure 35**). The graphene oxide sample for this experiment was the same as obtained in step 9 of the preparation protocol of GO described within **Figure 21**. As can be seen from the photos presented in **Figure 36A**, the surfaces of cellulose fibers are homogeneously covered by a thin layer of GO particles. More importantly, this carbon material does not fill the space between individual cellulose fibers. The same structure of the GO layer on cellulose fibers was observed under SEM imaging (**Figure 36B**). Based on this observation, it can be assumed that the movement of electrolyte and target analytes through a GO covered cellulose strip should be possible, similar to the original cellulose material. Results of the electromigration experiment using cellulose coated with GO are presented in **Figure 37**. As a target analyte, sunset yellow was applied. This colorant was found to have relatively high electroplanar migration measured under the plain cellulose stationary phase and boric acid electrolyte conditions that were tested in Chapter 4.3.1. The Sunset Yellow spot

was also characterized by no-tailing, which is an important feature due to the relatively low separation efficiency of the electrochromatographic system investigated (**Figure 37 1A**, **1B**). Interestingly, electromigration of the tested dye from start line was not observed in the case of GO covered cellulose strips (**Figure 37 2A**, **2B**).

To investigate this unexpected behavior of the analyte, different cellulose strip arrangements were prepared: (**i**) with a thin horizontal barrier of graphene oxide (**Figure 37 3A**, **3B**) and (**ii**) a reference strip with a horizontally positioned wall containing plain carbon in the form of graphene powder (**Figure 37 4A**, **4B**). This experiment clearly demonstrates that GO nanoparticles may act as an efficient barrier for sunset yellow electromigration. Under such conditions, the dye molecules tested cannot penetrate the barrier as it is visible to the graphite wall, but concentrates in front of the GO wall.

In subsequent experiments, commercially available TLC plates coated with cellulose stationary phase were tested. This surface was manually coated with a suspension of raw GO (as described above) and lyophilized GO reconstituted in distilled water. Cross-sections of the cellulose-coated chromatographic plates presented in **Figure 38** clearly indicate that carbon materials may penetrate the 100 μm thick stationary phase, however, there are some areas that carbon particles did not penetrate. Interestingly, even such a non-homogenous barrier was able to significantly change the migration distance of the dyes tested through the plate. This is demonstrated on electrochromatographic plate scans obtained using two testing dyes: Sunset Yellow and Ponceau 4R (**Figure 39**). As can be seen, there is a slightly different migration effect observed for the barriers generated from raw and lyophilized GO. Notably, the target analytes may form dense spots close to the GO barrier, indicating that separation efficiency can be significantly improved in such conditions.

The electropherograms in **Figure 40** clearly indicate that graphene oxide may work as an efficient barrier for different testing dye sets: Brilliant Blue and Ponceau 4R. In such case, the resolution of this process is deteriorating: $R_s$ value decreases in comparison to the experiment without the GO barrier (graphs A1 and A2 in **Figure 40**). However, it should be noted that overall separation efficiency increases since both spots located close to the barrier are narrow (graphs B1 and B2 in **Figure 40**), indicating that separation performance increased. In this case, the selectivity parameter ($\alpha$) value is still relatively high and was estimated as 2.21. The presented phenomenon can be applied for the efficient two-dimensional analysis of various target compounds by

forming different barriers as visualized in **Figure 41**. In this case, the electromigration direction of Ponceau 4R was modified by the repulsion effect from the horizontal wall printed parallel to the electromigration flow direction. This spatial arrangement was proposed by Prof. Jorge Pereira during experiment consultations based on cooperation with the University of Coimbra through the Erasmus program. It is hoped that such phenomenon, which to my knowledge had not been described previously, can be used for the design of selective barriers/membranes for the removal of micropollutants from wastewater or in portable microfluidic devices for the analysis of low molecular mass compounds using a thin-layer analytical approach.

### 4.4.2. Adsorption experiments based on results from electromigration studies

The unexpected phenomenon of dye immobilization on various cellulose stationary phases modified with graphene oxide reported in the experiments described above, resulted in the elaboration of an additional experimental setup concerning the adsorption of low-molecular mass compounds. This experiment is not directly associated with the main goals of this PhD thesis, but seems to be a good example of a side effect of the research conducted. In particular, cellulose strips coated with GO nanoparticles created according to the protocol visualized in **Figure 35** were folded and placed in the extraction devices presented in **Figure 42**. This experiment was an extension of different investigations described in detail in the PhD project of Fenert **[Fenert 2021]**, where raw cellulose, cellulose modified with *n*-alkanes and dandelion pappus were tested for analytical applications. These biopolymers were tested as adsorption matrices enabling the selective extraction of micropollutants and biomarkers, mainly chlorophylls, in surface water from lakes and the Baltic Sea. As an extension of this experiment, cellulose strips covered with GO were tested. This was performed during a research trip on the Baltic Sea in 2020 ***[S2]***, ***[S3]***. Results of studies concerning raw cellulose, cellulose modified with *n*-alkanes and dandelion pappus were described in the PhD thesis **[Fenert 2021]**. Data obtained from cellulose modified with GO were presented in book chapter **[Zarzycki 2022]**. Particularly, it has been revealed that cellulose modified with graphene oxide may adsorb different chlorophyll molecules in comparison with plain cellulose and dandelion pappus biomaterial. This can be clearly seen from the microchromatograms presented in **Figure 43**. The selectivity of cellulose with GO and dandelion pappus against chlorophyll dyes is also different. Additionally, dandelion pappus seems to be more effective in terms of the quantity of chlorophylls adsorbed (higher peaks on microchromatograms).

Therefore, for further analytical studies, dandelion pappus coated with graphene oxide should be tested. Moreover, both cellulose and dandelion pappus coated with GO biomatrices may be also considered for future research concerning the application of such biomaterials for the purification of micropollutants from sewage and during the technological processes of water purification.

## *4.5. Application of a hybrid system for elimination studies of selected dyes (24 h and 16 days multivariate statistical experiments) in the presence of inorganic and organic additives and duckweed plant*

### 4.5.1. General problem overview and experiment concepts

In this part, examination of various solid materials that may interact with selected low - molecular mass compounds and enable elimination of such molecules from liquid phase has been proposed. In particular, three different dyes were initially selected (Malachite Green, Brilliant Blue and Ponceau 4R) as micropollutants and their solutions combined with selected solids were tested. The testing protocol applied was described in **Figures 18** and adapted for the reported study according to literature data **[Piaskowski 2020]**. This simple and low-chemical consumption protocol enabled fast estimation of the quantity change of target components during the duration of the experiment.

As the first screening approach, samples after a 24 h adsorption period were photographed. As can be seen from the photographs presented in **Figure 44,** the selected proposed biomaterial (dandelion pappus) can be effective and selective for the adsorption of Malachite Green dye in comparison to Ponceau 4R and Brilliant Blue. The next photographs of experiments performed may also result in qualitative and/or semi-quantitative information about dye levels in solution since the target chemicals are colored and may be easy photographed. The results of these investigations are included in **Figures 45 - 47** for Malachite Green, Brilliant Blue and Ponceau 4R, respectively. The digital data related to the densitograms presented in the above-mentioned figures are listed in **Tables 7 - 9**, where data from the raw RGB and the extracted red channel were presented. There are several important observations that are clearly visible from such data:

[***i***] in all cases activated carbon eliminates the entire quantity of all dyes investigated from solution (up to the detection limit of the pictures acquired),

[***ii***] the selected additives can act selectively for the elimination of selected dyes from solution,

[***iii***] with the exception of activated carbon and graphene oxide, Brilliant Blue seems to be resistant to elimination under experimental conditions,

[***iv***] the cellulose material that was used for solution filtration after the test may affect quantification results (by simply acting as an adsorbent), this is strongly visible for Malachite Green **Figure 45** - vials No.1 and No.2,

[***v***] there are significant differences in interactions between Malachite green and Ponceau 4R in the case of vials from No.5 to No.10. These contain cellulose/biopolymer materials and Egyptian Blue additives. Confirmation of the strong interaction/adsorption of these dyes by biopolymers was presented in **Figure 44**, where dandelion pappus samples were colored by dyes from solution.

Considering the experimental data described above, it is clear to see that Brilliant Blue is the dye which is the most resistant to removal from the water phase in comparison to the remaining colorants. As mentioned in Chapter 1.3, it has been documented that this chemical is difficult to eliminate from the water environment. Based on these reasons, the main focus of the next piece of research was Brilliant Blue. In particular, the intention was to find new conditions for the elimination of such a resistant micropollutant. This may give ideas for future research involving hybrid elimination methods of resistant micropollutants.

In the case of the full quantitative analysis of Brilliant Blue that was performed using separation science protocol (micro-TLC), there is an additional problem related to the high polarity of this chemical. In particular, this analyte is strongly adsorbed by the chromatographic stationary phase (in planar chromatography, the analyte spot is adsorbed on the plate start line) or migrates with the solvent front, depending on the mobile phase/stationary phase properties (reversed or normal phase systems). It has been found that BB migration between these states (on the start line or close to the mobile phase front) results in broad and tailing spots that are inconvenient for quantitative analysis. For quantification purposes, the micro-plate mobile/stationary phase system where BB can migrate with the mobile phase front (the analyte is not retarded by the stationary phase) was selected. This is due to the presence of solid nanoparticle additives in raw samples that are also difficult to remove by centrifugation.

Such effect was obtained using 100% methanol as the mobile phase, which additionally simplified the proposed quantification system. The total migration distance of the analyte (BB) was 40 mm. The device and sample arrangement picture, as well as all key quantification steps, are visualized in **Figure 48**. According to this protocol, basic validation data for Methyl Red (applied as retention standard; *n* = 20) measured as peak intensity (PI; peak heights of green channel; 8 Bits resolution) and peak area (PA; number of pixels above baseline) resulted in an average PI = 185 ± 37 (relative standard deviation RSD = 5.07%) and a PA = 3946 ± 772 (relative standard deviation RSD = 5.11%). It should be noted that, using the proposed microanalytical device setup, up to five BB samples can be analyzed together with three points for the calibration line and one lane for the retention control standard (Methyl Red).

The quantitative experimental work proposed in this chapter involved a number of various nanomaterials/biopolymers, which were used in two different experimental modes involving real activated sludge microorganisms (24 h experiment; partial results based on the semi-quantitative approach were described above) and duckweed plant (16-day experiment). Detailed protocols concerning both experiments are described in **Figures 17 - 20**. A general view of the target component (Brilliant Blue) and additives investigated are present in **Figure 49**. Selection of these materials was proposed due to: (***i***) the expected different mechanisms that may occur during interaction with BB and active biomass (activated sludge and duckweed) and (***ii***) the presence of large quantities of the selected biomaterials in various ecosystems (pine tree pollen, duckweed plant or dandelion pappus biomass (**Figure 6**, **Figure 10**, and **Figure 7**, respectively).

Physicochemical analysis revealed that Brilliant Blue molecules are negatively charged (Zeta potential around -2 mV) in water solutions at pH = 5 - 6. Generally, the adsorption process occurs as a result of electrostatic attraction of ligands or the interaction of intermolecular forces between the non-polar fragments of dye and the adsorbent. This process depends on the nature of the adsorbent surface and can be characterized *e.g*. by electrokinetic potential **[Świderska 2004]**. The following possible mechanisms which can increase BB elimination from the water phase, mainly involving biodegradation, adsorption, or inclusion complexes formation include:

**(a)** activated carbon (AC)- Norit SA Super is a common adsorption base that is very efficient but predominantly not selective. The AC selected in this experiment is characterized by a particle size of 15 μm ($D_{50}$) and high surface area. This material is produced by steam activation resulting in a total surface area of 1150 $m^2$/g (BET). It has been found that the surface charge of activated carbon may be negative in a wide range of pH values ranging from 3.5 to 9.5. This allows for the efficient electrostatic attraction of target molecules that particularly consist of cationic ligands; however, different molecules can also be efficiently adsorbed on AC due to *e.g.*, dispersion forces **[Biswas 2016], [ Chang 2016], [Maddigpu 2018]**, **[Świderska 2018].**

**(b)** lyophilized graphene oxide (GO) may form individual nanoparticles and their conglomerates in water solution but is chemically and structurally non-homogenic. The physicochemical properties of GO may vary depending on the synthesis type and the drying methodology of the raw product. as well as storage time and conditions (temperature, oxygen contents, UV - Vis light exposition) **[Zarzycki 2020b]**. It has been documented that GO additive may significantly change the biological activity of activated sludge microorganisms **[Piaskowski 2020]**. Graphene oxide seems to be a promising material to develop new hybrid nanocomposites from, involving natural polysaccharides for the removal of dyes from wastewater **[Saya 2021]**. In this experiment, both direct interaction of BB with GO and the effects of GO on activated sludge microorganisms can be expected.

**(c)** β-cyclodextrin (CD) belongs to a chemical group called macrocyclic oligosaccharides. In polar solutions like water, this molecule may form stable inclusion complexes (host-guest interactions) and therefore native or derivatized cyclodextrins have a number of practical applications in pharmacy, food chemistry, and analytical chemistry. They may act as selective removal agents for micropollutants from wastewater **[Crini 2005]**, **[Armin 2014]**.

**(d)** raw dandelion pappus (DP); this organic structure is based on a cellulose biopolymer. This structure contains a number of different organic substances changing pappus surface polarity, *e.g.*, waxes. In this PhD project, a dandelion

pappus was used as a reaction mixture additive for dye elimination studies. In this case, direct adsorption of the target dye on pappus biomass, and its direct effect on the growth of activated sludge microorganisms can be expected. This may be due to an increase in the adsorption capacity, particularly the adsorption of small microorganism particles on the pappus lamels from the reaction mixture.

**(e)** microcrystalline cellulose (MC); this biopolymer, based on glucose monomers, is complex at any scale. It contains both crystalline and amorphous zones and may adsorb both polar as well as non-polar target chemicals from the water phase. It is commonly used in separation science due to the fact that it may work both in normal phase and reversed phase mode **[Włodarczyk 2017]**, **[Grumezescu 2016]**. In the proposed experiment MC should act similarly to the DP modifier.

**(f)** raw pine pollen (PP); This multicompartment biological microstructure can be locally present in the natural environment in large quantities. Pollen wall membranes contain highly resistant polymers like sporopollenin. Pollen can also be used as natural microcapsulation particles after isolation of clean sporopollenin exine capsules **[Li 2016a]**, **[Prabhakar 2017]**. In this experiment, multiple mechanisms can be expected in the presence of pollen in the reaction mixture, including physical and chemical adsorption as well as having an effect on activated sludge microorganisms. This material is a most complex additive as can be seen from the thermogravimetric analysis (TGA) graphs presented in **Figure 50**.

**(g)** Egyptian Blue mineral pigments (EB 1.1.1. and EB 1.1.1a.). This material can be relatively easily produced in different forms in the laboratory as described in Chapter 4.2. In the case of this experiment, interaction of EB nanoparticles containing copper ions with both Brilliant Blue and activated sludge microorganisms may be expected **[FitzHugh 1997/2012]**, **[Bianchetti 2000]**, **[Mozzocchini 2004]**, **[Errington 2016]**, **[Panagopoulou 2016]**.

### 4.5.2. Multivariate data analysis and discussion of experiment results

The data shows (**Table 10**) that the additives differ with regard to geometry, particle size and physicochemical properties which are collectively presented as their Zeta potential. The Zeta potential for each of these additives gives us a negative surface charge. In addition, some of them may have specific chemical and physicochemical structures notably activated carbon, cyclodextrin and graphene oxide. Each additive was the subject of experiments to evaluate their efficacy in promoting the removal of Brilliant Blue (BB) from water, the additives were utilized directly or indirectly in the experiments, the duration of which were either 24 hours or 16 days. The results of these experiments were analyzed using various chemometric exploratory tools, namely FA, PCA and AHC computations.

The results of the quantitative analysis are shown in **Tables 11** and **12**. The active carbon additive totally removed BB in the relatively short time of two hours confirming previous experiments **[Świderska 2018],** so results for this additive were not further evaluated. Factor score plots to show the principal component analysis are given in **Figure 51**, this data gave the results of the 16-hour procedures using parallel reaction mixtures with and without activated sludge organisms. They show that there is no discrimination between the types of additions to activated sludge (objects 1-7) and non-activated sludge (objects 8-14). In addition, all objects populate the F1/F2 factor space with random distribution suggesting that the experiment time needs to be prolonged in order to register real concentration changes. However, when the procedure was repeated using a 24-hour jar test using wastewater instead of BB molecules, significant changes were observed in the physicochemical properties of both the activated sludge and the processed wastewater. These results show that carbon-based materials, in particular various forms of graphene oxide, may greatly enhance the processing of wastewater in the presence of activated sludge micro-organisms. The results also show that Brilliant Blue molecules are highly resistant to short term biodegradation in the presence of the additives selected. From this it may be posited that an electrostatic interaction between ligands and the adsorbent surface may result in the effective adsorption of BB molecules.

It should be noted that under similar experimental setup (24 hours test) where wastewater instead of Brilliant Blue additive was exposed to carbon materials, major

changes were observed in given physicochemical parameters (SSV30, SVI, CST, pH, conductivity and total nitrogen concentration) of both: activated sludge and processed wastewater **[Piaskowski 2020]**. Current experiment confirmed that GO may change wastewater purification, especially, if activated sludge microorganisms are presented. However, Brilliant Blue dye is resistant for fast biodegradation, in spite of various additives, which were present in reaction mixture. Therefore it may be concluded that effective elimination of BB from water phase can be related to electrostatic interaction between active chemical centers (ligands) and the adsorbent surface.

According to their Zeta Potential, the additives presented in **Table 10** have a negatively charged surface in water solutions. In the case where the two surfaces, the adsorbate and the adsorbent, have uniform charges, multivalent cation bridging may an explanation for the adsorption process **[Świderska 2004]**. Conversely a BB molecule may be either neutral or may dissociate to mono- or bi- valent anions dependent on the pH of the mixture. These experiments were carried out in mixtures ranging from pH neutral to pH3 (graphene oxide additive). In these circumstances BB was not able to be adsorbed onto the additives used but the situation is more complex because it did adsorb well onto negatively-charged activated carbon.

The factor scores plot derived from PCA analysis of the data matrix produced from the 16-day experiment is presented in **Figure 52**. These calculations show that there is one dominating factor (F1) driving the experiment and this factor accounts for 74% of total variability. This was further confirmed by Factor Analysis (FA) calculations, notably the Scree Plot analysis (eigenvalues for F1 = 4.241 for F2 = 0.455; cumulative: F1 = 70.7 and F1 + F2 = 78.3 – the relevant graphs are presented in (S4)). So, by studying the object grouping along the F1 axis, it is apparent that sample 4 (containing β-cyclodextrin additive) is separated from the other objects. Referring to the quantitative data presented in **Table 12**, it can be seen that a systematic reduction in the concentration of BB was registered in this mixture. Data analysis, completed using Agglomerative Hierarchical Clustering (AHC), presented in the form of a dendogram, also evidenced the same clustering effect, i.e. that the β-CD reaction mixture clusters separately. By analyzing the PCA and AHC graphs and considering the possible mechanisms of BB interactions with the selected additives, it indicates that inclusion complex formation may provide an alternative method of BB micropollutant removal from the water phase.

Furthermore, graphene oxide, microcrystalline cellulose, duckweed, pine pollen, and a particular form of Egyptian Blue pigment (EB 1.1.1.) additives appear to have an effect on the elimination of BB removal according to the multivariate analysis results from PCA and AHC object grouping. However, further long-term experiments need to be performed involving wider ranges of BB concentration and the selected additives as well as temperature and pH. Additionally, a range of different target dyes should be processed as references in future studies.

# 5. CONCLUSIONS

This PhD manuscript contains new concepts focusing on experimental protocols and proposes new materials for hybrid methods allowing for the elimination of low-molecular-mass organic micropollutants from the water phase. In particular, the experimental work conducted was preceded by extensive literature research resulting in general procedures for nanomaterial synthesis and analysis, as well as experimental setups for micropollutant elimination studies based on multivariate analysis.

Elimination of organic micropollutants from the water phase and sewage is one of the more challenging problems of modern environmental engineering. Literature research focusing on this issue was summarized and discussed in the introduction to this PhD dissertation. It has been well documented that micropollutants have a strong negative impact on animal and human populations. This is the main reason why authorities from many countries around the world are trying to deal with this problem. Of note, the European Union has introduced a number of regulations in attempts to address this problem e.g. Directive 2000/60 EC. Based on such regulations, a number of micropollutants were indicated for permanent monitoring.

The data presented clearly indicate that there is no one efficient solution for micropollutant removal. This is because of the great diversity of target molecules in terms of their polarity and chemical structure, as well as their wide range of concentrations in the water phase. In addition, the parent molecules may transform into more toxic derivatives during the purification processes. It should be noted that classic technological processes for sewage purification may even generate a number of micropollutants, which can then be released to surface water ecosystems. For these reasons, the hybrid approach is indicated as a possible solution for micropollutant removal, especially using microfluidic technologies.

There are number of active materials that may be used concurrently during technological processes in treatment plants. They may work in complex ways using different phenomena *e.g.* oxidation, inclusion, adsorption or biodegradation. In recent years, two main approaches for active materials have been highlighted: the use of recycled biomaterials (*e.g.* fruit peels) and the application of nanocomposites involving *e.g.* carbon nanoparticles or supramolecular complexes involving macrocyclic compounds.

Colorants are common chemicals in a number of global industries which produce textiles, food products, cosmetics and pharmaceuticals as well as printer inks, leather and plastics. These substances can act as micropollutants or may generate toxic derivatives. Therefore, organic dyes namely Brilliant Blue, Malachite Green, Sunset Yellow and Ponceau 4R, were the target substances selected in this PhD thesis and extensive literature research on these colorants was performed.

The key part of the experimental work presented in this PhD dissertation was the proposal and testing of several nanomaterials/biopolymers as active substances enabling the elimination of organic micropollutants from the water phase. As new materials, pine pollen and dandelion pappus, biological structures containing biopolymers (cellulose, sporopollenin) were tested. As a reference, activated carbon was investigated as well as other different materials including β-cyclodextrin and microcrystalline cellulose. Moreover, graphene oxide and Egyptian Blue were produced. Successful synthesis and physicochemical characterization of Graphene Oxide and Egyptian Blue nanomaterials were performed. Graphene Oxide synthesis involved Hummers methodology adapted to the equipment available at TUK. Physicochemical analysis (SEM, EDS, Raman spectra) of the GO nanoparticles obtained, confirmed the high purity of such material but also the possible deterioration of its structure during storage. Moreover, the proposed drying step involving lyophilisation resulted in the creation of a specific form of GO that can easily be dispersed in the water phase, which property, to the best of the Author's knowledge, had not been described before. Egyptian Blue pigment was produced using Bologna methodology and this material was found to be identical to commercially available EB standard in respect of visual inspection, SEM, EDS and FTIR spectra. Testing of the above listed and additional nanomaterials, as well as biopolymers, was conducted by a number of experimental protocols including separation science technology and biological experiments also involving duckweed water organisms.

Separation science protocols were used for the fast screening and investigation of interactions between nanoparticles and target micropollutants. It has been demonstrated that the proposed electroplanar separation system can be used for the selection of active layer materials. Experimental data has revealed substantial differences between the electrophoretic migration of target dyes (in ion form) within cellulose type layers and also in comparison to the remaining stationary phases studied.

The obtained results, especially the recorded values of physicochemical parameters (the observed electric currents, migration distances, peak resolution for different electrolytes, layer type, and thickness), create a data set platform that may help in the further design of simple separation devices involving various active layers, particularly, modified with various nanoparticles. It is hoped that the described analytical protocol can be implemented for microfluidic paper based analytical devices (μPADs) enabling fast and non-expensive separation of complex samples and the generation of data for interactions of micropollutants with various adsorbents. This will also enable the selection of initial conditions for micropollutant removal experiments in the presence of graphene oxide nanoparticles. The experiments and data included in Chapter 4.4 have revealed that graphene oxide may generate a selective barrier, decreasing the migration of selected organic dyes in the water phase. The observed phenomena of decreased migration of dyes and the concentration of spots in the presence of a GO barrier may be predominantly caused by electrostatic interactions between polar dyes, consisting of negatively charged ligands, and negatively charged functional groups at the surface of GO particles. It is hoped that the described phenomena can be implemented for various microextraction bars and microfluidic paper-based analytical devices (μPADs), as well as being used for designing new filtrating materials that can be used for wastewater treatment and the purification of low-molecular mass micropollutants. This was proved by the application of GO coating to cellulose strips, which were used as selective adsorption matrices for chlorophyll and micropollutant extraction from surface water ecosystems. Such experiments were conducted during a research expedition on the Baltic Sea. The phenomenon described concerning the scientific experiments surrounding separation had, to the Author's knowledge, not been described in literature before.

Testing of a number of active materials including active carbon, lyophilized graphene oxide, β-cyclodextrin, raw dandelion pappus, microcrystalline cellulose, raw pine pollen, Egyptian Blue mineral pigment (1.1.1. and 1.1.1a.) was the main part of this PhD thesis. These materials were investigated as hybrid matrices for the potential elimination of the selected dye micropollutants *via* different and complementary mechanisms (adsorption, inclusion, biosorption, catalysis). Using these active additives, two experiments were proposed and performed as multivariate procedures in different modes (24 hours and 16 days). It should be noted that the experiment based

on a 16 days period involved duckweed organisms. From these experiments, quantitative data were generated using an optimized microfluidic device, namely a micro-TLC system, and the results were discussed using a multivariate statistic approach. The proposed quantification approach enabled direct determination of the target component without sample pre-treatment like pre-concentration or pre-purification. Within a single analytical run calibration line, retention standard spots (Methyl Red) and multiple samples were analyzed simultaneously. Noteworthily, target colorant pre-selection was performed using the simple colorimetric test that was described in Chapter 4.5.1. Based on these results, Brilliant Blue as the most stable molecule was selected for further research. Due to the multivariate nature of the proposed experiments, quantitative data were explored with chemometric tools including AHC (agglomerative hierarchical clustering), PCA (principal component analysis), and FA (factor analysis). Experimental data and multivariate calculations revealed that BB is strongly resistant to biodegradation. However, inclusion complexes formed with β - cyclodextrin may induce degradation of this dye in the presence of duckweed. Careful analysis of both PCA and AHC graphs, and consideration of the possible mechanisms of Brilliant Blue interactions with the given additives, may strongly indicate that inclusion complex formations can be an alternative way to remove BB molecules acting as micropollutants from the water phase. Moreover, multivariate data analysis resulting from PCA and AHC object grouping may suggest a potential effect of the given additive on BB elimination, particularly graphene oxide, microcrystalline cellulose, duckweed, pine pollen and Egyptian Blue pigment.

However, this must be confirmed by performing different long-term experiments involving a wide concentration range of BB, and the given additives, as well as different temperatures and pH. Moreover, to explain the potential mechanisms of BB elimination, a number of different target dyes should be processed as references. It is hoped that the results of the experimental work performed can be used in the design of future experiments for the fast screening of different additives and the improvement of technological processes, focusing on the purification of sewage and water from micropollutant.

# 6.TABLES

**Table 1.** Environmental Quality Standards (EQS) (in µg/L) for priority substances and certain other pollutants established on Annex I and II of Directive 2008/105/EC and that replaced Annex X of Water Frame Work Directive.

| No | Name of substances | CAS Number | AA-EQS inland surface waters | AA-EQS other surface waters | MAC-EQS inland surface waters | MAC-EQS other surface waters |
|---|---|---|---|---|---|---|
| 1 | Alachlor | 15972-60-8 | 0.3 | 0.3 | 0.7 | 0.7 |
| 2 | Antrachene | 120-12-7 | 0.1 | 0.1 | 0.4 | 0.4 |
| 3 | Atrazine | 1912-24-9 | 0.6 | 0.6 | 2.0 | 2.0 |
| 4 | Benzene | 71-43-2 | 10 | 8 | 50 | 50 |
| 5 | Brominated diphenylether | 32534-81-9 | 0.0005 | 0.0002 | na | na |
| 6 | Cadmium and its compounds | 7440-43-9 | ≤ 0.08<br>0.08<br>0.09<br>0.15<br>0.25 | 0.2 | ≤ 0.45<br>0.45<br>0.6<br>0.9<br>1.5 | ≤ 0.45<br>0.45<br>0.6<br>0.9<br>1.5 |

| | | | | | | |
|---|---|---|---|---|---|---|
| 6a | Carbon tetracloride | 56-23-5 | 12 | 12 | na | na |
| 7 | C10-C13-chloroalkanes | 85535-84-8 | 0.4 | 0.4 | 1.4 | 1.4 |
| 8 | Chlorfenvinphos | 470-90-6 | 0.1 | 0.1 | 0.3 | 0.3 |
| 9 | Chlorpyriphos-ethyl | 2921-88-2 | 0.03 | 0.03 | 0.1 | 0.1 |
| 9a | Cyclodiene pesticides:<br>Aldrin<br>Dieldrin<br>Endrin<br>Isodrin | <br>309-00-2<br>60-57-1<br>72-20-8<br>465-73-6 | 0.01 | Σ= 0.005 | na | na |
| 9b | Total DDT/p,p-DDT | 50-29-3 | 0.025/0.01 | 0.025/0.01 | na | na |
| 10 | 1,2-dichloroetane | 107-06-2 | 10 | 10 | na | na |
| 11 | Dichloromethane | 75-09-2 | 20 | 20 | na | na |
| 12 | DEHP | 117-81-7 | 1.3 | 1.3 | na | na |
| 13 | Diuron | 330-54-1 | 0.2 | 0.2 | 1.8 | 1.8 |
| 14 | Endosulfan | 115-29-7 | 0.005 | 0.0005 | 0.01 | 0.004 |
| 15 | Fluoranthene | 206-44-0 | 0.1 | 0.1 | 1 | 1 |
| 16 | Hexachlorobenzene | 118-74-1 | 0.01 | 0.01 | 0.05 | 0.05 |
| 17 | Hexachlorobutadiene | 87-68-3 | 0.1 | 0.1 | 0.6 | 0.6 |

| | | | | | | |
|---|---|---|---|---|---|---|
| 18 | Hexachlorocyclohexane | 608-73-1 | 0.02 | 0.002 | 0.04 | 0.02 |
| 19 | Isoproturon | 34123-59-6 | 0.3 | 0.3 | 1.0 | 1.0 |
| 20 | Lead and its compounds | 7439-97-6 | 7.2 | 7.2 | na | na |
| 21 | Mercury and its compounds | 7439-97-6 | 0.05 | 0.05 | 0.07 | 0.07 |
| 22 | Naphtalene | 91-20-3 | 2.4 | 1.2 | na | na |
| 23 | Nickel and its compounds | 7440-02-0 | 20 | 20 | na | na |
| 24 | 4-Nonylphenol | 104-40-5 | 0.3 | 0.3 | 2.0 | 2.0 |
| 25 | Octylphenol | 140-66-9 | 0.1 | 0.01 | na | na |
| 26 | Pentachlorobenzene | 608-93-5 | 0.007 | 0.0007 | na | na |
| 27 | Pentachlorophenol | 87-86-5 | 0.4 | 0.4 | 1 | 1 |
| 28 | PAH: | | | | | |
| | Benzo(a)pyrene | 50-32-8 | 0.05 | 0.05 | 0.1 | 0.1 |
| | Benzo(b)fluorantene | 205-99-2 | 0.03 | Σ= 0.03 | na | na |
| | Benzo(k)fluorantene | 207-08-9 | 0.002 | Σ= 0.002 | na | na |
| | Benzo(g,h,i)perylene | 191-24-2 | | | na | na |
| | Indeno(1,2,3-cd)pyrene | 193-39-5 | | | na | na |

| | | | | | | |
|---|---|---|---|---|---|---|
| 29 | Simazine | 122-34-9 | 1 | 1 | 4 | 4 |
| 29a | Tetrachloroethylene | 127-18-4 | 10 | 10 | na | na |
| 29b | Trichloroethylene | 79-01-6 | 10 | 10 | na | na |
| 30 | Tributhyl cations | 36643-28-4 | 0.0002 | 0.0002 | 0.0015 | 0.0015 |
| 31 | Trichlorobenzenes | 12002-48-1 | 0.4 | 0.4 | na | na |
| 32 | Trichloromethane | 67-66-3 | 2.5 | 2.5 | na | na |
| 33 | Trifluralin | 1582-09-8 | 0.03 | 0.03 | na | na |

na: not applicable

**Table 2**. Basic characteristic of colorants studied.

| No | Names of colorant | Category and CAS | Summary formula and molar mass | Characterization of the substance | Informations source |
|---|---|---|---|---|---|
| 1 | **Brilliant Blue E133; Acid Blue 9; Brilliant Blue FCF FD&C Blue No. 1** | Azo dyes 3844-45-9 | $C_{37}H_{34}N_2Na_2O_9S_3$ 792,84 g/mol | Synthetic organic compound used primarily as a blue colorant for processed foods, medications, dietary supplements, and cosmetics. Both the diammonium and disodium salts of are used. The disodium salt is used in foods, while the diammonium salt has limited usage in drugs and cosmetics. It is classified as a triarylmethane dye. It is soluble in water and glycerol, with a maximum absorption at about 628 nanometers. It is one of the oldest FDA-approved color additives and is generally considered nontoxic and safe. Has been used in foods in the US since 1929. | **[www 1] [www 2] [www 3] [Arabzadeh 2018]** |
| 2 | **Ponceau 4 R E 124; Cochineal Red A; Acid Red 18; BrillianScarlet 4R; New Coccine Brilliant Scarlet 3R** | 2611-82-7 Azo dye | $C_{20}H_{11}N_2Na_3O_{10}S_3$ 604.46 g x mol $^{-1}$ | Strawberry red powder, used in a variety of food products; it is stable to light, heat and acid but fades in the presence of ascorbic acid. It is used in Europe, Asia and Australia, but has not been approved for human consumption by the United States Food and Drug | **[Amri 2020]** |
| 3 | **Sunset Yellow E 110; Orange Yellow S; Sun Set Yellow FCF;** | 2783-94-0 Azo dye | $C_{16}H_{10}N_2Na_2O_7S_2$ 452.36 g·mol$^{-1}$ | Orange or yellow-orange powder is used in food, cosmetics and medicines; acceptable Daily Intake (ADI) 1.0 mg / kg (European Food Safety Authority); In Norway, Finland and Sweden was banned or restricted (around 2000) as a food additive | **[Peña-Gonzalez 2018] [Coros 2020]** |

| | | | | | |
|---|---|---|---|---|---|
| 4 | **Malachite Green Aniline green; Basic green 4; Diamond green B; Victoria green B China Gree Malachite green chloride** | 569-64-2<br><br>Triarylmethane dye | $C_{23}H_{25}ClN_2$<br><br>364.911 g/mol | Used as a green colored dye, as a counter dye in histology and for its antifungal properties in aquaculture. It acts as a fluorochrome, histological dye, antifungal and antibacterial drug, has carcinogenic and teratogenic properties. Key component in a fluorescence microscopy. Toxic and irritating: serious injury or death may result from inhalation, ingestion, or skin contact with the material. | **[www 4]**<br>**[Raducan 2008]** |

**Table 3**. Typical processes applied for removal of dyes from water/wastewater.

## A Adsorption process

| S. No. | Target compound | Experiment setup | Quantification protocols | Complementary data | Reference |
|---|---|---|---|---|---|
| 1. | Ponceau 4R (azo dye) | The insoluble polyamidoamine-cyclodextrin crosslinked copolymer (PAMAM-CD). Batch method: 50 mL aqueous solution of dye (130-350mg/L, pH5) with 50 mg PAMAM-CD was shaken (60 rpm) up to 12 h at set temperature (15-35ºC). Effect of pH in range 2-7 on the adsorption of dye was also determined. | Separation of dye by centrifugation and spectrophotometric analysis at 508 +/- 2 nm | The process was fast and spontaneous. Maximum adsorption capacity ( 254.3 mg/g) was achieved at the initial concentration of dye 340 mg/L. temperature 15 ºC and at pH below 5. The PAMAM-CD was easily recovered by 2 M HCl as washing solvent. | [Li 2012] |
| 2. | Malachite Green (cationic dye) | The magnetic β-cyclodextrin-graphene oxide nanocomposites. Batch method: 20 mL aqueous solution of dye (5-800 mg/L) with 5 mg adsorbent was shaken for 2 h at a variable temperature (25-45 ºC) and pH of solution (4-9). | Separation of dye by centrifugation and spectrophotometric analysis of dye concentration at 618 nm. | The adsorbent can effectively remove dyes from wastewater- the maximum adsorption capacity was 990.10 mg/g at 45ºC and pH 7. It can be repeatedly used thanks to its stability (after five cycles, the adsorption capacity only decreased by 20%) and magnetism 9ease of separation). | [Wang 2015] |

| | | | | | |
|---|---|---|---|---|---|
| 3. | Brilliant Blue (triphenylmethane dye) | Metal hydroxide sludge (in natura and calcined) from galvanic bath. The metal hydroxide sludge (LG-IN) was oven-dried at 110°C for 12 hours, ground and sieved until obtaining fine particles (<0.18 mm). The heat treatment of the samples was performed in an oven for 4 hours at temperatures of 250°C (LG-250), 400°C (LG-400) and 900°C (LG-900). This analysis consisted in investigating the initial pH of the solution of NB 180 dye with a concentration of 20 mg.L−1 at a range of 4–8, using a dosage of 5 g.L−1 (0.25 g / 50 mL). After three hours of stirring at 200 rpm and at a temperature of 25°C | Separation of dye by centrifugation and spectrophotometric analysis of BB concentration at 635 nm | For the conditions of 5 g./L and pH of 4, the sludge in natura (LG-IN) reached equilibrium after 60 min, removing 78% of dye, while the calcined sample at a temperature of 250°C (LG-250) removed 100% of dye in solution in 30 min. The presence of (Ca2+) ions in solution and metal oxides/hydroxides are the main factors responsible for the removal of colour. The parameters of the kinetics, equilibrium and intraparticle diffusion models demonstrated a better performance of the sample LG-250 (qe = 4.09 mg.g−1), when compared to the sample LGIN (qe = 2.76 mg.g−1). These results demonstrated that metal hydroxide sludge can be reused and applied in dye removal processes for the treatment of textile effluent. | [Baptisstella 2018] |

| | | | | | |
|---|---|---|---|---|---|
| 4. | Sunset Yellow (azo dyes) | Thermally reduced graphene oxide (TRGO) under argon. Adsorption was performed at room temperature in a total volume of 3 mL buffer (pH = 2 –HCl/KCl; pH = 4.2 – acetate; pH = 6 -phosphate; pH = 9 – Borax; pH = 10.7 - carbonate) containing predetermined amounts of Sunset yellow (10, 20, 30, 40, 50, 75 and 100 mg/L – for the thermodynamic investigations) and a known amount of thermally reduced graphene oxide (0.1; 0.2; 0.3; 0.4; 0.5; 0.75 and 1 mg/mL– for determining the influence of the initial adsorbent concentration), and left to stir for the specific amount of time. | The samples were filtered over Glass fiber syringe filters and the UV–Vis spectra were measured in order to obtain the absorbance at 470 nm. | The structural characterization of TRGO before and after SY dye adsorption demonstrate a favorable adsorption with structural changes in the FT-IR, XRD and XPS spectra and in the thermogravimetric analysis and BET surface area. The quantitative assessment of both thermodynamic and kinetic parameters also proves the efficiency of SY dye adsorption.. | (Coros 2020) |

## B Biodegradation and /or biosorption processes

| S. No. | Target compound | Experiment setup | Quantification protocols | Complementary data | Reference |
|---|---|---|---|---|---|
| 5. | Brilliant Blue (triphenylmethane dye) | Powdered grape seeds (PGS). Experimental steps: the effect of initial pH was studied (from 1.0 to 8.0) initial dye concentration of 50 mg/L, contact time of 1 h, volume of solution of 25 mL, PGS dosage of 2.00 g/L and temperature of 25°C. The effect of PGS dosage (from 0.25 to 5.00 g /L) was investigated under the same conditions, using the optimum pH. Kinetic experiments were performed using the optimum pH and PGS. The initial dye concentration was 50 mg/L, at 25°C with contact time from 0 to 120 min and the volume of solution 25 mL. Isotherm curves were constructed at 25, 35, 45 and 55°C, using the optimum pH and PGS. The initial dye concentration ranged from 25 to 300 mg/L and the volume of solution was 25 mL, with the aliquots stirred until the equilibrium (maximum 6 h). The biosorption experiments were realized in batch mode at 200 rpm using a thermostated agitator. | Centrifugation after the process at 4000 rpm for 20 min. and absorption maximum for dye was 408 nm. | At pH values lower than 6.85 the biosorbent is positively charged, while at pH values higher than 6.85, PGS is negatively charged. The material characterization revealed that PGS has potential features for biosorption, like functional groups on the surface, cavities and protuberances. The biosorption of BB was favored at pH of 1.0 and biosorbent dosage of 0.50 g/L, where the dye removal percentage was higher than 80%. The maximum biosorption capacities were 599.5 mg/g for BB at 328 K. | (Vanni 2017) |

| | | | | | |
|---|---|---|---|---|---|
| 6. | **Malachite Green** | Simultaneous biosorption on fungus biosorbent *Yarrowia lipolytica* ISF7 isolated from wastewater. Conditions of the process: mixing 0.04 g of biomass with solution containing 5-25 mg/L of dyes. Shaking rate of 160 rpm, temperature (15-35ºC) and contact times (0-24 h). | Centrifugation at 3000 rpm for 10 min and analysis of the supernatant by UV/Visible Spectrophotometer, 580 nm | The maximum biosorption efficiency (>99% for both dyes) at pH 7.0, T= 28ºC, 24h mixing and initial dyes concentrations-20 mg/L | [Asfaram 2017] |
| 7. | **Ponceau 4R** | Bio-Reduced Graphene Oxide (BRGO)-mediated bio-decolorization of P4R by *Shevanella algae*. Bio-decolorization system was 135 mL serum bottles containing 50 mL BRGO dispersion, bottles were sealed with rubber stoppers, and the gas headspace was flushed for 10 min with nitrogen gas. In an anaerobic chamber were added cells (0.025 g/ L) and P4R (1 mM). The serum bottles were incubated at 30 °C in a dark, shaker with 150 rpm. | The concentrations of dye was determined spectrophotometrically at corresponding maximum visible absorption wavelength (506 nm) | This experiment was confirmed that oxygen-containing functional groups of GO were partly removed, and GO was reduced to BRGO by *S. algae*. The electrical conductivity of RGO was found to be approximately 3 orders of magnitude higher than that of GO. Thus, it is possible for BRGO to be used as a mediator for transferring electrons from cells to azo dyes. 1 mM P4R could be decolorized by S. algae (0.025 g/L) in 10 h in the presence of 0.075 g/L BRGO, while the complete bio-decolorization of P4R needed 18 h without BRGO. BRGO could be used as a scaffold for bacterial attachment, which is beneficial for transferring electrons from cells to BRGO with the increase of BRGO concentration from 10 to 0.075 g/L, the decolorization efficiencies of P4R rose from 61 to 98 %, while P4R removal in the system without BRGO only reached 54 % in 10 h. This indicates that P4R bio-decolorization could be enhanced in a dose-dependent manner of BRGO. | [Zhang 2014] |

| | | | | | |
|---|---|---|---|---|---|
| 8. | **Sunset Yellow** | Microbial fuel cells (MFCs). Mixed cultures from different sources were first enriched and acclimated to cultures with an appropriate concentration under the toxicity threshold of model dye to isolate a promising azo dye decolorizer. After 6 h of secondary culture, model dyes were added to reach 100 mg/L for study. Only the microbial source which showed the most promising dye decolorization capability was taken for further acclimation.After decolorization of the azo dye, 1% v/v of the bacterial culture broth was inoculated into 100 mL of fresh medium as a secondary culture, then incubated for 6 h at 30 ◦C, 125 rpm. Afterwards, the azo dye sample was added until the concentration of the dye is 100 mg/L and the decolorization took place in static condition. This process was done repetitively until the maximum decolorization rate was reached. | Cell growth and dye decolorization were monitored using UV/Vissible Spectrophotometer, 474 nm. | The most appropriate decolorizer exhibited the extent of decolorization for Sunset Yellow FCF 93 % in 3 h respectively. | [Tacas 2021] |

## C Coagulation, filtration, membrane separation and other processes

| S. No. | Target compound | Experiment setup | **Quantification protocols** | **Complementary data** | **Reference** |
|---|---|---|---|---|---|
| 9. | Ponceau 4R (azo dye) | Electrocoagulation process (EC) against waste aluminium cans electrode. Batch monopolar experiments were carried out in a 1.1 L rectangular reactor,two pieces of flat waste aluminium cans (WAC) andcommercial aluminium (COM) plates were used as electrodes, the electrodes were connected to a DC Power supply (Dazheng PS-305D, 0–5 A, 0–30 V). All EC experiment was operated at the best-operating conditions (current density of 25 mA/cm2, pH of 3, initial concentration of P4R 100 mg/L, electrode distance of 0.5 cm, NaCl concentration of 2 g/L and reaction time of 25 min).The water solution (800 mL) was fed into the cell and was continuously stirred at 250 rpm. | The concentration of P4R dye solution was determined using a double beam UV-visible spectrophotometer at a wavelength of 507 nm. | The dye removal efficiency and changes in the solution pH with time as well as the quality of the treated water using WAC and COM electrodes via EC process were studied. The WAC electrode demonstrated better performance than COM electrode as it could decolorize the AR18 dye faster with 100% removal efficiency in 25 min and produced lower residual Al concentration of 0.6 ppm in the treated water after the EC treatment. During the EC process, it was also observed that pH of the solution increased considerably with both types of electrode materials reaching a maximum of 8.6, indicating that they performed similar dye removal mechanism due to the identical nature of the electrode. | [Amri 2020] |
| 10. | Malachite Green (cationic dye); Brilliant Blue | Photocatalytic oxidation process using ZnO as a photo-catalyst upon UV irradiation. The photocatalytic removal of Malachite Green (MG) and Brilliant Blue (BB) dyes was carried out in aqueous solutions containing the dye and suspended of ZnO. Pyrex glass beaker containing dye sample (100, 200 mL) and ZnO was placed in the reaction vessel. The concentrations of malachite green and brilliant blue dyes were (10 and 40 mg/L) and (50 and 100 mg/L) | Colour removal of dyes was assessed by Uv-Visible Spectrophotometer by fixing the maximum wavelength ëmax for each dye. | Photocatalytic removal of dye depends on initial concentration of dye, sample volume and treatment time.<br>In case of MG dye, the photocatalytic removal process was active at low initial concentration of MG dye (10 mg/L), small sample volume (100 mL) and long treatment time 30 min. However, the removal % was also found to be increased with the increasing of treatment time. For BB dye, it was favoured at low initial concentration of 50 mg/L and long treatment time (30 min) | [Mussa 2021] |

| | | | | | |
|---|---|---|---|---|---|
| 11. | Sunset Yellow | Photodegradation process using α-Fe2O3 nanostructures as a photo-catalyst upon visible beam sources irradiation. The experiments were performed with a Pyrex cylindrical photoreactor. The standard solution of SY (20 ppm) was prepared at six pH values: 8.0, 9.0, 10.0, 10.5, 11.0 and 12. At each pH, 50 mL of the solution was contacted with 0.002 g of iron oxide nanoparticles and 0.5 mL of H2O2 (2.5 mol $L^{-1}$). It was stirred throughout the experiment to hold the photocatalyst suspended and the reaction temperature was kept constant at 5° C. The solution was irradiated by the visible beam sources of a 400 W Krypton lamp with the range of the emitted beam 200 – 1000 nm | The sample was centrifuged at 3000 tr/min for 10 min. Then its spectrum was recorded using a UV – Vis spectrophotometer at 1 nm interval in wavelength range from 350 to 550 nm. | The results revealed that pH strongly affects the mechanism and the rate constants of the dye photoreactivity due to changing its-molecularstructure. Protonated/deprotonated structures with resonance forms were less degradable because of their stability and then showed lower rate constant (s). | [Rashidi 2019] |

**Table 4**. Synthesis conditions of Egyptian Blue samples.

| Name of EB samples | Chemical products | Amount [g] chemical compositions on 10 g sample weight | Synthesis temperature/time [°C]/[h] | Powder container used for synthesis | Additional information |
|---|---|---|---|---|---|
| **Comercial standard** | **$CaCuSi_4O_{10}$**<br>(final product accordingly to producer data) | ---------- | up to 1000 | ---------- | Kremer Pigmente GmbH&Co.KG; Aichstetten, Germany |
| **1.1.1.** | **$SiO_2$;**<br>**$NaHCO_3$**<br>**$CaCO_3$**<br>**CuO**<br>**$H_2O$**<br>(initial composition for synthesis) | 6.02<br>0.80<br>1.45<br>1.73<br>mix with water to form a plastic consistency | 860/4 and 950/4 | fireclay brick | After the first firing: cooling in a closed furnace oven for 20 hours and grinding in a ball mill. Then second firing at 950 ° C on a fireclay brick |
| **1.1.1a**. | **$SiO_2$**<br>**$NaHCO_3$**<br>**$CaCO_3$**<br>**CuO**<br>**$H_2O$**<br>(initial composition for synthesis ) | 6.02<br>0.80<br>1.45<br>1.73<br>mix with water to form a plastic consistency | 860/4 and 950/4 | porcelaine | After the first firing: cooling in a closed furnace oven for 20 hours and grinding in a ball mill. Then second firing at 950 ° C in a porcelaine, evaporating dish |

**Table 5.** Measured values of particles size and zeta potential for active carbon (Norit SA Super) obtained from Cabot Concern and distributed by Brenntag, Kędzierzyn Koźle, Poland) and graphene oxide (GO was produced in TUK laboratory using modified Hummers method). Both carbon materials were suspended in distilled water at concentration of 0.2 mg/mL, followed by 1 h shaking. Graphene oxide was reconstituted in water from dry lyophilizate. The pH value of the GO suspension was 3.4 and Norit SA Super was 8.2. The analysis was carried out at a temperature of 25°C using ZetaPALS device (Zeta Potential Analyzer, Brookhaven Instruments Corporation, Holtsville, New York, USA) working with ZetaPALS particle sizing software- 9 kpsdw ver. 2.31(1997) and PALS zeta potential analyzer software ver. 3.16 (1998).

| **Parameter measured** | | **Graphene oxide** | **Norit SA Super** |
|---|---|---|---|
| **Particle size [nm]** | Average (n= 20) | 20253 | 9566,9 |
| | Standard deviation | 7063,8 | 4631,7 |
| **Zeta Potential [mV]** | Average (n= 24) | -20,6 | -13,3 |
| | Standard deviation | 2,7 | 2 |

**Table 6.** List of layers and basic physical characterization of separation systems **[Lewandowska 2017]**; with permission from Journal of Planar Chromatography.

| Layer No | (I) Layer type<br>(II) Catalogue number<br>(III) Producer | Density (Producer specification) [g/m$^2$] | Density (Measured) [g/m$^2$] | Layer thickness (Producer specification) [µm] | Layer thickness (Measured) [µm] | Complementary data | Active layer working mode |
|---|---|---|---|---|---|---|---|
| **1** | **(I)** Filtrating paper (Bibuła filtracyjna jakościowa średnia)<br>**(II)** Not available<br>**(III)** Polska Grupa Laboratoryjna Sp. z o.o., PGL, Warszawa, Poland | 65 | --- | Not available | 100 ±2<br>(*n* = 7) | --- | **A** |
| **2** | **(I)** Office paper POL Jet 80, A4<br>**(II)** Not available<br>**(III)** International Paper - Kwidzyn Sp. z o.o., Kwidzyn, Poland | 80 | --- | Not available | 99 ± 3<br>(*n* = 14) | --- | **A** |
| **3** | **(I)** Whatman Chromatography paper 1CHR<br>**(II)** 3001-861<br>**(III)** GE Healthcare UK limited, Little Chalfont, UK, China | Not available | --- | 180 | 155 ± 3<br>(*n* = 14) | --- | **A** |

| | | | | | | | |
|---|---|---|---|---|---|---|---|
| **4** | **(I)** Thin Japanese paper for aircraft paper models<br>**(II)** Not available<br>**(III)** Distributed by www.modele.sklep.pl Warszawa, Poland | 12 | 13.04 ± 0.01 (*n*= 3) | Not available | 19 ± 3 (*n*= 7) | --- | **B** |
| **5** | **(I)** Thick Japanese paper for aircraft paper models<br>**(II)** Not available<br>**(III)** Distributed by www.modele.sklep.pl Warszawa, Poland | 21 | 21.241 ± 0.003 (*n* = 3) | Not available | 44 ± 3 (*n* = 7) | --- | **B** |
| **6** | **(I)** TLC Cellulose without fluorescence indicator, glass based pre-coated plates<br>**(II)** 5716<br>**(III)** Merck, Darmstadt, Germany | Not available | --- | 100 | --- | --- | **C** |
| **7** | **(I)** Potato starch (Potato flour)<br>**(II)** Not available<br>**(III)** Kupiec, Sp. z o.o., Krzymów, Poland | Not applicable | --- | Not applicable | 383 ± 23 (*n* = 7) | Starch layer on 100 µm filtrating paper strip | **B** |
| **8** | **(I)** TLC Polyamide 11 $F_{254}$, glass based pre-coated plates<br>**(II)** 5557<br>**(III)** Merck, Darmstadt, Germany | Not available | --- | 150 | --- | --- | **C** |

| | | | | | | | |
|---|---|---|---|---|---|---|---|
| **9** | **(I)** TLC Silica gel 60 W $F_{254}$ S, Glass based pre-coated plates<br>**(II)** 1.16485.0001<br>**(III)** Merck, Darmstadt, Germany | Not available | --- | 200 | --- | --- | **C** |
| **10** | **(I)** HPTLC Silica gel RP18W, glass based pre-coated plates<br>**(II)** 1.14296<br>**(III)** Merck, Darmstadt, Germany | Not available | --- | 150-200 | --- | --- | **C** |
| **11** | **(I)** TLC Aluminium oxide 60 F254 Type E, glass based plates<br>**(II)** 5713<br>**(III)** Merck, Darmstadt, Germany | Not available | --- | 250 | --- | --- | **C** |
| **12** | **(I)** Nutrient agar<br>**(II)** 1.05450.0500)<br>**(III)** Merck, Darmstadt, Germany | Not applicable | --- | Not applicable | 451 ± 68<br>(*n* = 7) | Working concentration 1.5% | **B** |
| **13** | **(I)** Nutrient agar<br>**(II)** 1.05450.0500)<br>**(III)** Merck, Darmstadt, Germany | Not applicable | --- | Not applicable | 1003 ± 139<br>(*n* = 7) | Working concentration 1.5% | **B** |

**A** - Without additional supporting material; active layer length = 180 mm (total 200 mm); 10 mm from each edge of active material strip dipped directly in cathode and anode electrolyte containers.

**B** - Glass plate (1.2 mm x 20 mm x 100 mm); active layer length 80 mm (total 100 mm); active material strip connected to cathode and anode electrolyte containers using additional strips 20 mm x 60 mm made of filtrating paper (Layer No1).

**C** - Active layer manufactured by producer on glass plate - TLC plate (20 mm x 100 mm); active layer length 80 mm (total 100 mm); TLC plate connected to cathode and anode electrolyte containers using additional strips 20 mm x 60 mm made of filtrating paper (Layer No1).

**Table 7.** Estimation of dye contents in reaction vials after 24 h of contact time based on digital pictures using raw RGB file (**A**) and extracted RGB channel (**B**) for **Malachite Green** (**MG**) dye samples.

**MG RAW RGB (A)**

| Sample ID | Spot intensity (SI) [max. avg. value; 8-Bit RGB space] | Background intensity (BI) [avg. value 8-Bit RGB space] | Difference SI-BI [avg. value 8-Bit RGB space] | Dye level decrease relatively to Sample 01 [%] | Dye level decrease relatively to Sample 02 [%] |
|---|---|---|---|---|---|
| **01** | 148 | 107 | 41 | 100 | 2.9 |
| **02** | 121 | 107 | 14 | 34 | 100 |
| **03** | 114 | 108 | 6 | 15 | 0.4 |
| **04** | 113 | 110 | 3 | 7 | 0.2 |
| **05** | 125 | 115 | 10 | 24 | 0.7 |
| **06** | 125 | 118 | 7 | 17 | 0.5 |
| **07** | 127 | 118 | 9 | 22 | 0.6 |
| **08** | 126 | 115 | 11 | 27 | 0.8 |
| **09** | 133 | 114 | 19 | 46 | 1.4 |
| **10** | 126 | 113 | 13 | 32 | 0.9 |

## MG RED CHANNEL RGB (B)

| Sample ID | Spot intensity (SI) [max. avg. value; 8-Bit RGB space] | Background intensity (BI) [avg. value 8-Bit RGB space] | Difference SI-BI [avg. value 8-Bit RGB space] | Dye level decrease relatively to Sample 01 [%] | Dye level decrease relatively to Sample 02 [%] |
|---|---|---|---|---|---|
| **01** | 201 | 110 | 91 | 100 | 2.8 |
| **02** | 145 | 113 | 32 | 35 | 100 |
| **03** | 124 | 114 | 10 | 11 | 0.3 |
| **04** | 121 | 116 | 5 | 6 | 0.2 |
| **05** | 145 | 126 | 19 | 21 | 0.6 |
| **06** | 144 | 128 | 16 | 18 | 0.5 |
| **07** | 144 | 127 | 17 | 19 | 0.5 |
| **08** | 136 | 123 | 13 | 14 | 0.4 |
| **09** | 156 | 118 | 38 | 42 | 1.2 |
| **10** | 141 | 114 | 27 | 30 | 0.8 |

**Table 8.** Estimation of dye contents in reaction vials after 24 h of contact time based on digital pictures using raw RGB file (**A**) and extracted RGB channel (**B**) for **Brilliant Blue** (**BB**) dye samples.

**BB RAW RGB (A)**

| Sample ID | Spot intensity (SI) [max. avg. value; 8-Bit RGB space] | Background intensity (BI) [avg. value 8-Bit RGB space] | Difference SI-BI [avg. value 8-Bit RGB space] | Dye level decrease relatively to Sample 01 [%] | Dye level decrease relatively to Sample 02 [%] |
|---|---|---|---|---|---|
| **01** | 121 | 85 | 36 | 100 | 1.0 |
| **02** | 120 | 82 | 38 | 105 | 100 |
| **03** | 110 | 82 | 28 | 78 | 0.7 |
| **04** | 83 | 81 | 2 | 6 | 0.1 |
| **05** | 118 | 81 | 37 | 103 | 1.0 |
| **06** | 120 | 84 | 36 | 100 | 1.0 |
| **07** | 123 | 85 | 38 | 105 | 1.0 |
| **08** | 124 | 89 | 35 | 97 | 0.9 |
| **09** | 126 | 92 | 34 | 94 | 0.9 |
| **10** | 129 | 95 | 34 | 94 | 0.9 |

## BB RED CHANNEL RGB (B)

| Sample ID | Spot intensity (SI) [max. avg. value; 8-Bit RGB space] | Background intensity (BI) [avg. value 8-Bit RGB space] | Difference SI-BI [avg. value 8-Bit RGB space] | Dye level decrease relatively to Sample 01 [%] | Dye level decrease relatively to Sample 02 [%] |
|---|---|---|---|---|---|
| **01** | 176 | 85 | 91 | 100 | 1.0 |
| **02** | 174 | 85 | 89 | 97 | 100 |
| **03** | 157 | 82 | 75 | 82 | 0.8 |
| **04** | 83 | 82 | 1 | 1 | 0.0 |
| **05** | 175 | 82 | 93 | 102 | 1.1 |
| **06** | 177 | 84 | 93 | 102 | 1.1 |
| **07** | 180 | 86 | 94 | 103 | 1.1 |
| **08** | 175 | 91 | 84 | 92 | 0.9 |
| **09** | 181 | 93 | 88 | 97 | 1.0 |
| **10** | 180 | 94 | 86 | 94 | 1.0 |

**Table 9.** Estimation of dye contents in reaction vials after 24 h of contact time based on digital pictures using raw RGB file (**A**) and extracted RGB channel (**B**) for **Ponceau 4R** (**P4R**) dye samples.

**P4R GREEN RGB CHANNEL (B)**

| Sample ID | Spot intensity (SI) [max. avg. value; 8-Bit RGB space] | Background intensity (BI) [avg. value 8-Bit RGB space] | Difference SI-BI [avg. value 8-Bit RGB space] | Dye level decrease relatively to Sample 01 [%] | Dye level decrease relatively to Sample 02 [%] |
|---|---|---|---|---|---|
| **01** | 132 | 113 | 19 | 100 | 0.8 |
| **02** | 140 | 117 | 23 | 1.2 | 100 |
| **03** | 137 | 121 | 16 | 0.8 | 0.7 |
| **04** | 128 | 125 | 3 | 0.2 | 0.1 |
| **05** | 141 | 133 | 8 | 0.4 | 0.4 |
| **06** | 138 | 131 | 7 | 0.4 | 0.3 |
| **07** | 142 | 127 | 15 | 0.8 | 0.7 |
| **08** | 148 | 126 | 22 | 1.2 | 1.0 |
| **09** | 146 | 122 | 24 | 1.3 | 1.0 |
| **10** | 138 | 118 | 20 | 1.1 | 0.9 |

**Table 10.** Measured values of particles size and zeta potential for additives studied. Raw materials were suspended in distilled water at concentration of 0.2 mg/mL, followed by 60 minutes of shaking. With permission from MDPI **[Zarzycki 2021]**.

| Material | Particle size value [nm] (standard deviation) *n*= 20 | Zeta Potential [mV] (standard deviation) *n*= 24 |
|---|---|---|
| **Graphene Oxide** | 20 253 (7 064) | -20.6 (2.7) |
| **Microcrystalline Cellulose** | 32 135 (5 816) | -4.9 (2.1) |
| **Pine Pollen** | 25-35 µm (approximate dimensions based on SEM measurement) | Not available |
| **β-Cyclodextrin** | 1.53* | Not available |
| **Dandelion Pappus** | Fiber length 3-5 mm Fiber diameter 25 µm (approximate dimensions based on SEM measurement) | Not available |
| **Active Carbon Norit SA** | 9567 (4632) | -13.3 (2.0) |
| **Egyptian Blue EB1** | 34 621 (12 683) | -14.9 (6.0) |
| **Egyptian Blue EB2** | 3 458 (942) | -23.3 (6.5) |

* Reference data **[Grumezescu 2016]**

**Table 11.** Quantitative data of Brilliant Blue concentration (mg/L) measured in presence of different active matrices during 24 hours test (involving activated sludge microorganisms). **Additive labels:** active carbon (**AC**), lyophilized graphene oxide (**GO**), β-cyclodextrin (**CD**), raw dandelion pappus (**DP**), microcrystalline cellulose (**MC**), raw pine pollen (**PP**), Egyptian Blue mineral pigment (**1.1.1a.**), activated sludge (**AS**). With permission from MDPI **[Zarzycki 2021]**.

| Time (hour)/Matrix tested | 1 | 2 | 3 | 6 | 24 |
|---|---|---|---|---|---|
| **BLANK** | 4.353 | 5.095 | 4.918 | 4.903 | 5.240 |
| **AC** | 0.000 | 0.000 | 0.000 | 0.000 | 0.000 |
| **GO** | 3.859 | 2.076 | 4.021 | 3.059 | 3.303 |
| **CD** | 4.353 | 5.095 | 4.470 | 4.376 | 4.755 |
| **DP** | 4.353 | 2.773 | 3.573 | 4.903 | 4.997 |
| **MC** | 6.211 | 5.899 | 8.351 | 5.382 | 6.952 |
| **PP** | 7.330 | 5.899 | 7.027 | 7.273 | 6.952 |
| **EB2** | 5.651 | 6.347 | 8.351 | 5.854 | 4.396 |
| **AS BLANK** | 5.479 | 5.833 | 4.921 | 4.611 | 3.427 |
| **AS+AC** | 0.000 | 0.000 | 0.000 | 0.000 | 0.000 |
| **AS+GO** | 4.789 | 5.833 | 4.184 | 3.278 | 3.427 |
| **AS+CD** | 5.479 | 5.833 | 4.184 | 5.278 | 2.536 |
| **AS+DP** | 4.789 | 4.167 | 5.289 | 2.278 | 3.724 |
| **AS+MC** | 3.544 | 5.197 | 4.285 | 5.779 | 4.241 |
| **AS+PP** | 4.152 | 3.586 | 6.100 | 5.377 | 4.664 |
| **AS+EB** | 3.848 | 4.553 | 5.737 | 3.771 | 5.086 |

**Table 12.** Quantitative data of Brilliant Blue concentration (mg/L) measured in presence of different active matrices during 16 days test (involving duckweed water plant). **Additive labels:** active carbon (**AC**), lyophilized graphene oxide (**GO**), β-cyclodextrin (**CD**), raw dandelion pappus (**DP**), microcrystalline cellulose (**MC**), raw pine pollen (**PP**), Egyptian Blue mineral pigment (**1.1.1.** and **1.1.1a.**), duckweed water plant (**DW**).
With permission from MDPI **[Zarzycki 2021]**.

| Time (day)/Matrix tested | 0 | 1 | 7 | 10 | 13 | 16 |
|---|---|---|---|---|---|---|
| **BLANK** | 4.364 | 5.346 | 5.595 | 4.846 | 4.709 | 4.828 |
| **DW** | 4.411 | 5.202 | 5.202 | 4.411 | 4.016 | 4.016 |
| **DW+AC** | 4.873 | 0.000 | 0.000 | 0.000 | 0.000 | 0.000 |
| **DW+GO** | 4.687 | 5.392 | 4.335 | 3.982 | 3.982 | 4.335 |
| **DW+CD** | 3.838 | 3.648 | 3.369 | 3.075 | 3.046 | 2.606 |
| **DW+DP** | 5.554 | 5.113 | 5.554 | 5.113 | 5.995 | 5.554 |
| **DW+MC** | 4.027 | 4.353 | 4.353 | 3.373 | 3.700 | 4.027 |
| **DW+PP** | 4.438 | 4.774 | 4.774 | 3.767 | 4.103 | 4.438 |
| **DW+EB 1.1.1.** | 3.700 | 5.779 | 4.888 | 4.294 | 4.591 | 3.700 |
| **DW+EB 1.1.1a.** | 4.411 | 5.597 | 5.202 | 5.597 | 4.411 | 4.806 |

# 7. FIGURES

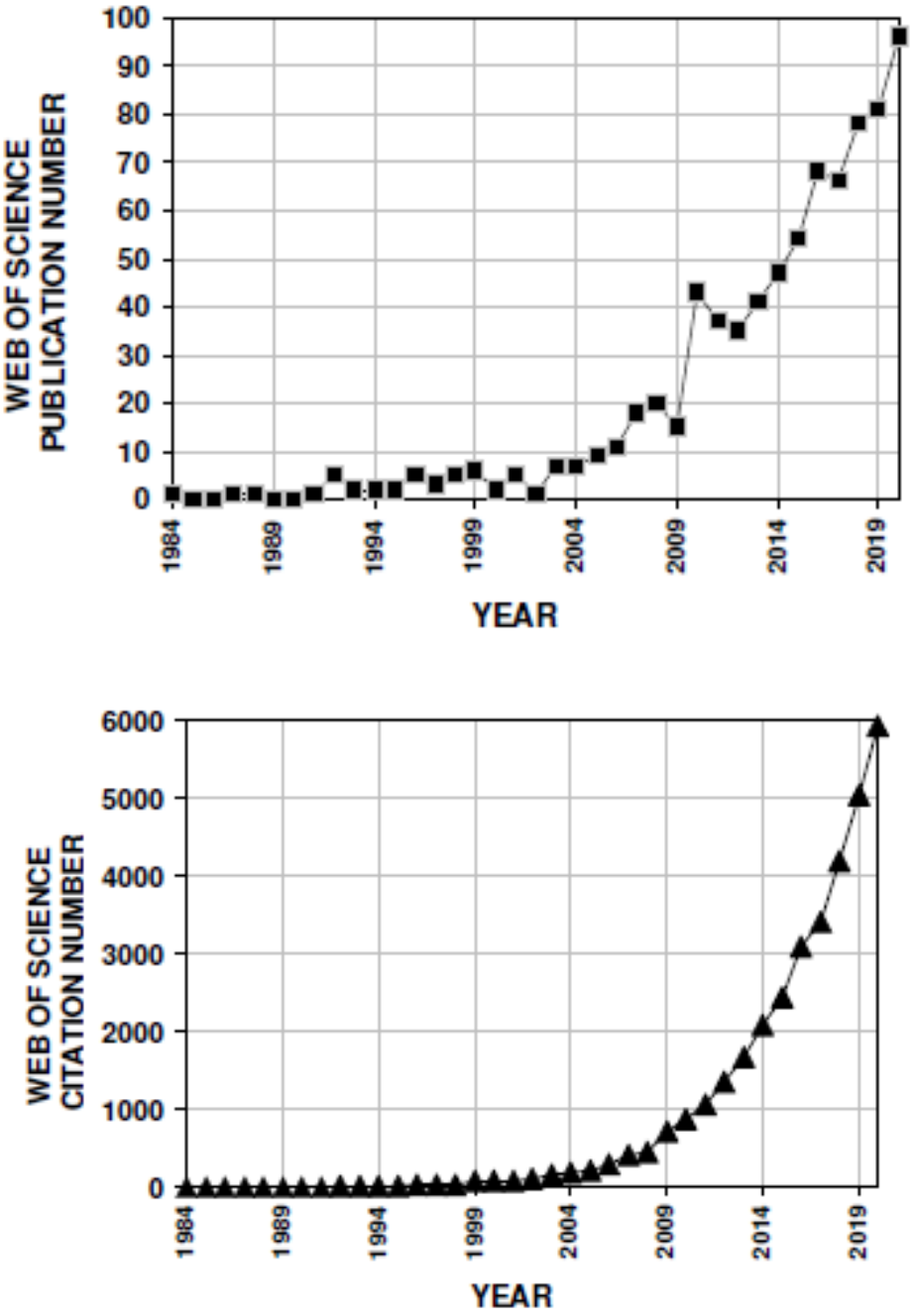


**Figure 1**. Scientific publications number (top graph; black squares) and their citations (bottom graph; black triangles) that are visible in the Web of Science database concerning "sewage micropollutants" term (Key words search: sewage micropollutants within Topic class) (total publications 815; number of citations 37972; time period 1984-2020; search performed: 22.06.2021).

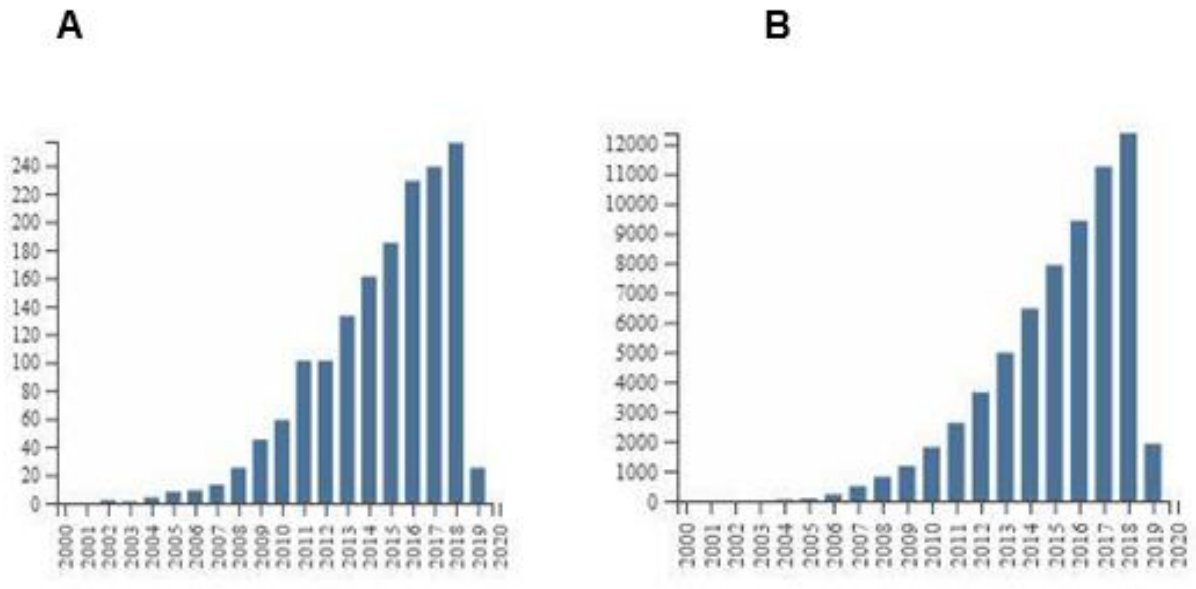


**Figure 2**. Papers number (**A**) and their citations (**B**) that are visible in the Web of Science database concerning "nanomaterials in environmental engeeniring" (Key words search: nanomaterals, environmental engineering within Topic class) (total publications 260; number of citations 1200; time period 1984-2019; search performed: 02.2019).

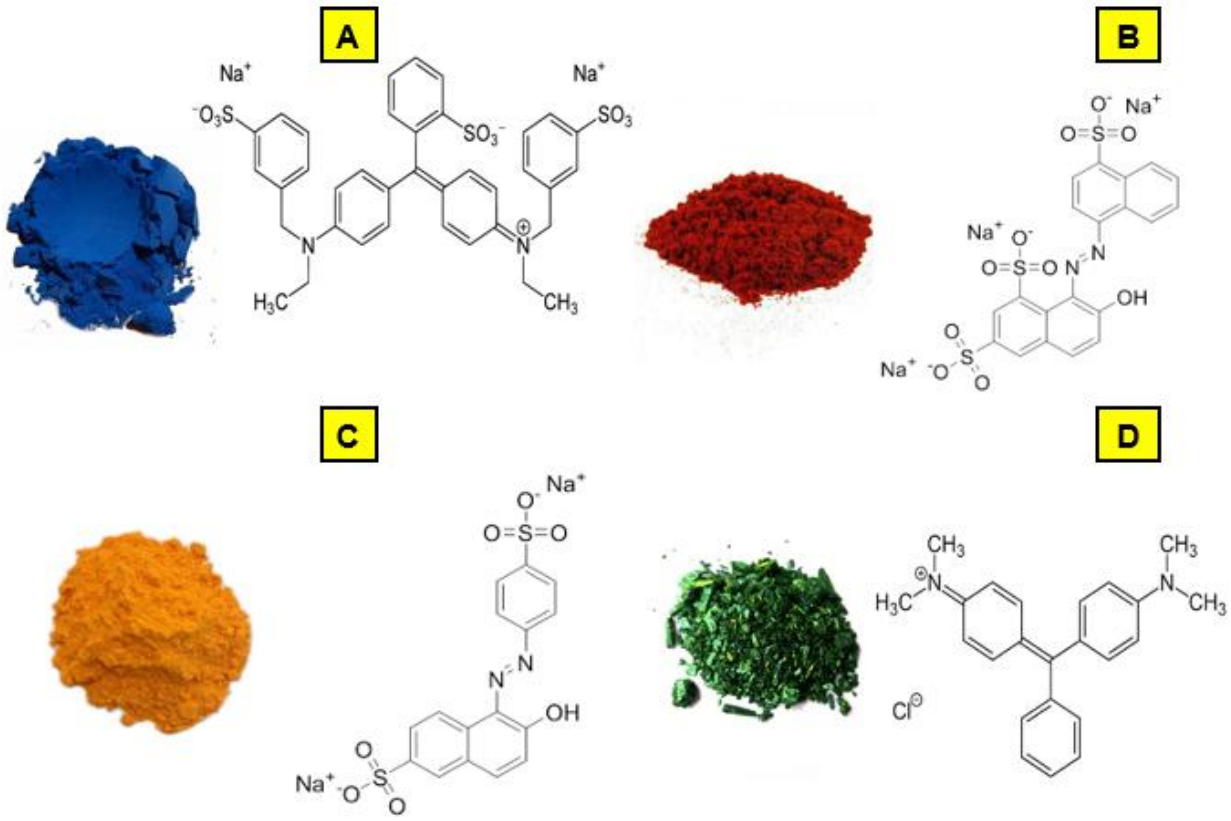


**Figure 3**. General view of solid colorants investigated and their chemical structure (**A** – Brilliant Blue; **B** – Ponceau 4R; **C**- Sunset Yellow; **D**- Malachite Green).

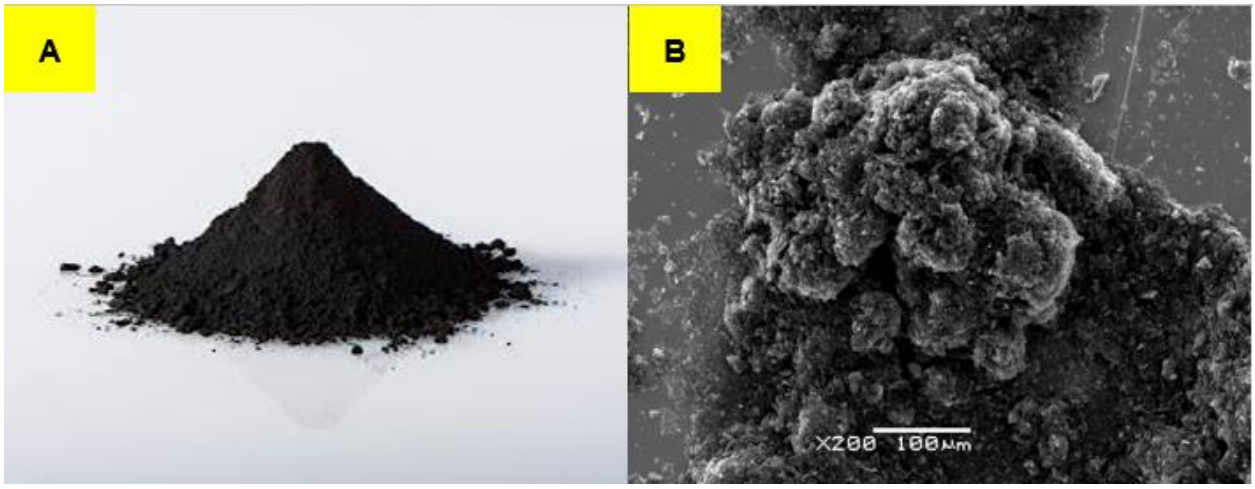


**Figure 4.** General (**A**) and electron microscope (**B**; SEM) views of activated carbon Norrit SA Super.

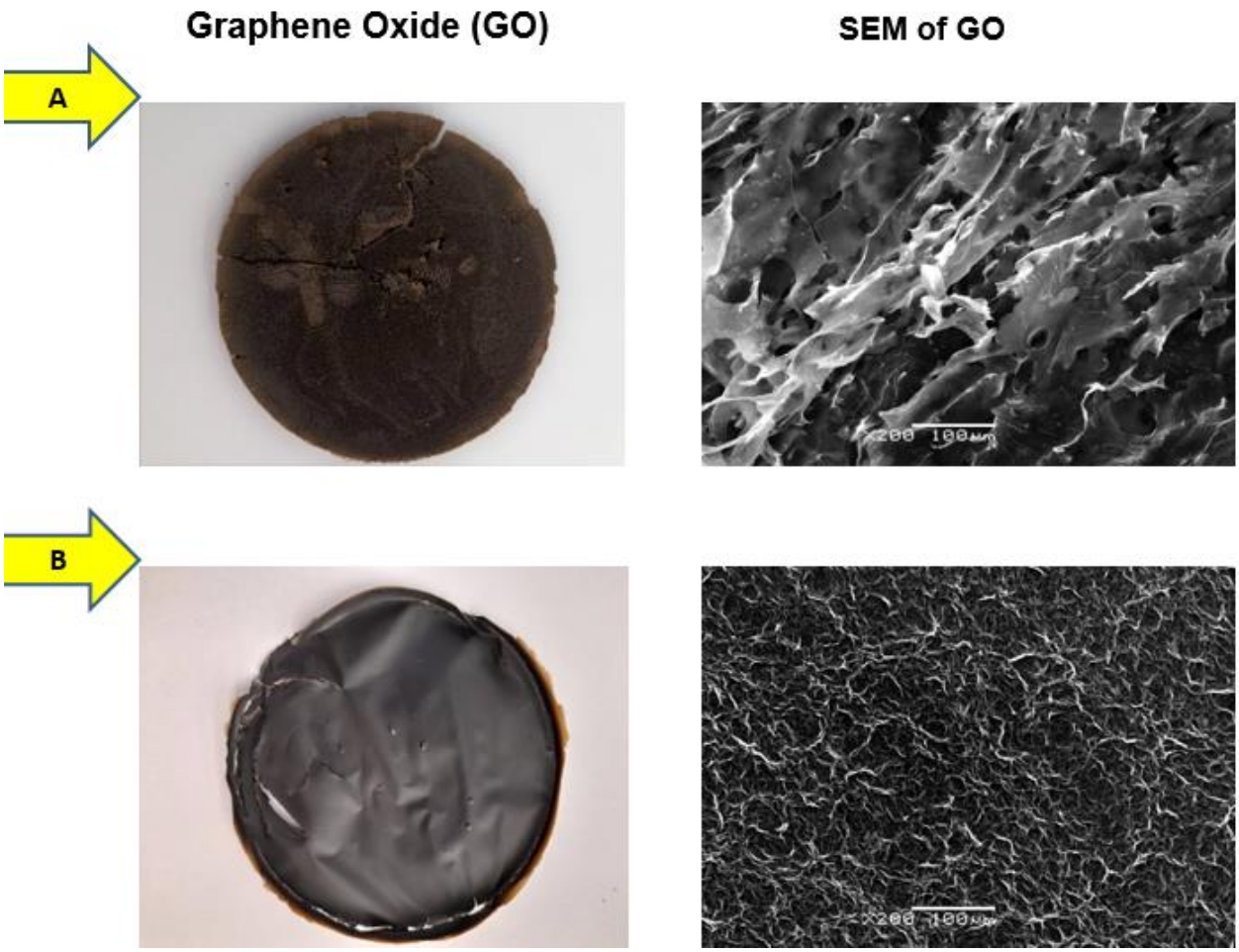


**Figure 5.** Macroscopic view of synthesized graphene oxide (left column; object diameter 90 mm, approximately) and pictures generated by scanning electron microscope SEM (right column) recorded for lyophilized (**A**) and air dried GO (**B**).

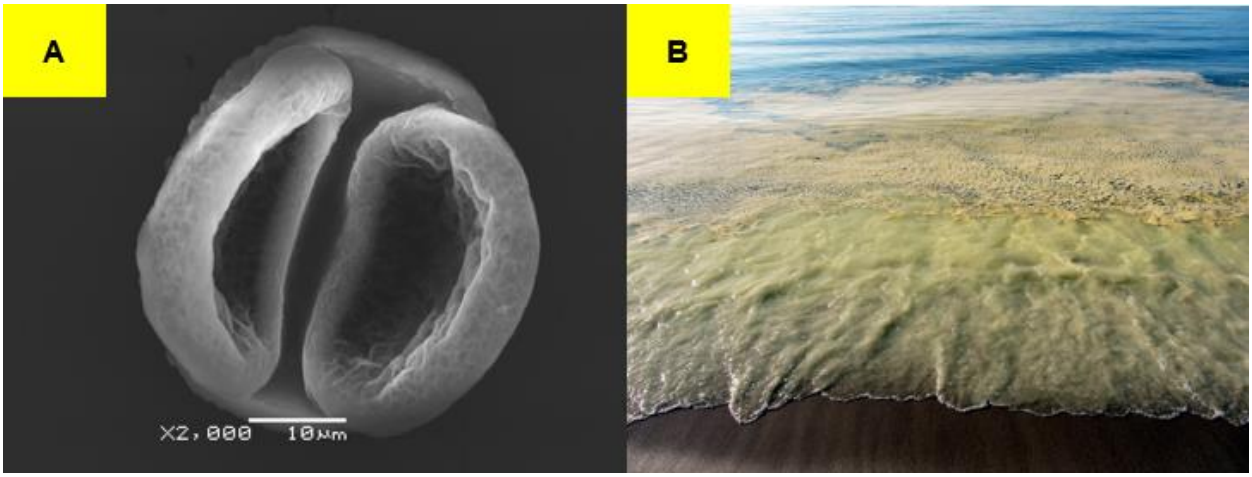


**Figure 6**. General view of pine pollen using scanning electron microscope SEM (**A**) as well as its presence in environment - the Baltic Sea shore (**B;** copyrights by Paweł. K. Zarzycki 2014 with permission).

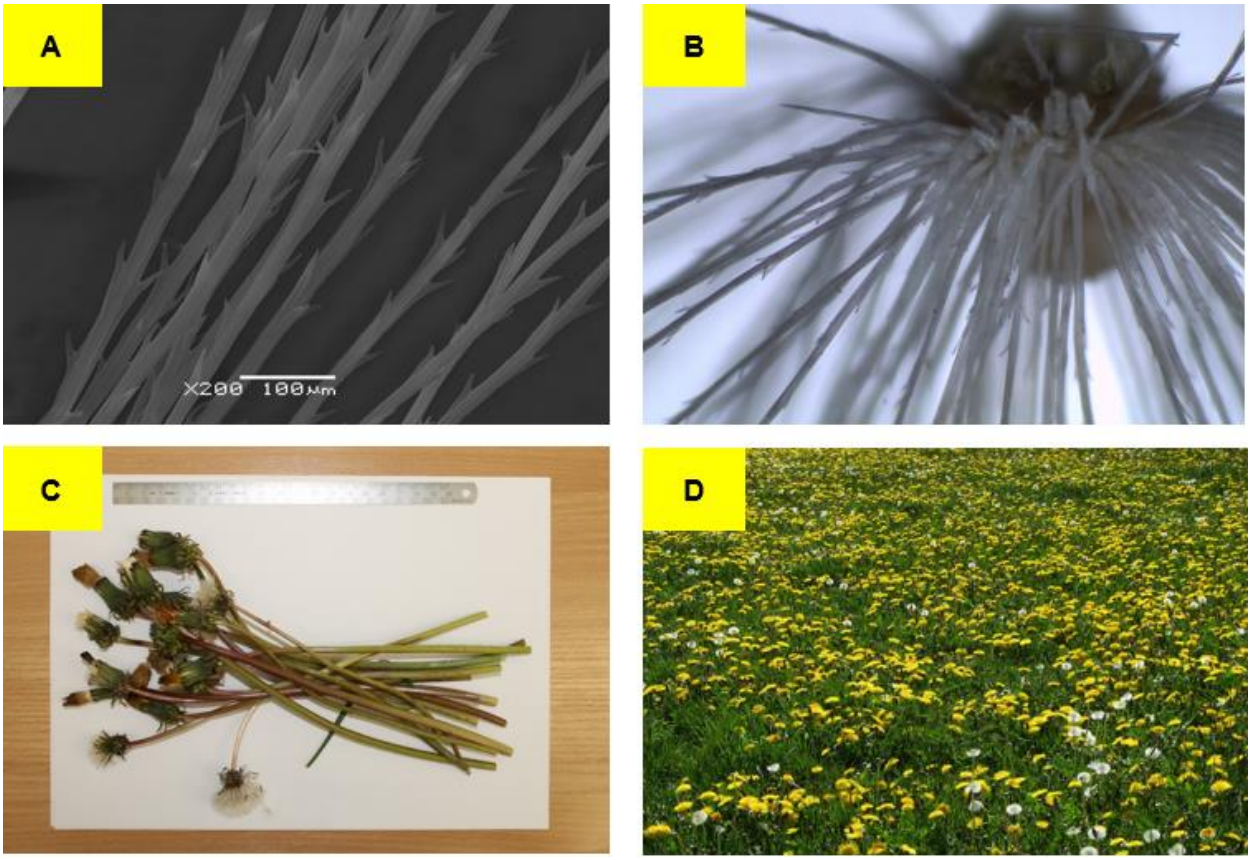


**Figure 7.** Detailed structure of dandelion pappus filaments visualized by scanning electron microscope SEM (**A**), optical microscope (**B**), general view of dandelion mature inflorescence (**C**) and typical view of dandelion organisms in their environment (**D**).

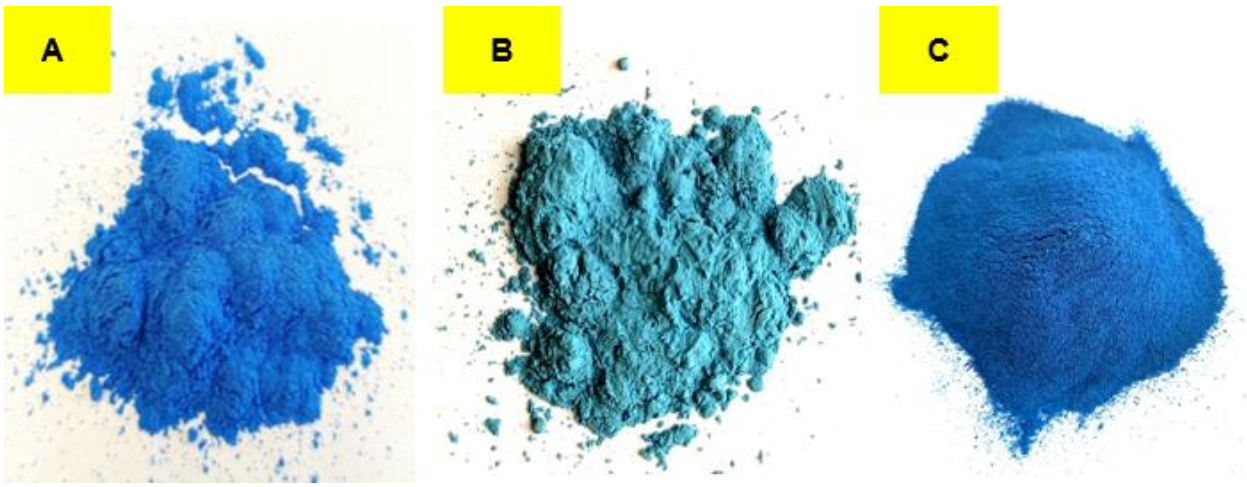


**Figure 8.** Egyptian Blue samples: commercially available standard (**A**) and EB pigments synthesized under different conditions: EB ID 1.1.1a (**B**), EB ID 1.1.1 (**C**).

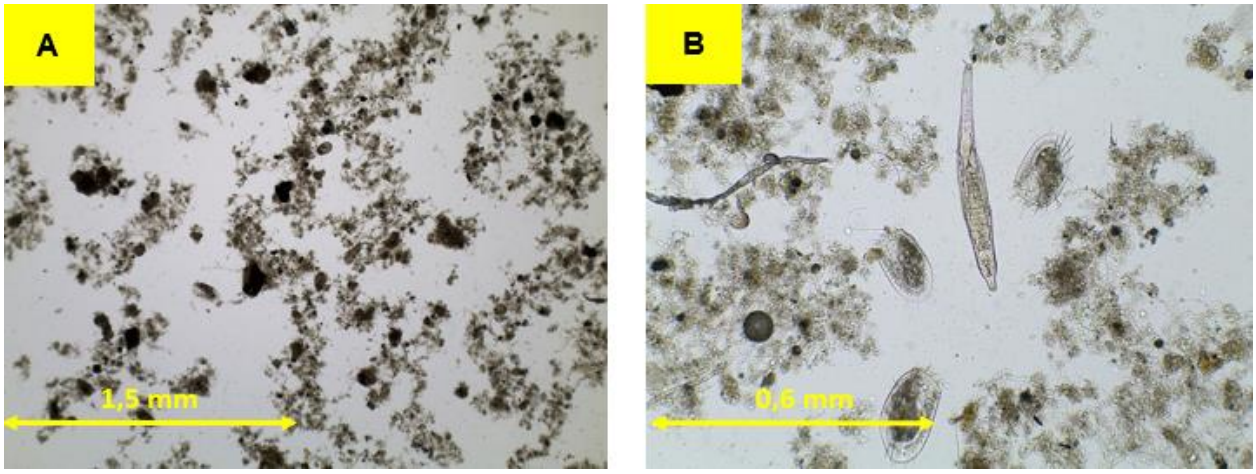


**Figure 9.** General view of activated sludge sample visualized by optical microscope (**A**) lens 4x; (**B**) lens 10x.

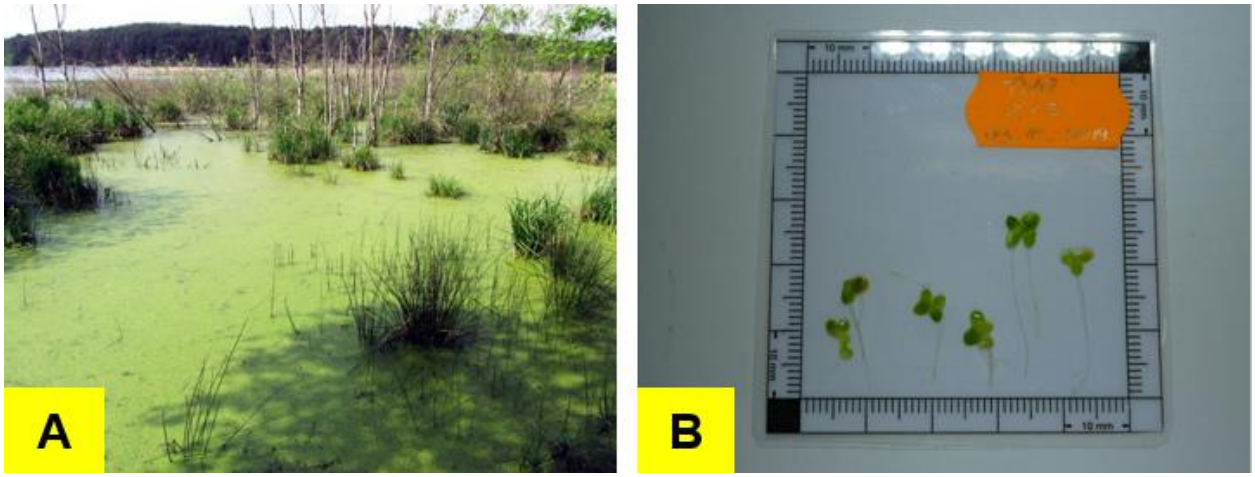


**Figure 10.** Typical duckweed organisms and their presence at surface water (**A**; copyrights by Paweł. K. Zarzycki 2014 with permission) and individual duckweed organisms (**B**).

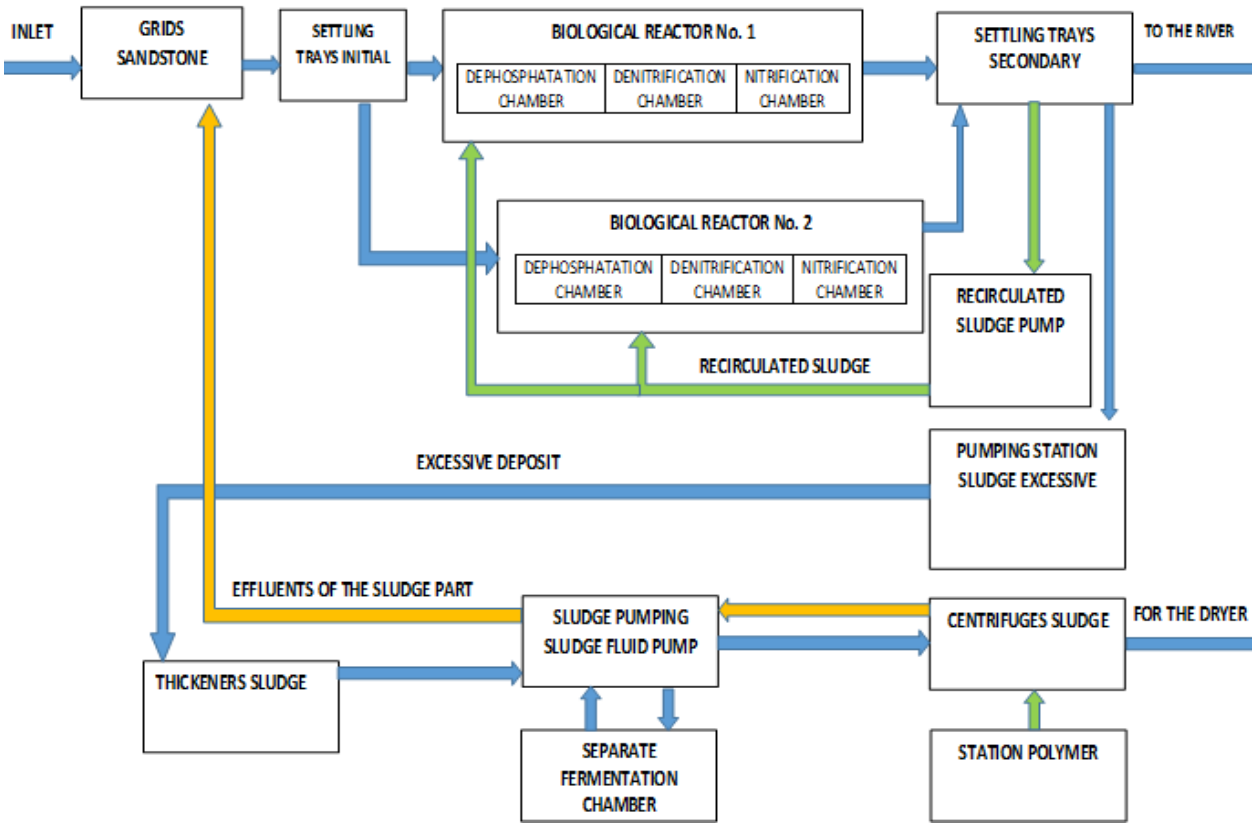


**Figure 11**. Sewage water treatment technological processes (Jamno Treatment Plant) adapted from **[Kozak 2007]**.

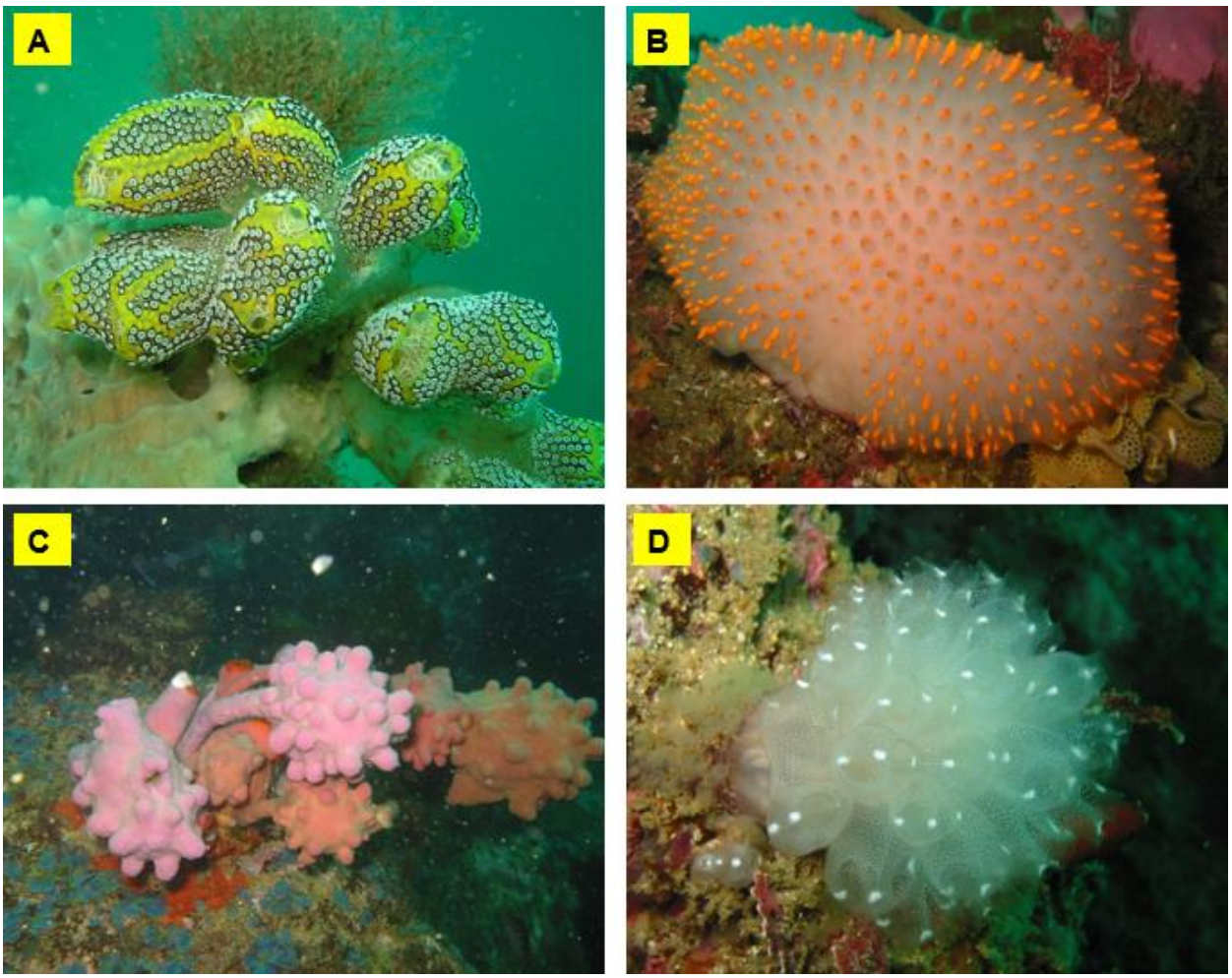


**Figure 12**. Australian Ascidians: (**A**) Magnificent ascidians (*Botrylloides magnicoecum*); (**B**) Giant jelly ascidian (*Polycitor giganteus*); (C) Sea Tulip (*Pyura spinifera*); (D) *Diazona violacea*. |Photos (**B**), (**C**), (**D**) captured at Pipeline, Nelson Bay NSW, Australia and (**A**) in Jervis Bay NSW, Australia Underwater macrophotography by P.K. Zarzycki with permission.

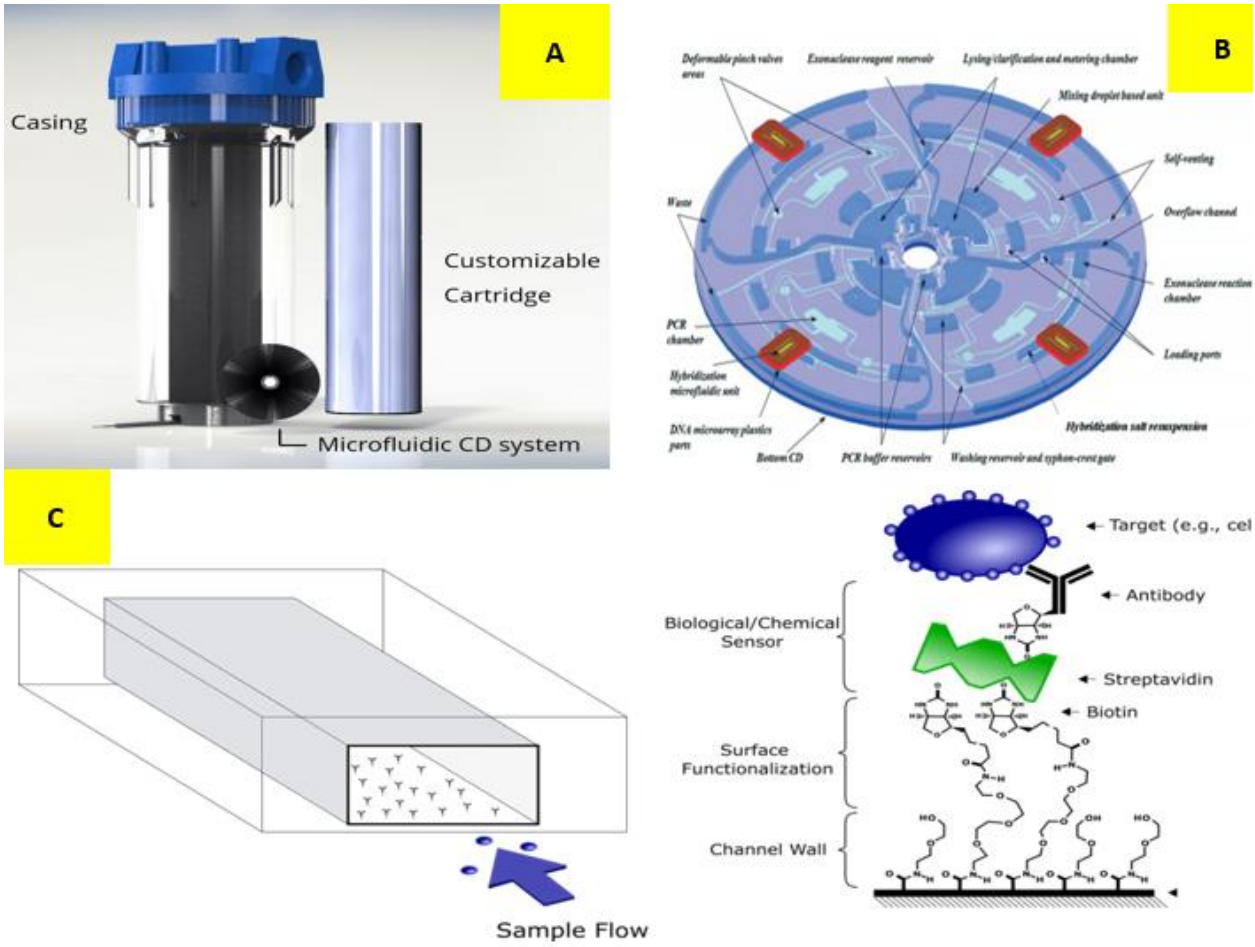


**Figure 13.** Microfluidic devices invented by Eden Microfluidics; Source: **[www 5]**: (**A**) AKVO intelligent microchannel networks recorded on CDs, which are stored in a cartridge for a water treatment system; (**B**) the use of a biocompatible material such as flexydym for applications in microfluidic diagnostics; (**C**) polymers for microfluidic devices: surface functionalization on the microfluidic channel wall.

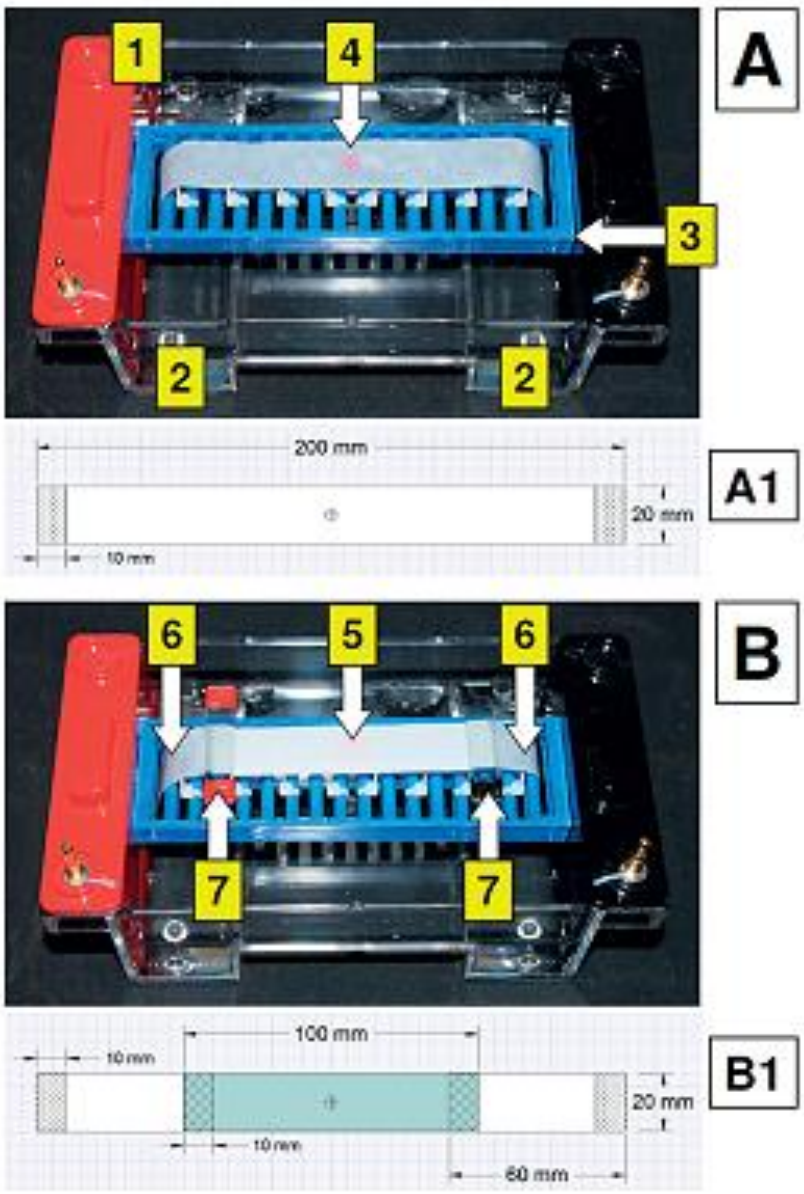


**Figure 14**. Horizontal electrophoresis chamber with different separation units: cellulose filtration paper (**A**) and TLC plate (**B**); gel box without cover (1), working electrolyte containers (2), separation unit suport (3), cellulose filtration paper (200 mm × 20 mm) as active separation stationary phase (4), TLC plate (10 mm × 20 mm) as active separation stationary phase (5), connection strips (6; cellulose filtration paper; 60 mm × 20 mm) and glass weights (glass plate 3.6 mm × 10 mm × 50 mm; ~5 g) for improving electrical connection between active TLC layer and cellulose filtration paper strips (7). Scheme of active layers: cellulose strip (**A1**), TLC plate combined with cellulose strips working as electrolyte connection layers (**B1**). With permission from Journal of Planar Chromatography **[Lewandowska 2017]**.

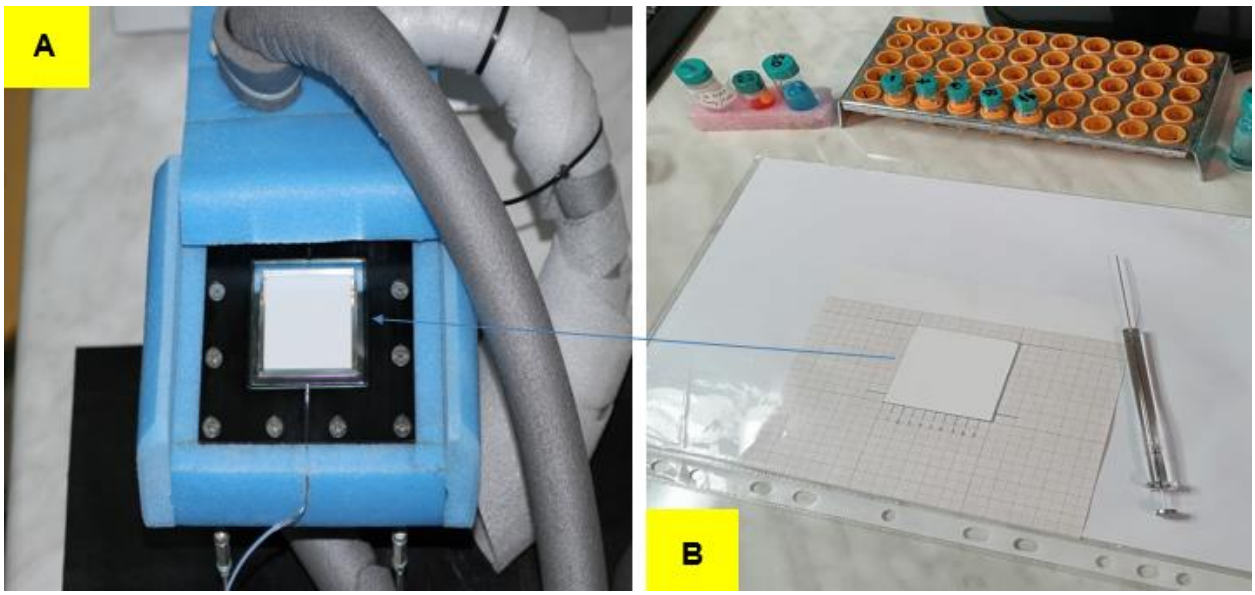


**Figure 15.** Micro- TLC removable unit working inside temperature controlled oven (**A**; **[Zarzycki 2008]**) and micro-TLC plate before samples application using Hamilton syringe (**B**).

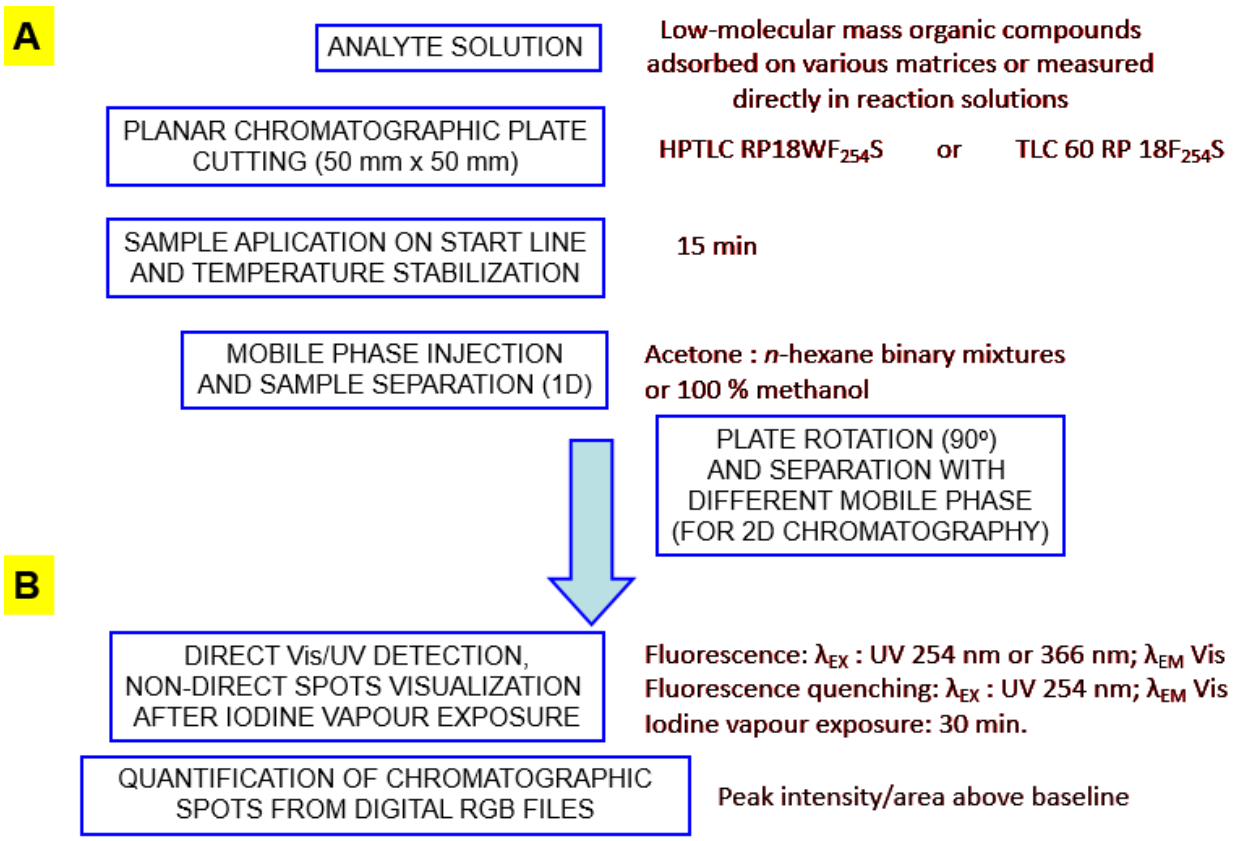


**Figure 16.** Main steps of samples separation using micro-TLC approach with different developing modes (1D and 2D) (**A**) and target components quantification (**B**).

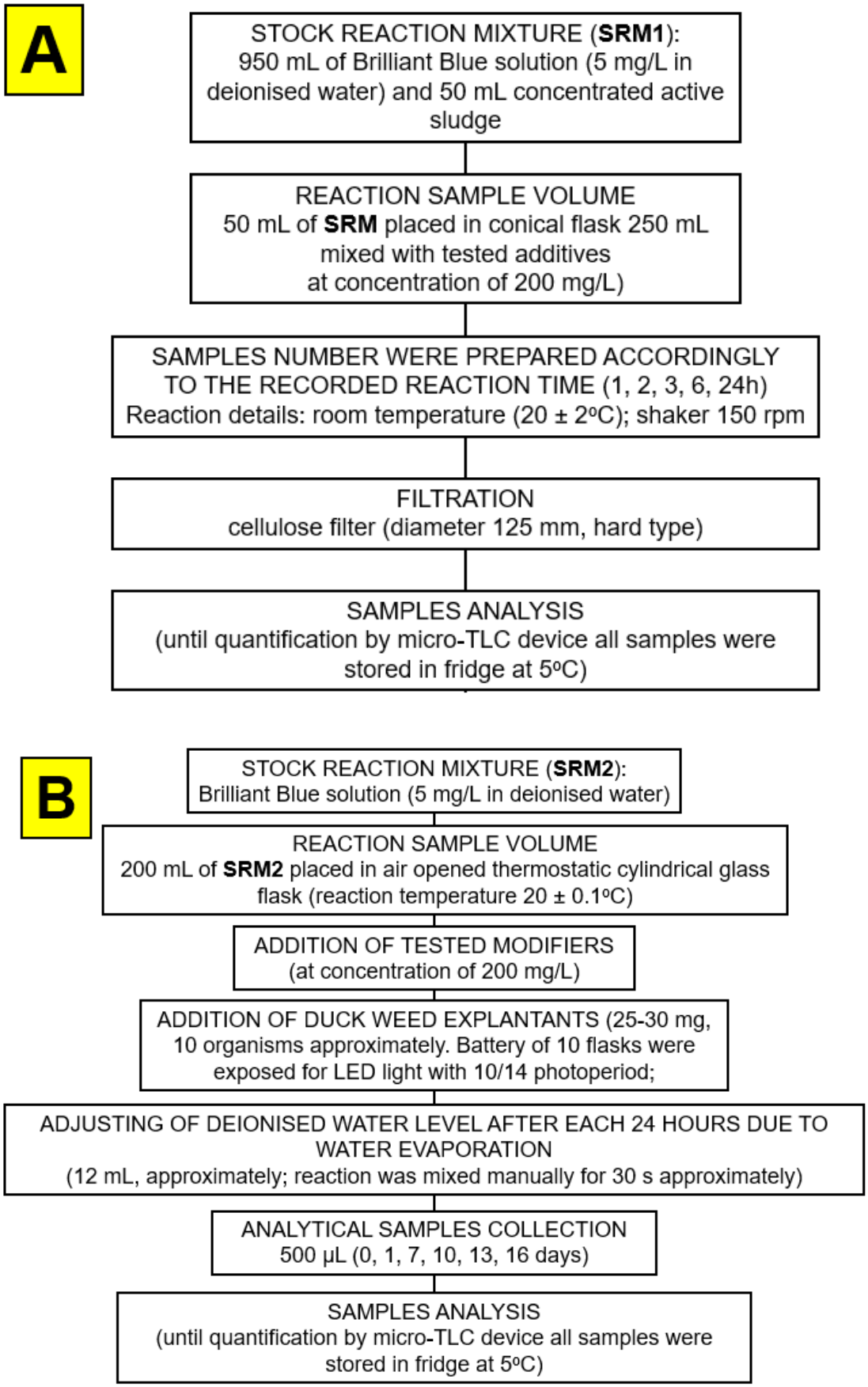


**Figure 17.** Protocol details and experiment sequence of 24 hour (**A**) and 16 days (**B**) tests.

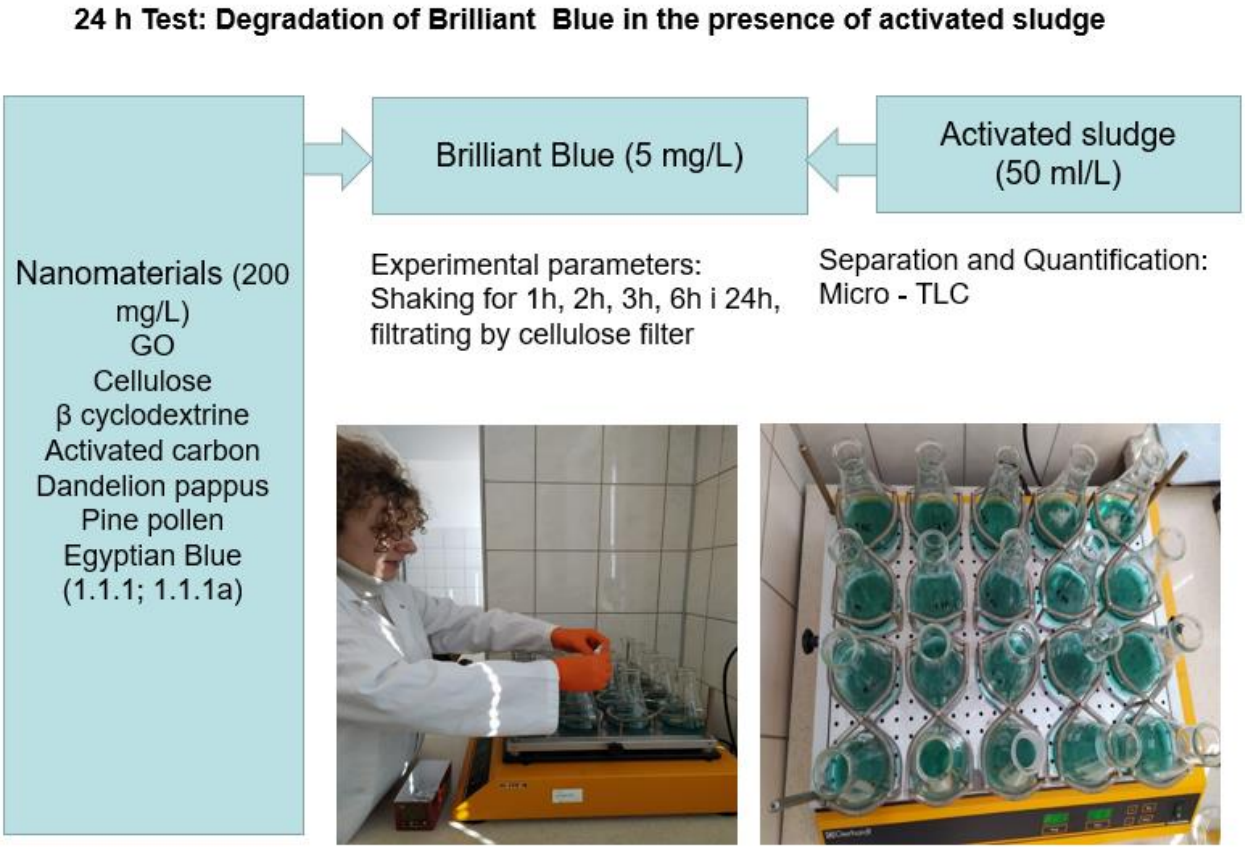


**Figure 18.** General view of conical flasks array used for 24 hours test.

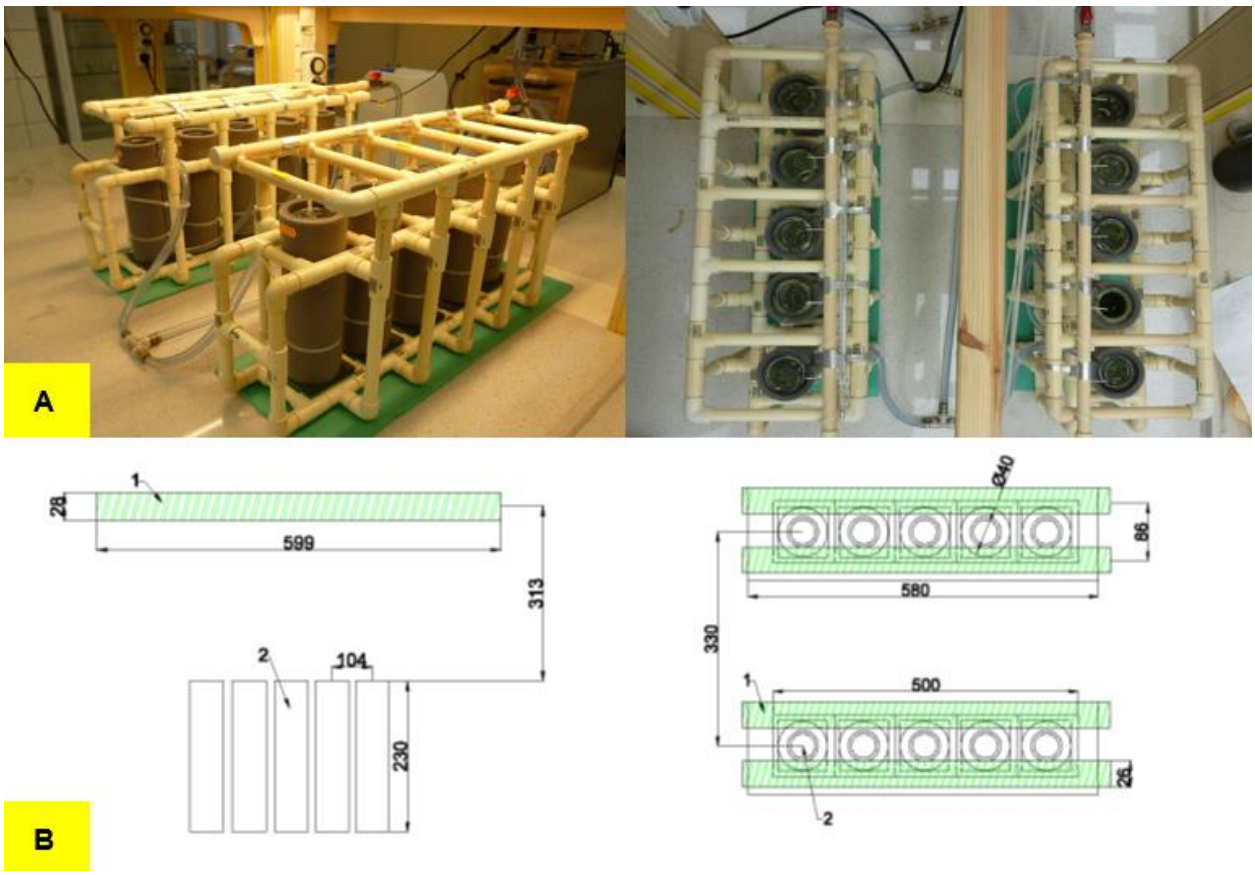


**Figure 19**. General view of duckweed cultivation chambers for 16 days test (**A**) and detailed dimensions of open-air dewar reactors (**B**).

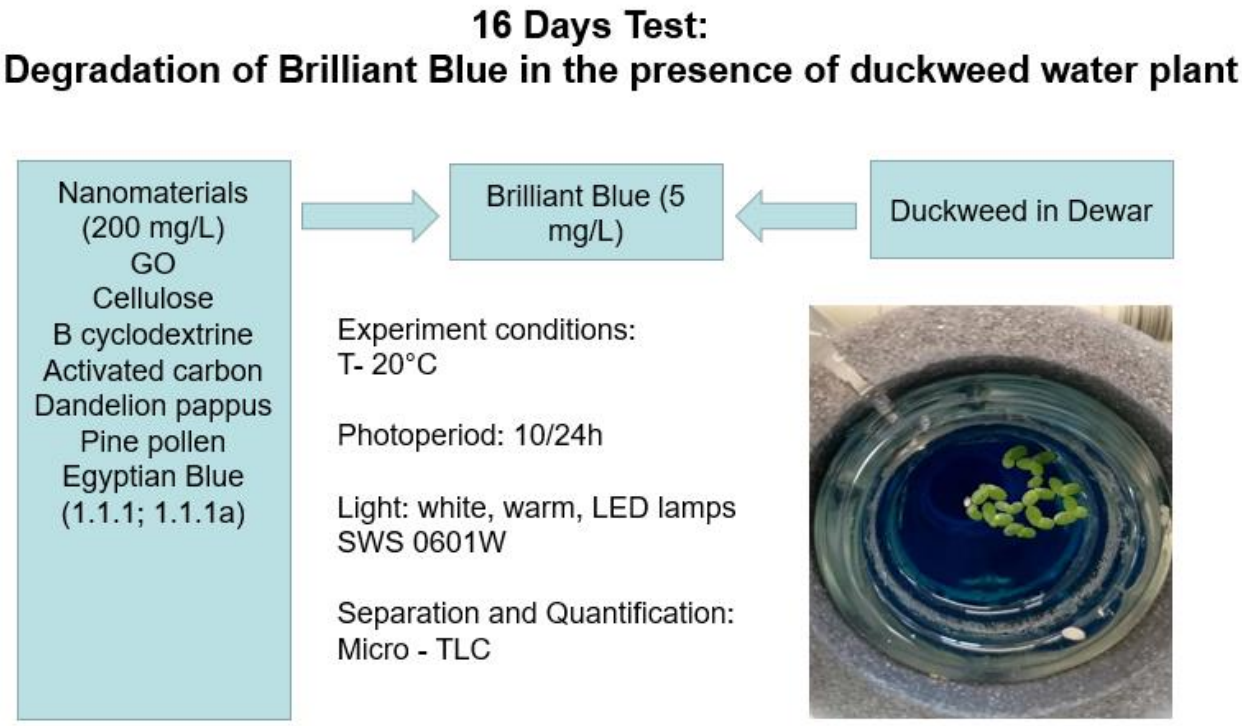


**Figure 20.** Detailed protocol scheme of 16 days test performed for degradation of Brilliant Blue in the presence of duckweed water plant and given nanomaterials

**A**

| MAIN STEPS OF GRAPHENE OXIDE (GO) SYNTHESIS: | OBSERVATIONS AND COMMENTS: |
|---|---|
| **1.** Mixing of graphite powder (0.75g) with solution composed of $H_2SO_4$ (90 mL, 96% w/w) and $H_3PO_4$ (10 mL, 85% w/w) by 30 min using mechanical stirrer (300 rpm).<br>**2.** Slow addition (by 30 min. approximately) of $KMnO_4$ crystals (4.5 g) and mixing for next 2 h. | Reaction container is placed in water bath providing reaction temperature close to 35°C.<br>Black colored suspension is stirred to obtain dark green material. |
| **3.** Reaction mixture stirring (300 rpm) by 18 h at temperature 50°C. | Suspension color is changing to pink-brown. |
| **4.** Cooling of the reaction mixture to room temperature by adding of crushed ice to water bath.<br>**5.** Adding to the reaction mixture: 100 g of crushed ice (prepared using distilled water) and 1.5 mL $H_2O_2$ (30%; slowly using dropper).<br>**6.** Reaction mixture stirring (300 rpm) for 15 min. | This reaction is highly exothermic.<br>Suspension is changing into mustard (yellowish) color. |
| **7.** Rising of graphene oxide sediment; 3 times using 100 mL of HCl 3.5% (v/v) and then 15 times using distilled water to obtain pH = 4, approximately. After each rising GO sample was concentrated by centrifugation (5000 rpm, 10 min.). | Graphene oxide is changing into mahogany color. Sample consistency is transforming to gel form. |
| **8.** Ultrasonication of graphene oxide suspension (40 kHz, 80 W, 1L volume, time: 45 min.). | Graphene oxide consistency changes to a more pouring material. |
| **9.** Centrifugation of graphene oxide suspension (700 rpm, 10 min) to remove non-delaminated graphite residues and remaining residues. | |
| **10.** Drying of graphene oxide suspension (14-22 g/L), which is present in supernatant, on (*i*) Petri dish within air circulated oven (60°C, 18 h) or (*ii*) using lyophilisation method (sample freezing -100°C for 1 h and transferring to evaporation chamber operating at room temperature for 18 h). | After drying in air circulating oven, a dark-brown film was formed.<br>After lyophilisation a light-brown, sponge-like structure was obtained (calculated apparent density: 14-22 mg/mL). |

**B**

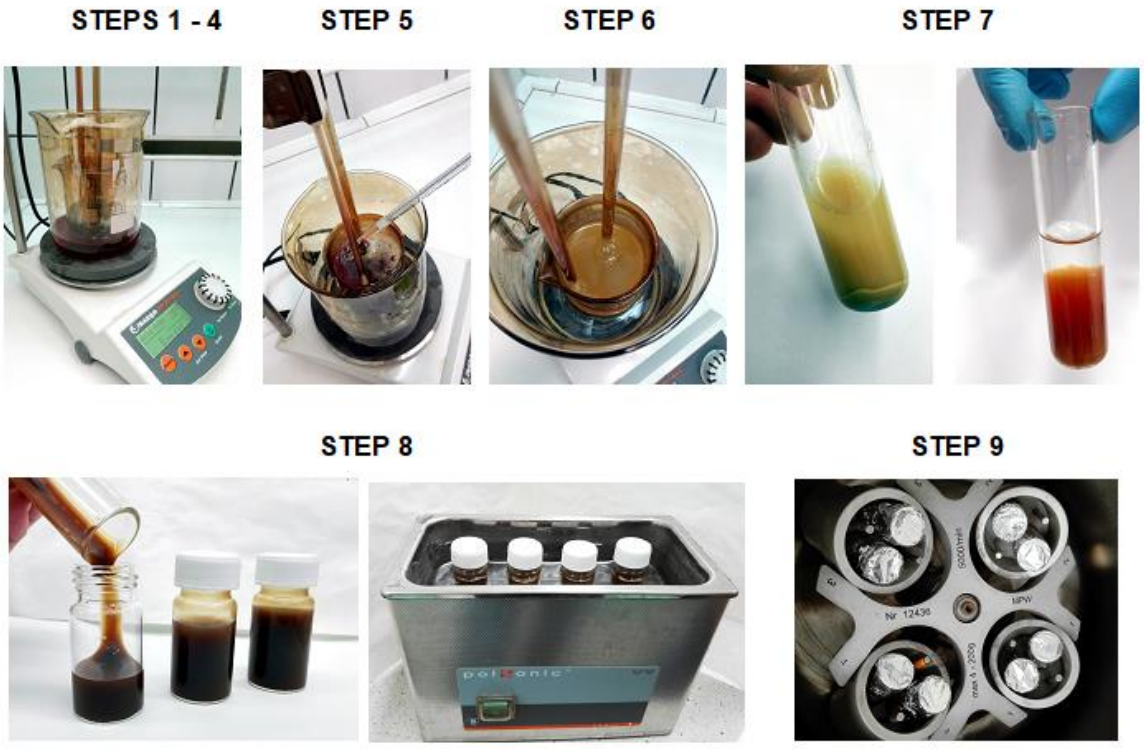


**Figure 21.** Synthesis of graphene oxide: (**A**) sequence of preparation protocol steps using improved Hummers method, (**B**) visualization of key experiment steps.
With permission from CRC Press Taylor & Francis Group **[Zarzycki 2020b]**.

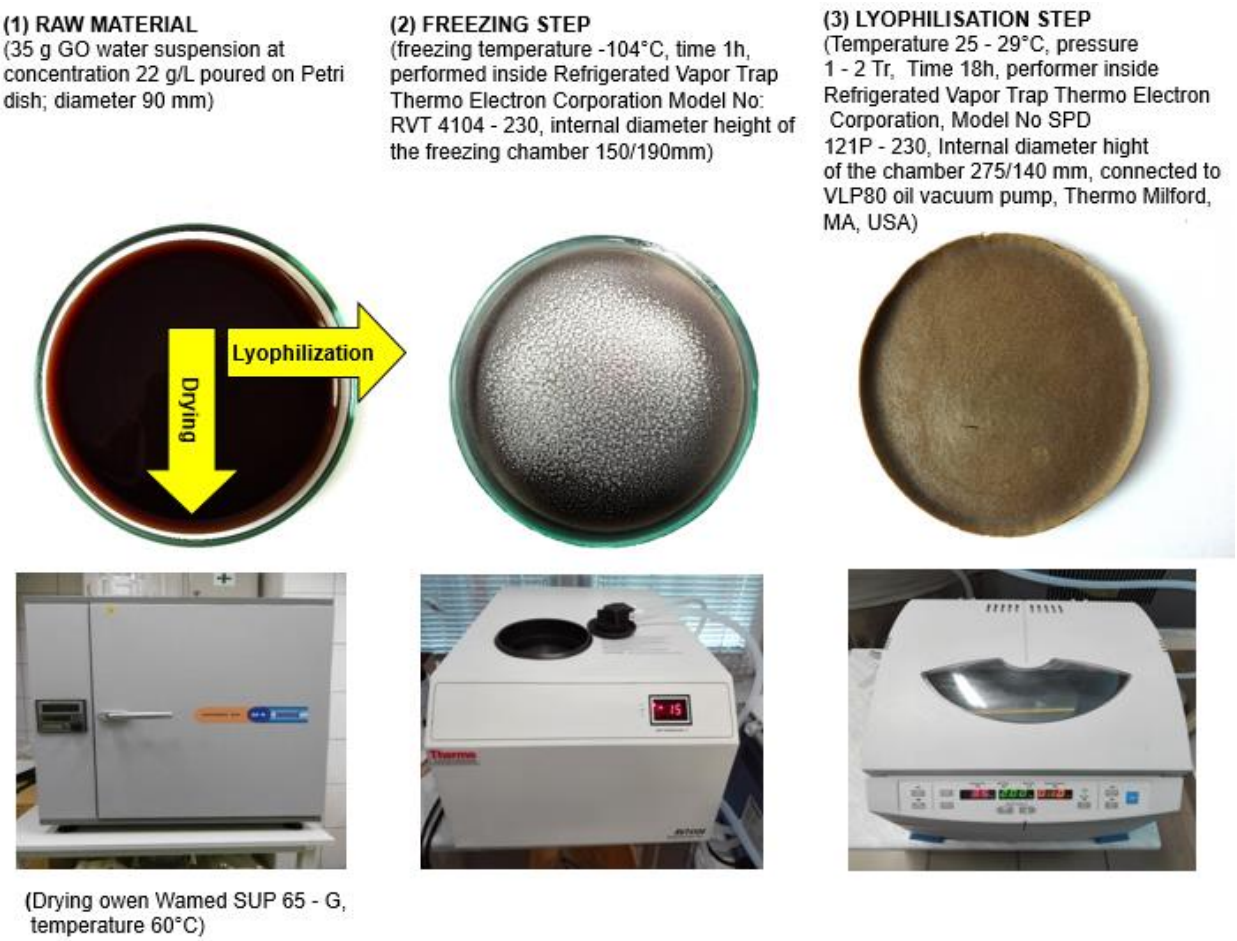


**Figure 22.** Lyophilization protocol of graphene oxide suspension (top), general view of GO during drying process (middle) and equipment (bottom).

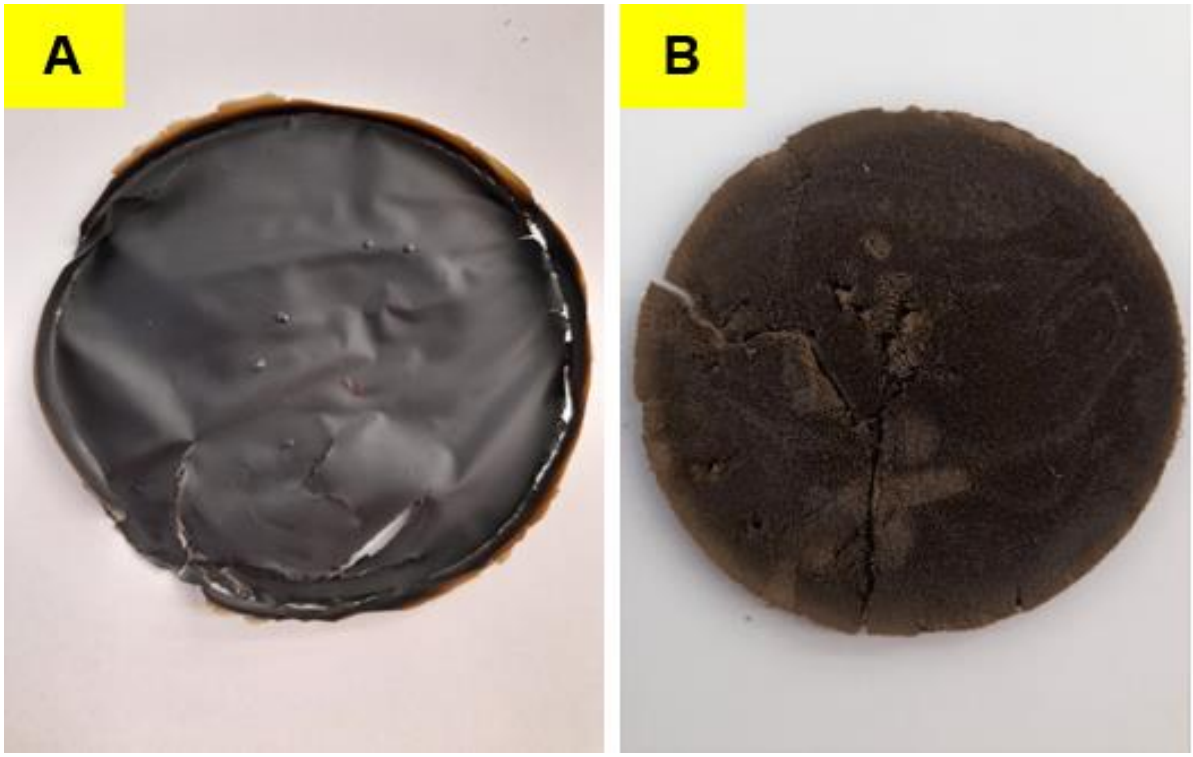


**Figure 23.** Graphene oxide after drying in different conditions: (**A**) air circulated oven and (**B**) lyophilization.

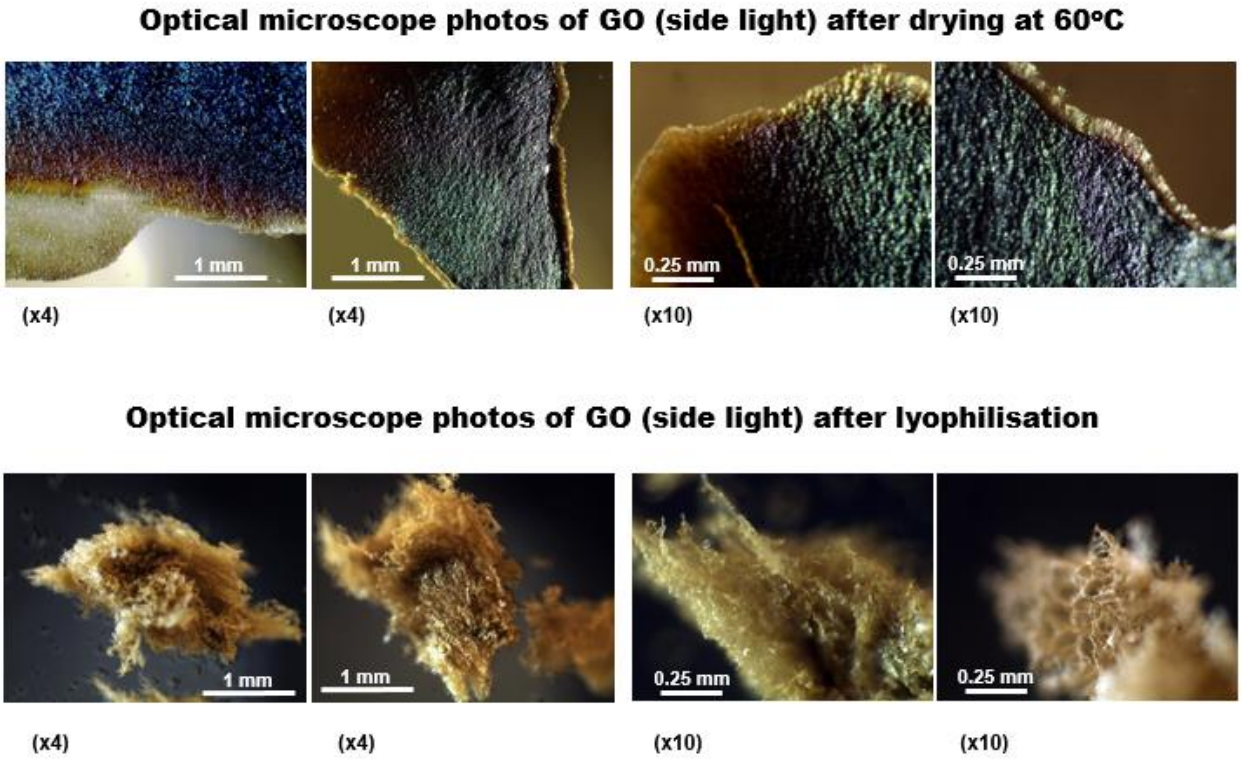


**Figure 24.** Visible light views of graphene oxide samples obtained after different drying conditions using Motic BA310 LED optical microscope (Motic China Group, Ltd., Xiamen, China) equipped with Moticam 3 (3.0 MP USB) CMOS digital camera under side light visualization mode. Digital pictures were acquired using Motic Image Plus 2.0 (Motic China Group Co., Ltd., 2007) software. With permission from CRC Press Taylor & Francis Group **[Zarzycki 2020b]**.

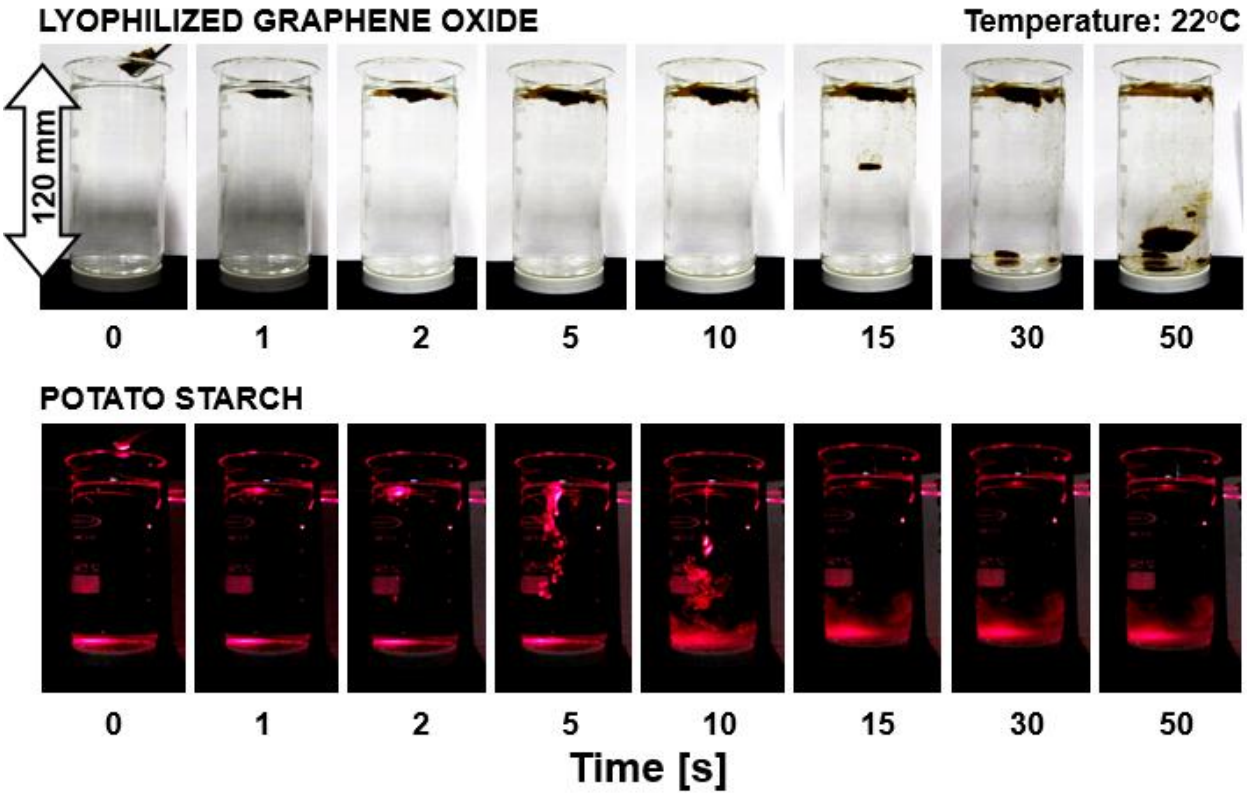


**Figure 25.** Spontaneous wetting, dispersion, and hydration of lyophilized graphene oxide sponge in distilled water (top sequence), in comparison to starch particles (bottom sequence). With permission from CRC Press Taylor & Francis Group **[Zarzycki 2020b]**.

## SEM

**A**

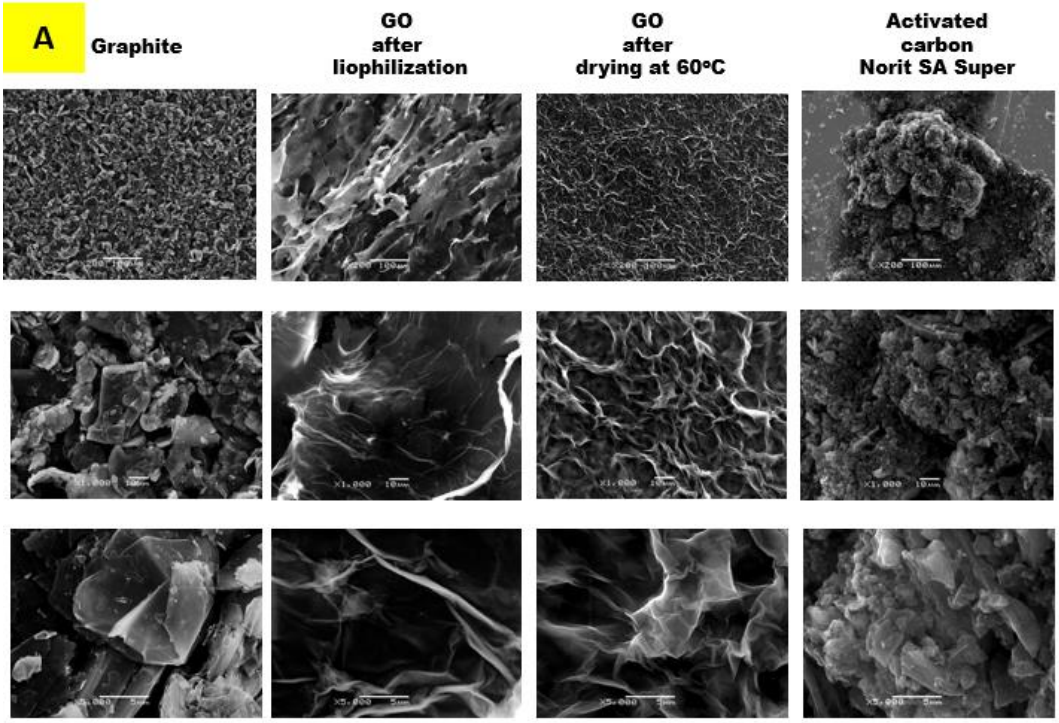


## EDS

**B**

**Graphite**

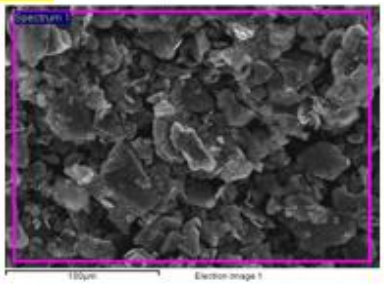

Spectrum processing :
Peak possibly omitted : 6.410 keV

| Element | Weight% | Atomic% |
|---|---|---|
| C | 100.00 | 100.00 |
| **Totals** | **100.00** | |

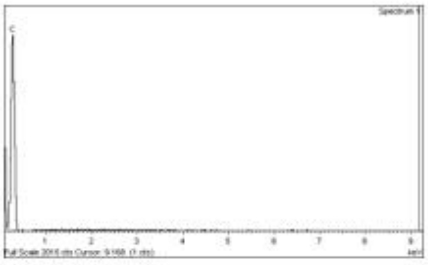

**Norit SA Super**

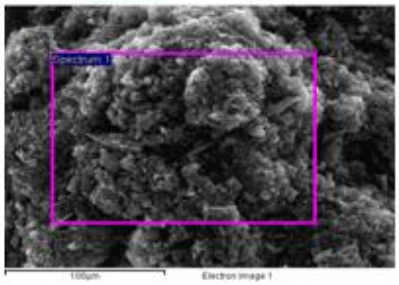

Spectrum processing :
Peak possibly omitted : 2.320 keV

| Element | Weight% | Atomic% |
|---|---|---|
| C | 90.28 | 94.38 |
| O | 5.01 | 3.93 |
| Mg | 0.91 | 0.47 |
| Al | 0.47 | 0.22 |
| Si | 0.54 | 0.24 |
| Ca | 1.51 | 0.47 |
| Fe | 1.28 | 0.29 |
| **Totals** | **100.00** | |

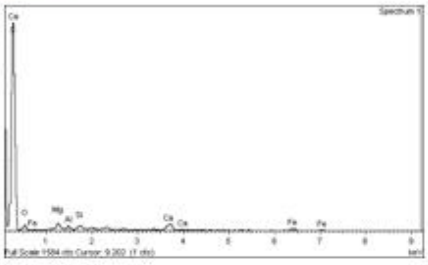

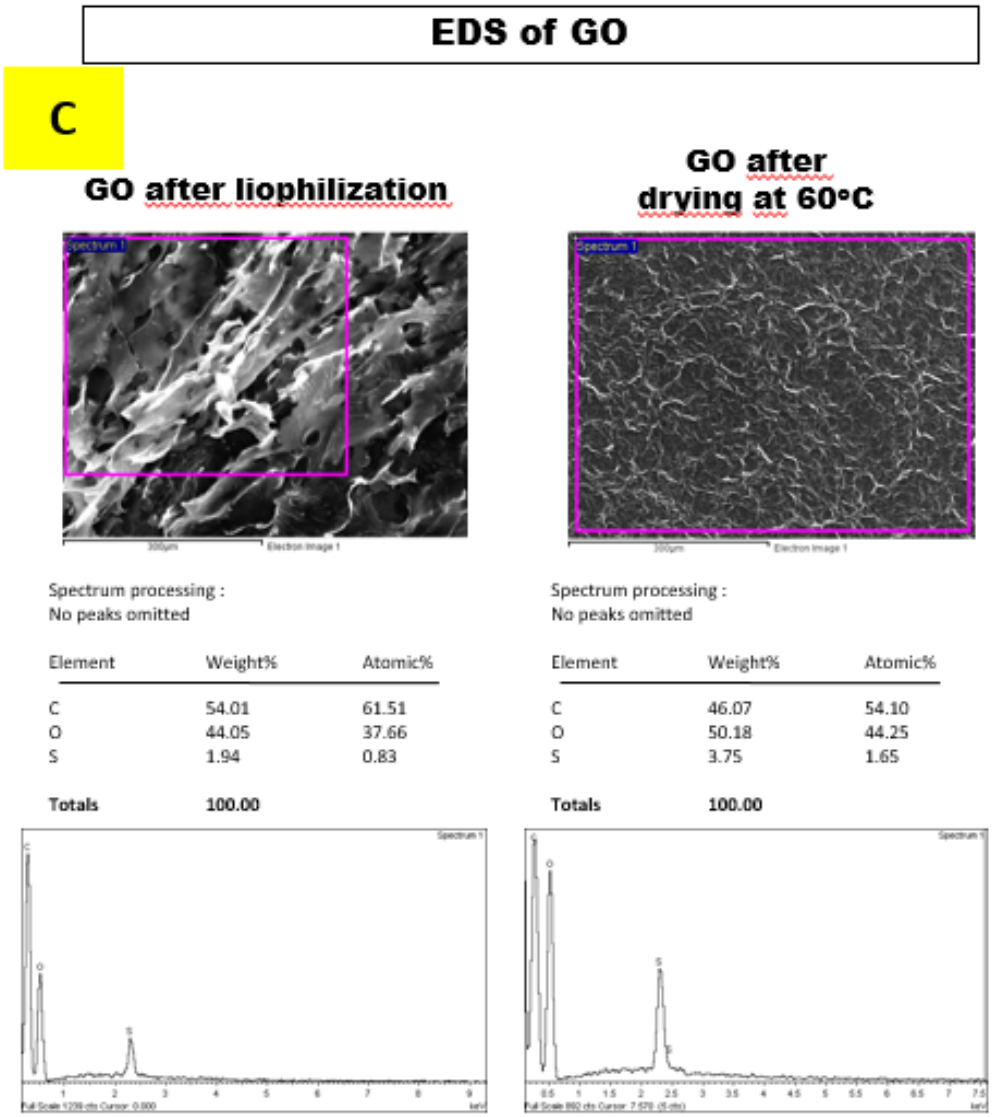


**Figure 26.** SEM images of various carbon materials (**A**) and results of EDS analysis (**B**, **C**). Scanning Electron Microscopy (SEM) and Energy X-ray Dispersive Spectroscopy (EDS) analyses were performed using JEOL JSM-5500LV electron microscope (JEOL Lts, Japan).

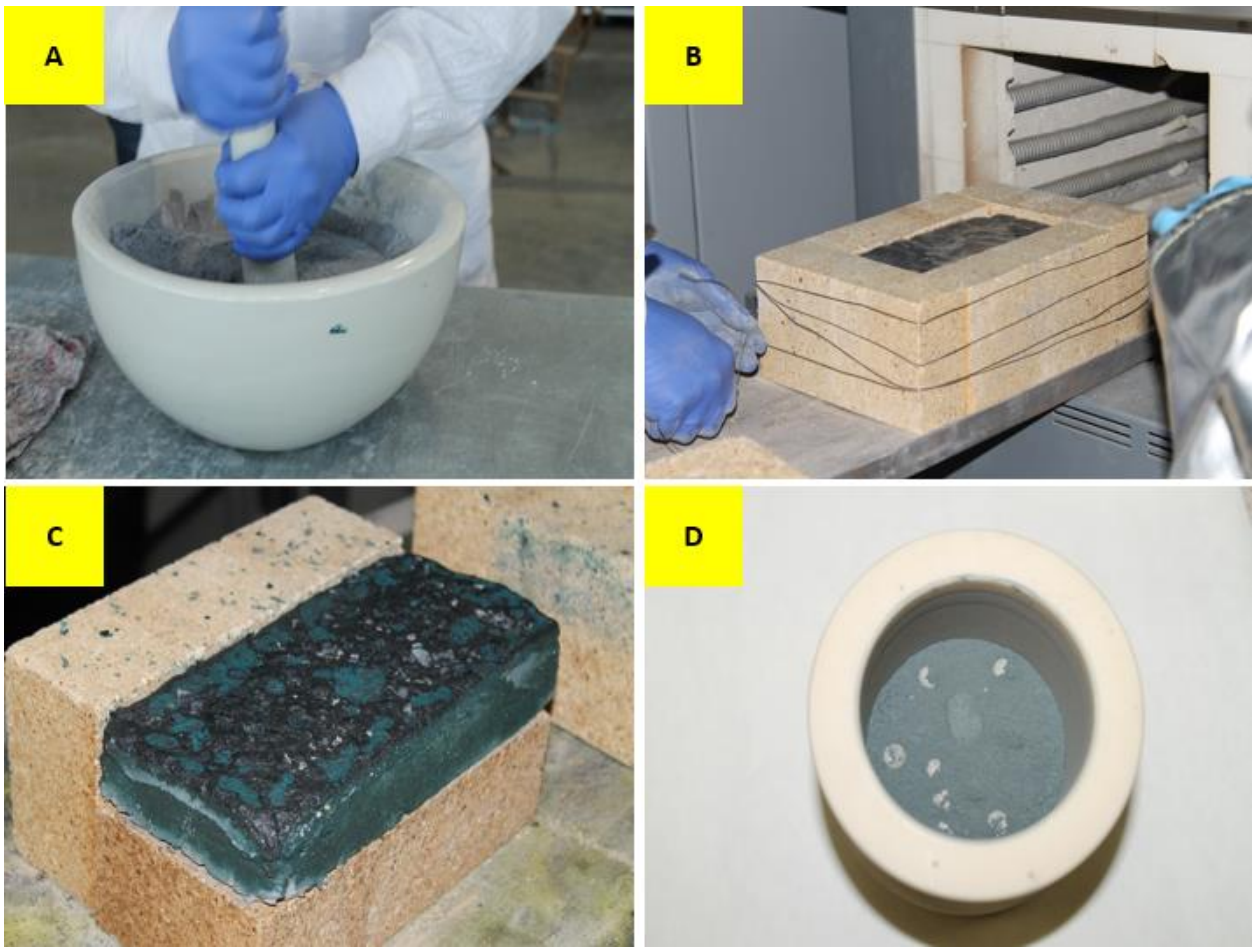


**Figure 27.** Preparation and synthesis steps of raw Egyptian Blue material: manual mixing and grinding of dry chemicals in large ceramic mortar (**A**), placing of water wetted chemicals inside brick container and ceramic oven (**B**); raw EB sinter after first heating step (**C**), automatic mechanical grinding of raw EB material in ball mill prepared for next heating steps (**D**).

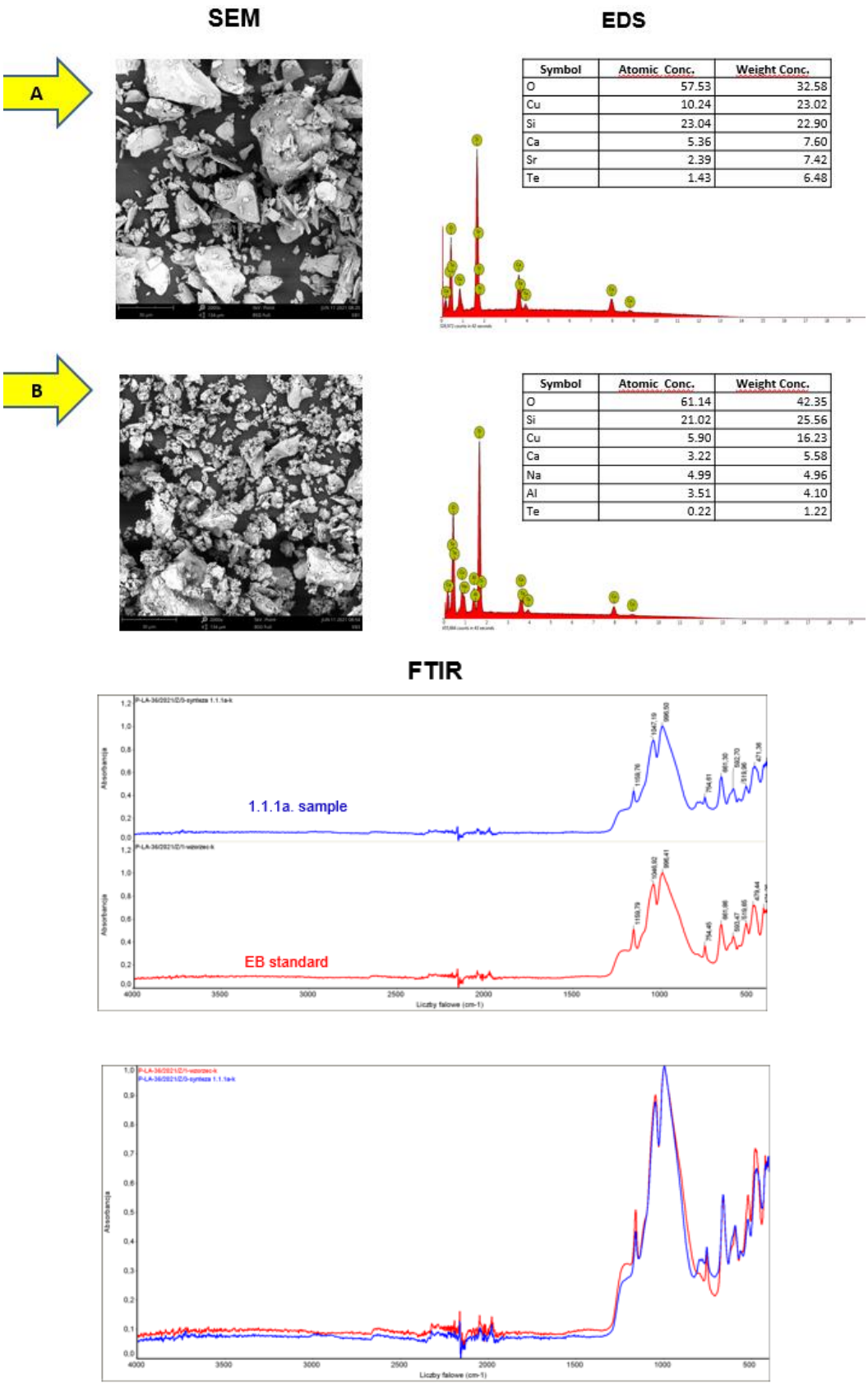


**Figure 28.** Physicochemical analysis of Egyptian Blue commercial standard and dye sythetized sample No 1.1.1a. using SEM, EDS and FTIR.

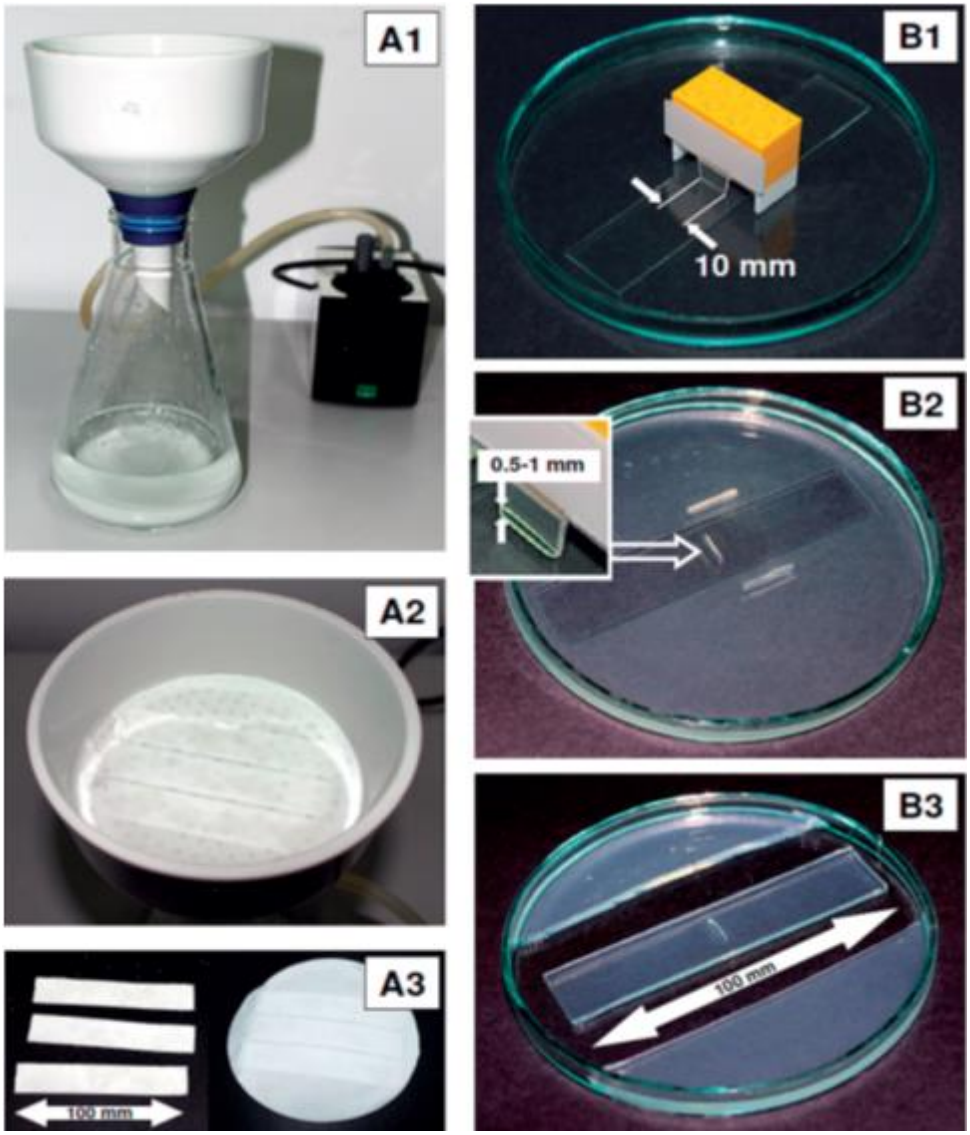


**Figure 29**. Sequence of the main steps for preparation of active thin-layers composed of starch powder on cellulose strips (**A**; 20 mm × 100 mm) and agar layer on glass plate support (**B**; 20 mm ×100 mm). Filtrating of starch suspension through filtrating paper with cellulose strips using ceramic Buchner funnel and vacuum pump (**A1**, **A2**); detaching of starch-cellulose strips from cellulose filter (**A3**); glass plate with sample hole positioning tool inside Petri dish (**B1**); fabricated agar layer with sample hole (**B2**); cut of 0.5 - 1.0 mm thick agar layer on glass plate support (**B3**). With permission from Journal of Planar Chromatography **[Lewandowska 2017]**.

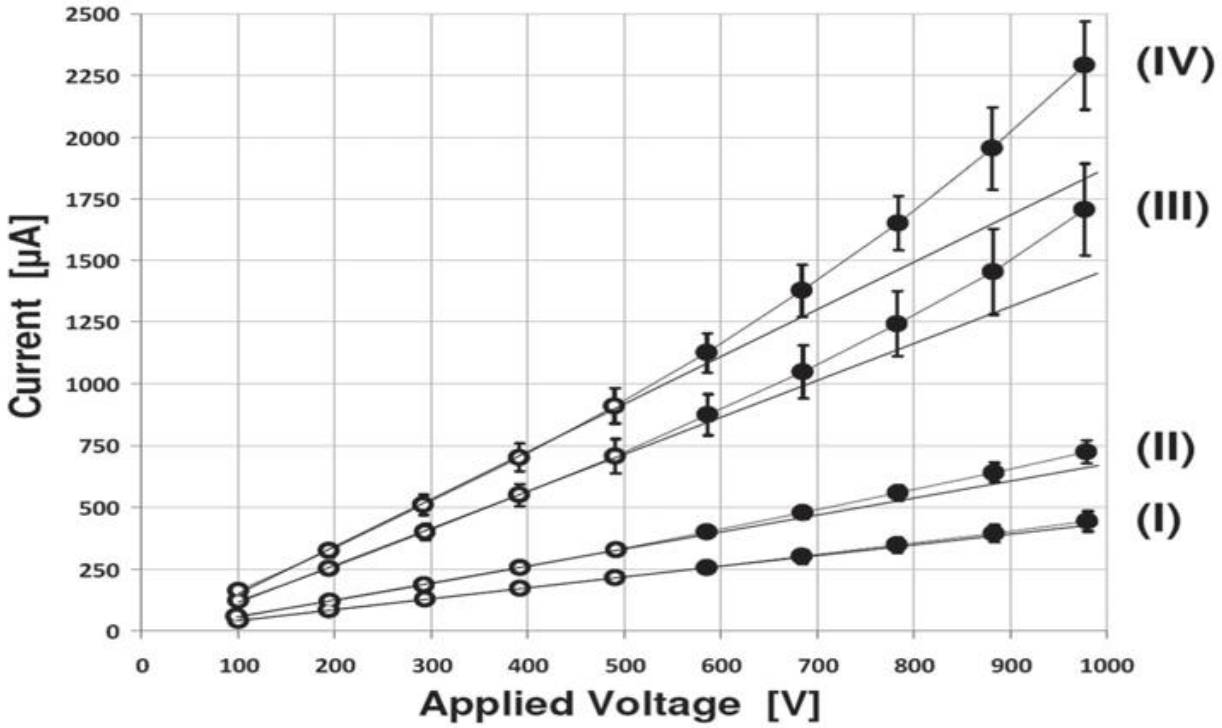


**Figure 30**. Ohm's Law plot illustrating observed current *versus* the applied voltage for different water-based electrolytes working on cellulose strip (200 mm × 20 mm × 0.1 mm). Electrolyte label: boric acid 100 mM, pH = 4.3 (I); 1:1 mixture of boric acid 90 mM and Tris base 90 mM, pH = 8.2 (II); boric acid 100 mM titrated with NaOH 1 M to obtain pH = 8.5 (III); formic acid 100 mM, pH = 2.4 (IV). With permission from Journal of Planar Chromatography **[Lewandowska 2017]**.

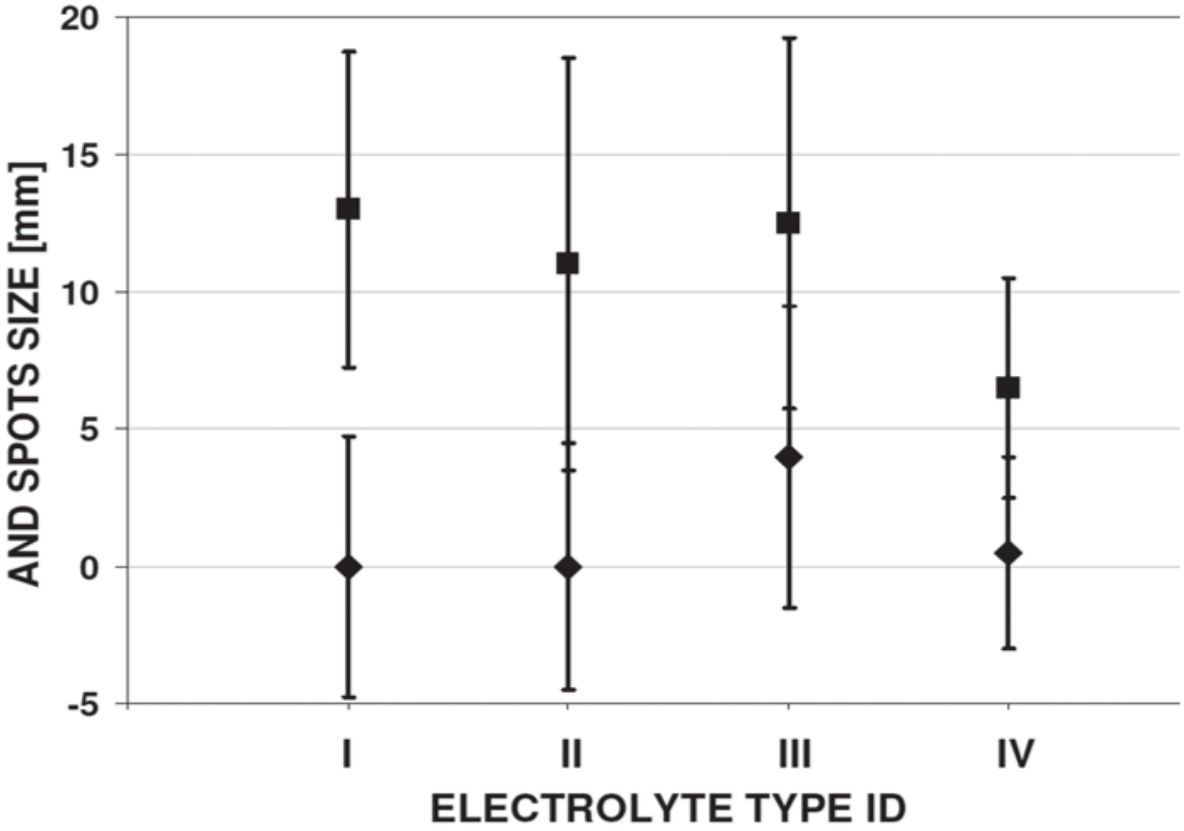


**Figure 31**. Migration distances of target dyes (measured from the application point to the spot center): Ponceau 4R (black squares) and Methyl Red (black diamonds) observed on cellulose strip (filtrating paper No.1) using different electrolytes. The bars connected to the points on this graph correspond to the dye spot size (peak base). Separation conditions: Δ*V* = 500 V; electrophoresis run time, 10 min; separated mass: 2.5 µg of each dye. Electrolyte label: boric acid 100 mM, pH = 4.3 (I); 1:1 mixture of boric acid 90 mM and Tris base 90 mM, pH = 8.2 (II); boric acid 100 mM titrated with NaOH 1 M to obtain pH = 8.5 (III); formic acid 100 mM, pH = 2.4 (IV). With permission from Journal of Planar Chromatography **[Lewandowska 2017]**.

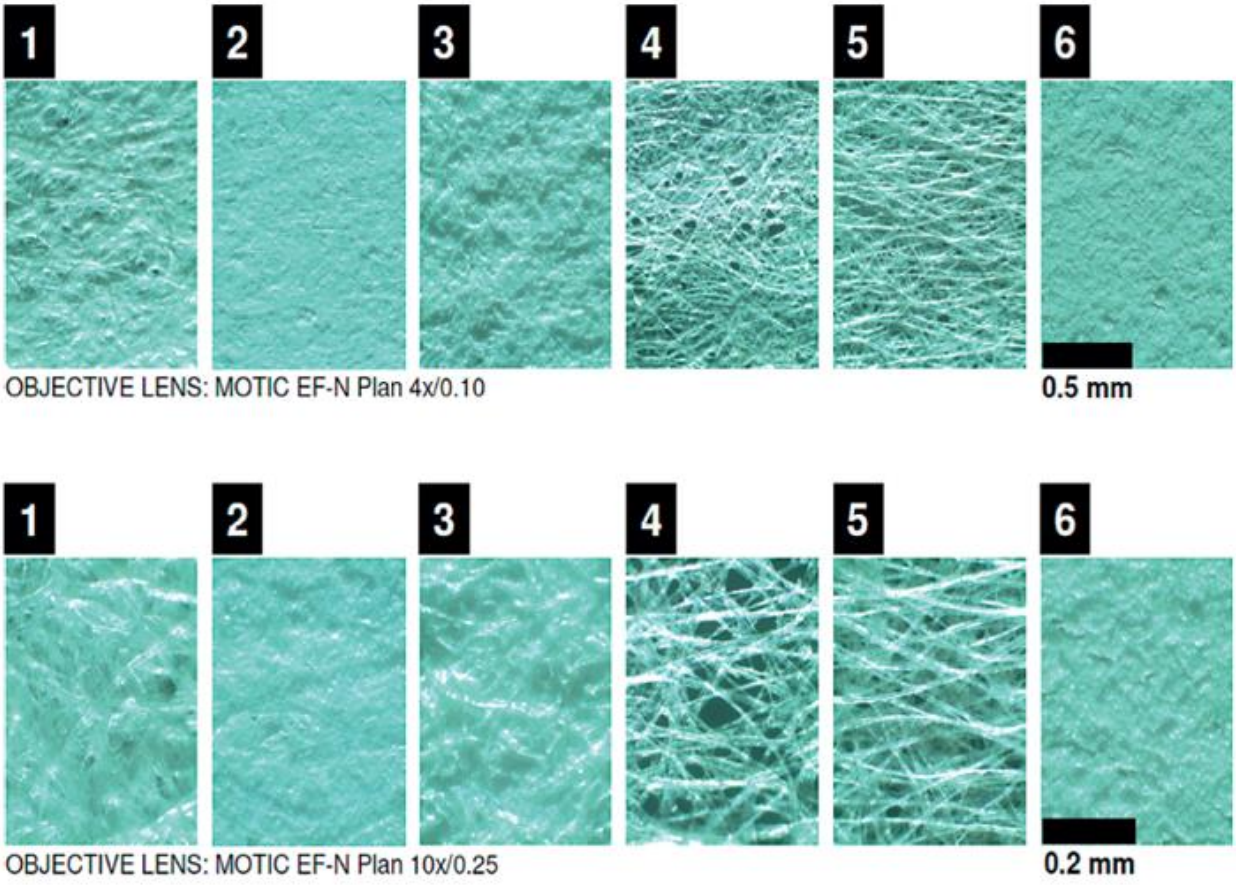


**Figure 32**. Optical microscope view of cellulose materials investigated using side light visualization mode. Sample labels: filtrating paper (**1**); office paper (**2**); Whatman chromatography paper (**3**); thin Japanese paper (**4**); thick Japanese paper (**5**); and TLC cellulose (**6**). With permission from Journal of Planar Chromatography **[Lewandowska 2017]**.

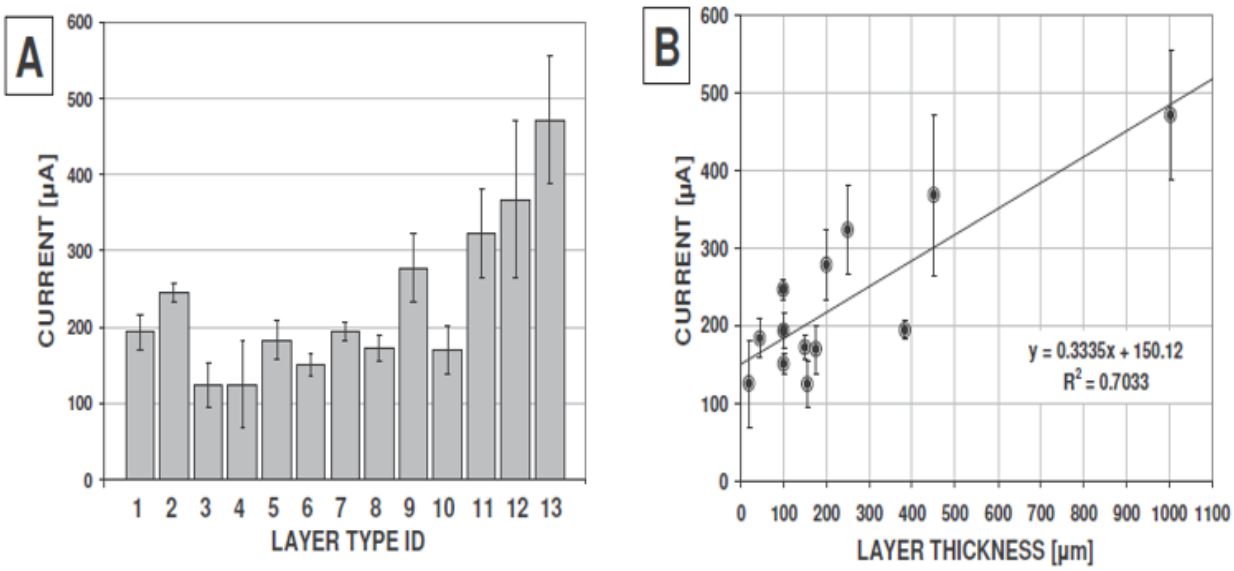


**Figure 33**. Current values measured on different layers (**A**) and the relationship between current and layer thickness (**B**). Sample labels: filtrating paper (**1**); office paper (**2**); Whatman chromatography paper (**3**); thin Japanese paper (**4**); thick Japanese paper (**5**); TLC cellulose (**6**); potato starch (**7**); TLC polyamide (**8**), TLC silica gel 60 W (**9**), HPTLC silica gel RP-18W (**10**), TLC aluminum oxide (**11**), nutrient agar 451 µm (**12**), nutrient agar 1003 µm (**13**). Electrophoresis conditions: applied voltage $\Delta V$ = 500 V; run time, 20 min; running electrolyte: boric acid 100 mM, pH = 4.3 (I). With permission from Journal of Planar Chromatography **[Lewandowska 2017]**.

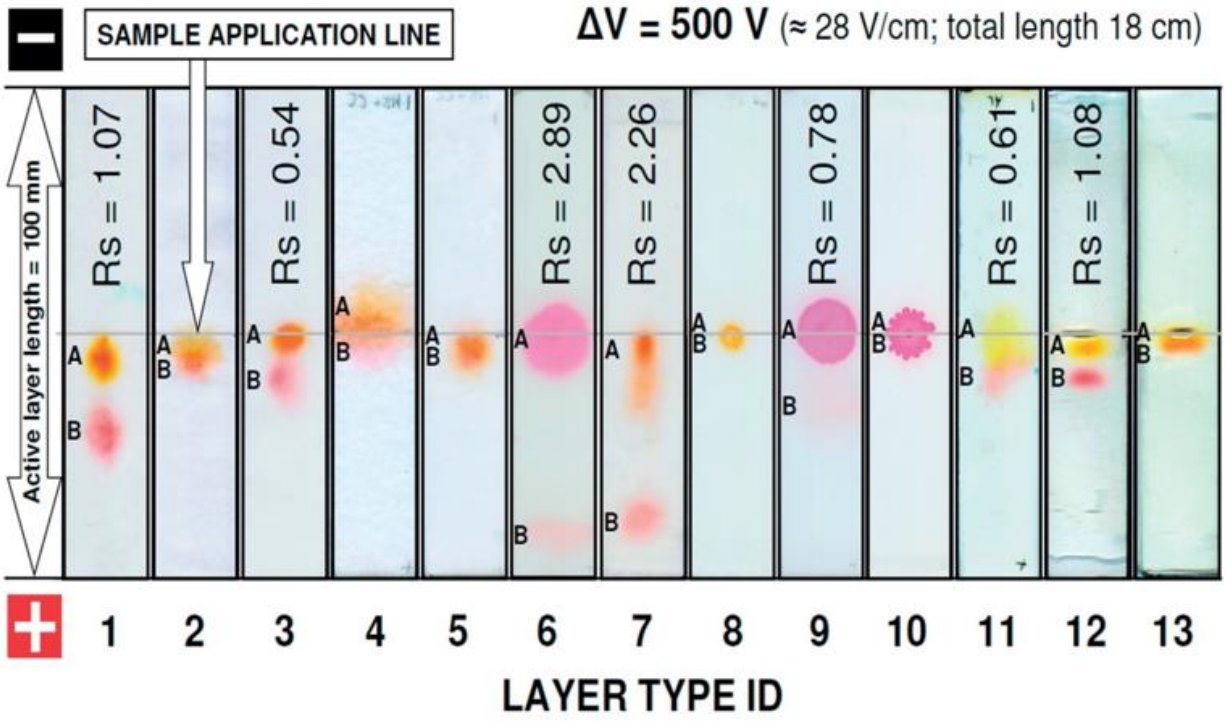


**Figure 34.** Electroplanar separation of Methyl Red (**A**) and Ponceau 4R (**B**) dyes on various layers. Sample labels: filtrating paper (**1**); office paper (**2**); Whatman chromatography paper (**3**); thin Japanese paper (**4**); thick Japanese paper (**5**); TLC cellulose (**6**); potato starch (**7**); TLC polyamide (**8**), TLC silica gel 60 W (**9**), HPTLC silica gel RP-18W (**10**), TLC aluminum oxide (**11**), nutrient agar 451 μm (**12**), nutrient agar 1003 μm (**13**). Electrophoresis conditions: applied voltage Δ*V* = 500 V; run time, 20 min; separated mass: 1.25 μg of each dye; running electrolyte: boric acid 100 mM, pH = 4.3; scanned as the wet strips. With permission from Journal of Planar Chromatography **[Lewandowska 2017]**.

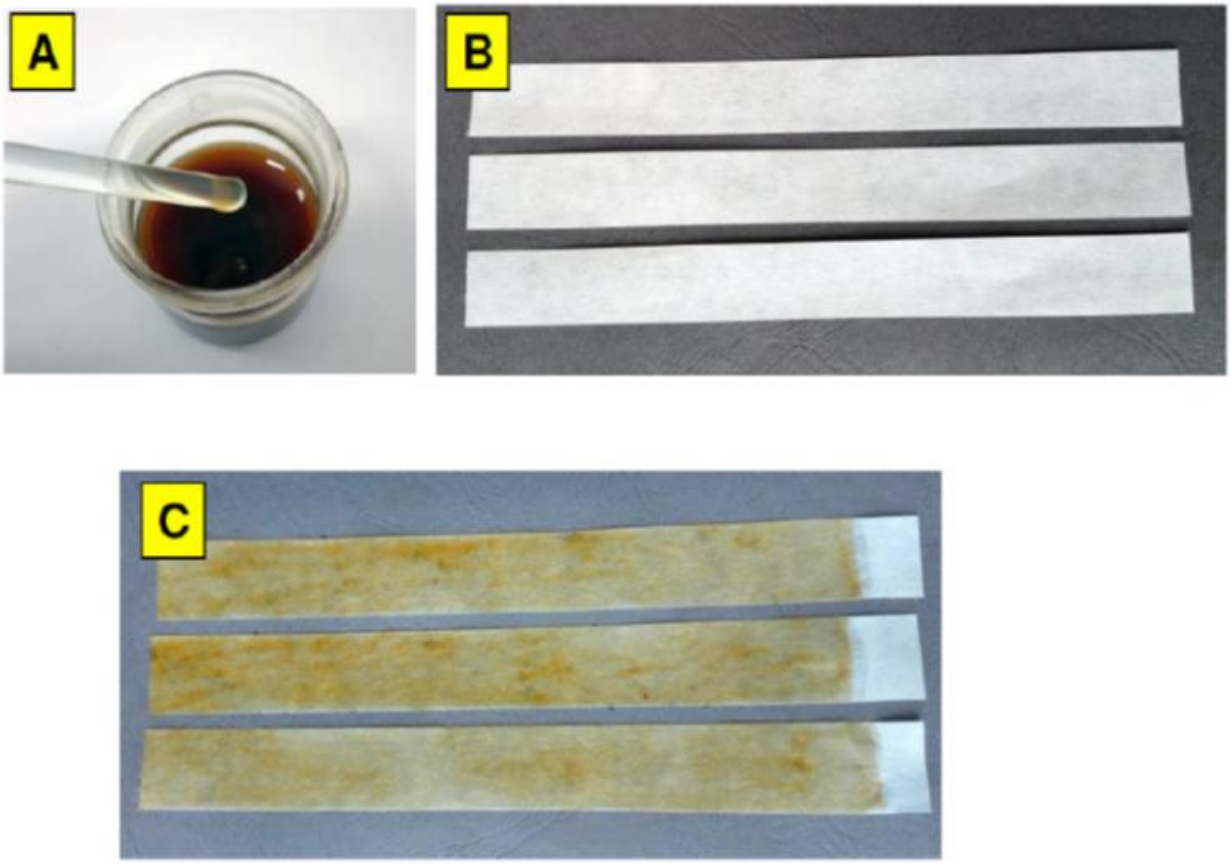


**Figure 35.** Manual application of graphene oxide water suspension with GO concentration ranging between 14–22 mg/mL (**A**) on filtrating paper strips: 200 mm × 20 mm, paper, thickness 100 µm (**B,C**). With permission from CRC Press Taylor & Francis Group **[Zarzycki 2020b]**.

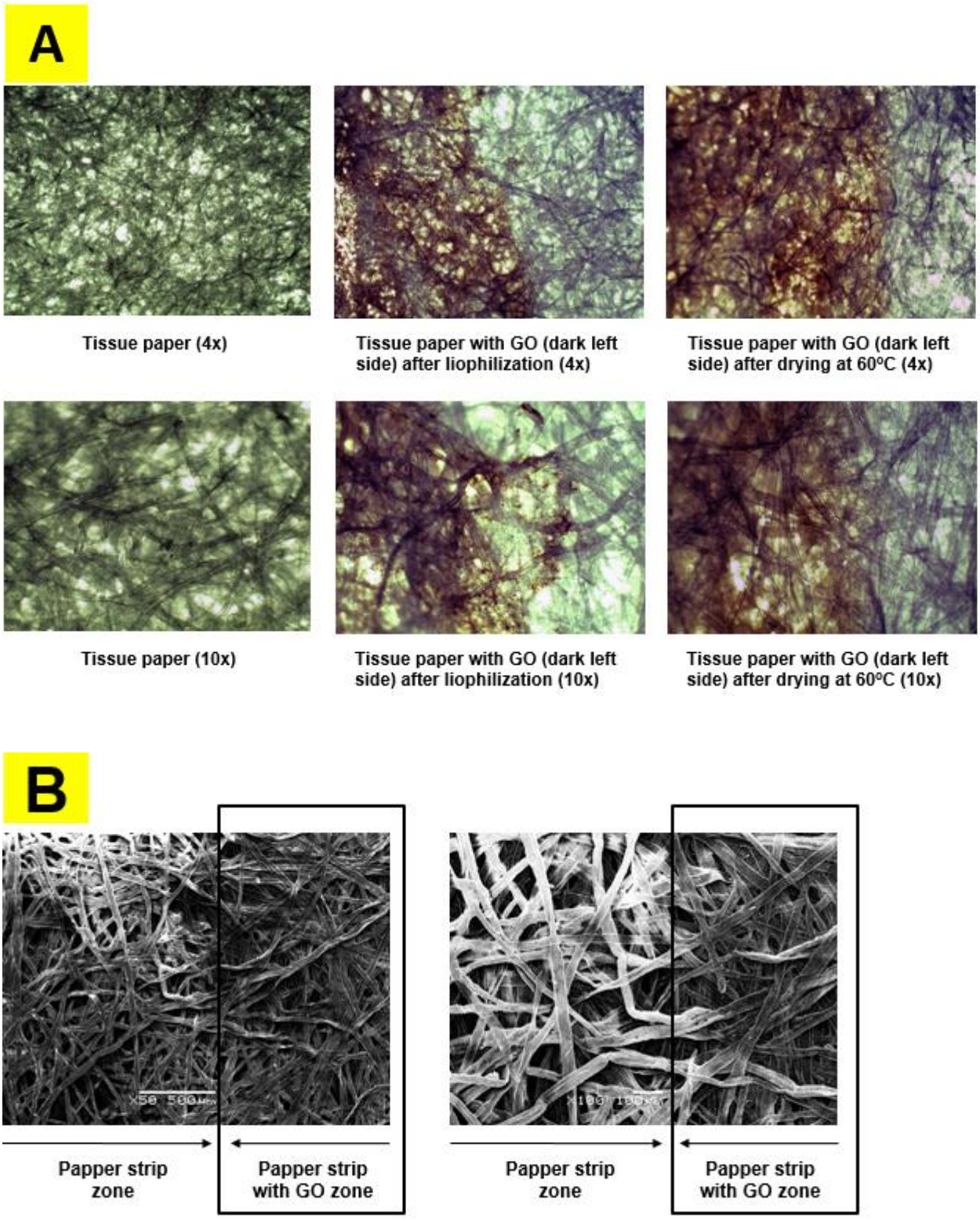


**Figure 36**. Cellulose fibers from filtrating paper coated with graphene oxide: (**A**) visible light views and (**B**) SEM images. With permission from CRC Press Taylor & Francis Group **[Zarzycki 2020b]**.

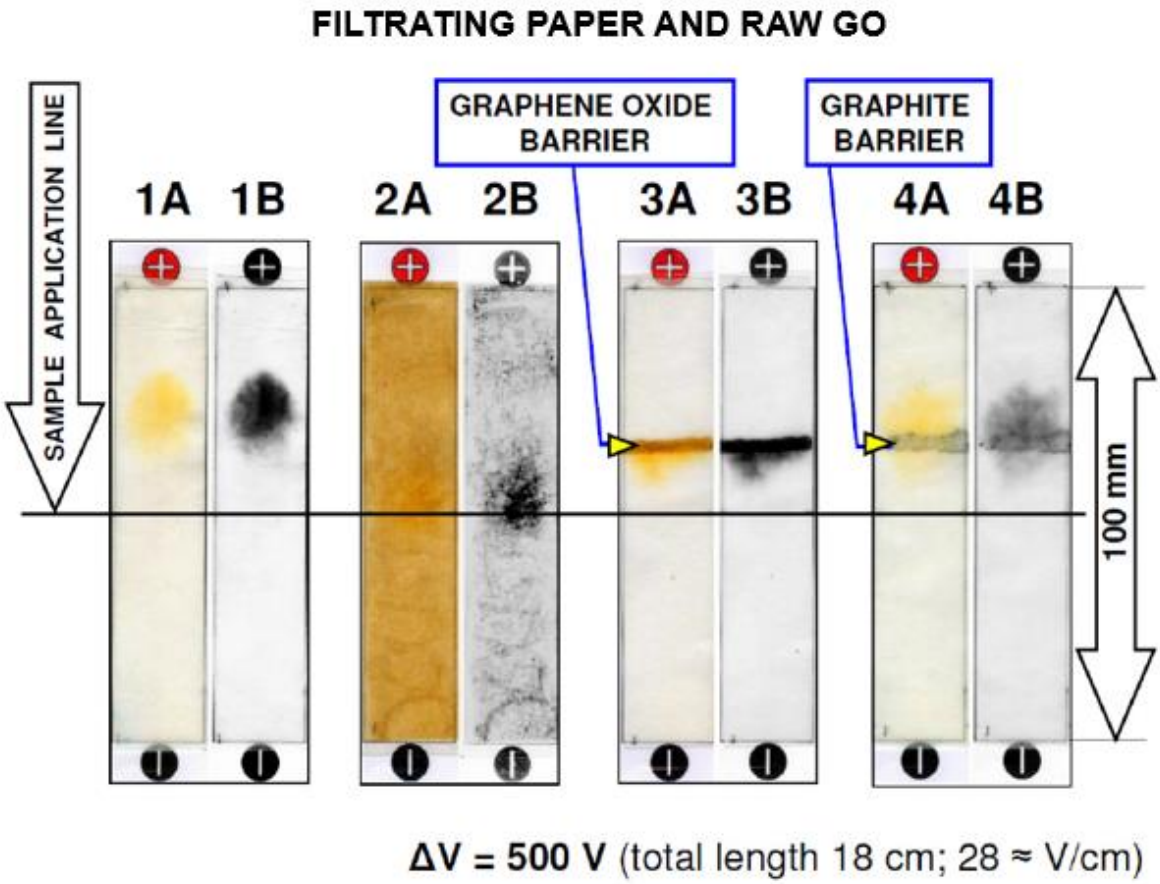


**Figure 37.** Electroplanar migration of Sunset Yellow dye on cellulose strips (filtrating paper, active layer length 100 mm): (**1A, 1B**) blank cellulose layer, (**2A, 2B**) cellulose coated with raw graphene oxide (GO applied from the top and bottom sides), (**3A, 3B**) cellulose strips with raw graphene oxide wall (applied to the top side), (**4A, 4B**) cellulose strips with graphite wall (applied to the top side); Electrophoresis conditions: applied voltage ΔV = 500 V; run time = 20 minutes; applied dye mass: 2.5 μg; running electrolyte: boric acid 100 mM, pH = 4.9; scanned as the wet strips. **A**—RGB picture with contrast auto-balance general filter applied; **B**—blue channel extracted from RGB picture. With permission from CRC Press Taylor & Francis Group **[Zarzycki 2020b]**.

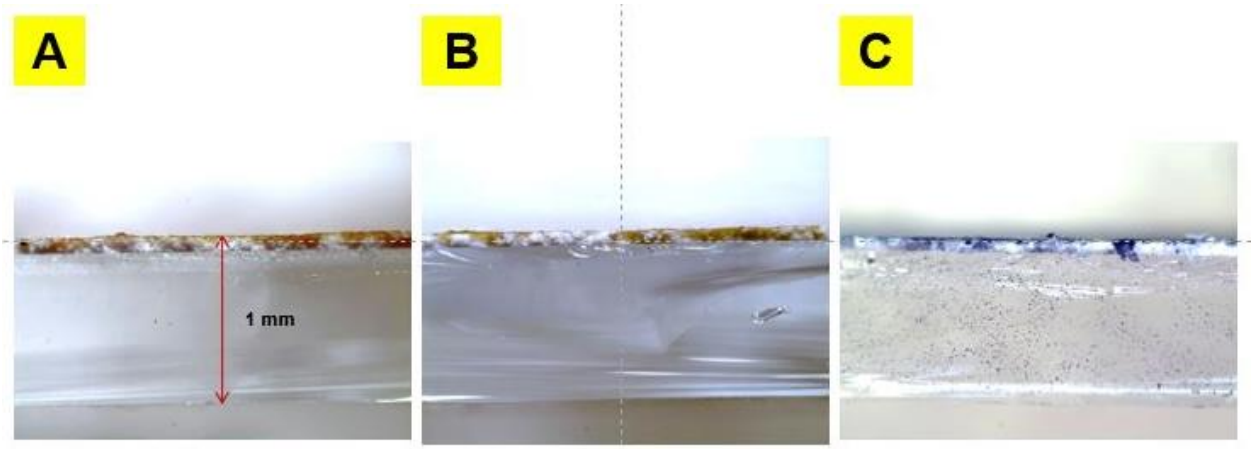


**Figure 38.** Cross-section of glass-based TLC plate with cellulose stationary phase (100 µm), manually coated with GO suspension in distilled water and dried at room temperature (**A**, raw GO suspension; **B**, lyophilized GO reconstituted in distilled water; **C**, activated carbon Norit Super SA). With permission from CRC Press Taylor & Francis Group **[Zarzycki 2020b]**.

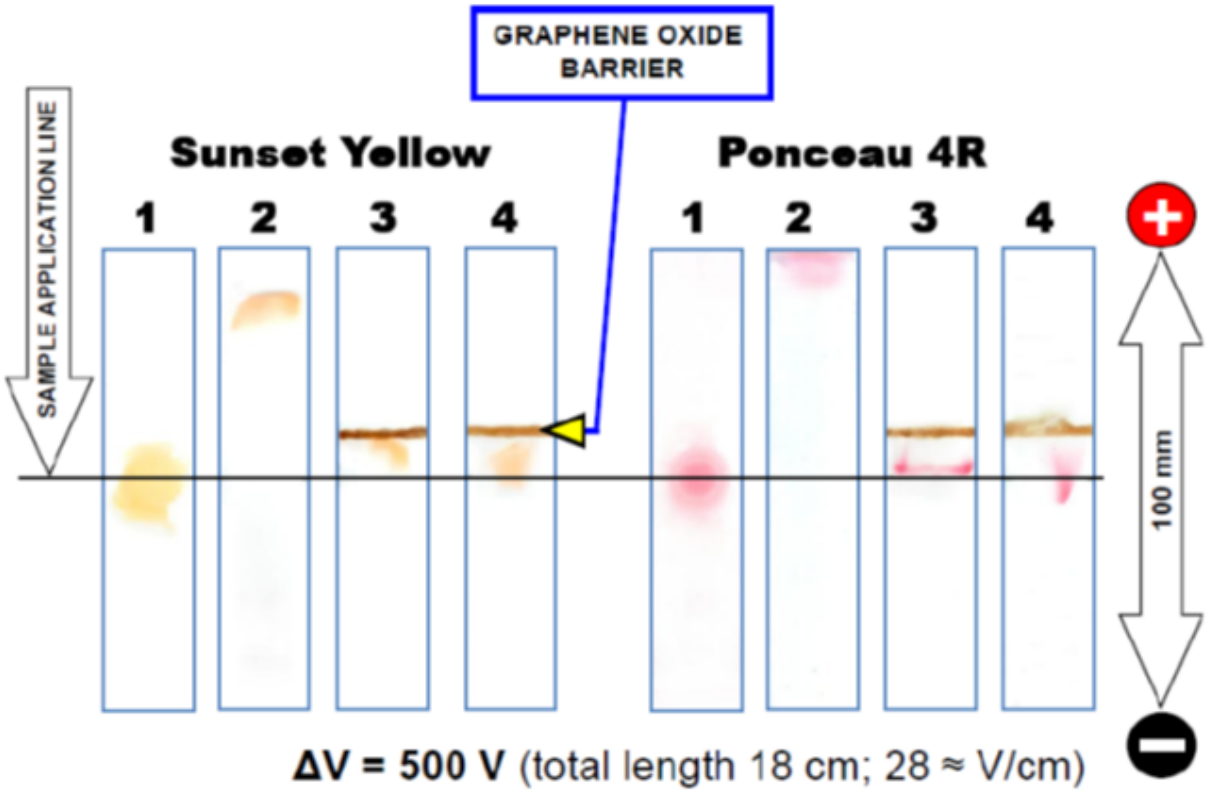


**Figure 39.** Electroplanar migration of Sunset Yellow and Ponceau 4R dyes on TLC cellulose plates: (**1**) dye sample application, (**2**) after 20 minutes electrophoresis, (**3**) after 20 minutes electrophoresis in the presence of raw graphene oxide wall, (40) after 20 minutes electrophoresis in the presence of lyophilized graphene oxide wall, Electrophoresis conditions: applied voltage ΔV = 500 V; run time = 20 minutes; applied dye mass: 2.5 µg; running electrolyte: boric acid 100 mM, pH = 4.9; scanned as the wet strips. Concentration of graphene in water suspension used for preparation of GO barriers was 22.7 mg/mL. With permission from CRC Press Taylor & Francis Group **[Zarzycki 2020b]**.

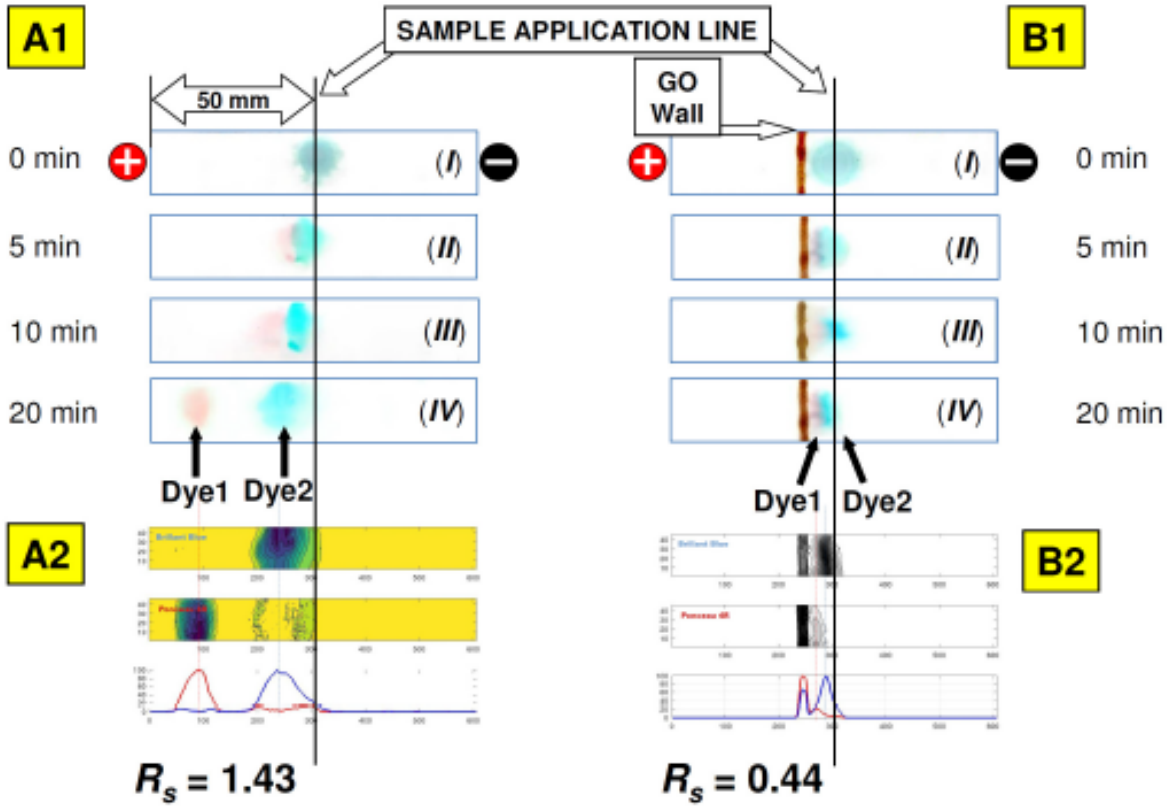


**Figure 40.** Electroplanar separation of Brilliant Blue and Ponceau 4R dyes mixture without and with GO vertical wall (perpendicularly to electromigration flow direction). Separated dyes: and Ponceau 4R (Dye 1) Brilliant Blue (Dye 2). Presented strips correspond to time sequence 0, 5, 10, and 20 minutes of electroseparation on plain cellulose based TLC plate (**A1**) and with graphene oxide barrier (**B1**). **A2** and **B2** gradient maps and profiles correspond to **A1** (IV) and **B1** (IV) strips. GO barrier was prepared from lyophilized material. Concentration of graphene in water suspension used for preparation of GO barriers was 22.7 mg/mL. Planar electrophoresis was performed on cellulose TLC plate using running electrolyte composed of boric acid 100 mM (pH 4.9). Remaining electrophoresis conditions: applied voltage ΔV = 500 V; separated mass: 1.25 µg of each dye. Resolution parameter (Rs) was calculated using formula (Rs) = 2(Lmig1 - Lmig2)/(Wb1 + Wb2), where Lmig1, Lmig2 denote migration distance of spot measured at spot maximum profile and Wb1, Wb2 correspond to peak base width of substance 1 and 2, assuming that substance 1 migrate far from start line than substance 2 (Rs ≥ 0). Total length of strips = 18 cm with 10 cm of TLC active layer (≈28 V/cm). Images of microelectropherograms were modified (a global balance filters were applied) to increase the contrast for spots for visual evaluation and printing. With permission from Elsevier **[Zarzycki 2022]**.

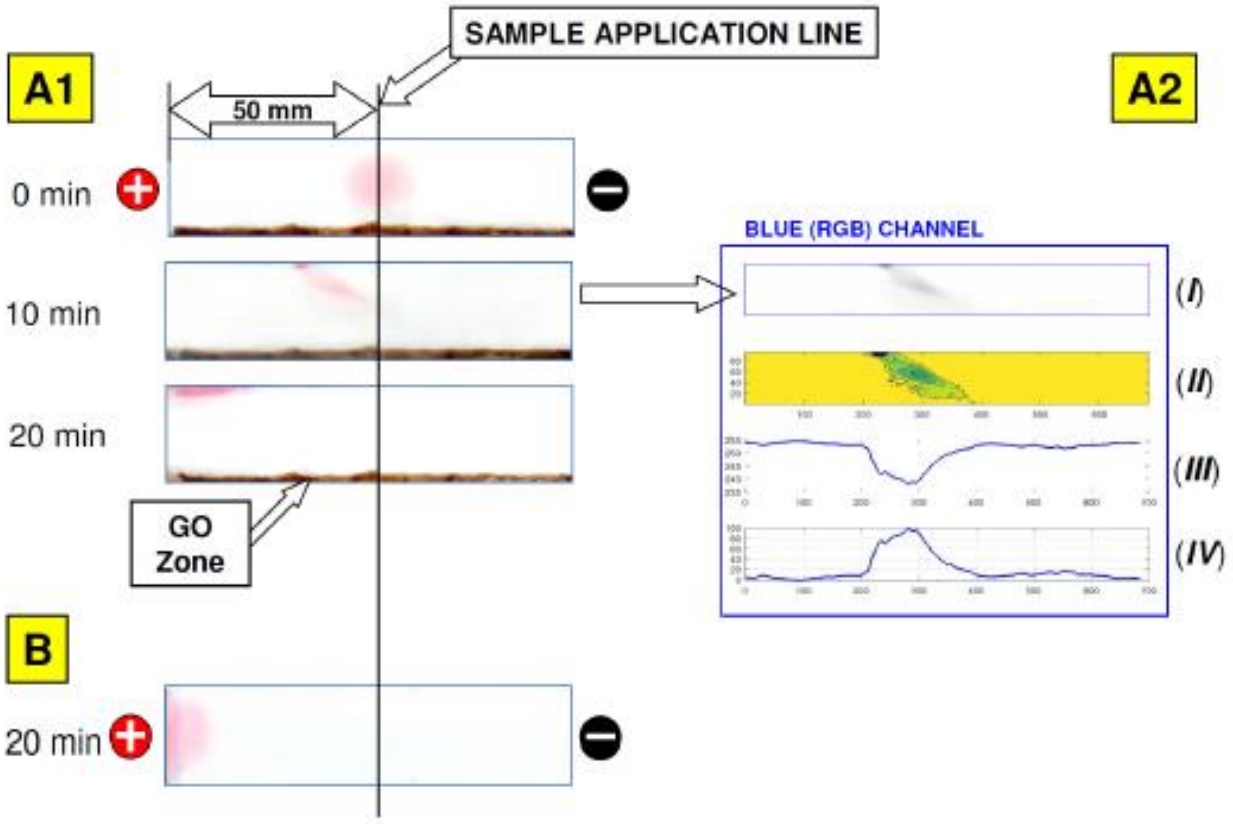


**Figure 41.** Repulsion effect observed for Ponceau 4R in the presence of GO horizontal wall (parallel with electromigration flow direction). Time sequence of electroseparation on cellulose based TLC plate with GO horizontal zone (**A1**), reference dye migration without GO zone (**B**) and dye jet structure formed after 10 minutes of electrophoresis and revealed at blue channel of RGB picture (**A2** I, II, III, IV). Experimental conditions as described in caption of **Figure 39**. Images of microelectropherograms were modified (a global balance filters were applied) to increase the contrast for spots for visual evaluation and printing. With permission from Elsevier **[Zarzycki 2022]**.

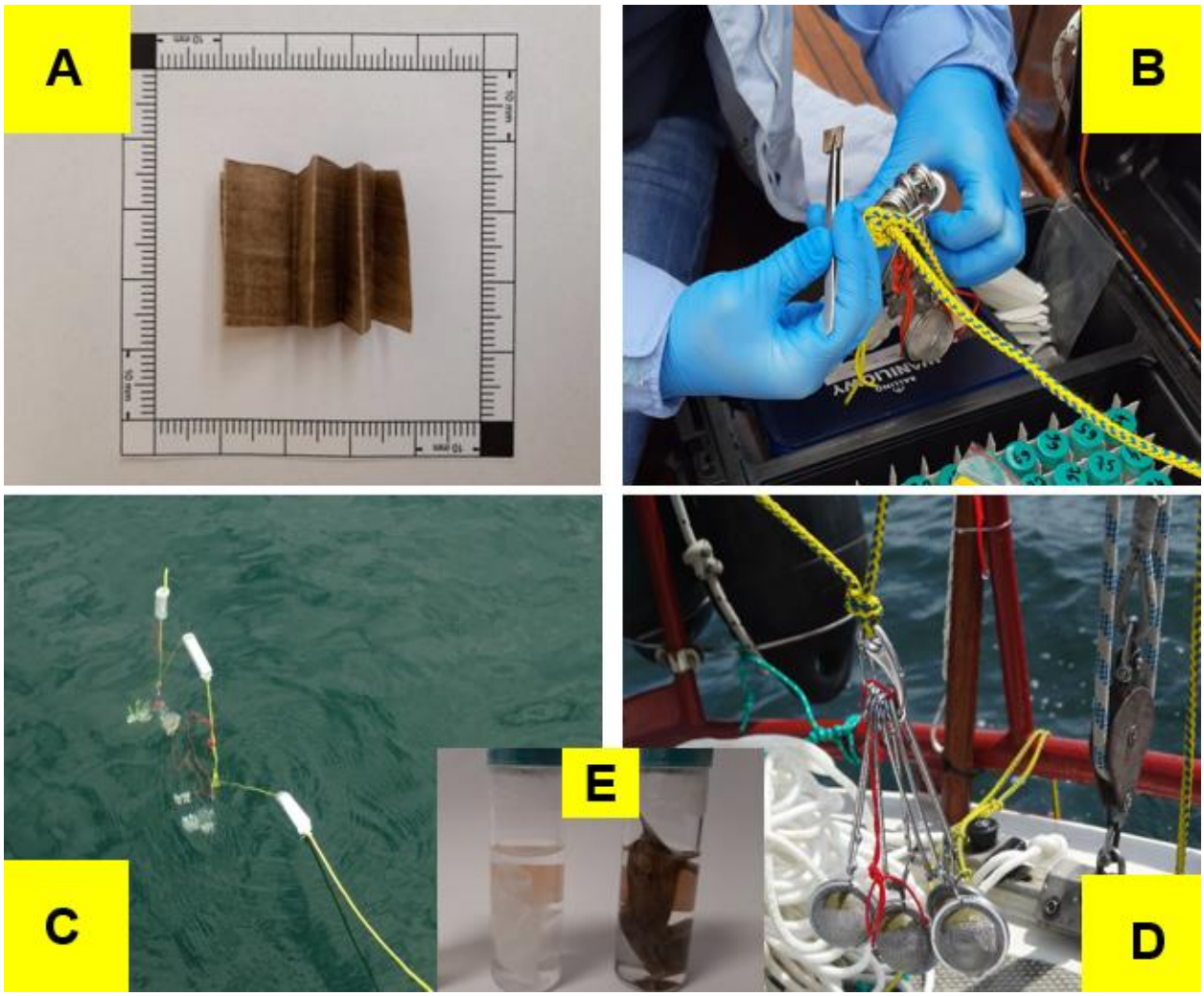


**Figure 42.** Rapid screening of organic particles and organic micropollutants that may be present in surface water and adsorbed on cellulose with a GO layer: cellulose with graphene oxide layer (**A**), placed inside metal wire mesh pocket (**B**), adsorbents probe in surface water (**C**), samples after 60 min adsorption (**D**) various adsorption strips preserved and stored in 95 % (v/v) ethanol (**E**).

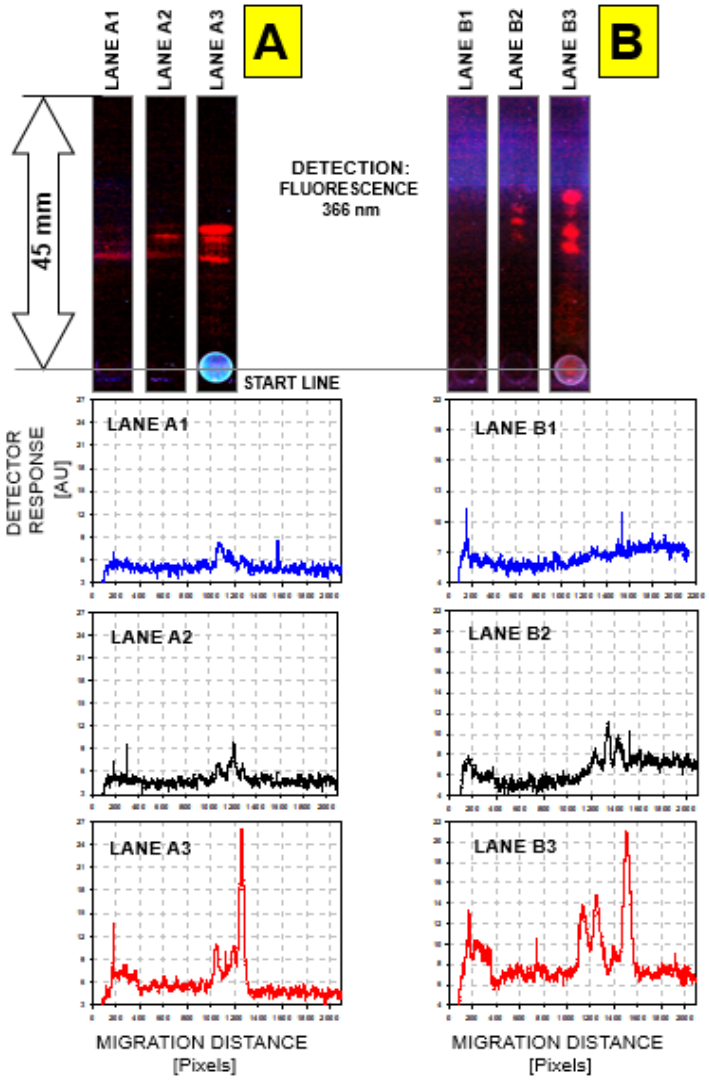


**Figure 43.** Rapid screening (fluorescence detection) of organic particles and organic micropollutants, which are present in surface water using different adsorption matrices: raw cellulose (Lanes **A1/B1**), cellulose coated with GO (Lanes **A2/B2**), raw dandelion pappus (Lanes **A3/B3**). Micro-TLC analysis was conducted using two different analytical systems: HPTLC RP18WF254S (**A**) and TLC RP18F254S (**B**). Separation was performed with two different mobile phases composed of 30% (v/v) acetone:n-hexane and 20% (v/v) acetone:*n*-hexane. Analysed samples were collected from the Baltic Sea (2020). Micro-TLC images were intentionally modified with a global balance filters, which increased the contrast for spots. Presented lane profiles (densitograms) were derived from raw and unprocessed files (red channel) using ImageJ 1.42q Wayne Rasband freeware (National Institute of Health, USA). With permission from Elsevier **[Zarzycki 2022]**.

.

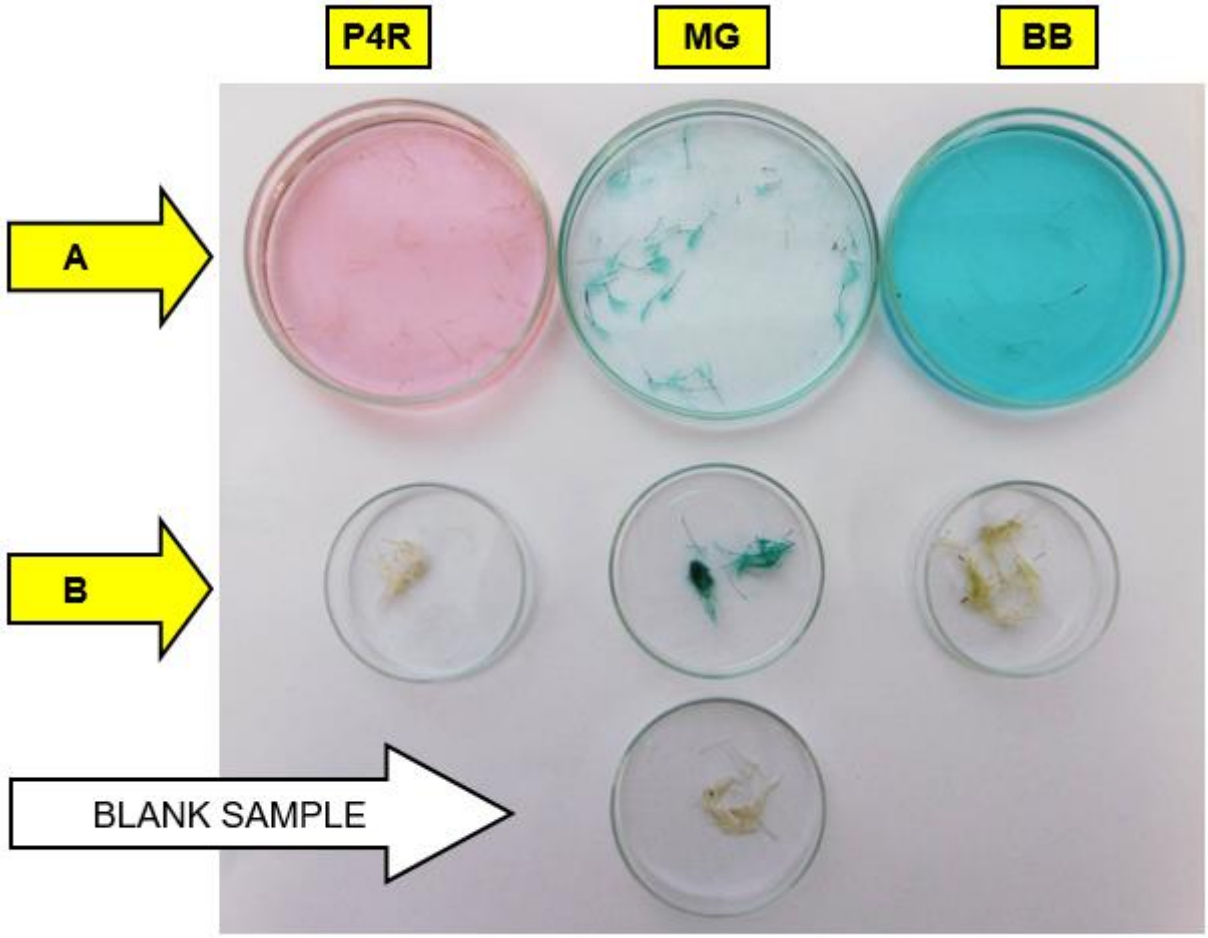


**Figure 44.** Adsorption of dyes on dandelion pappus after 24 h period. Sample labels: **P4R** - Ponceau 4R; **MG** - Malachite Green; **BB** - Brilliant Blue; Row **A** - dyes solution with dandelion pappus after 24 h contact time; Row **B** - isolated wet dandelion pappus; **Blank sample** - wet dandelion pappus from pure water.

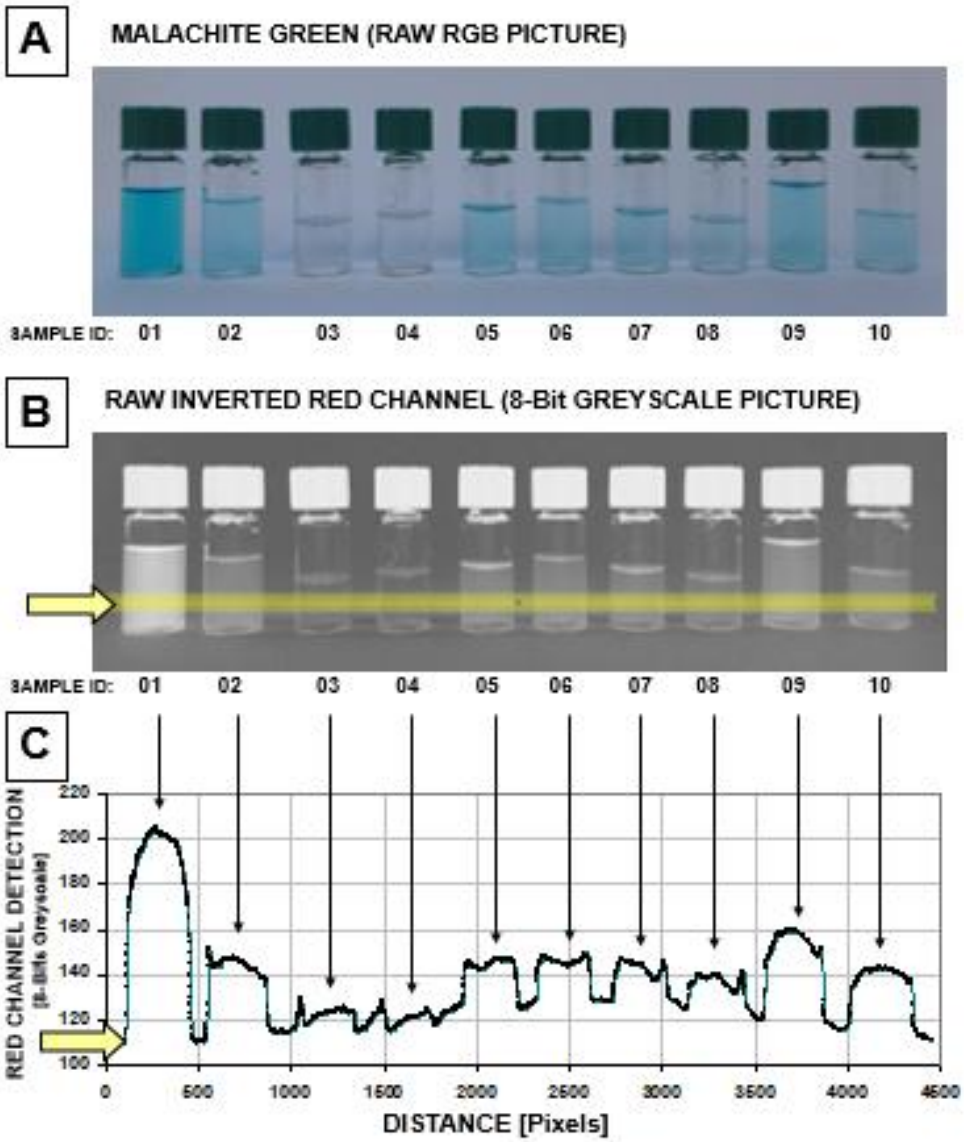


**Figure 45**. Screening test (24 h contact time) of Malachite Green interaction with additives investigated; **A** - raw picture; **B** - RED RGB channel (8-Bit gray scale); **C** - quantitative transsection across 2 mL vials picture. Sample labels: **01** Malachite Green blank solution 5 mg/L; **02** Malachite Green blank solution 5 mg/L filtered by cellulose membrane; **03** Malachite Green solution 5 mg/L with graphene oxide; **04** Malachite Green solution 5 mg/L with activated carbon; **05** Malachite Green solution 5 mg/L with β-cyclodextrin; **06** Malachite Green solution 5 mg/L with cellulose; **07** Malachite Green solution 5 mg/L with pollen; **08** Malachite Green solution 5 mg/L with dandelion pappus; **09** Malachite Green solution 5 mg/L with Egyptian Blue type 1.1.1.; **10** Malachite Blue solution 5 mg/L with Egyptian Blue type 1.1.1a. after 24 h of contact time.
Photo acquisition conditions: Panasonic Lumix DMC-SZ10 digital camera (Auto mode).

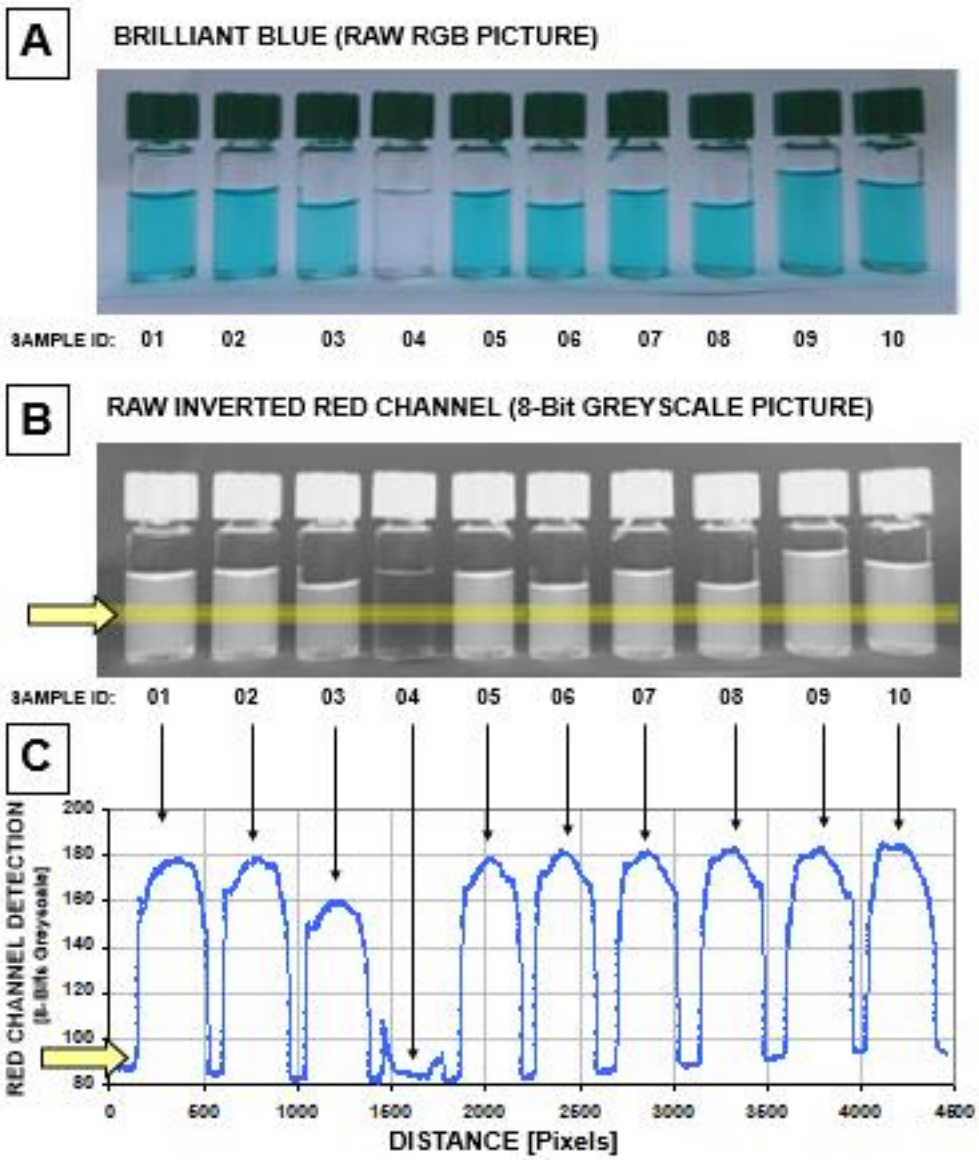


**Figure 46.** Screening test (24 h contact time) of Brilliant Blue interaction with additives investigated; **A** - raw picture; **B** - RED RGB channel (8-Bit gray scale); **C** -quantitative transsection across 2 mL vials picture . Sample labels: **01** - Brilliant Blue blank solution 5 mg/L; **02** - Brilliant Blue blank solution 5 mg/L filtered by cellulose membrane; **03** Brilliant Blue solution 5 mg/L with graphene oxide; **04** Brilliant Blue solution 5 mg/L with activated carbon; **05** Brilliant Blue solution 5 mg/L with β-cyclodextrin; **06** Brilliant Blue solution 5 mg/L with cellulose; **07** Brillint Blue solution 5 mg/L with pollen; **08** Brilliant Blue solution 5 mg/L with dandelion pappus; **09** Brilliant Blue solution 5 mg/L with Egyptian Blue type 1.1.1.; **10** Brilliant Blue solution 5 mg/L with Egyptian Blue type 1.1.1a. after 24 h of contact time.

Photo acquisition conditions: Panasonic Lumix DMC-SZ10 digital camera (Auto mode).

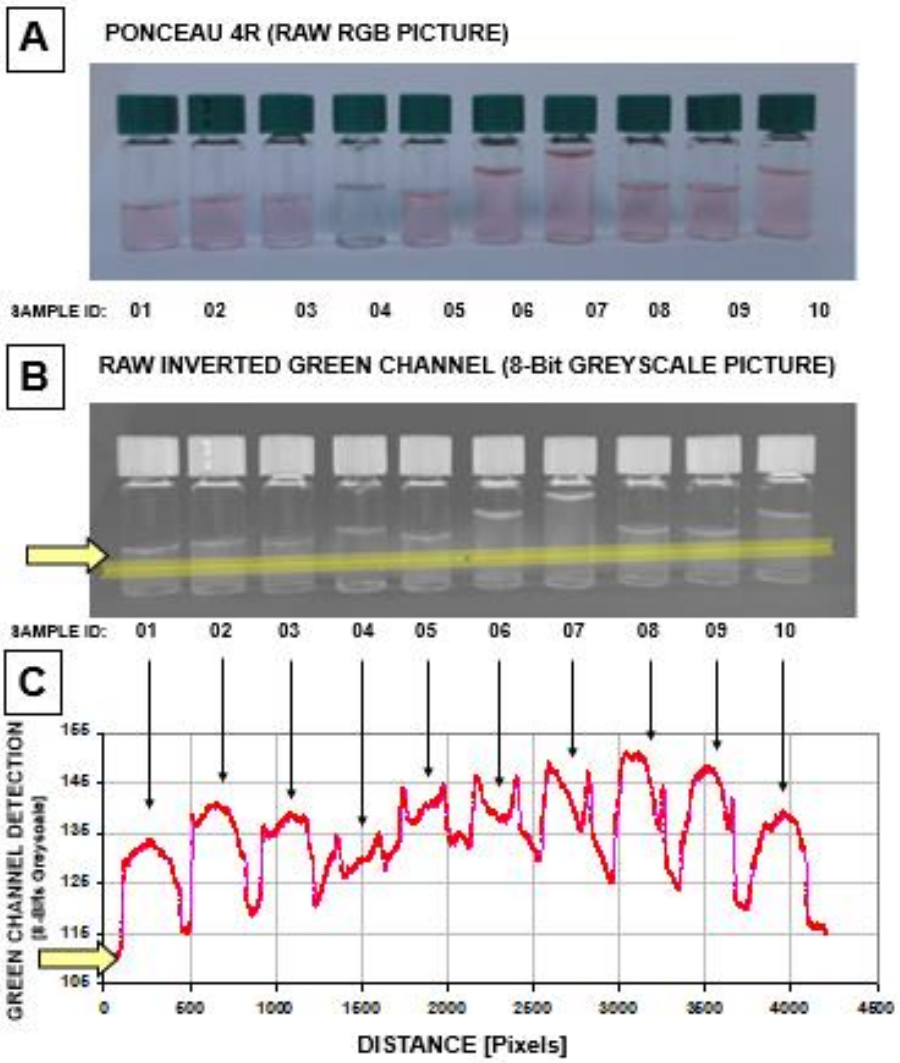


**Figure 47.** Screening test (24 h contact time) of Ponceau 4R interaction with additives investigated; **A** - raw picture; **B** - GREEN RGB channel (8-Bit gray scale); **C** - quantitative transsection across 2 mL vials picture . Sample labels: **01** - Ponceau 4R blank solution 5 mg/L; **02** - Ponceau 4R blank solution 5 mg/L filtered by cellulose membrane; ; **03** Ponceau 4R solution 5 mg/L with graphene oxide; **04** Ponceau 4R solution 5 mg/L with activated carbon; **05** Ponceau 4R solution 5 mg/L with β-cyclodextrin; **06** Ponceau 4R solution 5 mg/L with cellulose; **07** Ponceau 4R solution 5 mg/L with pollen; **08** Ponceau 4R solution 5 mg/L with dandelion pappus; **09** Ponceau 4R solution 5 mg/L with Egyptian Blue type 1.1.1.; **10** Ponceau 4 R solution 5 mg/L with Egyptian Blue type 1.1.1a. after 24 h of contact time. Photo acquisition conditions: Panasonic Lumix DMC-SZ10 digital camera (Auto mode).

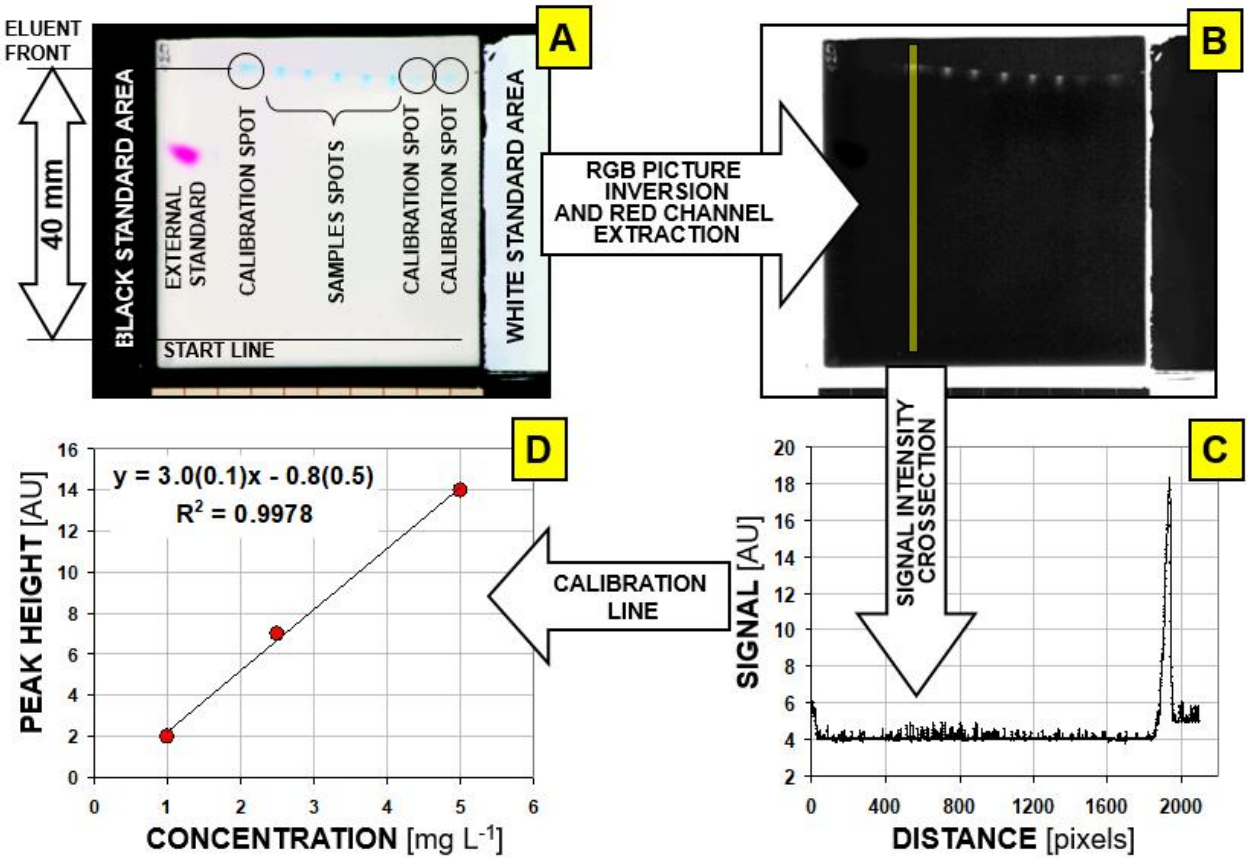


**Figure 48.** Applied sequence of quantification protocol for direct determination of Brilliant Blue dye in reaction mixtures using microfluidic analytical device based on micro-TLC plate. General view and spots arrangements of micro-TLC analytical device (**A**; to increase the contrast of spots for visual evaluation and printing a global balance filters were applied); converted picture prepared for spots quantification (**B**; to increase the contrast of spots for visual evaluation and printing a global balance filters were applied), Lane cross-section for given calibration spot (**C**; signal intensity data were derived from raw red channel without contrast enhancement); Calibration plot for individual m-TLC plate (**D**). External standard spot (Methyl Red; chromatographed mass 100 ng/spot) was used for accuracy of retention process and quantitative data validation. With permission from MDPI **[Zarzycki 2021]**.

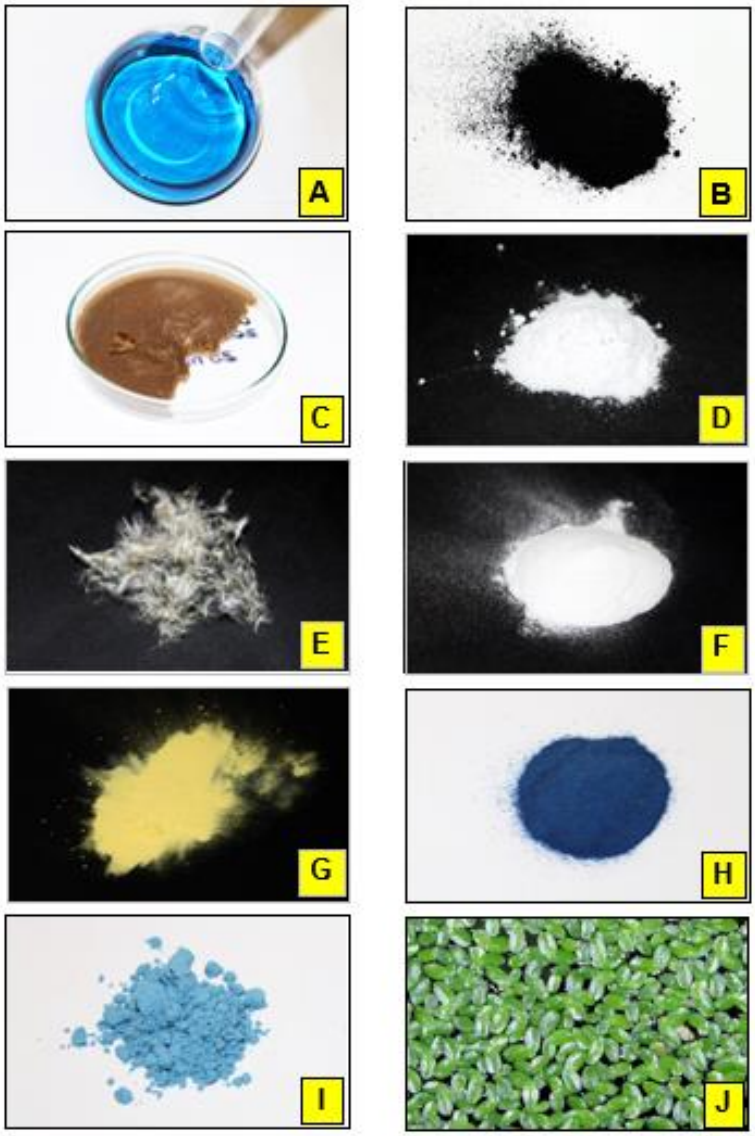


**Figure 49.** General view of target chemical stock solution (Brilliant Blue 5 mg/mL); (**A**) and additives studied: active carbon (**B**), lyophilized graphene oxide (**C**), β cyclodextrin (**D**), raw dandelion pappus without seeds (**E**), microcrystalline cellulose (**F**), raw pine pollen (**G**), Egyptian Blue (synthesis 1 EB1-(**H**); synthesis 2 EB2-(**I**), and duckweed water plant (**J**). With permission from MDPI **[Zarzycki 2021]**.

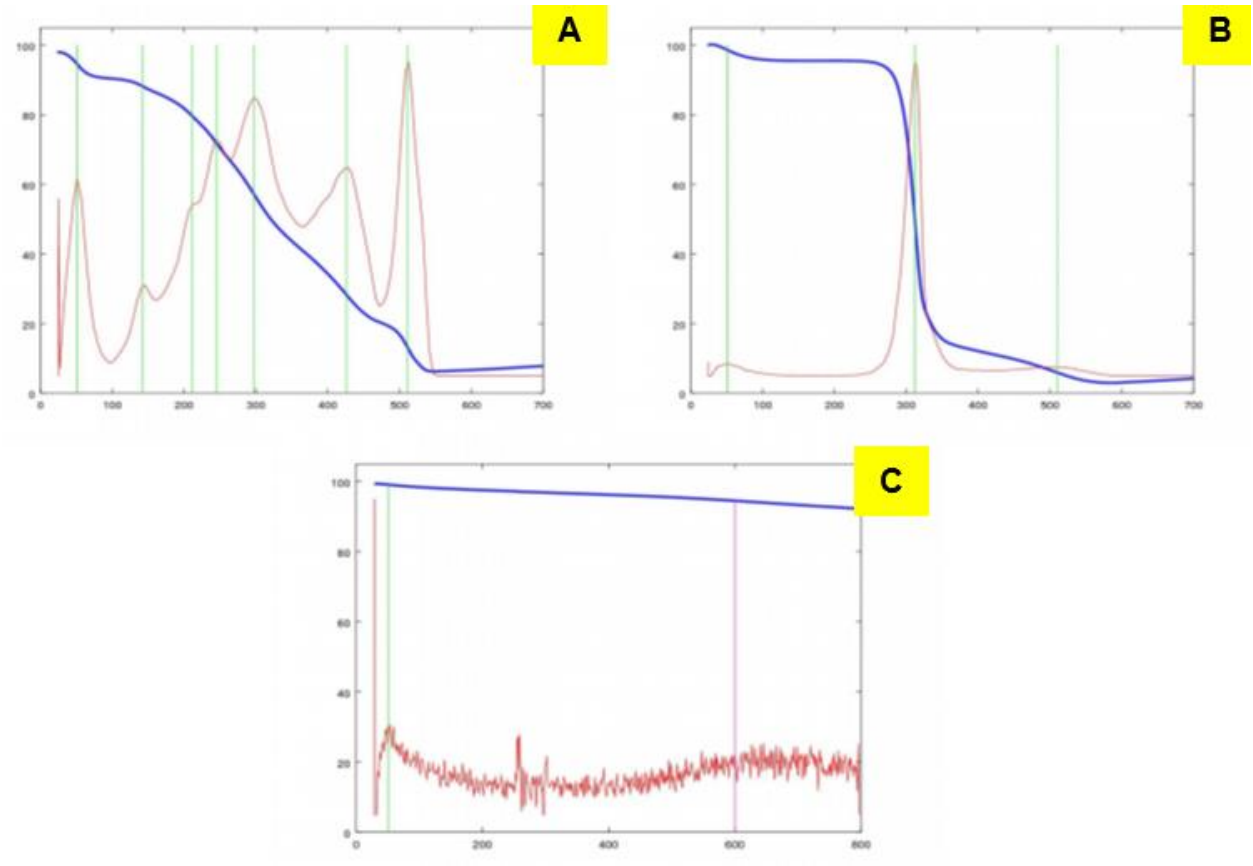


**Figure 50.** Results of thermogravimetric analysis of selected additives: (**A**) **Pine Pollen** (Atrium), sample mass = 4.5818 mg, 10 K $min^{-1}$, $N_2$ shield and purge highest weight losses at 51, 297, 426 and 511ºC, initial mass (25 ºC) = 4.5818 mg, dry mass (110ºC) = 4.1285 mg, residual mass (550ºC) = 0.2885 mg (7.0 %), dry mass loss = 3.8400 mg (93.0 % of dry mass), initial hydration = 11.0%; (**B**) **Cellulose microcrystalline**, sample mass = 5.2403 mg, 10 K $min^{-1}$, $N_2$ shield and purge, highest weight losses at 51.8, 311.9 and 509.7ºC, initial mass (25ºC) = 5.2403 mg, dry mass (110ºC) = 5.0151 mg, residual mass (580ºC) = 0.1572 mg (3.1 %), dry mass loss = 4.8579 mg (96.9 % of dry mass), initial hydration = 4.5%, suggestions: > heat at 350ºC under nitrogen flow/atmosphere; (**C**) **Activated Carbon**, 10 K $min^{-1}$, $N_2$ shield and purge, highest mass loss at 51ºC, initial mass (25ºC) = 7.30 mg, dry mass (110ºC) = 6.426 mg, residual mass (600ºC) = 5.522 mg (85.9 %), dry mass loss till 600ºC = 0.903 mg (14.1 % of dry mass), initial hydration = 13.6%. TG analysis was performed at the University of Coimbra (Portugal) in collaboration with Prof. Jorge C. Pereira and Prof. Jorge M. C. Marques.

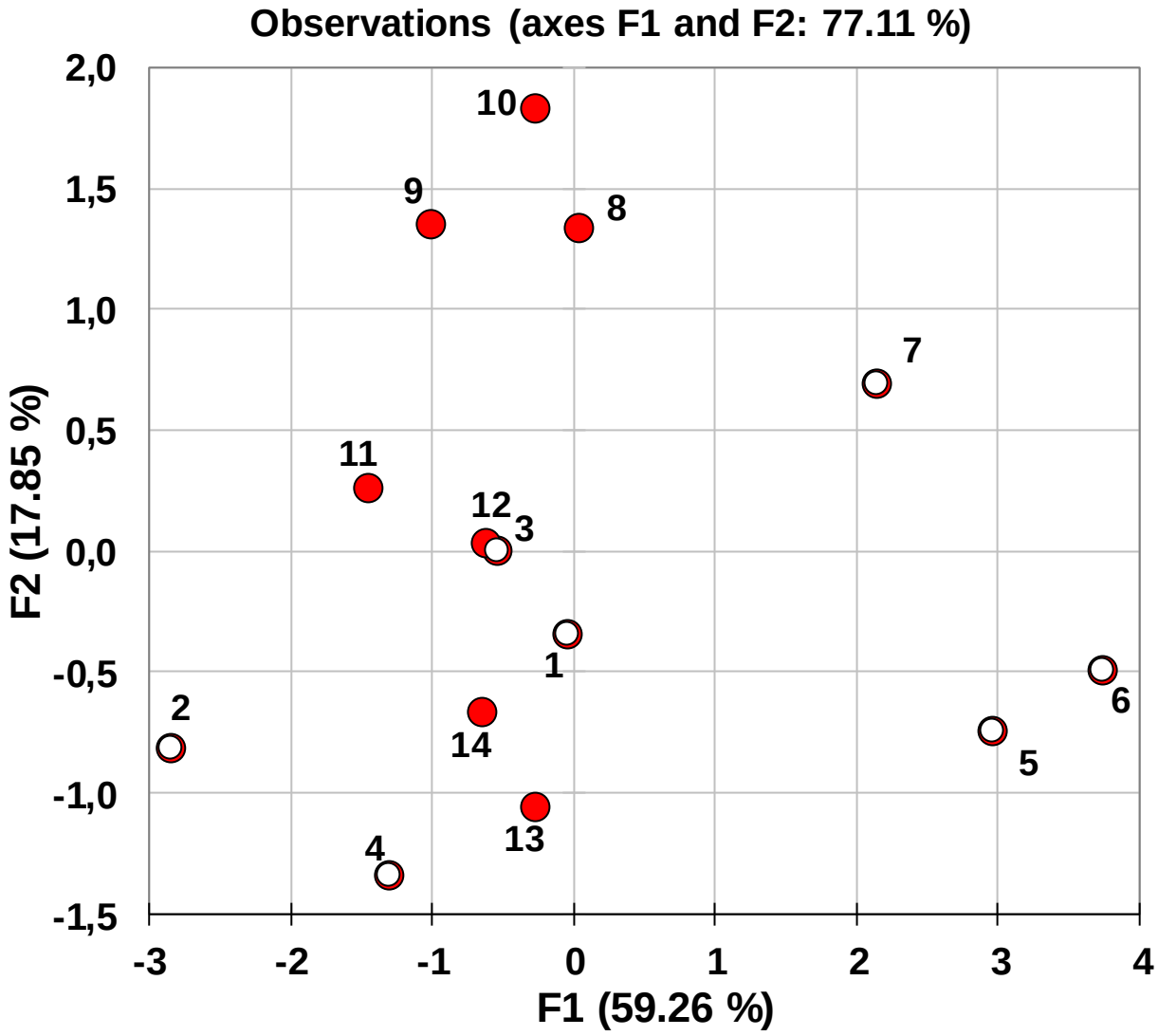


**Figure 51.** Factor scores plot (principal component analysis) related to 24 hours experiment and calculated from data matrix consisting of Brilliant Blue concentrations at different times of experiment duration (variables) and different additives (objects) listed in **Table 2**. Object labels (circles correspond to samples without activated sludge addition): water **BLANK** (**1**), water and graphene oxide **GO** (**2**), water and β-cyclodextrin **CD** (**3**), water and raw dandelion pappus **DP** (**4**), water and microcrystalline cellulose **MC** (**5**), water and raw pine pollen **PP** (**6**), water and Egyptian Blue mineral pigments **EB2** (**7**), activated sludge **AS BLANK** (**8**), activated sludge and graphene oxide **GO** (**9**), activated sludge and β-cyclodextrin **CD** (**10**), activated sludge and raw dandelion pappus **DP** (**11**), activated sludge and microcrystalline cellulose **MC** (**12**), activated sludge and raw pine pollen **PP** (**13**), activated sludge and Egyptian Blue mineral pigments **EB 1.1.1a.** (**14**). With permission. With permission from MDPI **[Zarzycki 2021]**.

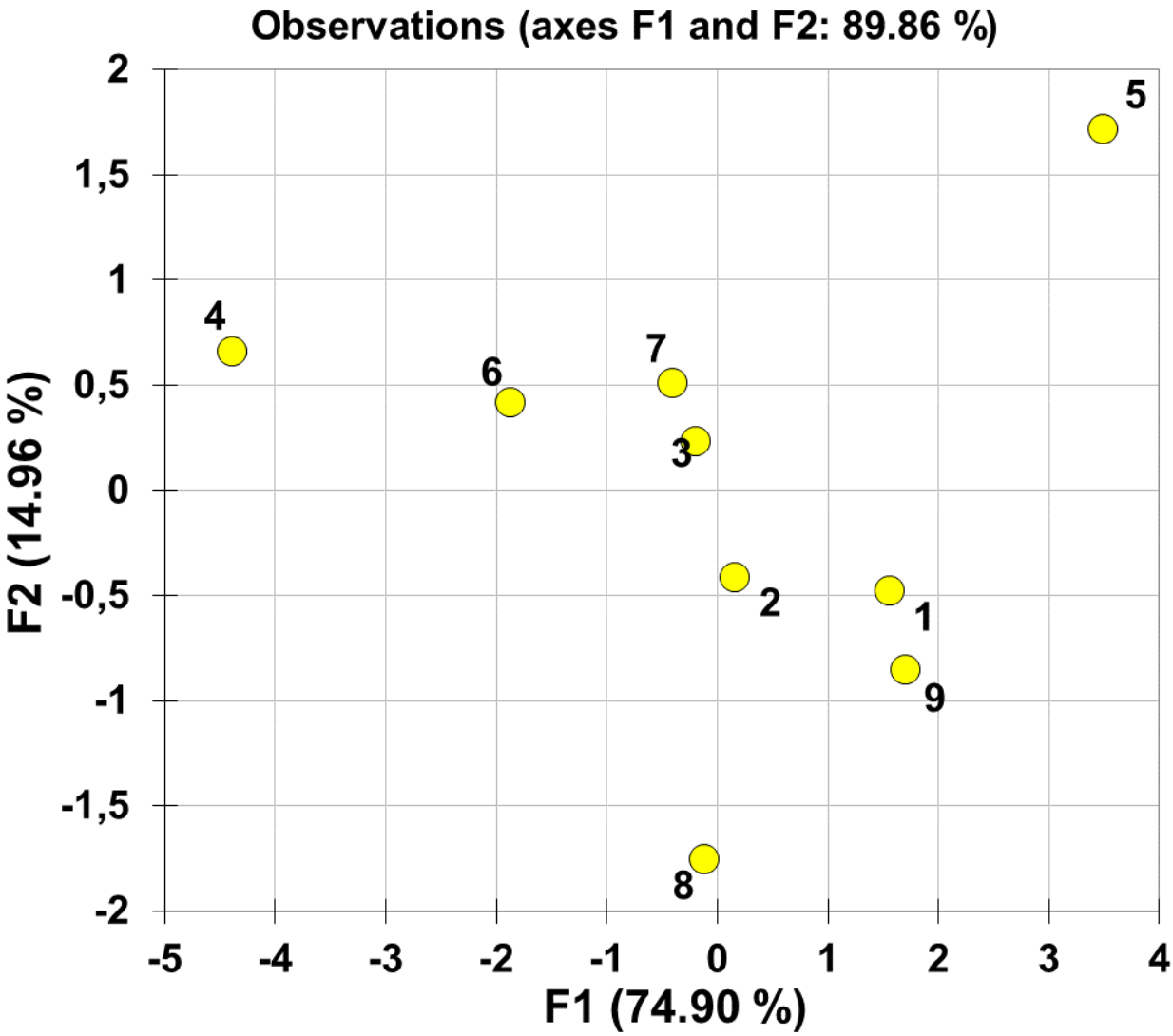


**Figure 52.** Factor scores plot (principal component analysis) related to 16 days experiment and calculated from data matrix consisting of Brilliant Blue concentrations at different times of experiment duration (variables) and different additives (objects) listed in **Table 3**. Object labels: water **BLANK** (**1**), duckweed water plant **DW** (**2**), **DW** and graphene oxide **GO** (**3**), **DW** and β-cyclodextrin **CD** (**4**), **DW** and raw dandelion pappus **DP** (**5**), **DW** and microcrystalline cellulose **MC** (**6**), **DW** and raw pine pollen **PP** (**7**), **DW** and Egyptian Blue mineral pigments **EB 1.1.1.** (**8**), **DW** and Egyptian Blue mineral pigments **EB 1.1.1a.** (**9**).With permission. With permission from MDPI **[Zarzycki 2021]**.

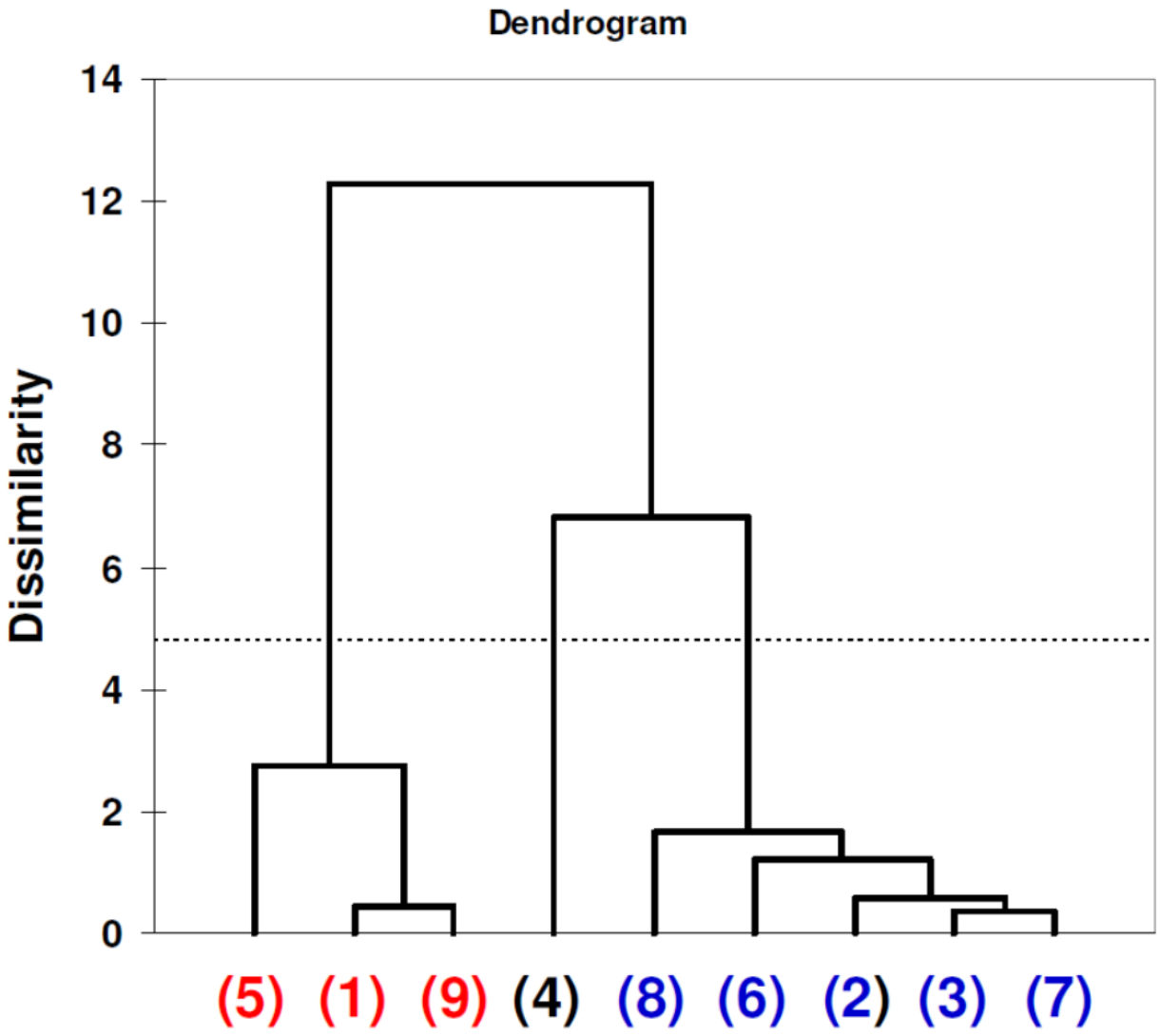


**Figure 53.** Dendrogram of agglomerative hierarchical cluster analysis involving Ward's method as the aggregation criterion. The graph represents the clustering of reaction mixtures (BB concentration) with different additives according to experiment time points listed in **Table 12** (16 days experiment). Object labels are identical to those listed in **Figure 52** caption. With permission from MDPI **[Zarzycki 2021]**.

# 8. LITERATURE

## *(a) References citied*


**----------2022----------**

**[Bridle 2022]** H. Bridle; Separation technologies in microfluidics; Micro and Nano-technology Enabled Applications for Portable Miniaturized Analytical Systems; Elsevier Book, Chapter 7 (2022), Pages 141-162

**[Zarzycki 2022]** P. K. Zarzycki, K. Piaskowski, L. Lewandowska, B. Fenert, R. Świderska-Dąbrowska, M. Ślączka-Wilk, A. Kaleniecka; Portable micro-planar extraction, separation and quantification devices for bioanalytical and environmental engineering applications. Elsevier book: Micro and Nano Technologies 2022, Chapter 8, Pages 163-196

**----------2021----------**

**[Alshehri 2021]** M. Alshehri, A. Bhardwa, M. Kumar, Sh. Mishra, J. Gyani; Cloud and IoT based smart architecture for desalination water treatment;Env Res 195 (2021) 110812

**[Aydin 2021]** S. Aydin, F. Beduk, A. Ulvi, M.E. Aydin; Simple and effective removal of psychiatric pharmaceuticals from wastewater treatment plant effluents by magnetite red mud nanoparticles; Sci. Total Environ, Volume 784, 25 August 2021, 147174

**[Binet 2021]** L**.** Binet; J. Lizon; S. Bertaina; D. Gourier; Magnetic and New Optical Properties in the UV–visible Range of the Egyptian Blue Pigment Cuprorivaite $CaCuSi4O_{10}$; J Phys. Chem C; Volume 125, Issue 45, Page 25189-25196, DOI10.1021/acs.jpcc.1c06060

**[El-Said 2021]** W. A. El-Said, A.S. Al-Bogami, W. Alshitari; Synthesis of gold nanoparticles-reduced porous graphene-modified ITO electrode for spectroelectrochemical detection of SARS-CoV-2 spike protein; Spectrochim Acta A-Molecular and Biomolecular Spectroscopy, Vol: 264: 120237, DOI:10.1016/j.saa.2021.120237

**[Ghoorchian 2021a ]** A. Ghoorchian, M. Kamalabadi, Z. Amouzegar, N. R. Jalal, H. M. A. Shawish, S. M. Saadeh, A. Afkhami, T. Madrakian, S. Thomas, T. A. Nguyen, M. Ahmadi; Lab-on-a-chip miniaturized analytical devices; Elsevier, Chapter 11

**[Ghoorchian 2021b]** A. Ghoorchiana, N. R. Jalala, M. Kamalabadia, F. Mollarasoulib, M. Moradia, S. Asadia, A. Afkhamia, T. Madrakiana, S. Thomasc, T. A. Nguyend, M. Ahmadia; Smartphone-enabled miniaturized analytical devices; Elsevier, Chapter 12

**[Jain 2021]** K. Jain, A. S. Patel, V. P. Pardhi, S. J. S. Flora;Nanotechnology in Wastewater Management: A New Paradigm Towards Wastewater Treatment; Molecules 26, 1797. https://doi.org/10.3390/molecules26061797

**[Lu 2021]** D. Lu, D. Z. Zhu, H. Gan, Z. Yao, Q. Fu, X. Zhang; Prospects and challenges of using electrochemical immunosensors as an alternative detection method for SARS-CoV-2 wastewater-based epidemiology; Sci Total Environ 777 (2021) 146239

**[Mussa 2021]** Z. H. Mussa, F. F. Al-Qaim, A. Yuzir, K. Shameli;
Photocatalytic Removal of Malachite Green and Brilliant Blue Dyes from its Aqueous Solution: A Case Study of Factorial Experimental Design; J. Mex. Chem. Soc. 2021, 65(2)

**[Saya 2021]** L. Saya, D. Gautam, V. Malik, W.R. Singh, S. Hooda; Natural Polysaccharide Based Graphene Oxide Nanocomposites for Removal of Dyes from Wastewater: A Review; J. of Chem. and Eng*. Data*, 2021**,** 66(1), pp 11-37

**[Srivastava 2021]** M. Srivastava, N. Srivastava, P.K. Mishra, B.D. Malhotra; Prospects of nanomaterials-enabled biosensors for COVID-19 detection; Sci Total Environ, Vol 754, 1 February 2021, 142363

**[Tacas 2021]** A. C. J. Tacas, P-W. Tsai, L. L. Tayo, C-C. Hsueh, S-Y. Sun, B-Y. Chen; Degradation and biotoxicity of azo dyes using indigenous bacteria-acclimated microbial fuel cells (MFCs); Process Biochem 102 (2021) 59–71

**[Vashisht 2021]** D. Vashisht, S. Sangarc, M. Kaura, E. Sharmac, A. Vashishtd, A. O. Ibhadonb, S. Sharmae, S.K. Mehtaa, K. Singh; Biosynthesis of silver nanospheres, kinetic profiling and their application in the optical sensing of mercury and chlorite ions in aqueous solutions; Environ Res 197 (2021) 111142

**[Zarzycki 2021]** P. K. Zarzycki, L. Lewandowska, B. Fenert, K. Piaskowski, J. Kobaka; Investigation of hybrid methods for elimination of micropollutants from water phase using Brilliant Blue as target chemical and various nanomaterials combined with activated sludge and duckweed; Nanomaterials 2021, 11(7), 1747; https://doi.org/10.3390/nano11071747

**[Zhang 2021]** F. Zhang, Z. Wang, M.G. Vijver, Willie J.G.M. Peijnenburg Probing nano-QSAR to assess the interactionsbetween carbon nanoparticles and a SARS-CoV-2 RNA fragment Ecotoxicol Environ Saf 219 (2021) 112357

**[Zhu 2021]** X. Zhu, G. Wu, N. Lu, X. Yuan, B. Li; A miniaturized electrochemical toxicity biosensor based on graphene oxide quantum dots/carboxylated carbon nanotubes for assessment of priority pollutants;J Hazard Mater 403 (2021) 123925

**----------2020----------**

**[Abdi 2020]** J. Abdi, H. Abedini; MOF-based polymeric nanocomposite beads as an efficient adsorbent for wastewater treatment in batch and continuous systems: Modelling and experiment. Chem. Eng. J. 2020, 400, 125862

**[Amri 2020]** N. Amri, A. Zuhairi Abdullah, S. Ismail; Removal Efficiency of Acid Red 18 Dye from Aqueous Solution Using Different Aluminium-Based Electrode Materials by Electrocoagulation Process; Indones. J. Chem. 20 (3), 536 - 544

**[Berggren 2020]** M. Berggren,E. S. Al-Kharusi; Decreasing organic carbon bioreactivity in European rivers;Freshwater Biol 2020, 00:1–11

**[Coros 2020]** M. Coros, C. Socaci, S. Pruneanu, F. Pogacean, M-C. Rosu, A. Turza, L. Magerusan; Thermally reduced graphene oxide as green and easily available adsorbent for Sunset yellow decontamination; Envi Res 182 (2020) 109047

**[Chenthattil 2020]** R. Chenthattil, J.G. Manjunatha; Fabrication of novel polymer-modified graphene-based electrochemical sensor for the determination of mercury and lead ions in water and biological samples; J Anal Sci Techn(2020) 11:3

**[Chunnathambi 2020]** S. Chinnathambi, S. Kumar, G.J.W. Euverink; Fabrication of a Nitrogen and Boron-Doped Reduced Graphene Oxide Membrane-Less Amperometric Sensor for Measurement of Dissolved Oxygen in a Microbial Fermentation;Chemosensors 2020, 8, 44; doi:10.3390

**[Duval 2020]** B. Duva, A. Gredilla, S. Fdez-Ortiz de Vallejuelo, E. Tessier; A simple determination of trace mercury concentrations in natural waters using dispersive Micro-Solid phase extraction preconcentration based on functionalized graphene nanosheets, Microchem J 154 (2020) 104549

**[Farmani 2020]** H. Farmani, A. Farmani, Z. Biglari;A label-free graphene-based nanosensor using surface plasmon resonance for biomaterials detection;Physica E 116 (2020) 113730

**[Faryadras 2020]** F. Faryadras, S. M. Yousefi, P. Jamshidi, F. Shemirani; Application of magnetic graphene-based bucky gel as an efficient green sorbent for determination of mercury in fish and water samples; Res Chem Intermediat (2020) 46:2055–2068

**[He 2020]** L. He, T. Hong, Y. Huang, B. Xiong, X. Hong, M. Tahir, W.A. Haider, Y. Han: Surface Engineering of Carbon-Based Microelectrodes for High-Performance Microsupercapacitors;Micromachines 2019, 10, 307

**[Jiang 2020]** K. Jiang, Q. Weng; Miniaturized Energy Storage Devices Based on Two-Dimensional Materials; ChemSusChem 2020, 13, 1420 – 1446

**[Kaleniecka 2020a]** A. Kaleniecka, P.K. Zarzycki; Degradation Studies of Selected Bisphenols in the Presence of β-Cyclodextrin and/or Duckweed Water Plant;J AOAC Int Vol. 103, 2020

**[Kaleniecka 2020b]** A. Kaleniecka, E. Włodarczyk, K. Piaskowski, L. Lewandowska, P. K. Zarzycki; Unexpected Encapsulation of Selected Polycyclic Aromatic Hydrocarbons by β-Cyclodextrin Studied Using UV-Vis Spectrophotometry, Micro-Planar Chromatography and Temperature Dependent Inclusion Chromatography; Symmetry 2020, *12*(12), 1967; https://doi.org/10.3390/sym12121967

**[Kazemi 2020]** E. Kazemi, Sh. Dadfarnia, A. M. H. Shabani, A. Abbasi, M.Reza, R. Vaziri, A. Behjat; Iron oxide functionalized graphene oxide as an efficient sorbent for dispersive micro-solid phase extraction of sulfadiazine followed by spectrophotometric and mode-mismatched thermallens spectrometric determination, Talanta147(2016) 561–568

**[Li 2020]** C. Li, Y. Wei, Sh. Zhang, W. Tan; Advanced methods to analyze steroid estrogens in environmental samples, Environ Chem Letters (2020) 18:543–559

**[Li 2020]** D. Li, T. Wang, Z. Li, X. Xu, C. Wang, Y. Duan; Application of Graphene-Based Materials for Detection of Nitrate and Nitrite in Water—A Review, Sensors2020, *20* (1), 54

**[Manoj 2020]** B. Manoj; Synthesis of Coal-based Nanocarbon- Advances and Applications; Pure and Functionalized Carbon Based Nanomaterials: Analytical, Biomedical, Civil and Environmental Engineering Applications, 1st ed.; Zarzycki, P.K.; CRC Press Taylor & Francis Group, Boca Raton, Florida, United States, 2020, pp. 326–363.

**[Piaskowski 2020]** K. Piaskowski, P.K. Zarzycki; Carbon-Based Nanomaterials as Promising Material for Wastewater Treatment Processes, Int J Environ Res Public Health 2020, 17, 5862

**[Rakkesh 2020]** R. A. Rakkesha, D. Durgalakshmia, S. Balakumar;Graphene based Nanoassembly for simultaneous Detection and Degradation of Harmful Organic Contaminants from Aqueous Solution, J Name., 2013, 00, 1-3

**[Setznagl 2020]** S. Setznagl, I. Cesarino; Copper nanoparticles and reduced Graphene oxide modified a glassy carbon electrode for the determination of glyphosate in water samples; Int J Environ Anal Chem, DOI:10.1080/03067319.2020.1720667

**[Tang 2020]** Ch. Tang, Y. Zhang, J. Han, Z. Tian, L. Chen, J. Chen; Monitoring graphene oxide's efficiency for removing Re(VII) and Cr(VI) with fluorescent silica hydrogels; Environ. Pollut. 262 (2020) 114246

.

**[Wang 2020]** W. Zhenxing, H. Fang, G. Jing, P. Shaogin, Ch. X. Quan, Z. Yingije, D. Enrico, F. Alberto, L. Yuexiang, Sh. Lu; The stability of a graphene oxide (GO) nanofiltration (NF) membrane in an aqueous environment: progress and challenges, Mater.Adv.,1,554

**[Yang 2020]** C. Yang, A. Qin, B. Z. Tang, X. Guo;Fabrication and functions of graphene–molecule–graphene single-molecule junctions; J Chem Physics 152, 120902 (2020)

**[Zarzycki 2020a]** P. K. Zarzycki (Ed.); Pure and Functionalized Carbon Based Nanomaterials: Analytical, Biomedical, Civil and Environmental Engineering Applications, 1st ed.; Zarzycki, P.K.; CRC Press Taylor & Francis Group, Boca Raton, Florida, United States, 2020

**[Zarzycki 2020b]** P. K. Zarzycki, K. Mitura, K. Piaskowski; L. Lewandowska, R. Świderska-Dąbrowska, M. Baran; Carbon and related nanomaterials as active media for analytical, pharmaceutical, biomedical and wastewater processing applications. Pure and Functionalized Carbon Based Nanomaterials: Analytical, Biomedical, Civil and Environmental Engineering Applications, 1st ed.; Zarzycki, P.K.; CRC Press Taylor & Francis Group, Boca Raton, Florida, United States, 2020, pp. 326–363

**----------2019----------**

**[Ahmad 2019]** Z. U. Ahmad, L.Yao, J. Wang, D.D. Gang, F. Islam, Q. Lian, M.E. Zappi; Neodymium embedded ordered mesoporous carbon (OMC) for enhanced adsorption of sunset yellow: characterizations, adsorption study and adsorption mechanism; Chem. Eng. J. 359, 814–826. https://doi.org/10.1016/j.cej.2018.11.174

**[Baruah 2019]** A. Baruah, V. Chaudhary, R. Malik, V.K.Tomer; Nanotechnology Based Solutions for Wastewater Treatment. In Nanotechnologyin Water and Wastewater Treatment: Theory and Applications; Elsevier: Amsterdam, The Netherlands, 2019; pp. 337–368

**[Chen 2019]** B. Chen, S. Chen, H. Zhao, Y. Liu, F. Long, X. Pan; A versatile _-cyclodextrin and polyethyleneimine bi-functionalized magnetic nanoadsorbent for simultaneous capture of methyl orange and Pb(II) from complex wastewater; Chemosphere 2019, 216, 605–616

**[Kaleniecka 2019]** A. Kaleniecka, P.K. Zarzycki; Analysis of Selected Endocrine Disrupters Fraction Including Bisphenols Extracted from Daily Products, Food Packaging and Treated Wastewater Using Optimized Solid-Phase Extraction and Temperature-Dependent Inclusion Chromatography**;** Molecules 2019, 24(7), 1285; https://doi.org/10.3390/molecules24071285

**[Le 2019]** G. Le, N. Chanlek, J. Manyam, P. Opaprakasit, N. Grisdanurak, P. Sreearunothai; Insight into theultrasonication of graphene oxide with strong changes in its properties and performance for adsorptionapplications; Chem. Eng. J. 375: 1212–1222

**[Lu 2019]** F. Lu, A. Dong, G. Ding, K. Xua, J. Li, L. You; Magnetic porous polymer composite for high performance adsorption of acid red 18 based on melamine resin and chitosan; J Mol Liq 294 (2019) 111515

**[Mirzajani 2019]** R. Mirzajani, S. Karimi; Ultrasonic assisted synthesis of magnetic Ni-Ag bimetallic nanoparticlessupported on reduced graphene oxide for sonochemical simultaneous removal of sunset yellow and tartrazine dyes by response surface optimization: application of derivative spectrophotometry; Ultrason. Sonochem. 50, 239–250, https://doi.org/10.1016/j.ultsonch.2018.09.022

**[Rashidi 2019]** M. Rashidi, S. M. Sajjadi, H. Z. Mousavi; Kinetic analysis of azo dye decolorization during their acid–base equilibria: photocatalytic degradation of tartrazine and sunset yellow; React. Kinet. Mech. Catal. (2019) 128:555–570, https://doi.org/10.1007/s11144-019-01654-1

**----------2018----------**

**[Alaba 2018]** P. A. Alaba, N.A. Oladoja, Y.M Sani, O.B. Ayodele, I.Y. Mohammed, S.F. Olupinla, W.M.W. Daud; Insight into wastewater decontamination using polymeric adsorbents; J. Environ. Chem. Eng. 2018, 6, 1651–1672.

**[Aliabadi 2018]** R. S. Aliabadi, N.O. Mahmoodi; Synthesis and characterization of polypyrrole, polyaniline nanoparticles and their nanocomposite for removal of azo dyes: sunset yellow and Congo red; J. Clean. Prod. 179, 235–245. https://doi.org/10.1016/j. jclepro.2018.01.035

**[Arabzadeh 2018]** N. Arabzadeh, R. Akbarzadeh, A. Mohammadi, M. Darwish; Green synthesis and application of nanomagnetic molecularly imprinted polimer for fast solid-phase extraction of brilliant blue FCF from real samples; J Polym Res 26: 8, https://doi.org/10.1007/s10965-018-1665-5

**[Baptisstella 2018]** A. M. S. Baptisttella, A. A. D. Araújo, M. C. Barreto, V. S. Madeira, M. A. da Motta Sobrinho;The use of metal hydroxide sludge (*in natura* and calcined) for the adsorption of brilliant blue dye in aqueous solution; Envi Technol 2019, VOL. 40, NO. 23, 3072–3085, https://doi.org/10.1080/09593330.2018.1466916

**[Berdahl 2018]** P. Berdahl; S.K. Boocock; G.C.Y. Chan; S.S. Chen; S. Sharon; R.M. Levinson; M.A. Zalich; High quantum yield of the Egyptian blue family of infrared phosphors (MCuSi4O10, M = Ca, Sr, Ba); J Appl. Phys. Vol. 123, Issue19, DOI10.1063/1.5019808

**[Bijelić 2018]** L. Bijelić, D., Puntarić, V. Gvozdić, D.Vidosavljević, D. Jurić, Z. Lončarić, A. Puntarić, E.Puntarić, M. Vidosavljević, I. Puntarić, A. Muller, S. Šijanović; Presence of war related elements in dandelion (*Taraxacum officinale*) as a possible consequence of military activities in east Croatia; *A. Agricult. Scandi. Sec. B- Soil & Plant Science*. 2018, 68 (3), pp 264-272; DOI:10.1080/09064710.2017.1394485

**[Gong 2018]** J. Gong, L. Mo, J. Li; A comparative study on the preparation and characterization of cellulose nanocrystals with various polymorphs; Carbohydrate Polymers 195 (2018) 18–28

**[Grumezescu 2018a]** A. M. Grumezescu (Ed.); Handbook of Food Bioengineering. In Role of Matial Science in Food Bioengineering; Academic Press/Elsevier: Cambridge, MA, USA, 2018; Volume 19, ISBN 978-0-12-811448-3, Chapter 3

**[Grumezescu 2018b]** A. M. Grumezescu (Ed.); Handbook of Food Bioengineering. In Role of Matial Science in Food Bioengineering; Academic Press/Elsevier: Cambridge, MA, USA, 2018; Volume 19, ISBN 978-0-12-811448-3, Chapter 6

**[Maddigpu 2018]** P. R. Maddigpu, B. Sawant, S. Wanjari, M.D. Goel, D. Vione, R.S. Dhodapkar, S. Rayalu; Carbon nanoparticles for solar disinfection of water; J. Hazard. Mater. 2018, 343, 157–165

**[Mitura 2018]** K. A. Mitura; E. Włodarczyk; Fluorescent nanodiamonds in biomedical applications. J. AOAC Int.101(5): 1297–1307

**[Neethirajan 2018]** S. Neethirajan, V. Ragavan, X. Weng, R. Chand; Biosensors for sustainable food engineering: challenges and perspectives. Biosensors 8, 23: 1–34.

**[Peña-Gonzalez 2018]** A. Peña-Gonzalez , O. García-Beltrán, E. Nagles; Detection of Sunset Yellow by Adsorption Voltammetry at Glassy Carbon Electrode Modified with Chitosan

**[Piaskowski 2018]** K. Piaskowski, R. Świderska-Dąbrowska, P. K. Zarzycki; Dye Removal from Water and Wastewater Using Various Physical, Chemical, and Biological Processes;J AOAC Int Vol. 101, No. 5

**[Ren 2018]** G. Ren, M. Tang, F. Chai H. Wu; One-pot synthesis of highly fluorescent carbon dots from spinach and multipurpose applications; Eur. J. Inorg. Chem. 153–158

**[Saleem 2018]** H. Saleem, M. Haneef, H.Y. Abbasi; Synthesis route of reduced graphene oxide via thermal reduction of chemically exfoliated graphene oxide. Mater. Chem. Phys. 204: 1–7. DOI: 10.1016/j.matchemphys.2017.10.020

**[Świderska-Dąbrowska 2018]** R. Świderska-Dąbrowska, K. Piaskowski, P.K. Zarzycki; Preliminary Studies of Synthetic dye adsorption on iron sludge and activated carbons, J AOAC Int 101 (2018) 1-8

**[Yakout 2018]** A. A. Yakout, M.E. Mahmoud; Fabrication of magnetite-functionalized-graphene oxide and hexadecyltrimethyl ammonium bromide nanocomposite for efficient nanosorption of sunset yellow; Mater. Sci. Eng. C 92, 287–296. https://doi.org/10. 1016/j.msec.2018.06.060

**[Yousefi 2018]** Z. Yousefi, A. Zafarzadeh, A. Ghezel; Application of Taguchi's experimental design method for optimization of Acid Red 18 removal by electrochemical oxidation proces; Environ Health Eng Manag J 2018, 5(4), 241–248

**----------2017----------**

**[Asfaram 2017]** A. Asfaram, M. Ghaedi, G.R. Ghezelbash, F. Pepe; Application of experimental design and derivative spectrophotometry methods in optimization and analysis of biosorption of binary mixtures of basic dyes from aqueous solutions;Ecotoxicol Environ Saf, 139 (2017) 219-227

**[Buntić 2017]** A. V. Buntić, M.D. Pavlović, D.G. Antonović, S.S Šiler-Marinković, S.I. Dimitrijević-Branković; A treatment of wastewater containing basic dyes by the use of new strain Streptomyces microflavus CKS6; (2017) J. Clean. Prod. 148, 347–354

**[Chatzimitakos 2017]** T. A. Chatzimitakos, L. Kasouni, A. Sygellou, A. Avgeropoulos, A.Troganis and C. Stalikas; Two of a kind but different: Luminescent carbon quantum dots from Citrus peels for iron and tartrazine sensing and cell imaging; Talanta 175: 305–312

**[Dil 2017]** E. A. Dil, M. Ghaedi, G.Reza, A. Asfaram; Multi-responses optimization of simultaneous biosorption of cationic dyes by live yeast Yarrowia lipolytica 70562 from binary solution: Application of first order derivative spectrophotometry; Ecotoxicol. Environ. Saf. (2017) 139, 158–164

**[Ferreira 2017]** G. M. D. Ferreira, M.C. Hespanhol, J.P. Rezende, A.C.S. Pires, L.V.A Gurgel, L.H.M. Silva;Adsorption of red azo dyes on multi-walled carbon nanotubes and activated carbon: A thermodynamic study; Coll. Surf. A. 529, 531–540

**[Gatidou 2017]** G. Gatidou,M.Oursouzidou, A. Stefanatou, A.S. Stasinakis (2017); Removal mechanisms of benzotriazoles in duckweed Lemna minor wastewater treatment systems; Sci Total Environ 596-597, 12-17

**[Gopinathan 2017]** R. Gopinathan, A. Bhowal, C. Garlapati; Thermodynamic study of some basic dyes adsorption from aqueous solutions on activated carbon and new correlations; J. Chem. Thermodynamics 107 (2017) 182–188

**[Grumezescu 2017]** A. M. Grumezescu, A.M. Holban (Eds.) Handbook of Food Bioengineering. In Ingredients Extraction by Physico-Chemical Method in Food; Academic Press/Elsevier: London, UK, 2017; Volume 4, ISBN 978-0-12-811521-3

**[Iatrou 2017]** E. I. Iatrou, G. Gatidou, D. Damalas, N.S. Thomaidis, A.S. Stasinakis; Fate of antimicrobials in duckweed Lemna minor wastewater treatment systems; J Hazard Mater 330, 116-126

**[Janović 2017]** B.S. Janović, A.R. Collins, Z.M. Vujčić, M.T. Vujčić; Acidic horseradish peroxidase activity abolishes genotoxicity of common dyes; J. Hazard. Mater. 321, 576–585. doi:10.1016/j.jhazmat.2016.09.037

**[Khan 2017]** Q. A. Khan, A. Shaur, T.A. Khan, Y.F. Joya, M.S. Awan; Characterization of reduced graphene oxide produced through a modified Hoffman method; Cogent. Chem. 2017, 3, 1298980

**[Kumawat 2017]** M.K. Kumawat, M. Thakur, R.B. Gurung, R. Srivastava; Graphene quantum dots from Mangifera indica: Application in near-infrared bioimaging and intracellular nanothermometry; ACS Sustainable Chem. Eng. 5: 1382–1391

**[Kuppusamy 2017]** S. Kuoousamy, M. Sethurajan, M. Kadarkarai, R. Aruliah; Biodecolourization of textile dyes by novel, indigenous Pseudomonas stutzeri MN1 and Acinetobacter baumannii MN3; J Environ Chem Eng (2017) 5: 716-724

**[Li 2017]** Q. Li, Y. Li, X. Maa, Q. Du, K. Sui, D. Wang, C. Wang, H. Li, Y. Xia; Filtration and adsorption properties of porous calcium alginatemembrane for methylene blue removal from water;Chem Eng J 316 (2017) 623–630

**[Lewandowska 2017]** L. Lewandowska, E. Włodarczyk, B. Fenert, A. Kaleniecka, P.K. Zarzycki; A Preliminary Study for the fast Prototyping of Simple Electroplanar Separation Systems Based on Various Natural Polymers and Planar Chromatographic Stationary Phases; JPC- J Planar Chromat- Modern TLC 30 (2017) 440-452

**[Manavi 2017]** N. Manavi, A.S. Kazemi, B. Bonakdarpour; The development of aerobic granules from conventional activated sludge under anaerobic-aerobic cycles and their adaptation for treatment of dyeing wastewater; Chem. Eng. J. 312, 375–384

**[Melo 2017]** R. P. F. Melo, E. L. de Barros Neto, M. C. P. de Alencar Moura, T. N. de Castro Dantas, A. A. D. Neto, S. K. da Silva Nunes; Removal of Direct Yellow 27 Dye by Ionic Flocculation: The Use of an Environmentally Friendly Surfactant; J Surfact Deterg (2017) 20:459–465, DOI 10.1007/s11743-016-1913-9

**[Nedyalkova 2017]** M. A. Nedyalkova, B. V. Donkova, V. D. Simeonov; Chemometrics Expertise in the Links Between Ecotoxicity and Physicochemical Features of Silver Nanoparticles: Environmental Aspects; J AOAC Int Vol. 100, No. 2, 2017

**[Ohta 2017]** H. Ohta, E. Włodarczyk, K. Piaskowski, A. Kaleniecka, L. Lewandowska**,** M. J. Baran, M. Wojnicz, K. Jinno., Y. Saito, P.K. Zarzycki; Unexpected differences between planar and column liquid chromatographic retention of 1-acenaphthenol enantiomers controlled by supramolecular interactions involving β-cyclodextrin at subambient temperatures; Anal Bioanal Chem – Springer 409 (2017) 3695-3706

**[Prabhakar 2017]** A-K. Prabhakar, H.Y Lai, M.G. Potroz, M.K Corliss, J.H Park, R.C Mundargi, D. Cho, S-I. Bang, N-J. Cho; Chemical processing strategies to obtain sporopollenin exine capsules multi-compartmental pine pollen. J. of Ind. and Eng. Chem., 53, pp 375–385

**[Rajasimman 2017]** M. Rajasimman, S. Venkatesh Babu, N. Rajamohan; Biodegradation of textile dyeing industry wastewater using modified anaerobic sequential batch reactor – Start-up, parameter optimization and performance analysis;J. Taiwan Inst. Chem. Eng. 72, 171–181. https://doi. org/10.1016/j.jtice.2017.01.027

**[Raval 2017]** N.P. Raval, P.U. Shah, N.K. Shah; REVIEW ARTICLE Malachite green ‘‘a cationic dye’’ and its removal from aqueous solution by adsorption; Appl. Water Sci. 7, 3407–3445. doi:10.1007/s13201-016-0512-2

**[Sun 2017]** X. Sun, Y. Lei; Fluorescent dots and their sensing applications. TRAC-Trend; Anal. Chem. 89: 163–180

**[Ślączka-Wilk 2017]** M.M. Ślączka-Wilk, E. Włodarczyk,. M.J. Baran, A. Kaleniecka, P.K. Zarzycki; Miniaturized Temperature-controlled Planar Chromatography (micro-TLC) as a Versatile Technique for Fast Screening of Micropollutants and Biomarkers Derived from Surface Water Ecosystems and During Wastewater Technological Processes of Wastewater Treatment; JAOAC, Vol. 100 (2017) 935-949

**[Vanni 2017]** G. Vanni, L. B. Escudero, G.L. Dotto; Powdered grape seeds (PGS) as an alternative biosorbentto remove pharmaceutical dyes from aqueous solutions; Water Sci Techn 76.5 2017

**[Virtanem 2017]** J. Virtanem,A. Pammo,J. Keskinen, E. Sarlin, S. Tuukkanen; Pyrolysed cellulose nanofibrils and dandelion pappus in supercapacitor application; *Cellulose,* 2017, 24 (8), pp 3387-3397

**[Włodarczyk 2017]** E. Włodarczyk, P.K. Zarzycki; Chromatographic behaviour of selected dyes on micro-TLC plates under NP and RP conditions - potential application as the internal standards substances for chromatographic and/or microfluidic systems. J. of Liq. Chromatogr.& Relat. Technologies, 2017**,** 40, pp 5-6, DOI:10.1080/10826076.2017.1298028

**[Xu 2017]** F. Xu, X.Y. Qi, Q. Kong, L. Shu, M.S. Miao, S. Xu, Y.D. Du, Q. Wang, Q. Liu, S.S. Ma; Adsorption of sunset yellow by luffa sponge, modified luffa and activated carbon from luffa sponge. Desalin. Water Treat. 96, 86–96. https://doi.org/10.5004/ dwt.2017.20925

**[Yuan 2017]** R.J. Yuan, Y. Yuan, , L. WuChen, H. Zhou, J. Chen; Efficient synthesis of graphene oxide and the mechanisms of oxidation and exfoliation. Appl. Surf. Sci. 416: 868–877

**[Zaaba 2017]** N.I. Zaaba, K.L. Foo, U. Hashim, S.J. Tan, W.-W. Liu, C.H. Voon; Synthesis of graphene oxide usinmodified hummers method: solvent influence. Procedia Engineer. 184: 469–477

**----------2016----------**

**[Arabzadeh 2016]** N. Arabzadeh, A. Khosravi, A. Mohammadi, N. M. Mahmoodi; Enhanced photodegradation of hazardous tartrazine by composite of nanomolecularly imprinted polymernanophotocatalyst with high efficiency; Des Water Treat 57(7):3142–3151

**[Atta-ur-Rahman 2016]** Atta-ur-Rahman (Ed.);Studies in Natural Product Chemistry. In Bioactive Natural Products; Elsevier Science Publishers: Amsterdam,
The Netherlands, 2016; Volume 48, ISBN 978-0-444-63602-7.

**[Biswas 2016]** P. Biswas, R. Bandyopadhyaya; Water disinfection using silver nanoparticle impregnated activated carbon: Escherichia coli cell-killing in batch and continuous packed column operation over a long duration; Water Res. 2016, 100, 105–115

**[Chang 2016]** Y-N. Chang, J-L. Gong, G-M. Zeng; X-M. Ou, B. Song, M. Guo, J. Zhang, H.-Y. Liu; Antimicrobial behavior comparison and antimicrobial mechanism of silver coated carbon nanocomposites; Process. Saf. Environ. 2016, 102, 596–605

**[Errington 2016]** B. Errington, G.Lawson, S.W. Lewis, G.D. Smith; Micronised Egyptian blue pigment: A novel near-infrared luminescent fingerprint dusting powder; Dye Pigm, 2016**,** 132, pp 310-315, DOI:10.1016/j.dyepig.2016.05.008

**[Flores-Cano 2016]** J.V. Flores-Cano, M. Sanchez-Polo, J. Messoud, I. Velo-Gala, R. Ocampo-Perez, J. Rivera-Utrilla;Overall adsorption rate of metronidazole, dimetridazole and diatrizoate on activated carbons prepared from coffee residues and almond shells**;**J. Environ.Manage. 169, 116–125. doi:10.1016/j.jenvman.2015.12.001

**[Grumezescu 2016]** A.M. Grumezescu. (Editor); Cyclodextrins-based nanocomplexes for encapsulation of bioactive compounds in food, cosmetics, and pharmaceutical products: principles of supramolecular complexes formation, their influence on the antioxidative properties of target chemi-cals, and recent advances in selected industrial applications.*Encap.,* Nanotech. in the Agri-Food Ind., 2016**,** 2; Chap. 17 by **Zarzycki**, P.K., Fenert, B., Głód, B.K., Elsevier*,* 2016**,** pp 717-767*;* ISBN: 978-0-12-804307-3

**[Irikura 2016]** K. Irikura, N. Bocchi, R.C. Rocha-Filho, S.R. Biaggio, J. Iniesta, V. Montiel; Electrodegradation of the Acid Green 28 dye using Ti/beta-PbO2 and Ti-Pt/beta-$PbO_2$ anodes; J Environ Manage 2016; 183: 306-13. doi: 10.1016/j. jenvman.2016.08.061

**[Ismail 2016]** M.A. Ismail, S.M. Sakr; Validation of replacement of the synthetic food dye ‘Sunset Yellow’-induced hepatotoxicity and genotoxicity with the nutraceutical ‘curcumin’ in mice. Merit Res. J. Med. Med. Sci. 4, 25–50

**[Jin 2016]** E. Jin, J. Guo, F.Yang, Zhu, Y., Song, J., Jin, Y., O.J. Rojas; On the polymorphic andmorphological changes of cellulose nanocrystals (CNC-I) upon mercerization andconversion to CNC-II. Carbohydrate Polymers, 143(5), 327–335

**[Lech 2016]** K. Lech, M. Jarosz; Identification of Polish cochineal (Porphyrophora polonica L.) in historical textiles by high-performance liquid chromatography coupled with spectrophotometric and tandem mass spectrometric detection; Anal Bioanal Chem **408,** 3349–3358

**[Lee 2016]** S. Lee, R. Doong; Design of size-tunable molecularly imprinted polymer for selective adsorption of pharmaceuticals and biomolecules; J Biosens Bioelectron 7:228–235

**[Li 2016]** X. Li, Y. Wu, W. Zhu, F. Xue, Y. Qian, C. Wang; Enhanced electrochemical oxidation of synthetic dyeing wastewater using $SnO_2$-Sb-doped $TiO_2$-coated granular activated carbon electrodes with high hydroxyl radical yields; Electrochim Acta 2016; 220: 276-84. doi: 10.1016/j. electacta.2016.09.109

**[Li 2016a]** Q. Li, J. Gluch, P. Krüger, M. Gall, Ch. Neinhuis, E. Zschech; Pollen structure visualization using high-resolution laboratory-based hard X-ray tomography. Biochem. and Biophysic. Research Communicat; 479, pp 272-276

**[Mirzajani 2016]** R. Mirzajani, M. Bagheban; Simultaneous preconcentration and determination of malachite green and fuchsine dyes in seafood and environmental water samples using nano-alumina-based molecular imprinted polymer solid-phase extraction; Inter J Environ Anal Chem 96(6):576–594

**[Nazerah 2016]** A. Nazerah, A.F. Ismail, J. Jaafar; Incorporation of bactericidal nanomaterials in development of antibacterial membrane for biofouling mitigation: A mini review; Jurnal Teknologi (Sciences & Engineering) 78:12: 53–61

**[O'Connor 2016]** E.F. O'Connor, S. Paterson, R. de la Rica; Naked-eye detection as a universal approach to lower the limit of detection of enzyme-linked immunoassays;Anal Bioanal Chem, 408(2016) 3389–3393

**[Panagopoulou 2016]** A. Panagopoulou, K.. Karanasios, G. Xanthopoulou; Ancient Egyptian Blue ($CaCuSi_4O_{10}$) Pigment by Modern Solution Combustion Synthesis Method.; Eurasian Chem.-Technol. J. 2016, 18. pp. 31-37

**[Pezoti 2016]** O. Pezoti, A.L. Cazetta, K.C. Bedin, L.S. Souza, A.C. Martins, T.L Silva, O.O. Santos Junior, J.V. Visentainer, V.C. Almeida; NaOH-activated carbon of high surface area produced from guava seeds as a high-efficiency adsorbent for amoxicillin removal: Kinetic, isotherm and thermodynamic studies; Chem. Eng. J.288, 778–788. doi:10.1016/j.cej.2015.12.042

**[Rybczyńska-Tkaczyk 2016]** K. Rybczyńska-Tkaczyk, T. Korniłłowicz-Kowalska; Biosorption optimization and equilibrium isotherm of industrial dye compounds in novel strains of microscopic fungi; Int. J. Environ. Sci. Technol. (2016)13, 2837–2846. https://doi.org/10.1007/s13762-016-1111-3

**[Rajasulochana 2016]** P. Rajasulochana, V. Preethy; Comparison on efficiency of various techniques in treatment of waste and sewage water—A comprehensive review. Resour. Technol. 2016, 2, 175–184

**[Zinicovscaia 2016]** I. Zinicovscaia; Conventional Methods of Wastewater Treatment. In Cyanobacteria for Bioremediation of Wastewaters; Springer: Cham, Switzerland, 2016; pp. 17–25

**[Zarzycki 2016]** Zarzycki P.K., Fenert B., Głód B.K., Cyclodextrins-based nanocomplexes for encapsulation of bioactive compounds in food, cosmetics, and pharmaceutical products: principles of supramolecular complexes formation, their influence on the antioxidative properties of target chemicals, and recent advances in selected industrial applications, A. M. Grumezescu (Editor), Encapsulations, Nanotechnology in the Agri-Food Industry, Volume 2; Chapter 17717-767, Elsevier

**----------2015----------**

**[Ahmad 2015]** A. Ahmad, S.H. Mohd-Setapar, C.S. Chuong, A. Khatoon, W.A. Wani, R. Kumar, M. Rafatullah; Recent advances in new generation dye removal technologies: novel search for approaches to reprocess wastewater; RSC Adv. 5, 30801–30818. https://doi.org/10.1039/c4ra16959j

**[Amchova 2015]** P. Amchova, H. Kotolova, J. Ruda-Kucerova; Health safety issues of synthetic food colorants. Regul. Toxicol. Pharmacol. 73, 914922.https://doi.org/10.1016/j.yrtph.2015.09.026

**[Bergstorm 2015]** L. Bergstrom, R. Mezzenga; Understanding nanocellulose chirality and structure–properties relationship at the single fibril level; Nat Commun 6:7564, 1–11

**[Hazzaa 2015]** R. Hazzaa, M. Hussein; Adsorption of cationic dye from aqueous solution onto activated carbon prepared from olive stones; Environ Technol Innovation4, 36–51. doi:10.1016/j.eti.2015.04.002

**[Hyde 2015]** A. Hyde, O. Batishchev; Undergraduate physics laboratory: Electrophoresis in chromatography Paper; Am J Phys83

**[Kiziltas 2015]** Synthesis of bacterial cellulose using hot water extracted wood sugars Esra Erbas Kiziltasa, Alper Kiziltasa, Douglas J. Gardner; Carbohydr Polym 124 (2015) 131–138

**[Mu 2015]** X. Mu, D.G. Gray; Droplets of cellulose nanocrystal suspensions on drying give iridescent 3-D “coffee-stain” rings; Cellulose 22, 1103–1107

**[Panjali 2015]** Z. Panjali, A.A. Asgharinezhad, H. Ebrahimzadeh, S. Karami, M. Loni, M. Rezvani, R. Yarahmadi, S.J.; Development of a selective sorbent based on a magnetic ion imprinted polymer for the preconcentration and FAAS determination of urinary cadmium; Anal Met 7(8):3618–3624

**[Panwar 2015]** V.Panwar, A. Chattree, K. Pal. 2015; A new facile route for synthesizing of graphene oxide using mixture of sulfuric-nitric-phosphoric acids as intercalating agent; Physica E73: 235–241

**[Poole 2015]** C.F. Poole; Instrumental Thin-Layer Chromatography; Amsterdam: Elsevier

**[Popowicz 2015]** J. Popowicz; P. Koszelnik; The Influence of the physicochemical properties on the methods of inactivation and removal of cytostatic drugs from water and wastewater; Acta Sci. Pol., Form. Circumiectus, Vol.14, Issue 3, Pages: 107-125; DOI: 10.155

**[Rajamanickam 2015]** D. Rajamanickam, P. Dhatshanamurthi, M. Shanthi; Preparation and characterization of SeO2/TiO2 composite photocatalyst with excellent performance for sunset yellow azo dye degradation under natural sunlight illumination. Spectrochim. Acta A.138, 489–498. https://doi.org/10.1016/j.saa.2014.11.070

**[Roosta 2015]** M. Roosta, M. Ghaedi, R. Sahraei, M.K. Purkait; Ultrasonic assisted removal of sunset yellow from aqueous solution by zinc hydroxide nanoparticle loaded activated carbon: optimized experimental design. Mater. Sci. Eng. C 52, 82–89. https://doi.org/10.1016/j.msec.2015.03.036

**[Sasmaz 2015]** M. Sasmaz, E.I. Topal, E. Obek,A. Sasmaz; The potential of Lemna gibba L. and Lemna minor L. to remove Cu, Pb, Zn, and As in gallery water in a mining area in Keban, Turkey; J Environ Manage. 163: 246–253

**[Suszyński 2015]** Suszyński Z., Zarzycki P.K., New approach for sensitive photothermal detection of C60 and C70 fullerenes on micro-TLC plates, Analytica chimica acta 863 (2015) 70-77.76/ASP.FC/2015.14.3.107

**[Tsai 2015]** C.-F. Tsai, C.-H Kuo, D.Y.-C. Shih; Determination of 20 synthetic dyes in chili powders and syrup-preserved fruits by liquid chromatography/tandem mass spectrometry; J Food Drug Anal 23(3):453–462

**[Usov 2015]** I. Usov, G. Nystrom, J. Adamcik, S. Handschin, C. Schutz, A. Fall, L. Bergström, R. Mezzenga; Understanding nanocellulose chirality and structure–properties relationship at the single fibril level; Nature Communications volume 6, Article number: 7564 (2015)

**[Yeh 2015]** C-N. Yeh, K. Raidongia, J. Shao, Q-H. Yang, J. Huang; On the origin of the stability of graphene oxide membranes in water;Nature Chemistry,volume 7, pages 166–170

**[Wang 2015]** D. Wang, L. Liu, X. Jiang, J. Yu, X. Chen; Adsorption and removal of malachite green from aqueous solutionusing magnetic -cyclodextrin-graphene oxide nanocompositesas adsorbents; Colloid Surf. A 466, 166–173

**----------2014----------**

**[Armin 2014]** M.T. Amin, A.A. Alazba, U. Manzoor; A review of removal of pollutants from water/wastewater using different types of nanomaterials; Adv. Mater. Sci. Eng. 2014, pp 1–24; DOI:10.1155/2014/825910

**[Azarian 2014]** G. Azarian, D. Nematollahi, A.R. Rahmani, K. Godini, M. Bazdar, H. Zolghadrnasab; Monopolar electro-coagulation process for azo dye C.I. Acid Red 18 removal from aqueous solutions; Avicenna J Environ. Health Eng., 1 (1)

**[Chandrasekaran 2014]** S. Chandrasekaran, Y. Sameena, I.V.M.V. Enoch; Modulation of the interaction of Coumarin 7 with DNA by- cyclodextrin; J Incl Phenom Macrocycl Chem, 81, 225–236

**[French 2014]** A. French, P. Langan; 100 years of cellulose fiber diffraction and the emergence of complementary techniques; Cellulose 21, 1087–1089

**[Goswami 2014]** C. Goswami, A.Majumder, A.K.Misra, K.Bandyopadhyay; Arsenic Uptake by Lemna minor in Hydroponic System; Int J Phytoremediation 16 (12): 1221–1227

**[Kumar 2014]** S. Kumar, W. Ahlawat, G. Bhanjana, S. Heydarifard, M.M. Nazhad, N. Dilbaghi; Nanotechnology-Based Water Treatment Strategies. J. Nanosci. Nanotechnol, 14, 1838–1858

**[Lin 2014]** C-W. Lin, Z. Zhao, J. Kim, J. Huang; Pencil Drawn Strain Gauges and Chemiresistors on Paper; Sci Rep 4, 1–5; article, No.: 3812

**[Mackenzie 2014]** G. Mackenzie, S. Beckett, S. Atkin, A. Diego-Taboada; Hollow pollen shells to enhance drug delivery. Pollen and Spore Shells—Nature's Microcapsules; Chapter 24

**[Mackenzie 2014]** G. Mackenzie, S. Beckett, S. Atkin, A. Diego-Taboada;
Pollen and Spore Shells—Nature's Microcapsules; Part IV Materials used in Microencapsulation, Chapter 24; University of Hull, Hull, UK and Sporomex Ltd

**[Ozdemir 2014]** I. Ozdemir, M. Şahin, R. Orhan, M. Erdem; Preparation and characterization of activated carbon from grape stalkby zinc chloride activation; Fuel Process. Technol. 125, 200–206. doi:10.1016/j.fuproc.2014.04.002

**[Rajamanickam 2014]** D. Rajamanickam, M. Shanthi; Photocatalytic degradation of an azo dye Sunset Yellow under UV-A light using TiO2/CAC composite catalysts. Spectrochim. Acta 128,100–108. https://doi.org/10.1016/j.saa.2014.02.126

**[Reinholt 2014]** S.J. Reinholt, A. Sonnenfeldt, A. Naik, M.W. Frey, A.J. Baeumner; Developing new materials for paper-based diagnostics using electrospun nanofibers;
Anal Bioanal Chem406, 3297–3304

**[Roosta 2014]** M. Roosta, M. Ghaedi, N. Shokri, A. Daneshfar, R. Sahraei, A. Asghari; Optimiza-tion of the combined ultrasonic assisted/adsorption method for the removal ofmalachite green by gold nanoparticles loaded on activated carbon: experimen-tal design; Spectrochim. Acta A 118 (2014) 55–65

**[Wang 2019]** S.Wang, Y. Zhai, Q. Gao,W. Luo, H. Xia, C. Zhou; Highly efficient removal of Acid Red 18 from aqueous solution by magnetically retrievable chitosan/carbon nanotube: batch study, isotherms, kinetics, and thermodynamics; J. Chem. Eng. Data 59 (2014) 39–51

**[Włodarczyk 2014]** E. Włodarczyk, M.J. Baran, M.M. Ślączka, J.K. Portka, P.K. Zarzycki; Fingerprinting of soot dust materials using micro-TLC; J. Liquid Chromatogr. Related Technol. 37 (2014) 2846–2856

**[Yagub 2014]** M.T.Yagub, T.K. Sen, S. Afroze, H.M. Ang; Dye and its removal from aqueous solution by adsorption: a review; Adv. Colloid Interface Sci. 209, 172–184. https://doi.org/10.1016/j.cis.2014.04.002

**[Zhang 2014]** H-K. Zhang, H. Lu, J. Wang, G.-F. Liu, J-T. Zhou; Accelerating Effect of Bio-Reduced Graphene Oxide on Decolorization of Acid Red 18 by Shewanella algae; Appl Biochem Biotechnol (2014) 174:602–611; DOI 10.1007/s12010-014-1106-9

**----------2013----------**

**[Appenroth 2013**] K. J. Appenroth, B. Nikolai,L. Eric (2013); Telling duckweed apart: genotyping technologies for the Lemnaceae; Chin J Appl Environ Biol**19**: 1–10. doi:10.3724/sp.j.1145.2013.00001

**[Abbey 2013]** J Abbey, et at.; Colorants. pp 459-465 in Encyclopedia of Food Safety; Vol 2: Hazards and Diseases. Eds, Motarjemi Y et al. Academic Press, 2013. ISBN 9780123786135

**[Arqiani 2013]** M. Arqiani, J. A. Jonidi, K.R. Rezaeei, M. Gholami; Study of the aniline removal from industrial wastewater by electrochemical proces; Iran Occup Health J 2013; 10(1): 70-8

**[Chowdhury 2013]** I. Chowdhury, M. C. Duch, N. D. Mansukhani, M.C. Hersam, D. Bouchard;Colloidal Properties and Stability of Graphene Oxide Nanomaterials in the Aquatic Environment; Environ Sci Technol, 47, 12, 6288–6296

**[Khandegar 2013]** V. Khandegar, A.K. Saroha; Electro coagulation for the treatment of textile industry effluent–A review; J. Environ. Manage., 128, 949–963

**[Khan 2013]** A.A. Khan, R. Ahmad, A. Khan, P.K. Mondal; Preparation of unsaturated polyesterCe (IV) phosphate by plastic waste bottles and its application for removal ofMalachite green dye from water samples; Arab. J. Chem. 6 (2013) 361–368

**[Kurra 2013]** N. Kurra, G.U. Kulkarni; Pencil-on-paper: electronic devices; Lab Chip13, 2866–2873

**[Lisowski 2013]** P**.** Lisowski, P.K. Zarzycki; Microfluidic paper based analytical devices (μPADs) and micro total analysis systems (μTAS): development, applications and future trends; Chromatographia 76, 1201-1214

**[Malakootian 2013]** M. Malakootian, M. Asadi, A.H. Mahvi; Evaluation of electro-Fenton process performance for COD and reactive Blue 19 removal from aqueous solution; Iranian J Health Environ 2013; 5(4): 433-44

**[Marcinkowska 2013]** A. Marcinkowska, M. Legan, J. Jezierska; Molecularly imprinted polymeric Cu (II) catalysts with modified active centres mimicking oxidation enzymes; J Polym Sci 20:317–321

**[Mirnaghi 2013]** F.S. Mirnaghi, D. Hein, J. Pawliszyn; Thin-Film Microextraction Coupled with Mass Spectrometry and Liquid Chromatography–Mass;SpectrometryChromatographia 76**,** 1215–1223

**[Reddy 2013]** D.H.K. Reddy; S.-M. Lee; Application of magnetic chitosan composites for the removal of toxic metal and dyes from aqueous solutions; Adv. Coll. Interface Sci. 2013, 68–93

**[Siti Zuraida 2013]** M. Siti Zuraida, C.R. Nurhaslina, K.H. Ku Halim; Removal of Synthetic Dyes from Wastewater by Using Bacteria, Lactobacillus delbruckii; IRJES**2**, 1–7

**[Saravana 2013]** K. K. Saravana, M. Sushma, R.R. Prasanna; Dissolution enhancement of poorly soluble drugs by using complexation technique—a review; J Pharm Sci Res, 5:120–4.

**[Shen 2013]** Y. Shen, A.C. Lua; A facile method for the large-scale continuous synthesis of graphene sheets using a novel catalyst; Sci. Rep. 2013, 3, 1–6

**[Shirmardi 2013]** M. Shirmardi, A.H. Mahvi, B. Hashemzadeh, A. Naeimabadi, G. Hassani, M.V. Niri; The adsorption of malachite green (MG) as a cationic dye onto functionalizedmulti walled carbon nanotubes; Korean J. Chem. Eng. 30 (2013) 1603–1608

**[Zhang 2013]** C. Zhang, Y. Jiang, Y. Li, Z. Hu, L. Zhou, M. Zhou; Three-dimensional electrochemical process for wastewater treatment: a general review; Chem Eng J 2013; 228: 455-67. doi: 10.1016/j.cej.2013.05.033

**[Zukunft 2013]** S. Zukunft, M. Sorgenfrei, C. Prehn, G. Moller, J. Adamski; Targeted metabolomics of dried blood spot extracts; Chromatographia, 76, 1295–1305

**----------2012----------**

**[Abid 2012]** M.F. Abid, M.A. Zablouk, A.M. Abid-Alameer; Experimental study of dye removal fromindustrial wastewater by membrane technologies of reverse osmosis and nanofiltration; J. Environ. Health Sci. Eng. 9, 1–9 doi:10.1186/1735-2746-9-17

**[FitzHugh 1997/2012]** E.W. FitzHugh, (editor); Artists' Pigments: A Handbook of Their History and Characteristics, 1997/2012, 3, National Gallery of Art, Washington Archetype Publications, London

**[Ghaedi 2012]** M. Ghaedi, J.A. Hekmati, S. Khodadoust, R. Sahraei, A. Daneshfar, A. Mihandoost, M.K.Purkait; Cadmium telluride nanoparticles loaded on activated carbon as adsorbent for removal of sunset yellow; Spectrochim. Acta Part A Mol Biomol Spectrosc 90, 22–27. https://doi.org/10.1016/j.saa.2011.12.064

**[Kant 2012]** R. Kant; Textile dyeing industry an environmental hazard; Natural Sci; 4, 22-26, http://dx.doi.org/10.4236/ns.2012.41004

**[Koupaie 2012**] E.H. Koupaie, M.R.A. Moghaddam, S.H. Hashemi; Investigation of decolorization kinetics and biodegradation of azo dye Acid Red 18 using sequential process of anaerobic sequencing batch reactor/moving bed sequencing batch biofilm reactor, Int. Biodeterior. Biodegradation 71 (2012) 43–49

**[Li 2012]** N. Li, X.L. Lei; Adsorption of ponceau 4R from aqueous solutions by polyamidoamine–cyclodextrin crosslinked copolymer; J. Incl. Phenom. Macrocycl. Chem. 74, 167–176. doi:10.1007/s10847-011-0096-2

**[Shiri 2012]** S. Shiri, T. Khezeli, S. Lotfi, S. Shiri; Aqueous two-phase systems: a new approach for the determination of brilliant blue FCF in water and food; J Chemistry 2013:6–12

**[Verlicchi 2012]** P. Verlicchi, M. Al Aukidy, E. Zambello; Occurrence of pharmaceutical compounds in urban wastewater: Removal, mass loadand environmental risk after a seconda ry treatment—A review; Sci. Total Environ. 2012, 429, 123–155

**----------2011----------**

**[Cazetta 2011]** A.L. Cazetta, A.M.M.Vargas, E.M. Nogami, M.H. Kunita, M.R. Guilherme, A.C. Martins, T.L. Silva, J.C.G. Moraes, V.C. Almeida; NaOH-activated carbon of high surface area produced from coconut shell: Kinetics and equilibrium studies from the methylene blue adsorption; Chem. Eng. J. 174, 117–125.doi:10.1016/j.cej.2011.08.058

**[Hayenga 2011]** I. Hayenga, M. Nold; Food Color and Other Dye Standards, in: Analytix, Vol. 5, Sigma-Aldrich Marketing Communications Europe, Buchs, 4–7

**[Pourreza 2011]** N. Pourreza, M. Ghomi; Simultaneous cloud point extraction and spectrophotometric determination of carmoisine and brilliant blue FCF in food samples; Talanta 84(1):240–243

**[Srivastava 2011]** M.Srivastava; High-Performance Thin-Layer Chromatography. Berlin: Springer-Verlag

**[Vargas 2011]** A.M.M.Vargas, A.L. Cazetta, C.A., Garcia, J.C.G.,Moraes, E.M. Nogami, E. Lenzi, W.F. Costa, V.C.Almeida; Preparation and characterization of activated carbon from a new raw lignocellulosic material: Flamboyant (Delonix regia) pods; J. Environ. Manage. 92, 178–184. doi:10.1016/j. jenvman.2010.09.013

**[Yamamura 2011]** H. Yamamura, M. Hashino, N. Kubota; Membrane Filtration: Principle and Applications inWater Treatment. SEN-I GAKKAISHI, 2011, 67, 3

**[Zarzycki 2011]** P.K. Zarzycki, M.M. Ślączka,M.B. Zarzycka, E. Włodarczyk, M.J. Baran; Application of micro-thin-layer chromatography as a simple fractionation tool for fast screening of raw extracts derived from complex biological, pharmaceutical and environmental samples; Analytica Chimica Acta 688 (2011) 168-174

**----------2010----------**

**[Aguilar 2010]** F. Aguilar, B. Dusemund, P. Galtier, J. Gilbert, D. Gott, S. Grilli, R. Gürtler, J. König, C Lambré, J. Larsen; Scientific opinion on the re-evaluation of Brown FK (E 154) as a food additive; EFSA J 8:1853–1889

**[Arabzadeh 2010]** N. Arabzadeh, M. Abdouss; Synthesis and characterization of molecularly imprinted polymers for selective solid-phase extraction of pseudoephedrine. Colloid J 72(4):446–455

**[Astec Cellulose 2010]** Astec Cellulose Efficient, Rugged, and Economical Columnsfor Chiral HPLC & SFC, Supelco Analytical, Sigma-Aldrich

**[Baby 2010]** J. Baby, J. Raj, E.T. Biby, P. Sankarganesh, M.V. Jeevitha, S.U. Ajisha, S.S. Rajan (2010); Toxic effect of heavy metals on aquatic environment; IJBCS 4 (4): 939–952

**[Habibi 2010]** Y. Habibi, L. A. Lucia, O. J. Rojas; Cellulose nanocrystals: Chemistry, selfassembly,and applications. Chemical Reviews, 110(6), 3479–3500

**[Marcano 2010]** D.C.Marcano, D.V. Kosynkin, J.M. Berlin, A. Sinitskii, Z.Z. Sun, A. Slesarev et al.; Improved synthesis of graphene oxide; ACS Nano 4(8): 4806–4814

**[Ngah 2010]** W.S.W. Ngah, N.F.M. Ariff, A. Hashim, M.A.K.M. Hanafiah; Malachite greenadsorption onto chitosan coated bentonite beads: isotherms, kinetics andmechanism; CLEAN – Soil Air Water 38 (2010) 394–400

**[Okutucu 2010]** B. Okutucu, A. Akkaya, N.K. Pazarlioglu; Molecularly imprinted polymers for some reactive dyes; Prep Biochem Biotechnol 40(4):366–376

**[Parisi 2010]** O. Parisi, G. Cirillo, M. Curcio; Surface modification of molecularly imprinted polymers for improved template recognition in water media; J Polym Res 17:355–362

**[Sabnis 2010]** R.W. Sabnis; Handbook of biological dyes and stains: synthesis and industrial applications. John Wiley & Sons

**----------2009----------**

**[Fraige 2009]** K. Fraige, N.A. Assuncao, R. de Souza Pinto, E. Carrilho; Analytical assessment of a home made capillary electrophoresis equipment with linear charge coupled device for visible light absorption detection in the determination of food dyes; J Liq Chromatogr Relat Tech 32(13):1862–1878

**[Morlock 2009]** G.E. Morlock, C. Oellig, J. Rapid; Planar Chromatographic Analysis of 25 Water-Soluble Dyes Used as Food Additives; AOAC Int. 92, 745–756

**[Zarzycki 2009]** P.K.Zarzycki, E. Włodarczyk, M.J. Baran; Determination of endocrine disrupting compounds using temperature-dependent inclusion chromatography: II. Fast screening of free steroids and related low-molecular-mass compounds fraction in the environmental samples derived from surface waters, treated and untreated sewage waters as well as activated sludge material; J Chromatogr A, Vol. 1216, Issue 44, Pages 7612-7622

----------2008----------

**[Alves 2008]** S.P. Alves, D.M. Brum, É.C.B. de Andrade, A.D.P. Netto; Determination of synthetic dyes in selected foodstuffs by high performance liquid chromatography with UV-DAD detection; Food Chem 107(1):489–496

**[Gupta 2008]** V.K. Gupta, Suhas; Application of low-cost adsorbents for dye removal--a review; J Environ Manage 2009; 90(8): 2313-42. doi: 10.1016/j.jenvman.2008.11.017

**[Hamdaoui 2008]** O. Hamdaoui, F. Saoudi, M. Chiha, E. Naffrechoux; Sorption of malachite green by a novel sorbent, dead leaves of plane tree: Equilibrium and kinetic modeling; Chem. Eng. J. 143, 73–84

**[Raducan 2008]** A. Raducan, A. Olteanu, M. Puiu, D. Oancea; Influence of surfactants on the fading of malachite green; Cent. Eur. J. Chem. 6(1) 2008 89-92DOI: 10.2478/s11532-007-0066-0

**[Srour 2008]** Srour R.K., L.M.McDonald;Determination of the Acidity Constants of Methyl Red and Phenol Red Indicators in Binary Methanol− and Ethanol−Water Mixtures; J. Chem. Eng. Data 53 (2008) 116–127

**[Waksmundzka-Hajnos 2008]** M. Waksmundzka-Hajnos, J. Sherma, T. Kowalska;Thin layerchromatography in phytochemistry; Taylor & Francis Group, Boca Raton, FL, 2008

**[Zarzycki 2008]** P.K. Zarzycki, Simple horizontal chamber for thermostated micro-thin-layer chromatography. J. Chromatogr A 2008, Vol. 1187, pp 250-259

**[Zarzycki 2008]** P.K. Zarzycki, H. Ohta, Y. Saito, K. Jinno; Interaction of native α-cyclodextrin, β-cyclodextrin and γ-cyclodextrin and their hydroxypropyl derivatives with selected organic low molecular mass compounds at elevated and subambient temperature under RP-HPLC conditions; Anal Bioanal Chem, 391:2793–801

----------2007----------

**[Kozak 2007] M. Kozak;** Wspomaganie chemiczne przeróbki osadów ściekowych na oczyszczalni ścieków „Jamno”; Przegląd Komunalny 5/2007

**[Minotti 2007]** K.S. Minioti, C.F. Sakellariou, N.S. Thomaidis; Determination of 13 Synthetic Food Colorants in Water- Soluble Foods by Reversed-Phase High-Performance Liquid Chromatography Coupled with Diode-Array Detector;Anal Chim Acta 583**,** 103–110

**[Punt 2007]** W.Punt, P.P. Hoen,S. Blackmore,S. Nilsson, A.Le Thomas; Glossary of pollen and spore terminology. Rev. Palaeobot. Palynol. 143,1-81

**[Stncanelli 2007]** R. Stancanelli, A. Mazzaglia, S. Tommasini, M. Calabrò, V. Villari, M. Guardo, P. Ficarra, R. Ficarra; The enhancement of isoflavones water solubility by complexation with modified cyclodextrins: A spectroscopic investigation with implications in the pharmaceutical analysis. J. Pharm. Biomed. Anal, 44, 980–984

----------2006----------

**[Gosetti 2006]** F. Gosetti, V. Gianotti, E. Mazzucco, S. Polati, M.C. Gennaro; Sunlight induced degradation of E133 in a commercial beverage; Dyes and Pigments 74 (2007) 424-432

**[Movahedian 2006]** A.H. Movahedian, R. Rezaee; Investigating the efficiency of advanced photochemical oxidation (APO) technology in degradation of direct azo dye by UV/H2O2 process; J WW 2006; 17(3): 75-83.

**[Ma 2006]** M. Ma, X. Luo, B. Chen, S. Su, S. Yao; Simultaneous determination of water-soluble and fat-soluble synthetic colorants in foodstuff by high-performance liquid chromatography–diode array detection–electrospray mass spectrometry; J Chromatogr A1103(1):170–176

----------2005----------

**[Crini 2005]** G. Crini; Recent developments in polysaccharide-based materials used as adsorbents in wastewater treatment; Prog. Polym. Sci. 2005, 30, pp 38–70

**[Huang 2005]** H.Y. Huang, C.L. Chuang, C.W. Chiu, M.C. Chung; Determination of food colorants by microemulsion electrokinetic chromatography. Electrophoresis 26(4–5):867–877

**[Mozia 2005]** S. Mozia, M.Tomaszewska, A.W. Morawski; Photocatalytic degradation of azo-dye Acid Red 18; Desalination 2005; 185(1-3): 449-56.

**[Tauber 2005]** F. Tauber, K-Ch. Emeis; Sediment mobility in the Pomeranian Bight (Baltic Sea):a case study based on sidescan-sonar imagesand hydrodynamic modeling;Geo-Mar Lett, 2005, 25, pp 221–229

**----------2004----------**

**[Huang 2004]** Huang JW, Poynton CY, Kochian LV, Elless MP (2004). "Phytofiltration of arsenic from drinking water using arsenic hyperaccumulating ferns". Environ Sci Technol. 38 (12): 3412–3417

**[Mozzocchin 2004]** G.A. Mozzocchin, D. Rudello, C. Bragato, F. Angoli; A short note on Egyptian Blue. J Cult Herit 2004, Vol. 5, pp. 129-133.

**[Świderska 2004]** R. Świderska, A.M. Anielak; The significance of Electrokinetic potential in the adsorpion process of humic substances; Rocznik Ochrony Środowiska*,* 2004*,* 6, pp 31-49

**----------2003----------**

**[Hunger 2003]** K. Hunger; Industrial Dyes. Chemistry, Properties, Applications; Wiley-VCH Verlag GmbH & Co. KGaA, Weinheim

**[Sherma 2003]** J. Sherma, B. Fried, Handbook of Thin-Layer Chromatography, Marcel Dekker, New York, 2003

**----------2002----------**

**[Eskilsson 2002]** C.S. Eskilsson, R. Davidsson, L. Mathiasson; Harmful azo colorants in leather determination based on their cleavage and extraction of corresponding carcinogenic aromatic amines using modern extraction techniques; J Chromatogr A 2002;955:215-27.

**[Florian 2002**] M. Florian, H. Yamanaka, P. Carneiro, M.V.B.Zanoni; Determination of brilliant blue FCF in the presence and absence of erythrosine and quinoline yellow food colours by cathodic stripping voltammetry; Food Addit Contam 19(9):803–809

**[Gottlieb 2003]** A. Gottlieb, C. Shaw, A. Smith, A. Wheatley, S. Forsythe;The toxicity of textile reactive azo dyes after hydrolysis and decolourisation; J Biotechnol 2003;101:49-56

**[Laima 2002]** M. Laima,D. Maksymowska-Brossard, P.G. Sauriau, P. Richard, M.Girard, D. Gouleau, L. Joassard;Fluffdeposition on intertidalsediments: effects on benthic biota, ammoniumfluxes and nitrificationrates**;** Biogeochemistry*,* 2002,Vol. 61, pp 115–133

**----------2001----------**

**[Baraldi 2001]** P. Baraldi, F. Bondioli, C. Fagnano, A.M. Ferrari, A. Tinti, M.Vinella; Study of the vibrational spectrum of cuprorivaite; Annali di Chimica 91 (2001) 679–692

**[Perez-Urquiza 2001]** M. Perez-Urquiza, J.L. Beltran; Determination of the dissociation constants of sulfonated azo dyes by capillary zone electrophoresis and spectrophotometry methods; J Chromatogr A 917, 331–336

**[Sumiko Tsuji 2001]** Y.A. Sumiko Tsuji, Y. Umino, M. Nishi, T. Nakanishi, Y.Tonogai; Structural determination of the subsidiary colors in food blue No. 1 (brilliant blue FCF) aluminum lake detected by paper chromatography; Shokuhin Eiseigaku Zasshi 42(4):243–248

**----------2000----------**

**[Bianchetti 2000]** P. Bianchetti, F. Talarico, M.G. Vigliano, M.F. Ali; Production and characterization of Egyptian blue and Egyptian green frit; Journal ofCultural Heritage 1 (2000) 179–188

**----------1999----------**

**[Jinno 1999]** K. Jinno (ed.); Separation of Fullerenes by Liquid Chromatography; RSC Chromatography Monographs, TheRoyal Society of Chemistry, Cambridge, UK.

**[Punt 1999]** W. Punt, S. Blackmore, S. Nilsson,A. Le Thomas; In: Hoen, P. (Ed.); Glossary of Pollen and Spore Terminology, second ed. Laboratory of Palaeobotany and Palynology, Utrecht

**[Rahmani 1999]** G.N. Rahmani, S.P. Sternberg: Bioremoval of lead from water using Lemna minor; Bioresource Technol 70 (3): 225–230. doi:10.1016/s0960-8524(99)00050-4

**[Saito 1999]** Y. Saito, I. Tanemura, T. Sato, H. Ueda; Interaction of Fragrance Materials with 2-Hydroxypropyl-beta-Cyclodextrin by Static and Dynamic Head-space Methods. Int. J. Cosmet. Sci 1999, 21, 189–198

**----------1998----------**

**[Delamare 1998a]** F. Delamare; De la composition du bleu égyptien utilisé en peinture murale gallo-romaine, Scienze e materiali del patrimonio culturale 4, (1998) 177–195

**[Delamare 1998b]** F. Delamare, Le bleu éegyptien, essai de bibliographie critique, Scienzee materiali del patrimonio culturale 4 (1998) 143–163

**----------1997----------**

**[Riederer 1997]** J. Riederer; Egyptian blue, in: E.W. FitzHugh (Ed.), Artists' Pigments: a Handbook of their History and Characteristics, vol. 3,Washington, National Gallery of Art, 1997, pp. 23–45.

**----------1996----------**

**[Capitán-Vallvey 1996]** L. Capitán-Vallvey, N.N. Iglesias, I. de Orbe Payá, R.A. Castañeda; Simultaneous determination of quinoline yellow and brilliant blue FCF in cosmetics by solid-phase spectrophotometry; Talanta 43(9):1457–1463

**----------1995----------**

**[Lehn 1995]** J.M. Lehn; Supramolecular Chemistry: Concepts and Perspectives; VCH Verlagsgesellschaft: Weinheim, Germany, 1995; p. 2617

**[Saito 1995]** Y. Saito, H. Ohta, H. Nagashima, K. Itoh, K. Jinno, M. Okamoto et al.; Separation of fullerenes with novelstationary phases in microcolumn high performance liquid chromatography; J. Liq. Chromatogr. 18: 1897–1908

**----------1994----------**

**[Ohta 1994]** H. Ohta, Y. Saito, K. Jinno, H. Nagashima, K. Itoh; Temperature effect in separation of fullerene by highperformance liquid chromatography. Chromatographia 39: 453–459

**----------1993----------**

**[Häusler 1993]** O. Häusler, C. Műller-Goymann; Properties and structure of aqueous solutions of hydroxypropyl-ß-cyclodextrin; Starch, 45:183–7

**[Jinno 1993]** K. Jinno, H. Ohta, Y. Saito, T. Uemura, H. Nagashima, K. Itoh; Dimethoxyphenylpropyl bonded silicaphase for higher fullerenes separation by high-performance liquid chromatography; J. Chromatogr. 648: 71–77

**[Skillicorn 1993]** Skillicorn P, Spira W and Journey W (1993), Duckweed aquaculture a new aquatic farming system for developing countries, The International Bank for Reconstruction and Development/The World Bank

**----------1992----------**

**[Chatjigakis 1992]** A.K. Chatjigakis, C. Donzé, A.W. Coleman; Solubility behaviour of β-cyclodextrin in water/cosolvent mixtures; Anal Chem, 64:1632–4

**[Lamparczyk 1992]** H. Lamparczyk; Analysis and Characterization of Steroids; CRC Handbook of Chromatography; 1992 by CRC Press, 176 Pages

**----------1990----------**

**[Borzelleca 1990]** J.Borzelleca, K. Depukat, J. Hallagan; Lifetime toxicity/carcinogenicity studies of FD & C blue No. 1 (Brilliant blue FCF) in rats and mice; Food Chem Toxicol 28(4):221–23

----------1989----------

**[Vesterberg 1989]** O. Vesterberg; History of electrophoretic methods; J Chromatogr A 480, 3–19

----------1987----------

**[Connors 1987]** K.A. Connors; Binding Constats—The Measurement of Molecular Complex Stability; JohnWiley&Sons: New York, USA; Chichester, UK; Brisbane, Australia; Toronto, ON, Canada; Singapore, 1987; p. 86

**[Ullrich 1987]** D. Ullrich; Egyptian blue and green frit: charact erization, history and occurence, synthesis, PACT 17 (II.3.1) (1987) 323–332

----------1984----------

**[Okamoto 1984]** Y. Okamoto, M. Kawashima, K. Hadata; Useful chiral packing materials for high-performance liquid chromatographic resolution of enantiomers: phenylcarbamates of polysaccharides coated on silica gel;J Am Chem Soc 106, 5357–5359

----------1978----------

**[Brooks 1978]** J. Brooks, G. Shaw; Sporopollenin a review of its chemistry, paleochemistry and geochemistry; Grana. 17, 91-98.

**[Hillman 1978]** S. W. Hillman, D. D. Culley Jr. (1978); The Uses of Duckweed; American Scientist. 66 (4): 442–451. Bibcode:1978AmSci..66..442H

----------1964----------

**[Feagri 1964]**I. Feagri, J. Iverson; Textbook of Pollen Analysis;1964, Blackwell, London

----------1961----------

**[Wunderly 1961]** Ch. Wunderly; Principles and Applications of Paper Electrophoresis; Elsevier Publishing Company, Amsterdam, pp. 4–17

----------1958----------

**[Hummers 1958]** W.S.Hummers, R.E. Offeman; Preparation of graphitic oxide; J Am Chem Soc 80(6): 1339–1339

----------1954----------

**[Brown 1955]** C. Brown, P.L. Kirk, J. Crim; Paper electophoresis in the identification of writing inks; Law Criminol Police Sci 45,473–480

**[Martin 1954]** N.H. Martin, G.T. Franglen; The use and limitations of filter-paper electrophoresis; J Clin Path 7, 87–105.

----------1951----------

**[Kunkel 1951]** H.G. Kunkel, A. Tiselius, J. Gen; Elecyrophoresis of proteis on filter paper; Physiol35, 89–118

## *(b) PhD Thesis*

**[Fenert 2021]** B. Fenert; Studies of novel micromethods for determination of various micropollutants and biomarkers in selected environmental and/or technological processes related to surface water ecosystems and wastewater treatment; PhD DSc

**[Kaleniecka 2018]** A. Kaleniecka; Investigation of supramolecular encapsulation as potential tool foranalysis and removal of selected micropollutants from liquid phases, Phd DSc

**[Ślączka 2013]** M. Ślączka; biodegradation of selected hormone modulators in technological processes and in natural conditions; PhD DSc

## *(c) Directives and regulations*

**[EU 2013]** DIRECTIVE OF THE EUROPEAN PARLIAMENT AND OF THE COUNCIL 2013/39 / EU of 12 August 2013 amending Directives 2000/60 / EC and 2008/105 / EC

as regards priority substances in the field of water policy (Text with EEA relevance)

**[Veterinary Residues Committee 2012]** Annual Report on Surveillance for Veterinary Residues in Food in the UK for 2001, 2002, and 2003 Archived 2012-02-11 at the Wayback Machine

**[The Merck Index 1976]** The Merck Index, 9th edn., Rahway, Merck & Co. Inc., Kenilworth, NJ, 1976.

**[Uchwała Rady Miejskiej 2020]** Załącznik nr 1 do Uchwały Rady Miejskiej w Koszalinie z dnia 03.12.2020r. w sprawie wyznaczenia obszaru i granic aglomeracji Koszalin

## *(d) WWW sources*

**[www 1]** https://culinarylore.com/ingredients:fdc-blue-no-1-brilliant-blue-fcf-food-dye/

**[www 2]** https://web.archive.org/web/20190506202301/

**[www3]** https://www.iacmcolor.org/safety-of-color/safety-synthetic-certified-colors/blue

**[www 4]** https://pubchem.ncbi.nlm.nih.gov/compound/11294

**[www 5]** www.eden-microfluidics.com/

**[www 6]** https://eden-microfluidics.com/eden-cleantech/

**[www 7]** http://rsb.info.nih.gov/ij

# 9. LIST OF THE OWN PAPERS

This PhD thesis is based on experimental/review data that were partially published as experimental papers, book chapters and/or conferences abstracts.

## *A. List of research papers and book chapters*

**----------2010----------**

**(*) [Anielak 2010]** K. Piaskowski, M. Wojnicz, M. Grzegorczuk, **L. Lewandowska**; Wastewater Treatment with Zeolites at Dygowo Wastewater Treatment Plant; Monograph: Envirenmental Engineering III. CRC Press, Boca Raton, New York 2010

**----------2017----------**

**(*) [Ohta 2017]** H. Ohta, E. Włodarczyk, K. Piaskowski, A. Kaleniecka, **L. Lewandowska,** M.J. Baran, M. Wojnicz, K. Jinno, Y. Saito, P.K. Zarzycki; Unexpected differences between planar and column liquid chromatographic retention of 1-acenaphthenol enantiomers controlled by supramolecular interactions involving β-cyclodextrin at subambient temperatures; Anal Bioanal Chem – Springer 409 (2017) 3695-3706

**[Lewandowska 2017]** L. Lewandowska, E. Włodarczyk, B. Fenert, A. Kaleniecka, P.K. Zarzycki; A Preliminary Study for the fast Prototyping of Simple Electroplanar Separation Systems Based on Various Natural Polymers and Planar Chromatographic Stationary Phases, Journal of Planar Chromatography- Modern TLC 30 (2017) 440-452.

**----------2020----------**

**(*) [Kaleniecka 2020]** A. Kaleniecka, E. Włodarczyk, K. Piaskowski, **L. Lewandowska**, P.K. Zarzycki; Unexpected Encapsulation of Selected Polycyclic Aromatic Hydrocarbons by β-Cyclodextrin Studied Using UV-Vis Spectrophotometry, Micro-Planar Chromatography and Temperature Dependent Inclusion Chromatography; Symmetry 2020, *12*(12), 1967; https://doi.org/10.3390/sym12121967

**[Zarzycki 2020]** P.K**.** Zarzycki, K. Mitura, K. Piaskowski, **L. Lewandowska,** R. Świderska-Dąbrowska, M.J. Baran; Carbon and related nanomaterials as active media

for analytical, pharmaceutical, biomedical and wastewater processing applications; Pure and Functionalized Carbon Based Nanomaterials: Analytical, Biomedical, Civil and Environmental Engineering Applications, 1st ed.; Zarzycki, P.K.; CRC Press Taylor & Francis Group, Boca Raton, Florida, United States, 2020, pp. 326–363

**----------2021----------**

**[Zarzycki 2021a]** P. K. Zarzycki, **L. Lewandowska**, B. Fenert, K. Piaskowski, J. Kobaka; Investigation of hybrid methods for elimination of micropollutants from water phase using Brilliant Blue as target chemical and various nanomaterials combined with activated sludge and duckweed; Nanomaterials 2021, 11(7), 1747; https://doi.org/10.3390/nano11071747

**[Zarzycki 2021b]** P.K**.** Zarzycki, K. Piaskowski, **L. Lewandowska**, B. Fenert, R. Świderska-Dąbrowska, M. Ślączka-Wilk, A. Kaleniecka; Portable micro-planar extraction, separation and quantification devices for bioanalytical and environmental engineering applications; Elsevier book: Micro and Nano Technologies 2022, Chapter 8, Pages 163-196

**(*)** Research papers which experiments were not included in this PhD dissertation

## *B. Research communications published as conference abstracts*

**[Zarzycki 2016]** P.K. Zarzycki, M.J. Baran, **L. Lewandowska**, E. Włodarczyk, R. Świderska-Dąbrowska, K. Piaskowski, M. Wojnicz, R. Nowak, A. Kaleniecka, B. Fenert; Wyniki Wstępnych badań batymetrycznych oraz metodologii poboru prób wody i osadów dennych wybranych ekosystemów wód powierzchniowych Pomorza Środkowego; XVIII th Annual meeting of the Polish Hyperbaric Medicine and Technology Society, 24-27 November 2016, Jurata, Poland

**[Zarzycki 2017]** P.K. Zarzycki, **L. Lewandowska**, B. Fenert, A. Kaleniecka; Electronic nose on small sailing yacht; XIX th Annual meeting of the Polish Hyperbaric Medicine and Technology Society, 16-19 November 2017, Jastrzębia Góra, Poland

**[Ohta 2017]** H. Ohta, E. Włodarczyk, K. Piaskowski, A. Kaleniecka, **L. Lewandowska**, M.J. Baran, M. Wojnicz, K. Jinno, Y. Saito, P.K. Zarzycki; Adjustment of phenomenological model describing liquid chromatography retention controlled by supramolecular interactions with natural cyclodextrins; EMN (Energy, Materials, Nanotechnology) Meeting on Biomaterials, August 14-18, Milan, Italy

**[Lewandowska 2018]** L. Lewandowska**,** E. Włodarczyk, B. Fenert, A. Kaleniecka, A. J. M. Valente, J. C. Pereira, P. K. Zarzycki; Biocomposites related stationary phases for microplanar electrophoresis; International Conference on Advanced Structural and Functional Materials/Energy Materials and Nanotechnology, August 2018, Kraków, Poland

# 10. ABBREVIATIONS

**AC**- activated carbon

**ADI**- Acceptable Daily Intake

**AOP**- advanced oxidation process

**ARAMIS**- Antibiotic and Endocrine Disruptor Removal From Wastewater By Absorption In Microfluidics Systems

**AS**- activated sludge

**BAT**- Brunauer-Emmett-Teller theory

**BB**- Brilliant Blue

**BF**- Bożena Fenert

**CD**- cyclodextrin

**DMF**- 7,8 dimethoxyflavone

**DP**- dandelion pappus

**EDS**- Energy Dispersive Spectroscopy

**EFSA**- European Food Safety Authority

**FAO**- Food and Agriculture Organization

**GO**- graphene oxide

**HPTLC**- high-performance thin layer chromatography

**JMWTP**- Jamno Municipal Wastewater Treatment Plant

**LED**- light-emitting diode

**MG**- Malachite Green

**MMIP**- magnetic molecularly imprinted polymer

**NP**- normal phase

**PA**- peak intensity

**PAD**- Pressure Activated Devices

**PCA**- Principal Component Analysis

**PI**- peak area

**p*K*$_{a}$** - acid dissociation constant

**PKZ**.- Paweł Konrad Zarzycki

**PP**- pine pollen

**PS**- priority substances

**P4R**- Ponceau 4 R

**RGB**- color values specified with: red, green, blue

**rpm**- revolutions per minute

$\boldsymbol{R_s}$- resolution parameter

**SCF**- scientific committee for food

**SEM**- Scanning Electron Microscopy

**SLR**- Single-Lens Reflex

**SPE**- solid-phase extraction

**SY**- Sunset Yellow

**TGA**- thermogravimetric analysis

**TLC**- thin layer chromatography

**TUK**- Technical Universiti of Koszalin

**WHO**- World Health Organization

# 11. ABSTRACT

**PhD Thesis: "*Hybrid methods enabling elimination of organic micropollutants in water and sewage*"**

This PhD manuscript contains new concepts focusing on experimental protocols and a proposal of new materials/nanomaterials for hybrid methodologies allowing for the elimination of low-molecular-mass organic micropollutants from the water phase. The introduction to the manuscript consists of a problem overview and extensive discussion of current literature in the field of micropollutants and technological processes for their removal. As target micropollutants, four common dyes were selected and investigated: Brilliant Blue, Malachite Green, Sunset Yellow and Ponceau 4R. Various experiments involving these chemicals were proposed including separation science and biological investigations (activated sludge, duckweed organisms). As active matrices, a number of both simple and complex substances were investigated, namely: active carbon, lyophilized graphene oxide, β-cyclodextrin, raw dandelion pappus, microcrystalline cellulose, raw pine pollen, and Egyptian Blue mineral pigments (1.1.1. and 1.1.1a.). A new approach for the synthesis of the selected nanomaterials were described in the details concerning lyophilised Graphene Oxide and Egyptian Blue dye. These materials were extensively characterized using a number of different physicochemical methods such as SEM, EDS, Raman and FTIR. In addition, new simple analytical protocols based on direct colorimetry and/or microplanar chromatographic separation for the fast estimation and quantification of target micropollutants during elimination studies were elaborated. Molecular interactions between inorganic adsorbents and various biopolymers (cellulose in different forms, potato starch, nutrient agar, TLC cellulose, TLC polyamide, TLC silica gel 60 W, HPTLC silica gel RP-18W), nanoparticle additives (graphene oxide) and selected charged micropollutants (organic dyes ions) were investigated using electroplanar separation protocols. The results of these studies enabled the rapid and preliminary selection of further active matrices in ion form for elimination from the water phase. As a side effect of the conducted research, it has been found that cellulose coated with graphene oxide can be applied as an efficient adsorbent for the analytical application of micropollutants.

Using a number of active additives described in this PhD dissertation, two experiments were proposed and performed as multivariate procedures in different modes (24-hour and 16-day). Due to the multivariate nature of the proposed experiments, quantitative data were explored with chemometric tools including AHC

(agglomerative hierarchical clustering), PCA (principal component analysis), and FA (factor analysis). Based on a simple colorimetric test (24h) involving three dyes: BB, P4R, MG, Brilliant Blue dye was selected for follow up investigations due to its high stability. Multivariate data analysis resulting from PCA and AHC object grouping may suggest a potential effect of the given additive on BB elimination, particularly in the cases of graphene oxide, microcrystalline cellulose, duckweed, pine pollen, and Egyptian Blue pigment. Experimental data and multivariate calculations revealed that BB is strongly resistant to biodegradation, however, inclusion complex formations with β-cyclodextrin may induce degradation of this dye in the presence of duckweed. It is hoped that the results of the experimental work performed can be used in the design of future experiments for the fast screening of different additives and the improvement of technological processes focusing on the purification of sewage and water from micropollutants.

# 12. STRESZCZENIE

**Praca doktorska: "*Hybrydowe metody eliminowania mikrozanieczyszczeń organicznych z wody i ścieków*"**

W niniejszej rozprawie doktorskiej przedstawiono szereg nowych propozycji dotyczących badań eksperymentalnych oraz nowych materiałów (w tym nanomateriałów) umożliwiających eliminację małocząsteczkowych mikrozanieczyszczeń organicznych z fazy wodnej, w procesach o charakterze hybrydowym. Wstęp pracy zawiera opis problemu mikrozanieczyszczeń w różnych kontekstach oraz usuwanie tych substancji w procesach technologicznych oczyszczania ścieków komunalnych. Jako mikrozanieczyszczenia wybrano oraz badano cztery barwniki: Błękit Brylantowy, Zieleń Malachitową, Żółcień Pomarańczową i Czerwień Koszenilową. Praca opisuje szereg badań w/w barwników w różnych warunkach, włączając w to techniki rozdzielania oraz organizmy żywe (osad czynny, rzęsa wodna). Jako materiały aktywne będące aktywnymi składnikami wielowariancyjnych eksperymentów hybrydowych użyto: węgiel aktywny, liofilizowany tlenek grafenu, β-cyklodekstrynę, puch mniszka lekarskiego, pyłek sosnowy, celulozę mikrokrystaliczną oraz dwa rodzaje Błękitu Egipskiego. W pracy opisano modyfikowane procedury syntezy dwóch nanomateriałów: liofilizowanego tlenku grafenu oraz mikronizowanego Błękitu Egipskiego. Jakość otrzymanych produktów była sprawdzona poprzez badania fizykochemiczne, obejmujące analizy SEM, EDS, widma Ramana i FTIR. Dodatkowo opracowano metody analityczne (jakościowe oraz ilościowe) oznaczania barwników w trakcie procesów eliminacji z fazy wodnej, w oparciu o techniki kolorymetryczne oraz rozdzielania na płytkach mikro-TLC. Za pomocą chromatografii elektroplanarnej zbadano oddziaływania międzycząsteczkowe pomiędzy adsorbentami nieorganicznymi, różnymi biopolimerami (różne formy celulozy, mąka ziemniaczana, agar odżywczy, komercyjne płytki do TLC pokryte celulozą, poliamidem, żelem krzemionkowym typ 60 W, płytki do HPTLC pokryte żelem krzemionkowym typ RP-18W), jak również dodatkami nanocząsteczek (tlenek grafenu), a wybranymi jonami barwników. Uzyskane rezultaty umożliwiają szybki dobór aktywnych matryc do eliminacji mikrozanieczyszczen w postaci jonów organicznych z fazy wodnej, wykorzystując zjawisko barierowania. Dodatkowo, uzyskane wyniki wskazują na możliwość zastosowania warstw cellulozowych, modyfikowanych tlenkiem grafenu, jako efektywnych i selektywnych adsorbentów do zastosowań analitycznych (analiza ilościowa mikrozanieczyszczeń w

wodach powierzchniowych).

W opisanej pracy eksperymentalnej zaproponowano dwa doświadczenia, umożliwiające analizę wielowariancyjną otrzymanych wyników: test 24 godzinny oraz 16 dniowy. Uzyskane dane ilościowe były analizowane przy pomocy algorytmów analizy czynnikowej (PCA, FA, AHC). Przeprowadzone badania kolorymetryczne, z wykorzystaniem próbek testu 24 godzinnego z barwnikami BB, P4R oraz MG wykazały, że cząsteczki BB są najmniej podatne na usuwanie z fazy wodnej. Wyniki analizy chemometrycznej, grupowania obiektów w oparciu o PCA i AHC, sugerują potencjalną możliwość eliminacji BB poprzez dodatki tlenku grafenu, celulozy mikrokrystalicznej, pyłku sosnowego, błękitu egipskiego oraz rzęsy wodnej. Wykazano, że w warunkach prowadzenia eksperymentu najbardziej efektywnym dodatkiem jest β-cyklodekstryna w obecności rzęsy wodnej. Zjawisko to może wynikać z tworzenia kompleksów inkluzyjnych i zwiększonej bioadsorpcji takich kompleksów z wody. W ocenie Autorki, przeprowadzone wyniki badań umożliwią w przyszłości projektowanie dedykowanych systemów hybrydowych do usuwania z wody i ścieków różnych mikrozanieczyszczeń organicznych.

# 13. SUPPLEMENTS LIST

***[S1]*** Raman spectra of carbon materials used in laboratory tests.

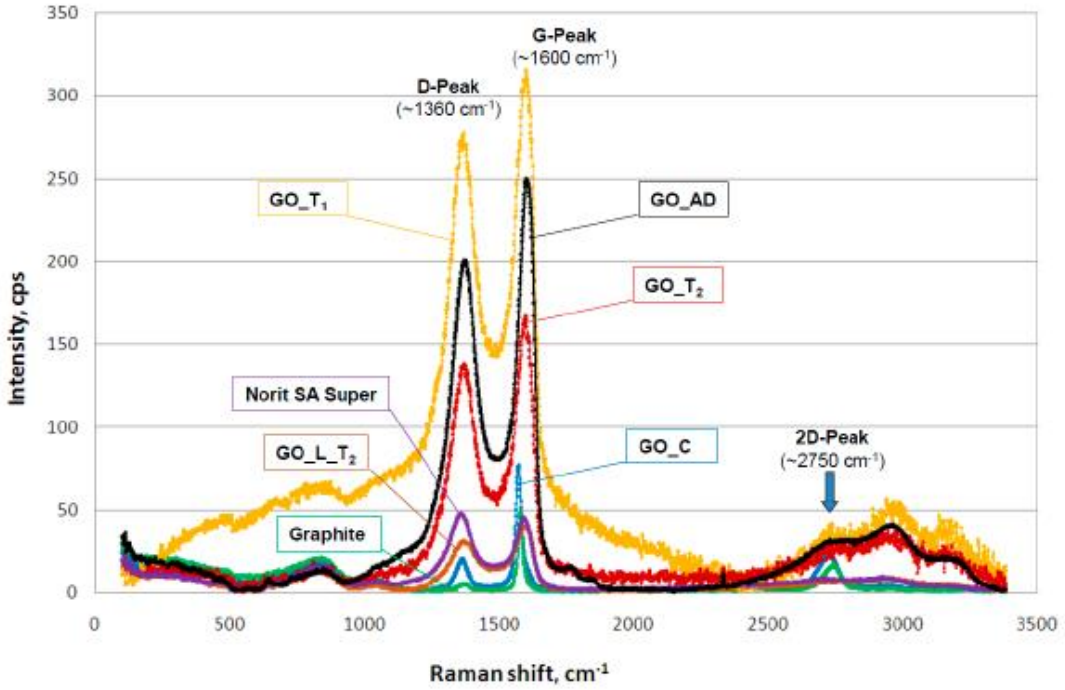


Raman spectra of carbon materials used in laboratory tests. Activated carbon Norit SA Super; commercial graphene oxide—GO_C, graphene oxide—GO_T1 (after 3 weeks from synthesis time); graphene oxide—GO_T2 (after 36 weeks from synthesis time); graphene oxide after air drying—GO_AD and GO after lyophilization GO_L **[Piaskowski 2020;** Figure 4, page 5869; with permision from MDPI**]**

***[S2]*** Copy of permission from Danish Defence authorities to conduct research cruse inside Danish territorial waters.

MINISTRY OF FOREIGN AFFAIRS

JTHAV 2020-18590

NOTE VERBALE

Referring to Note No. 2992.5.2020 of 27 May 2020 from the Embassy of the Republic of Poland concerning a research cruise with the Polish research vessel "TOBIAS" during the period of 27th June – 4th July 2020, the Ministry of Foreign Affairs has the honour to inform the Embassy that the competent Danish Defence authorities have no objections to the proposed cruise provided that the Danish Environmental Protection Agency or the Danish Energy Agency recommend the cruise to be conducted and thereby recommend the permission issued.

According to the application the research cruise with the Polish research vessel "TOBIAS" will take place in the Baltic Sea inside Danish territorial waters (less than 12 nautical miles from the baselines). No contact has been made with the Danish Technical University and there are no plans for the participation of Danish researchers on this cruise.

In connection to the research cruise there has been asked permission to call at the ports of Roenne, Svaneke, Hammerhavn and on Christiansoe. During the outbreak of CORONA VIRUS (COVID-19) in Denmark, all calls to port, including call to port under the rules of Force Majeure are made under certain restrictions. Only visits to Danish harbour for logistic purpose and resupply are allowed. It is not allowed to perform any kind of shore leave for the crew when inside Danish harbour. Information on CORONA VIRUS in Denmark can be sought through the homepage of the Danish Ministry of Foreign Affairs which directs you to the homepage of the Danish Health Department; https://www.sst.dk/da/Viden/Smitsomme-sygdomme/Smitsomme-sygdomme-A-AA/Coronavirus/Spoergsmaal-og-svar/Questions-and-answers and on the joint homepage of Danish authorities; https://politi.dk/coronavirus.

While the vessel is in Danish EEZ, it must broadcast continuously on the vessel's Automatic Identification System (AIS) and in connection with entering and departing Danish EEZ report to Maritime Surveillance Centre.

Attention is drawn to the fact that navigation and research will take place in areas in which unexploded ammunition (UXO), including chemical ammunition, as remains from World War II may be found. In the case that remains of ammunition or other unidentified objects are spotted during the research the work must be stopped immediately and the ship must contact the National Maritime Operations Centre i.a.w. Danish Regulation 1351 of 29 November 2013, para. 14.

The Embassy of the Republic of Poland
COPENHAGEN

*The Joint GeoMETOC Support Centre* under Danish Defense Department, Materiel and acquisitions board, requests a copy of the bathymetric data (incl. relevant metadata e.g. Cruise Reports, Calibration Reports etc.) collected within 200NM from the baseline.

The bathymetric data is to be delivered as cleaned XYZ data (in full resolution). Metadata can be delivered as PDF or Word documents. Furthermore all data concerning the ocean water physical (temperature, salinity, currents) and chemical (oxygen, nutrients) composition, specifically measurements from CTD/LACP (conductivity/temperature/depth – lowered acoustic current profiler) is to be forwarded. All data can be delivered to POC Charlotte Wiin Havsteen, fmi-ma-cho@mil.dk.

Contact information for National Maritime Operations Centre;
Duty officer: +45 7285 0361, E-mail: Opscent@sok.dk
Maritime Surveillance Centre (MSC) +45 7285 0654 moc-orum@mil.dk
Maritime Assistance Service: +45 7285 0371, E-mail: Mas@sok.dk
Front desk: +45 7285 0000.

The study area covers the Baltic Sea between: S: 54 19.9 N, N: 55 21.3 N, W: 014 37.6 E, E: 015 29.7 E. The purpose of the cruise is to investigate floatable biopolymers in surface water. Operational methods floating extraction microdevice attached to S/Y Tobias.

The Danish Environmental Protection Agency (MST) recommends, that the permission is granted, provided that:

The Danish Environmental Protection Agency receives all provisional and subsequent reports including publications of the findings of the cruise. Regarding the provisional report, a chart shall be attached showing on the largest scale possible the navigation route and the positions of sampling (submitted not later than 2 months after completion of the cruise).

The research result of any biological/hydrological/geological description of the seabed samples, together with any analyses conducted on the sample material including the exact positions will be forwarded The Danish Environmental Protection Agency not later than 3 months after completion of the cruise.

The Danish authorities are entitled to use the research data in connection with publication of own research results.

The Agency for Culture and Palaces (Slots- og Kulturstyrelsen) is notified immediately of any vestiges of stone-age villages or historical wrecks.

The applicants fill in a spreadsheet (to be provided by the ministry of foreign affairs) where information as date, position, activity (e.g. echosounding and the vmADCP) and sound level of the activity is registered for each day the activity is performed. The spreadsheet must be returned to the Danish Environmental Agency (MST) on fyn@mst.dk.

Finally, it would be appreciated that hydrographical data collected in Danish waters be forwarded to the International Council for the Exploration of the Sea (ICES/CIEM), Service Hydrographique within a year after the conclusion of the research cruise. The hydrographical data should be forwarded on a computer compatible medium, if applicable, in accordance with the agreement between Poland and the ICES/CIEM.

Copenhagen, 12 June 2020

***[S3]*** Copy of Provisional Research Report concerning research cruise on the Baltic Sea with the polish research vessel S/Y Tobias; Koszalin, 02.09.2020

Koszalin, 02.09.2020

Paweł K. Zarzycki, M.Pharm., Ph.D., DSc, A/Professor
Faculty of Civil Engineering, Environmental and Geodetic Sciences
Koszalin University of Technology
Śniadeckich 2, 75-453 Koszalin
Poland

Ph.: 48-94-3478671; 8559; 8560; Fax: 48-94-3427652
E-mail: pkzarz@wp.pl

**PROVISIONAL RESEARCH REPORT**
**CONCERNING RESEARCH CRUISE ON THE BALTIC SEA**
**WITH THE POLISH RESEARCH VESSEL S/Y TOBIAS**

Referring to Permission No **JTHAV 2020-18590** issued by Danish Ministry of Foreign Affairs (Copenhagen, 12 June 2020) and recommendations of the Danish Environmental Protection Agency (MTS) that were specified in this Permission, namely:

1. "The Danish Environmental Protection Agency receives all provisional and subsequent reports including publications of the findings of the cruise. Regarding the provisional report, a chart shall be attached showing on the largest scale possible the navigation route and the positions of sampling (submitted not later than 2 month after completion of the cruise)."

2. "The research results of any biological/hydrological/geological description of the seabed samples, together with any analyses conducted on the sample material including the exact positions will be forwarded The Danish Environmental Protection Agency not later than 3 months after completion of the cruise."

3. "The applicant fill in a spreadsheet (to be provided by the ministry of foreign affairs) where information as date, position, activity (e.g. echosounding and vmADCP) and sound level of the activity is registered for each day the activity is performed. The spreadsheet must be returned to the Danish Environmental Agency (MTS) on fyn@mst.dk."

hereby, I would like to provide requested data and current research advances concerning samples collected during research cruise with the Polish research vessel S/Y Tobias, which was recently performed inside Polish and Danish territorial waters within Bornholm island area.

Research cruise with S/Y Tobias lasted from 27th June to 4th July 2020. Planned and conducted studies were predominantly focused on testing of natural and chemically modified biopolymers based on cellulose as the potential selective extraction matrices enabling isolation and measurement of various micropollutants and biomarkers that may be present in surface water of the Baltic Sea. Expected target chemicals are characterized by different polarity (e.g. polycyclic aromatic hydrocarbons, *n*-alkanes, chlorophyll dyes or steroids and related endocrine disrupting compounds). We have invented analytical system composed of portable cage devices containing an appropriate extracting biopolymers attached to 50 m long floating line (**Figure 1A**). Extraction time for each sampling position/route was performed within 1 hour period. Using this system we collected multiple samples (**Figure 1B**) involving different extraction matrices based on various raw cellulose or modified cellulose layers with *n*-alkanes and graphene oxide active coatings (**Figure 1 C1/C2/C3**). This chemical modification affected active layers polarity and consequently changed selectivity of the extraction process.

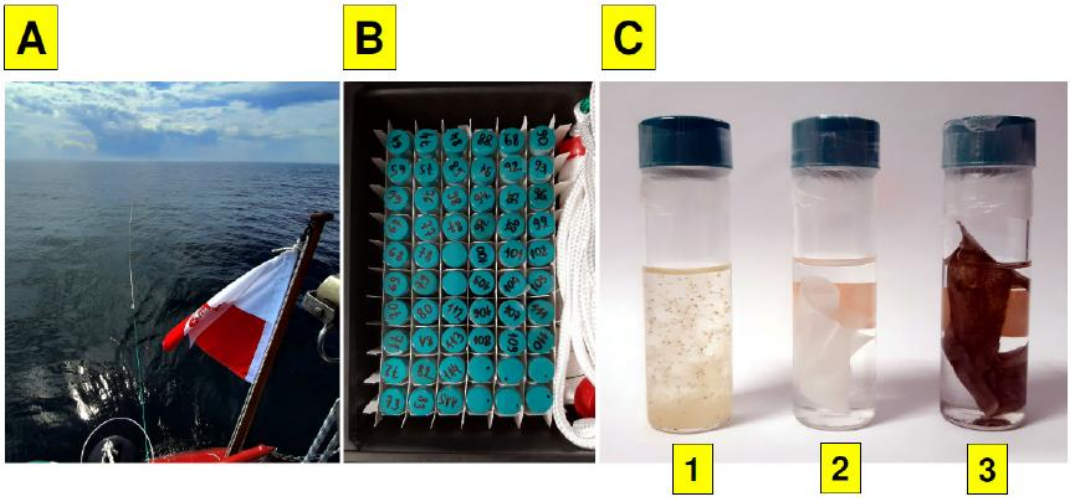


**Figure 1.** General view of applied sampling technique (**A**), all samples collected (**B**) and extraction matrices types (**C**): *Taraxacum officinale* derived raw pappus cellulose (**1**), cellulose layer (plain and modified with *n*-alkanes; **2**), cellulose layer coated with graphene oxide (**3**).

During this research cruise 52 individual samples were collected that were *in situ* preserved in ethanol (95%) for storage, until chemical analysis time. **Table 1** contains detailed data for each sample including sampling point/route ID, coordinates, date, time and surface water temperature.

| LOCALIZATION | SAMPLING POINT No or ROUTE No | COORDINATES OF SAMPLING POINT/ROUTE [Latitude] | [Longitude] | SAMPLING DATE | SAMPLING TIME | YACHT SAILING MODE | SURFACE WATER TEMPERATURE [C] | COLLECTED SAMPLES LABELS | NUMBER OF SAMPLES COLLECTED |
|---|---|---|---|---|---|---|---|---|---|
| KOŁOBRZEG (PL) | 01 (START) | 54 10.699 N | 015 33.663 E | 27.06.2020 | 21:53 (START) | SAILS OFF; ENGINE OFF | 23.0 | 64,65,66,67,88,89,90,91,108,109,110,111,112,113,114,115 | 16 |
| KOŁOBRZEG (PL) | 01 (END) | 54 10.699 N | 015 33.663 E | 27.06.2020 | 22:53 (END) | | | | |
| BALTIC SEA (PL) | 02 (START) | 54 13.707 N | 015 30.844 E | 28.06.2020 | 14:40 (START) | SAILS ON; ENGINE OFF | 19.0 | 68,69,70,71,92,93,94,95 | 8 |
| BALTIC SEA (PL) | 02 (END) | 54 13.562 N | 015 29.896 E | 28.06.2020 | 15:40 (END) | | | | |
| BALTIC SEA (DK) | 03 (START) | 55 05.381 N | 015 12.553 E | 29.06.2020 | 11:51 (START) | SAILS OFF; ENGINE ON | 18.5 | 72,73,74,75,96,97,98,99 | 8 |
| BALTIC SEA (DK) | 03 (END) | 55 07.874 N | 015 09.981 E | 29.06.2020 | 12:55 (END) | | | | |
| SVANEKE,BORNHOLM (DK) | 04 (START) | 55 08.190 N | 015 08.702 E | 30.06.2020 | 12:02 (START) | SAILS OFF; ENGINE OFF | 18.0 | 76,77,78,79,100,101,102,103 | 8 |
| SVANEKE,BORNHOLM (DK) | 04 (END) | 55 08.190 N | 015 08.702 E | 30.06.2020 | 13:03 (END) | | | | |
| BALTIC SEA (DK) | 05 (START) | 55 13.632 N | 015 09.263 E | 01.07.2020 | 10:15 (START) | SAILS ON; ENGINE OFF | 15.5 | 80,81,82,83 | 4 |
| BALTIC SEA (DK) | 05 (END) | 55 18.300 N | 015 10.513 E | 01.07.2020 | 11:15 (END) | | | | |
| HAMMERSHAVN,BORNHOLM (DK) | 06 (START) | 55 16.707 N | 014 45.326 E | 02.07.2020 | 21:50 (START) | SAILS OFF; ENGINE OFF | 19.0 | 84,85,86,87,104,105,106,107 | 8 |
| HAMMERSHAVN,BORNHOLM (DK) | 06 (END) | 55 16.707 N | 014 45.326 E | 02.07.2020 | 22:50 (END) | | | | |
| | | | | | | | | TOTAL NUMBER OF SAMPLES COLLECTED: | 52 |

**Table 1.** List of sampling points and sampling routes as well as individual samples labels collected for given localization.

S/Y Tobias was equipped with Autohelm ST50 echo sounder, however, using this equipment we were unable to record the bathymetric data in electronic form. It should be noted that our samples were collected using both sailing modes (sailing on sails only or with working engine). Therefore, the maximum sound level generated by our vessel was related to the sound of S/Y Tobias engine (Leyland-Thornycroft 154; 46.3 kW). Detailed navigation route of the research cruise and the positions of sampling points/areas were presented on chart in **Figure 2**.

All samples collected during this research cruise are presently stored at Koszalin University of Technology (TUK) and will be subsequently analyzed, mainly using chromatographic techniques including high performance micro-thin layer chromatography (micro-TLC), planar electrophoresis and temperature depended inclusion chromatography (HPLC) involving fluorescence and/or chemical derivatization detection protocols. In the future we plan to analyze collected samples using mass spectrometry, to identify chemical structures which were adsorbed on cellulose layers.

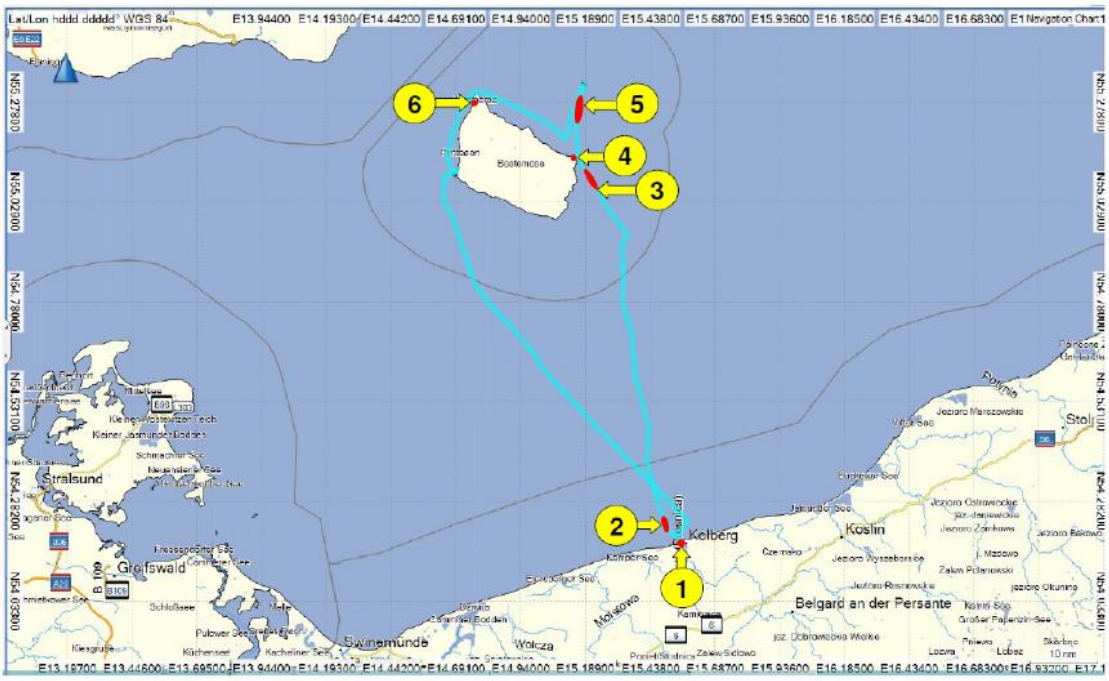


**Figure 2.** Navigation route chart of research cruise and localization of sampling points/routes positions (Labels 1-6 relate to data presented in **Table 1**).

Quantitative data concerning biomarkers/micropollutants composition will be processed using multivariate statistics to compare present results with previously obtained samples collected from different surface water ecosystems. We plan to collect more samples in the future to get more accurate information about time driven changes of micropollutants and biomarkers levels in the Baltic Sea. It is also planned to test improved sampling devices (*e.g.* semi-automatic) to increase spatial resolution of the measurements.

Results of this study will be subsequently reported in SCI research journals and presented as part of PhD thesis by Lucyna Lewandowska and Bożena Fenert (PhD students at TUK supervised by PZ). Selected information about this research trip and results obtained will be also reported as RoSSY (Research on Small Sailing Yacht) project through YouTube video channel (PK Zarzycki: https://www.youtube.com/channel/UCWH1_gXZitvk7KXNHeRGYwA

Yours faithfully

Zarzycki

Paweł K. Zarzycki

4

***[S4]*** Factor analysis od data matrices generated during the 16 days esperiment.

| | F1 | F2 | F3 | F4 | F5 | F6 |
|---|---|---|---|---|---|---|
| Eigenvalue | 4,784 | 1,068 | 0,060 | 0,038 | 0,035 | 0,015 |
| Variability (%) | 79,737 | 17,793 | 1,003 | 0,634 | 0,579 | 0,254 |
| Cumulative % | 79,737 | 97,530 | 98,533 | 99,167 | 99,746 | 100,000 |

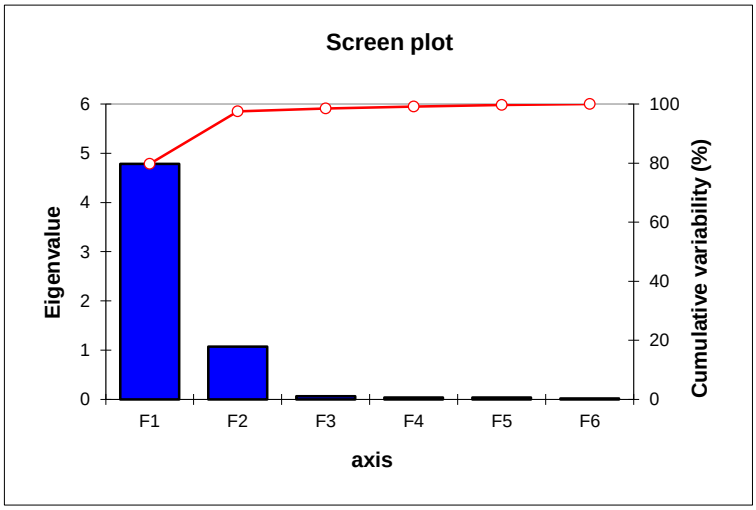

# A Preliminary Study for the Fast Prototyping of Simple Electroplanar Separation Systems Based on Various Natural Polymers and Planar Chromatographic Stationary Phases

Lucyna Lewandowska, Elżbieta Włodarczyk, Bożena Fenert, Aleksandra Kaleniecka, and Paweł K. Zarzycki*

**Key Words:**

Planar electrochromatography
Food dyes
Biomaterials
Natural and biodegradable polymers
Cellulose materials
Potato starch
Nutrient agar

## Summary

**This experimental work deals with preliminary studies concerning combined planar electrophoresis–electrochromatography system involving stationary phases composed of various natural materials applied for the separation of selected colorants. The main goal of the presented experiment is to investigate the key parameters (applied voltage, electrolyte composition, pH) and separation protocol setup (stationary phase/connection strips type and geometry) enabling the fast prototyping of simple analytical systems for the fractionation and/or separation of low-molecular mass compounds. Four water-based electrolytes that are as simple as possible (without additional organic liquid components or modifiers), including boric acid 100 mM (pH = 4.3), 1:1 mixture of boric acid 90 mM and Tris base 90 mM (pH = 8.2), boric acid 100 mM titrated with NaOH 1 M (pH = 8.5), and formic acid 100 mM (pH = 2.4), were tested. As target analytes, two colorants, namely, methyl red and ponceau 4R, were selected. These dyes are commonly used as printing inks component or pH indicator (methyl red) and food products colorant (ponceau 4R). Electroseparation experiments were conducted using commercially available, temperature non-controlled, open-air electrophoresis box equipped with homemade support for the positioning of active separation layers and electrodes connection strips. Thirteen types of separation layers (working zone = 20 × 100 mm; total length with connection strips = 20 cm) including cellulose-based polymers (filtrating paper, office paper, chromatography paper, and two Japanese papers for aircraft paper models), potato starch on cellulose support, common thin-layer chromatography–high-performance thin-layer chromatography (TLC–HPTLC) glass-based plates coated with cellulose, silica gel 60W (wettable with water), silica gel RP-18W, and aluminum oxide as well as glass-based nutrient agar layers (0.5 and 1.0 mm, approximately) were investigated. Moreover, detailed preparation procedure for manufacturing starch layer on cellulose and agar glass plate supports is described. Conducted investigations have revealed substantial differences between the electrophoretic migration of target dyes within cellulose type layers and also in comparison to the remaining stationary phases studied. The best separation under the given analytical conditions (voltage applied $\Delta V$ = 500 V and run time 20 min) was observed for cellulose pre-coated TLC plate ($R_s$ = 2.89) and starch layer on filtrating paper support ($R_s$ = 2.26). Baseline separation of investigated dyes was observed for filtrating paper strip and agar 0.5-mm thick layer ($R_s$ = 1.07 and 1.08, respectively). There was no electrophoretic mobility shift of the tested dyes on polyamide and RP-18W coated TLC–HPTLC plates, while dye short migration without separation was observed on the remaining layers. The obtained results, especially the recorded values of physicochemical parameters (the observed electric currents, migration distances, and peak resolution for different electrolytes, layer type, and thickness) create initial data set platform that can help in the further design of simple separation devices involving natural polymeric layers. Particularly, the described analytical protocol may be implemented for microfluidic paper-based analytical devices (μPADs) enabling fast and non-expensive separation of complex samples.**

## 1 Introduction

Modern separation science methods including chromatography, electrophoresis, and microfluidic devices are generally based on two spatial concepts: column or plate. Both systems may work in one-, two-, or three-dimensional separation modes usually involving multispace detection regimes. This approach highly improves the separation/quantification ability of target components in complex matrices. However, in practice, one- or two-dimensional and isocratic systems should be selected for fast, non-expensive, and robust separation and quantification of the components of interest. Therefore, a number of simple and fairly primitive analytical techniques based on planar separation concept are still developed and invented, particularly including dried blood spot (DBS) [1], thin-film microextraction (TFME) [2], or microfluidic paper-based analytical devices (μPADs) [3]. These analytical systems usually work as pre-purification and/or sample fractionation tools combined with more complex and sophisticated detectors including pattern recognition systems involving ultraviolet–visible (UV–Vis) and fluorescence data

L. Lewandowska, E. Włodarczyk, B. Fenert, A. Kaleniecka, and P.K. Zarzycki, Department of Environmental Technologies and Bioanalytics, Faculty of Civil Engineering, Environmental and Geodetic Sciences, Koszalin University of Technology, Śniadeckich 2, 75-453 Koszalin, Poland.
E-mail: pkzarz@wp.pl



DOI: 10.1556/1006.2017.30.5.15

# Chapter 14

# Carbon-based and Related Nanomaterials as Active Media for Analytical, Biomedical, and Wastewater Processing Applications

*Paweł K. Zarzycki*,[1,*] *Renata Świderska-Dąbrowska*,[1] *Krzysztof Piaskowski*,[1] *Lucyna Lewandowska*,[1] *Bożena Fenert*,[1] *Katarzyna A. Mitura*[2] and *Michał J. Baran*[1]



## 1. Introduction and Problems Overview

Pure carbon and carbon-related nanomaterials may be considered the most versatile particles that are presently studied in physics, chemistry, and bioengineering. Extensive research focusing on classical and new carbon particles is being carried out worldwide, and a number of new commercial products have been successfully implemented in different industries and technology areas, including electronic, medicine/pharmacy, cosmetic, food and agriculture, wastewater treatment or environmental protection, as well as civil engineering (Grumezescu 2017). From principles, carbon nanoparticles are easy to functionalize with various organic ligands and therefore, there are virtually an unlimited number of derivatives available, which can be adapted to the given application (Sun and Lei 2017). Particularly, carbon nanoparticles based on fullerenes, nanotubes, graphene, as well as nanodiamonds or carbon dots (CDs) are presently of great interest due to their relatively low toxicity, biocompatibility, easy synthesis, and unique physicochemical properties (Grumezescu and Holban 2018, Neethirajan et al. 2018). On the other hand, low-molecular mass carbon chemicals, such as fullerenes, are extremely difficult to analyze using classical chromatographic or electrophoretic methods. This is due to low solubility of such substances in both polar and non-polar organic solvents and the presence of higher

[1] Department of Environmental Technologies and Bioanalytics, Faculty of Civil Engineering, Environmental and Geodetic Sciences, Koszalin University of Technology, Śniadeckich 2, 75-453 Koszalin, Poland.
[2] Department of Biomedical Engineering Division, Faculty of Technology and Education, Koszalin University of Technology Śniadeckich 2, 75-453 Koszalin, Poland.
* Corresponding author: pkzarz@wp.pl

nanomaterials

MDPI

Article

# Investigation of Hybrid Methods for Elimination of Brilliant Blue Dye from Water Phase Using Various Nanomaterials Combined with Activated Sludge and Duckweed

Paweł K. Zarzycki [1,*], Lucyna Lewandowska [1], Bożena Fenert [1], Krzysztof Piaskowski [1] and Janusz Kobaka [2]

[1] Faculty of Civil Engineering, Environmental and Geodetic Sciences, Koszalin University of Technology, 75-453 Koszalin, Poland; lucyna.lewandowska@tu.koszalin.pl (L.L.); bozena.fenert@gmail.com (B.F.); Krzysztof.piaskowski@tu.koszalin.pl (K.P.)

[2] Faculty of Geoengineering, University of Warmia and Mazury in Olsztyn, 10-720 Olsztyn, Poland; janusz.kobaka@uwm.edu.pl

* Correspondence: pkzarz@wp.pl

**Abstract:** The main goal of this experimental work is screening of different natural and synthetic nanomaterials and biopolymers that may improve elimination of stable micropollutants from water phase. In this work, as a target chemical acting as the micropollutant molecule, the Brilliant Blue (BB) dye was selected. We tested different active matrices dispersed in water phase including activated carbon (AC), lyophilized graphene oxide (GO), β-cyclodextrin (CD), raw dandelion pappus (DP), microcrystalline cellulose(MC), and raw pine pollen (PP), as well as two types of Egyptian Blue mineral pigments (EB1 and EB2). Graphene oxide and Egyptian Blue nanomaterials were synthesized in our laboratory. We investigated potential application of such nanoparticles and biopolymer conglomerates as additives that may tune the activated sludge (AS) microorganisms or duckweed water plant (DW) and increase efficiency of micropollutants removal from wastewater. Studied nanomaterials/biopolymers were used in two different experimental modes involving real activated sludge microorganisms (24 h experiment) as well as duckweed plant (16 day experiment). Quantitative data of BB were obtained using microfluidic type device based on micro-TLC plate. This approach enabled direct determination of target component without sample pre-treatment like pre-concentration or pre-purification. Within single analytical run calibration line, retention standard spots (methyl red) and multiple samples were analyzed simultaneously. Due to the multivariate nature of these experiments, quantitative data were explored with chemometric tools including AHC (agglomerative hierarchical clustering), PCA (principal component analysis), and FA (factor analysis). Experimental data and multivariate calculations revealed that BB is strongly resistant on biodegradation, however, inclusion complexes formation with β-cyclodextrinmay induce degradation of this dye in the presence of duckweed. It is hoped that results of our experimental work can be used for designing of future experiments for fast screening of different additives and improvement of technological processes, focusing on purification of sewage and water from micropollutants.

**Keywords:** micropollutants; wastewater; microanalysis; chemometrics; duckweed; cyclodextrin; activated sludge; hybrid nanomaterials



**Citation:** Zarzycki, P.K.; Lewandowska, L.; Fenert, B.; Piaskowski, K.; Kobaka, J. Investigation of Hybrid Methods for Elimination of Brilliant Blue Dye from Water Phase Using Various Nanomaterials Combined with Activated Sludge and Duckweed. *Nanomaterials* **2021**, *11*, 1747. https://doi.org/10.3390/nano11071747

Academic Editors: Varsha Srivastava and Weiming Zhang

Received: 14 May 2021
Accepted: 29 June 2021
Published: 2 July 2021



## 1. Introduction

Over the last decade there has been a growing interest in the development of non-expensive hybrid technologies, combining nanoparticles generated from recycled waste materials that may work as selective media enabling micropollutants removal from wastewater. This is a complex task, and therefore, a number of different approaches to this problem were proposed and studied. The main issue is that micropollutants form a highly non-homogenous mixture and are present at different concentrations level, usually ranging from pg to ng per liter. They can be chemically resistant, but even under particular condi-

# 8

# Portable microplanar extraction, separation, and quantification devices for bioanalytical and environmental engineering applications

P.K. Zarzycki[a], K. Piaskowski[a], L. Lewandowska[a], B. Fenert[a], R.K. Świderska-Dąbrowska[a], M.M. Ślączka-Wilk[b], J.C. Pereira[c]

[a]FACULTY OF CIVIL ENGINEERING, ENVIRONMENTAL AND GEODETIC SCIENCES, KOSZALIN UNIVERSITY OF TECHNOLOGY, KOSZALIN, POLAND, [b]INSTITUTE OF MATHEMATICS, PHYSICS AND CHEMISTRY, MARITIME UNIVERSITY OF SZCZECIN, SZCZECIN, POLAND, [c]CQC, DEPARTMENT OF CHEMISTRY, UNIVERSITY OF COIMBRA, COIMBRA, PORTUGAL

## 8.1 Occurrence and quantification of priority substances in water ecosystems—the problem overview based on the European Union Water Framework Directive

There are number of micropollutants that can be present, generated, and transported via water ecosystems. They may strongly affect animals and human populations and therefore, number of countries worldwide try to deal with this problem. Particularly, on the 23rd of October 2000 Directive 2000/60/EC—The Water Framework Directive (WFD) of the European Parliament and of the Council came to light. This document established a framework for "*Community action in the field of water policy*" with the purpose of creating a framework for the protection of inland surface waters, transitional, coastal, and groundwaters [6] including a procedure for dealing with water pollution that was revealed in Article 16 of the WFD Directive 2000/60/EC. The first step of the procedure or in other words a strategy was to provide a list of priority substances that was finally adopted by way of Decision 2455/2001/EC and included 33 priority substances or groups of priority substances (PS). Among the PS substances the priority hazardous substances, mainly toxic, persistent and with possibility to bioaccumulate were also identified [4, 6]. Beside that certain definitions were introduced including for instance surface waters, inland waters, transitional waters, river basin as *"the area of land from which all surface run-off flows through a sequence of streams, rivers and also possible lakes into the sea at a single river mouth, estuary or delta"* [6]. What it is worth of pointing out within the Article 16 of the WFD Directive 2000/60/EC the Member States were supposed to implement

**Micro- and Nanotechnology Enabled Applications for Portable Miniaturized Analytical Systems.**
**DOI:** https://doi.org/10.1016/B978-0-12-823727-4.00013-4

***[S6]*** YouTube presentations that were created by P.K.Z., partially as the research performed for this PhD thesis. These movies summarize and illustrate various aspects of experiments performed: collecting of adsorbing biomaterials, sampling collection during research cruises on the Baltic Sea and Polish inland lakes, research presentation during research workshop at Kusy Dwór (Czaplinek/Drawsko Lake) as well as Egyptian Blue synthesis.

1. SeaHungry human droid is devouring of dandelion seeds (RoSSY project).


Video link: https://youtu.be/SlVAbeF6tYw

2. Incoming publication reporting bioanalysis of water ecosystems via microseparation (RoSSY project).

Video link: https://youtu.be/KrdhRKXsoHs

3. Incoming publication: nanomaterials and quantitative microfluidic device in action.


Video link: https://youtu.be/m4NO-GRrkfE

4. Bornholm research cruise with S/Y Tobias (the RoSSY project 2020).


Video link: https://youtu.be/QK7JKqBS47k

5. Research workshop focusing on various hybrid systems. Drawsko Lake, Poland (RoSSY project)

 Video link: https://youtu.be/I6pdgvcIlIo

6. Synthesis of miraculous ancient pigment by human droids.

 Video link: https://youtu.be/Ou5OG1tFvbQ

7. RoSSY bioanalytical/environmental research: pipe microsampler for underwater sediments collection

 Video link: https://youtu.be/IKaI663KMAo